UNIVERSITÉ DE STRASBOURG

EDSC Ecole Doctorale des Sciences Chimiques

ÉCOLE DOCTORALE DES SCIENCES CHIMIQUES

Laboratoire de Chimie des Matériaux Moléculaires - UMR 7509

THÈSE

présentée par

Meera MOHANKUMAR SREELATHA

soutenue le : **14 décembre 2012**

pour obtenir le grade de

Docteur de l'université de Strasbourg

Discipline / Spécialité : Chimie

Synthèse de complexes cuivreux luminescents

THÈSE dirigée par :

Jean-François NIERENGARTEN Directeur de Recherche au CNRS, Université de Strasbourg

RAPPORTEURS :

Peter FALLER Professeur, Université Paul Sabatier de Toulouse

Stéphane P. VINCENT Professeur, Université de Namur (FUNDP), Belgique

---

MEMBRE DU JURY :

Dominique ARMSPACH Professeur, Université de Strasbourg

MEMBRE INVITE :

Jean-Pierre SAUVAGE Professeur, Université de Strasbourg

Acknowledgement

I would like to express my sincere gratitude to my thesis supervisor Dr. Jean-François Nierengarten, who has given me the opportunity to be in an international working environment. Your scientific knowledge and expertise on planning the very complex systems have always been fantastic. The way you used to go deep into a problem and to come up with a convincing explanation has been amazing to me. During those hard days of my thesis you always used to cheer me up by saying 'That's Chemistry!' Thank you so much for your constant support.

I would like to thank Dr. Michel Holler, who trained me to work with almost all dangerous chemicals! Thanks for being an outstanding teacher with huge amounts of patience, for your ability to treat the problems in a wiser way, for being a good listener of my silly problems, for teaching me French (and sometimes Alsatian!), more than that for being a good friend during all the three years. Mimiche, all these makes you unique!

Many thanks to Dr. Jean Pierre Sauvage, for his collaboration and the discussions which were always been encouraging. The ideas and suggestions from you have always been impulsive. You have shown me how humble a person should be! I would also like to thank Frédéric Niess for providing me the samples of M30 and for the scientific discussions.

I would like to thank my examiners - Prof. Dominique Armspach, Prof. Peter Faller and Prof. Stéphane P. Vincent - for accepting our request to be in the jury and also for their interest in my research work.

I am grateful to Dr. Nicola Armaroli (ISOF – CNR, Bologna, Italy) for the effective collaboration and for the stimulant lectures in photophysics. Thanks to you for giving me an opportunity to be a part of FINELUMEN. I would also like to thank his group members John Mohanraj, Filippo Monti and Joanna Malicka for the fruitful and friendly discussions. Thanks to Raffaella Amodio for taking care of the issues related to my work contract.

Many thanks to Dr. Béatrice Delavaux-Nicot for the electrochemistry experiments and for the friendly collaboration.

Thanks as well to Dr. Kristiaan Neyts (ELIS department, Ghent University, Belgium) for giving me an opportunity to have secondments in his lab. Thanks to Oksana Drobchak for explaining the experiments which were really sophisticated and completely new to me.

I am thankful to Dr. Michel Schmitt for the huge number of NMR experiments that he has performed for me. I would like to thank Dr. Lydia Brelot and Dr. Corinne Bailly for the X-ray diffraction experiments. Many thanks to Dr. Jean-Marc Strub for the mass spectral analysis. Thank you to Mathieu Chesse for the UV measurements. I would also like to thank

Agnès Schmitt for helping me in taking care of all the administrative issues I had gone through.

I would like to thank Dr. Maida Vartanian for being a friend and a travel mate during the three years. The early wake up calls, the overnight chats, the journeys, the Bollywood movies, the list is never ending! The very next person whom I would like to thank is Luis Moreira Navarro, for being a very friendly person from the right beginning of my thesis. The enormous number of jokes that we shared still used to make me laugh. My huge thanks goes to Dr. Rubén Caballero Briceño for his friendly help, his jokes, his Spanish, for the movies, and for the Indian food . Hope that you are taking care of the pink dinosaur nicely.

A big thanks to David Sigwalt for being there as a good friend in the lab and sometimes an eternal Guru! I am thankful to you for the same radio songs which we learned along with AC/DC! Thanks a lot Piou for the late drop outs to Rotonde after the lab during the heavy winter. I would like to thank also Dr. Julien Iehl and Dr. Juan José Cid Martín for their company during my stay in Strasbourg. Thanks to Mathilde Berville for always being a true friend (Since we share the same karma!). Many thanks to María Vizuete Medrano, Rocio Risquez Cuadro, and the rest of the Spanish mafia for the friendly evenings.

I would like to thank Dr. Uwe Hahn for his help and scientific discussions. I know that you will miss my camera for your colourful compounds. I am thankful to Dr. Iwona Nierengarten for her understanding and support. My sincere thanks to Dr. Sebastiano Guerra for his help and friendship during the last couple of months. Thanks a lot to Haifa Ben Aziza for being there as a good friend (don’t laugh at pizzas anymore!). I would also like to thank Nico, Thomas, Annie, Shiva, Franck, Pauline, Radian, Ellodie and Lucie for their friendship.

I am indebted to Dr. S. Prathapan for being an enthusiastic teacher and for introducing me to the vast field of research.

I would like to thank Puja Dey and her family for being a huge support during my stay in Strasbourg. I am thankful to Rahul, Murali, Prasad, Jino, Dhanya, Deepak, Midhun, Ajin, Shaneesh and Jamsad for their support and friendship.

My deep thanks to my brother, sister-in-law and also to their lovely son for keeping me in good pace with their affection. Finally I would like to thank My mom and dad for their love, encouragement, prayers and for their faith in me. I thank The Almighty for helping me to go through all the hard times and making only good memories behind.

Meera Mohankumar Sreelatha

"Nothing in life is to be feared, it is only to be understood. Now is the time to understand more, so that we may fear less."

Marie Curie

Résumé en Français

Le travail réalisé au cours de cette thèse est centré sur la synthèse de composés de coordination dans le but de développer des composés possédants des propriétés de luminescence intéressantes, et d'élaborer des assemblages supramoléculaires pour l'obtention de matériaux originaux.

Chapitre 1.

L'élaboration de diodes électroluminescentes stables est un défi technologique majeur. La forte demande pour des écrans plats de grandes tailles ou pour des dispositifs d'éclairage consommant peu d'énergie motive la recherche dans ce domaine. Si les polymères conjugués organiques ont été les premiers matériaux utilisés pour l'élaboration de dispositifs électroluminescents, le problème majeur réside dans le fait que l'émission se fait à partir d'un état excité singulet n'offrant ainsi qu'une performance théorique maximale de 25%. Afin d'optimiser l'efficacité de ces systèmes et dépasser cette limite, le matériau photo-actif doit émettre à partir d'un état excité triplet. Dans ce cas, un rendement théorique de 100% est possible. L'un des enjeux actuels de cette technologie repose donc sur l'élaboration de nouveaux complexes de métaux de transition phosphorescents pour la production de lumière. Des complexes d'iridium, d'osmium, de ruthénium et de platine sont actuellement les plus utilisés. Cependant leur stabilité n'est pas toujours très bonne, leur prix est élevé et certains posent des problèmes environnementaux. Les complexes de cuivre ont été peu étudiés dans la perspective d'applications dans ce domaine. Ils représentent pourtant une alternative intéressante du fait du faible coût de ce métal et de sa faible toxicité. Ceci nous a conduit à nous intéresser à la préparation de nouveaux complexes cuivreux phosphorescents.

Chapitre 2.

Des complexes homoleptiques de Cu(I) préparés à partir de ligands P-N possèdent des propriétés de luminescence intéressantes, néanmoins ils sont peu stables en solution et

plusieurs espèces peuvent être en équilibre. C'est par exemple le cas des complexes cuivreux obtenus avec la 2-diphénylphosphinopyridine (dpPy). Afin de stabiliser cette famille de complexes du Cu(I), nous avons substitué le cycle pyridine du ligand par un groupement CH_3. La réaction de 2-diphenylphosphino-6-methylpyridine avec $[Cu(CH_3CN)_4]BF_4$ conduit bien à un seul un complexe de Cu(I) qui comporte 3 ligands, deux cations cuivreux et une molécule d'acétonitrile. Les groupements CH_3 permettent de masquer un des deux centres métalliques et ainsi d'empêcher les réactions avec des nucléophiles conduisant à la dissociation du ligand. Nous avons également montré que le ligand acétonitrile peut être échangé avec divers ligands R-CN ou Ph_3PO afin de moduler les propriétés photophysiques de ces complexes. Tous ces complexes sont stables en solution et à l'état solide et certain d'entre eux possèdent des rendements quantiques d'émission allant de 20 à 46%.

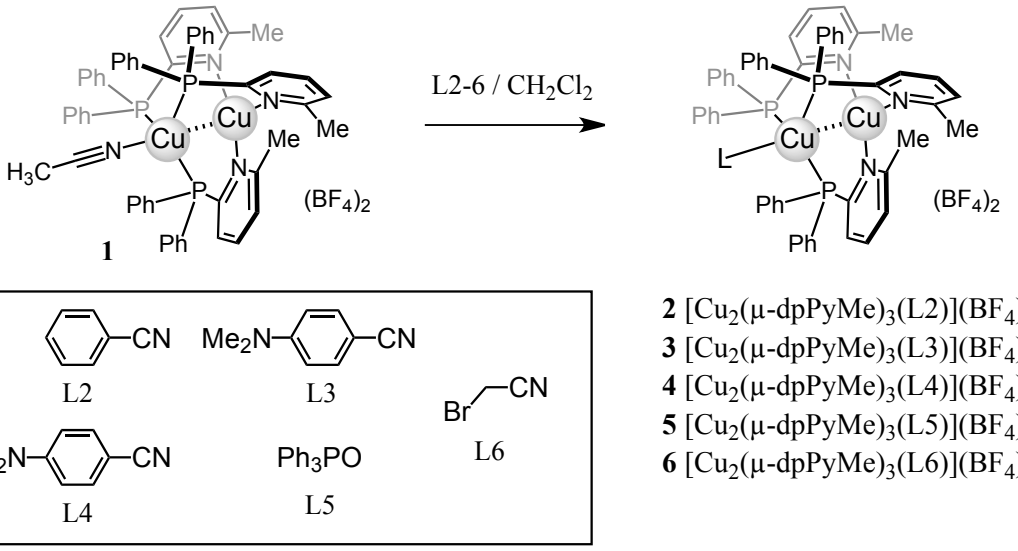

2 $[Cu_2(\mu\text{-dpPyMe})_3(L2)](BF_4)_2$
3 $[Cu_2(\mu\text{-dpPyMe})_3(L3)](BF_4)_2$
4 $[Cu_2(\mu\text{-dpPyMe})_3(L4)](BF_4)_2$
5 $[Cu_2(\mu\text{-dpPyMe})_3(L5)](BF_4)_2$
6 $[Cu_2(\mu\text{-dpPyMe})_3(L6)](BF_4)_2$

Chapitre 3.

Nous nous sommes également intéressés à des complexes hétéroleptiques du Cu(I) combinant des ligands bis-phosphines et phénanthrolies. De fait, McMillin et ses collaborateurs avaient élaboré des complexes hétéroleptiques de type $[Cu(POP)(NN)].BF_4$ (POP : bis[2-(diphénylphosphine)phényl]éther ; NN : dérivé de la 1,10-phénanthroline) fortement luminescents en solution. En nous inspirant de ces résultats, nous avons préparé de nombreux complexes analogues en faisant systématiquement varier la nature des ligands

phénanthrolines et bis-phosphines. Ces dérivés ont été obtenus en traitant un dérivé de la 1,10-phénanthroline (NN) avec un mélange équimolaire de $Cu(CH_3CN)_4BF_4$ et d'une bis-phosphine. Ces complexes hétéroleptiques ($[Cu(phen)(PP)]BF_4$) sont stables à l'état solide, cependant un équilibre entre complexes homoleptique et hétéroleptique est observé en solution dans un certain nombre de cas. Cet équilibre est lié à la stabilité thermodynamique exceptionnelle des complexes homoleptiques ($[Cu(PP)_2]^+$ et $[Cu(phen)_2]^+$).

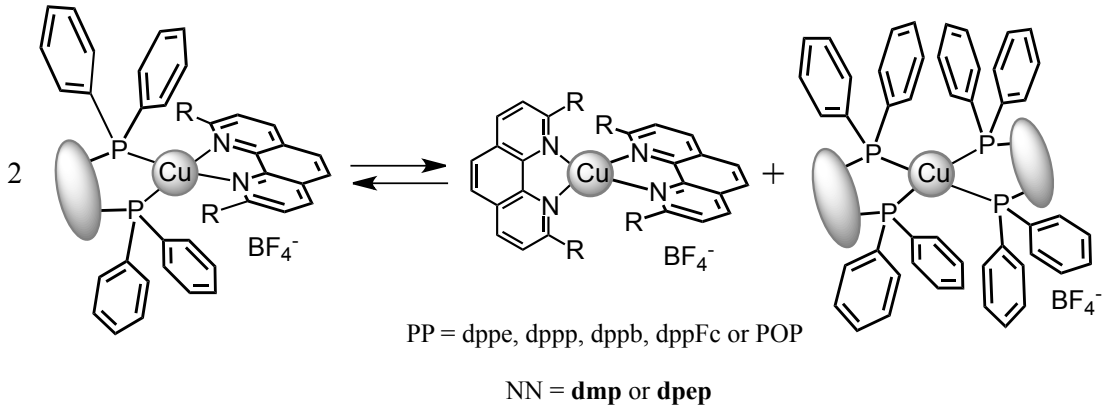

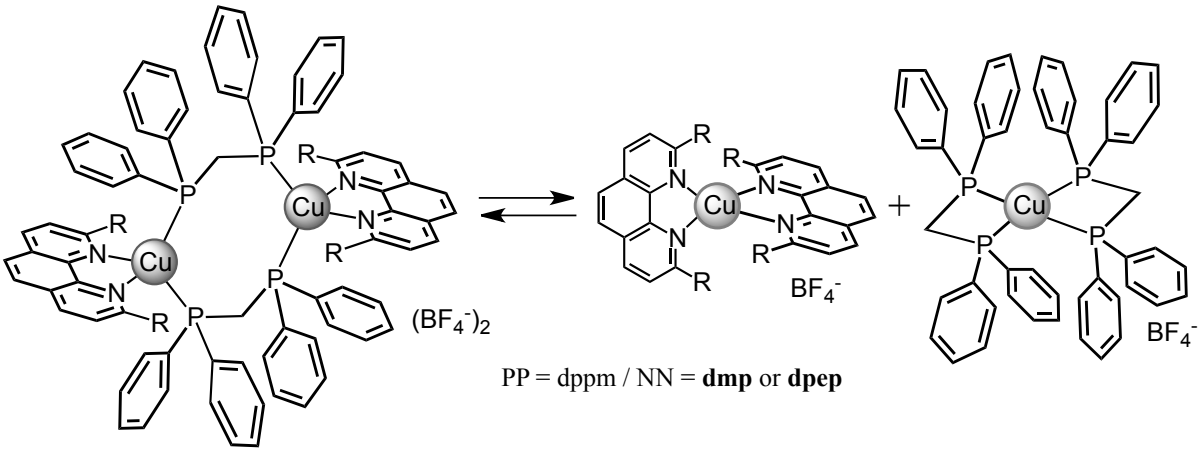

Chapitre 4.

La dernière partie de la thèse a été consacrée à l'élaboration d'une nouvelle stratégie permettant d'obtenir sélectivement des complexes hétéroleptiques. Afin d'empêcher la formation des complexes homoleptiques stables, les sous unités 1,10-phénanthrolines substituées en position 2 et 9 ont été incorporées dans des structures macrocycliques. Ainsi, les composés traités avec du Cu^I et un ligand bis-phosphine donnent exclusivement les

pseudo-rotaxanes correspondant. Ce travail a été réalisé en collaboration avec le Prof. Jean-Pierre Sauvage (ISIS, Strasbourg).

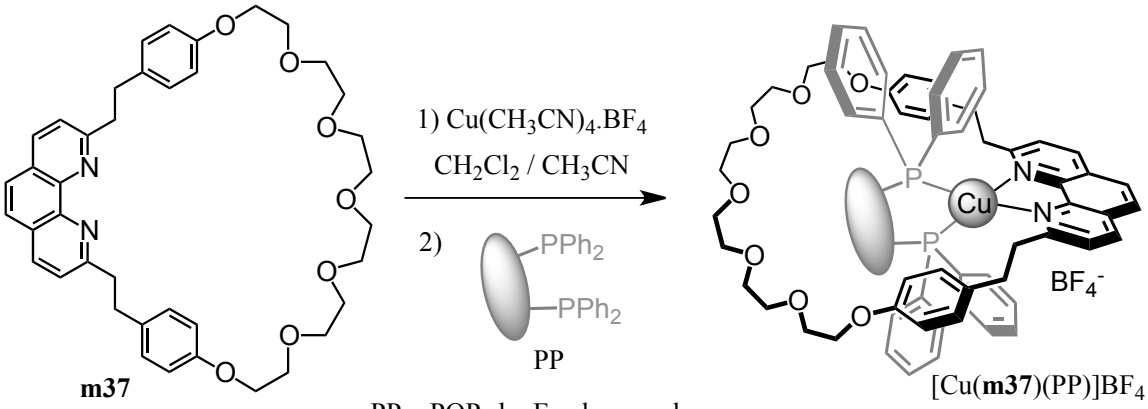

PP = POP, dppFc, dppe or dppp

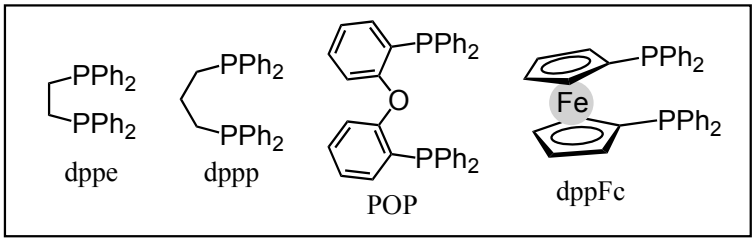

Table of content

CHAPTER 1

Introduction

The photophysical properties of coordination compounds displaying a metal-to-ligand charge transfer (MLCT) absorption have been intensively investigated since the 1960s.[1] In particular, compounds based on second and third row transition metals utilizing bi- or tri-dentate aromatic heterocyclic ligands have focused a major attention.[1-2] The classic example is $[Ru(bpy)_3]^{2+}$ (bpy: 2,2'-bipyridine).[1] This compound has highly desirable properties including microsecond lifetimes in fluid solution, intense visible absorption and emission, well defined redox chemistry, and high stability under many conditions.[1] All these characteristics make them attractive for the study of fundamental processes such as photoinduced energy- and electron-transfer under diffusional (bimolecular) conditions or within multicomponent supramolecular arrays.[1-2] Furthermore, practical devices based on Ru(II) polypyridyl derivatives now exist for solar energy conversion.[3] On the other hand, Ir(III) derivatives have been extensively investigated for applications in the field of light emitting diodes.[4] However, there are some potential drawbacks of Ru(II)- and Ir(III)-based devices, including high costs and environmental concerns. Existing alternatives, such as Re(I) and Os(II), have the same inherent limitations. It is therefore worthwhile to develop alternatives that circumvent these difficulties. In recent years, an attractive alternative has emerged in the form of Cu(I) coordination compounds.[5] Importantly, copper is less toxic, less expensive, and environmentally friendly when compared to ruthenium or iridium.

Cationic Cu(I) complexes show a very rich photophysical behavior. Among them, the most extensively investigated are $[Cu(NN)_2]^+$ and $[Cu(NN)(PP)]^+$ derivatives (where NN indicates a chelating imine ligand, typically 1,10-phenanthroline, and PP denotes two phosphine ligands or a bis-phosphine chelate).[5] The coordination behavior of Cu(I) is strictly related to its electronic configuration. The complete filling of *d* orbitals (d^{10} configuration) leads to a symmetric localization of the electronic charge. This situation favors a tetrahedral disposition of the ligands around the metal center in order to locate the coordinative sites far from one another and minimize electrostatic repulsions. Clearly, the complete filling of *d* orbitals prevents *d-d* metal-centered electronic transitions in Cu(I) compounds. On the contrary, such transitions are exhibited by d^9 Cu(II) complexes and cause relatively intense

absorption bands in the visible (VIS) spectral window.[5] The resulting excited states deactivate *via* ultrafast non-radiative processes making Cu(II) complexes far less interesting from the photophysical point of view.

A review of $[Cu(NN)_2]^+$ crystal structures show considerable deviation from the tetrahedral geometry.[6] Typically, $[Cu(NN)_2]^+$ complexes display distorted tetrahedral geometries and the two NN ligands are not in a perfect perpendicular arrangement. This flattening of the ligands lowers the symmetry from D_{2h} to D_2. Since the solid state structures are influenced by crystal packing forces, it might be expected that the solution geometry of $[Cu(NN)_2]^+$ is closer to tetrahedral. Indeed, their ^1H NMR spectra are sharp, with equivalent phenanthroline and substituent resonances on the NMR timescale at room temperature.[6]

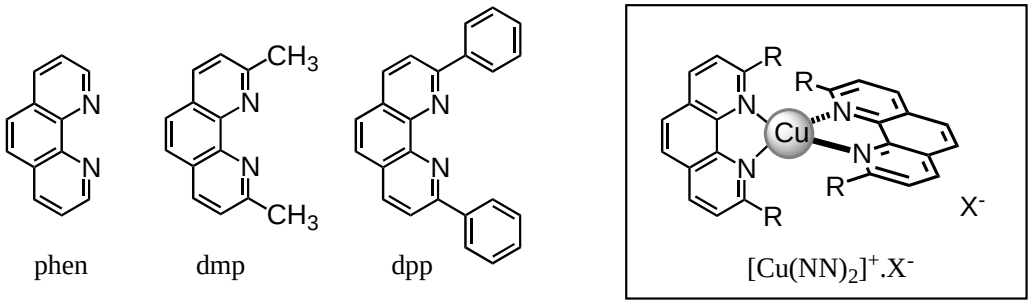

phen dmp dpp $[Cu(NN)_2]^+.X^-$

An interesting property inherent to copper coordination compounds is the structural difference between the Cu(I) and Cu(II) oxidation states.[5] Whereas Cu(I) generally prefers to be four-coordinate with a nearly tetrahedral geometry, Cu(II) adopts a Jahn–Teller distorted geometry that is usually 5- or 6-coordinate. This inner sphere reorganizational change has a dramatic influence on the Cu(II/I) redox chemistry and in the MLCT excited state behavior of $[Cu(NN)_2]^+$ derivatives. Crystal structures of Cu(II) bis-phenanthroline or bis-bipyridine compounds are numerous.[7] A large class of compounds of the general form $[Cu(NN)_2X]^{2+}$ are known, where X is a halide or counterion.[7] Examples where the fifth ligand is derived from solvent are also known, for example $[Cu(dmp)_2(H_2O)]^{2+}$ (dmp: 2,9-dimethyl-1,10-phenanthroline). When the 2,9-substituents of the phenanthroline ligand are large, coordination of a fifth ligand is not possible anymore. Indeed, crystal structures of both $[Cu(dpp)_2]^+$ and $[Cu(dpp)_2]^{2+}$ (dpp: 2,9-diphenyl-1,10-phenanthroline) shows both oxidation states to be four-coordinate in the solid state.[8]

Substituents in the 2- and 9-positions of 1,10-phenanthroline play an important role in the redox properties when coordinated to Cu(I). These substituents interact in a destabilizing manner with the 2- and 9-substituents of the opposite ligand in the Cu(II) state. As a result, this interaction dramatically stabilize the Cu(I) state. Electrochemically, it was effectively found that it is easier to oxidize $[Cu(phen)_2]^+$ than $[Cu(dmp)_2]^+$ (ΔE ~ 400 to 800 mV depending on the solvent).[5,9] This observation cannot be rationalized through inductive effects of the methyl groups or coordination number changes. Rather, it is most easily rationalized through steric effects, as the two dmp ligands can not achieve a high degree of planarity with respect to one another in the Cu(I) state. One interesting development in the electrochemistry of $[Cu(NN)_2]^+$ systems is related with molecular motions in multicomponent arrays where a coordinating ligand is kept free of coordination, but made available upon oxidation.[10] Sauvage and co-workers have demonstrated that in a suitably designed catenate, reversible molecular motions can be electrochemically induced by taking advantage of the different coordination environment of Cu(I) and Cu(II). This compound represents one of the very early examples of molecular machines.[11]

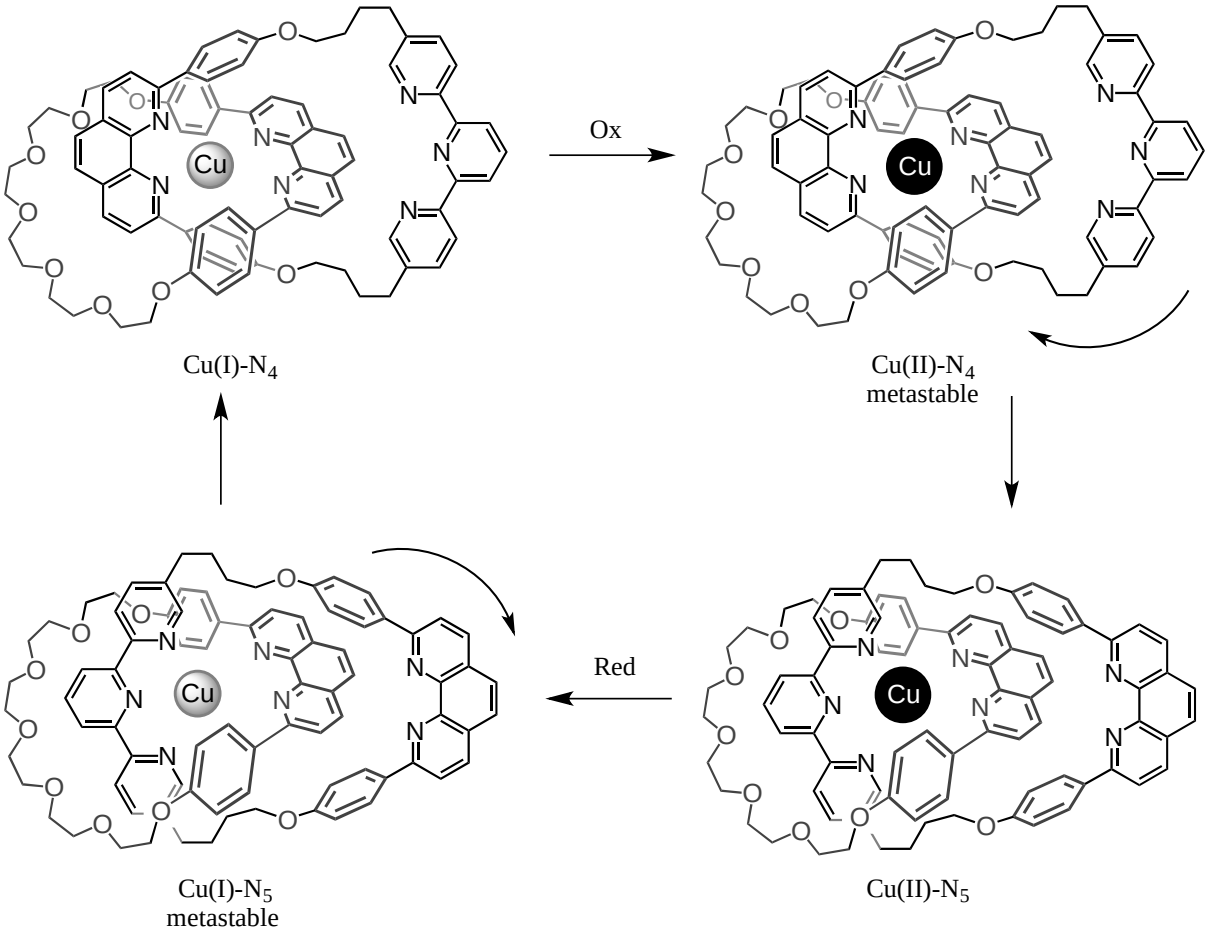

Upon light excitation followed by intersystem crossing (IC), the lowest ^{3}MLCT excited state is populated, thus the metal center changes its formal oxidation state from Cu(I) to Cu(II); the latter tends to assume a more flattened coordination geometry.[13] In this flattened structure a fifth coordination site is made available for the newly formed Cu(II), that can be attacked by nucleophilic species such as solvent molecules and counterions, leading to penta-coordinated excited complexes (exciplexes), that deactivate *via* non-emissive deactivation pathways.

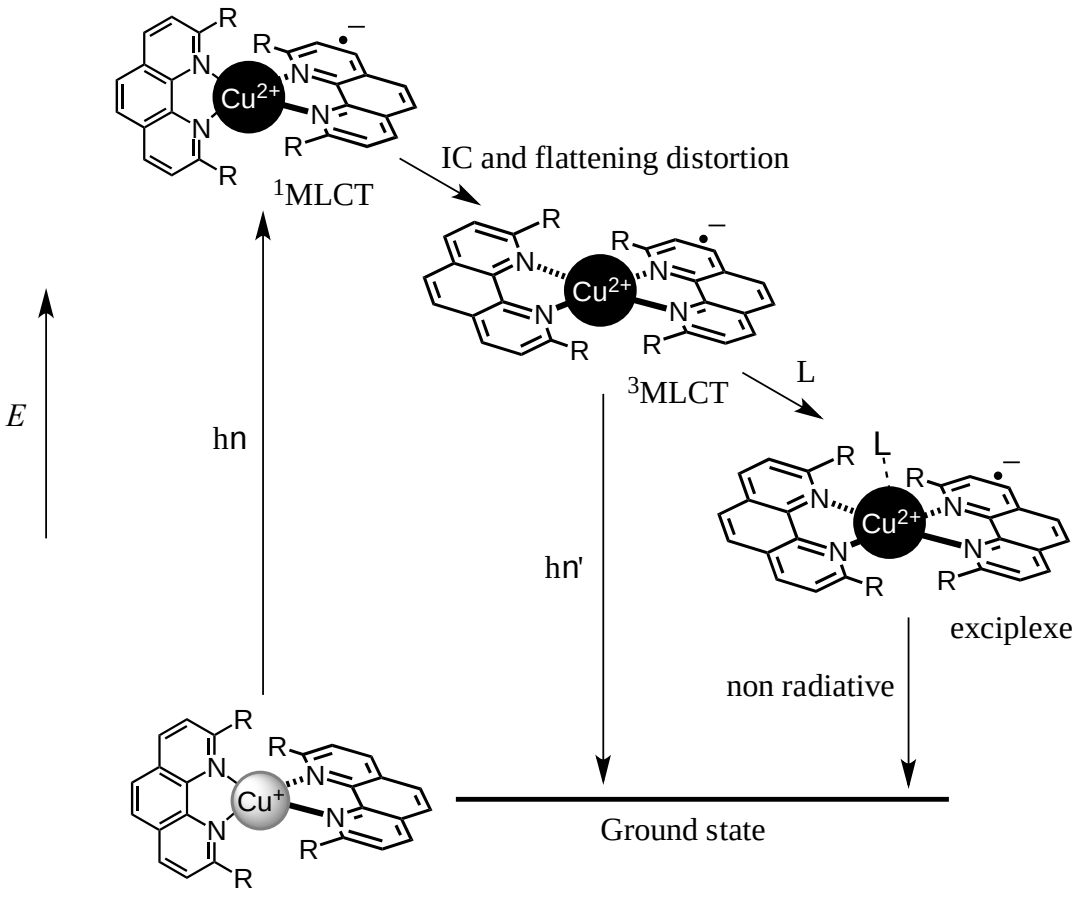

Direct spectroscopic evidence for these exciplexes is still lacking, however convincing clues for their formation have been given by McMillin and co-workers in a variety of investigations where the effect of the solvent, of the counterion, and of external molecules on the excited state lifetime of several $[Cu(NN)_2]^+$ have been examined.[13] Clearly, any factor which can limit the formation of the exciplexes is able to increase the luminescence quantum yield and excited state lifetime of Cu(I)–phenanthrolines. Practically, one can act on three factors: (i) solvent nature; (ii) chemical nature, size, and number of the substituents; (iii) type of counterion. In order to maximize the luminescence performances, poor donor solvents, large substituents (which physically prevent the undesired nucleophilic attack), and poor donor

counterions must be utilized. As a matter of fact, most of the photophysical investigations on copper phenanthrolines are reported in CH_2Cl_2, phenyl or long alkyl substituents are usually appended to the chelating unit, and BF_4^- or PF_6^- counterions are employed. In general, the emission quantum yields are low (< 0.1%) in solution and in the solid state at room temperature.[5] However, some complexes are strong emitters in rigid matrices at 77 K.[14] Very recently, it was successfully prepared the most sterically encumbered homoleptic Cu(I)-bisphenanthroline complex, $[Cu(dtbp)_2]^+$ (dtbp = 2,9-di-*tert*-butyl-1,10-phenanthroline), which exhibits the longest MLCT emission lifetime (τ = 3260 ns) and largest emission quantum yield (Φ = 5.6%) ever reported for a $[Cu(NN)_2]^+$ derivatives.[15] However, despite its outstanding photophysical properties, $[Cu(dtbp)_2]^+$ undergoes facile ligand replacement reactions, where one dtbp ligand is lost. Thus, this compound is not very stable in the presence of nucleophiles and coordinating solvents. Indeed, even weakly coordinating solvents such as acetone are capable of displacing one dtbp ligand.[15]

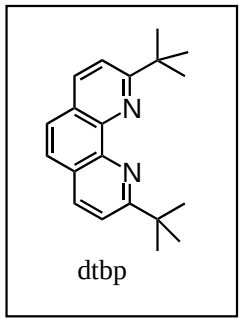

dtbp

In photochemistry, the *excited state* electrochemical potentials are also important parameters to quantify the 'abilities' of a given excited state. These quantities can be obtained from the *ground state* electrochemical potentials and the spectroscopic energy ($E^{\circ\circ}$, in eV units, to be considered divided by a unitary charge) related to the involved transition:[5]

$$E(A^+/{}^*A) = E(A^+/A) - E^{\circ\circ} \quad (1)$$

$$E({}^*A/A^-) = E(A/A^-) + E^{\circ\circ} \quad (2)$$

Hence the variation of the electron-donating or accepting capability of a given molecule A, upon light excitation, can be assessed. In eq. (1) and (2) *A denotes the lowest-lying electronically excited state; $E^{\circ\circ}$ can be estimated from emission spectra.[5] As expected, $*[Cu(NN)_2]^+$ is a better oxidant *and* reductant in the excited state than in the ground state. For example, $*[Cu(dpp)_2]+$ is a more powerful reductant than $*[Ru(bpy)_3]^{2+}$ [$E(A^+/A^*)$ = -1.11 and -0.85 V, respectively) owing to its more favorable ground state 2+/+ potential (+0.69 *vs*. +1.27 V), that largely compensates for the lower content of excited state energy (1.80 *vs*. 2.12 eV).[5,16] This peculiar property of $*[Cu(NN)_2]^+$ has been widely exploited for the preparation

of multicomponent molecular devices in which light-induced electron transfer could be evidenced.[17-18] As typical examples, fullerene-substituted $[Cu(NN)_2]^+$ derivatives have been prepared and investigated in details.[18] Upon excitation of the Cu(I)-complexed moiety and population of the related MLCT level, electron transfer to the fullerene subunit has been observed.

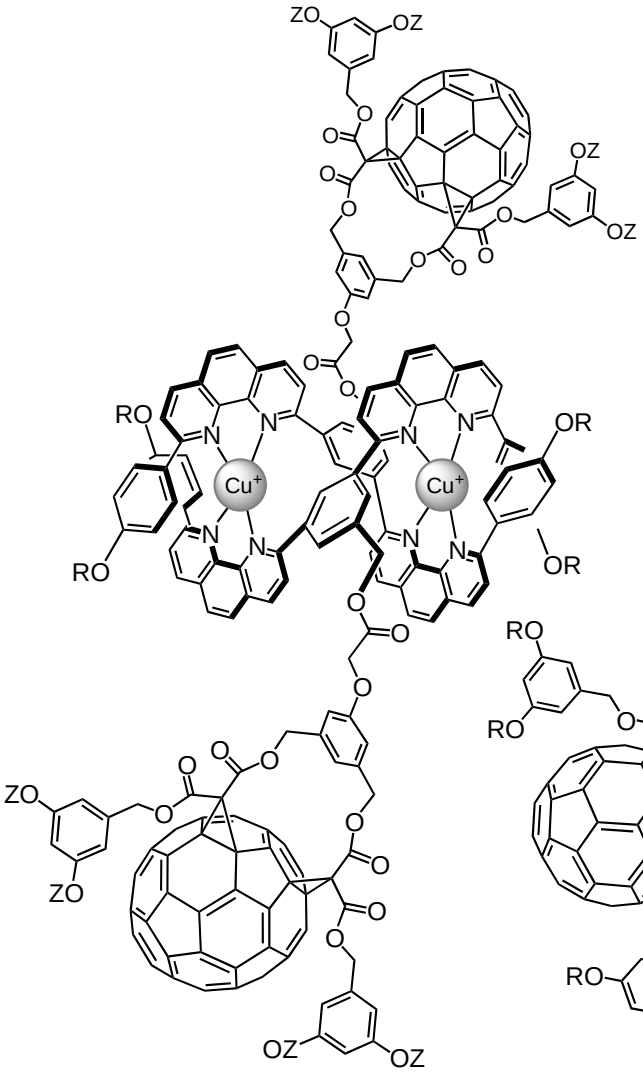

$[Cu_2(L1)_2]^{2+}$ Z = C_8H_{17}, R = $C_{12}H_{25}$

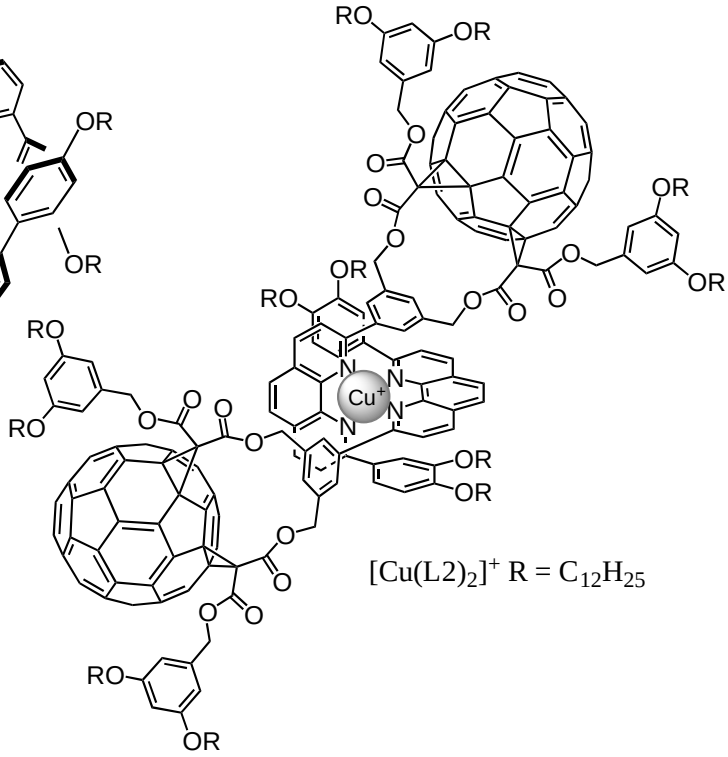

$[Cu(L2)_2]^+$ R = $C_{12}H_{25}$

Owing to their excited state redox potentials, $[Cu(NN)_2]^+$ derivatives are also suitable compounds for photovoltaic applications. The first example of dye-sensitized solar cell prepared from a $[Cu(NN)_2]^+$ derivative has been reported in 1994.[19] Research on solar cells was not particularly popular at that time and it is only recently that solar energy conversion

became a field of general interest.[20] In recent years, several reports on such applications with $[Cu(NN)_2]^+$ complexes have been published.[21]

A completely different approach to improve substantially the luminescence performance of Cu(I) complexes is that of using heteroleptic coordination with imine- and phosphine-type ligands.[22-28] Initially, such systems generally prepared with PPh_3 as the P-ligands looked promising because they exhibit long lifetimes in the solid state as well as in frozen solution.[22] They also display interesting photochemical properties in relation to light-induced electron transfer.[22] However, detailed studies have shown that exciplex quenching is important even for compounds incorporating bulky phosphines such as PPh_3.[23] Moreover, the speciation of these compounds was hard to control even in non-coordinating solvents such as CH_2Cl_2.[22] McMillin and co-workers have also reported mixed-ligand Cu(I) complexes prepared from 1,10-phenanthroline derivatives and bis[2-(diphenylphosphino)-phenyl]ether (POP).[24,25] Not only ligand dissociation is essentially suppressed for the complexes prepared from this particular chelating bis-phosphine ligand,[25] but these compounds are also characterized by remarkably high emission quantum yields from their long lived metal-to-ligand charge transfer (MLCT) excited state. Following this key finding, numerous examples of related heteroleptic Cu(I) complexes have been prepared from bis-phosphine and aromatic diimine ligands.[26,27] Their outstanding emission properties have been exploited to produce efficient light emitting devices thus showing that inexpensive and earth-abundant Cu(I) is an attractive alternative to noble metal ions for such applications.[28]

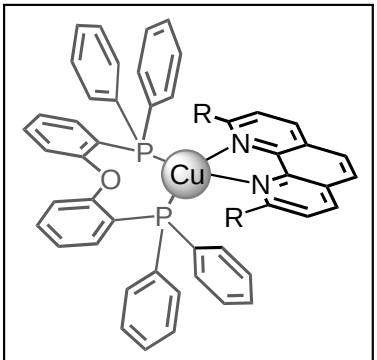

$[Cu(NN)(POP)]^+$

Unfortunately, $[Cu(NN)(PP)]^+$ complexes often exhibit poor stability in solution and are more difficult to handle. Preliminary investigations performed in our group have shown that $[Cu(NN)(PP)]^+$ complexes are stable in the solid state but equilibration between the heteroleptic complex and the corresponding homoleptic species is observed for most of them as soon as dissolved.[29] This equilibrium is affected by the nature of both NN and PP chelating ligands, however systematic studies have not been performed so far to elucidate the structural factors that influence the stability of the $[Cu(NN)(PP)]^+$ derivatives. *This is one of the*

objectives of the present PhD thesis (Chapter 3). The next challenge was then to develop a new strategy to stabilize [Cu(NN)(PP)]$^+$ complexes (Chapter 4).

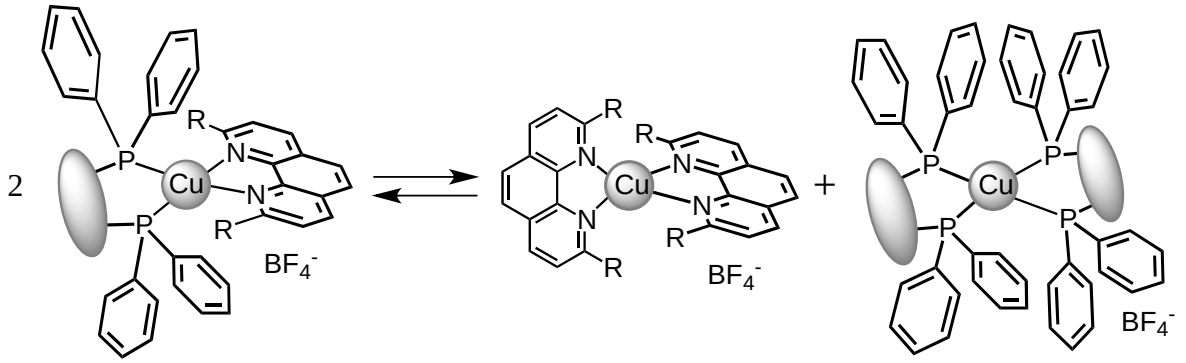

In order to prevent the equilibration between different species observed for [Cu(NN)(PP)]$^+$ derivatives, homoleptic complexes have been prepared from P,N-ligands. The [Cu(PN)$_2$]$^+$ derivatives prepared from 8-diphenylphosphinoquinolines[30] (dpqn and dpmqn) or 4-diphenylphosphino-1,5-naphthyridines[31] (dpnt and dpmnt) are stable in solution, however photophysical investigations revealed very low emission quantum yields for these compounds.

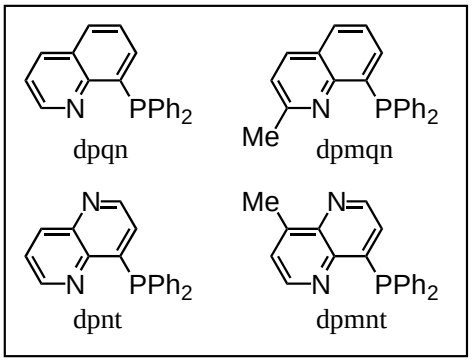

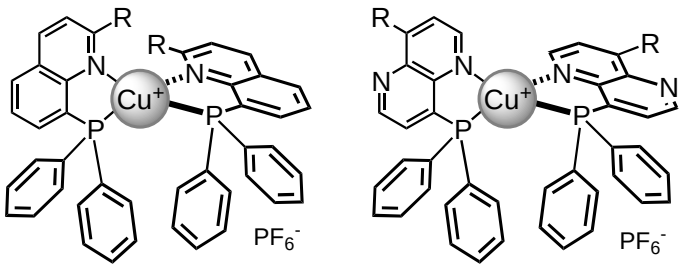

The combination of dpqn and dpmqn with a bis-phosphine ligand, namely POP, lead to interesting [Cu(PN)(PP)]$^+$ derivatives.[32] The X-ray crystal structures of both [Cu(PN)(PP)]$^+$ derivatives has been reported but their stability in solution is not commented.[32] In CH_2Cl_2, complexes [Cu(dpqn)(POP)]$^+$ and [Cu(dpmqn)(POP)]$^+$ emit with maximum at 642 nm and 608 nm, respectively. The introduction of methyl group on the quinoline group shifts the absorption and emission bands towards the blue, it also significantly increases the emission quantum yield from 0.0013 for [Cu(dpqn)(POP)]$^+$ to 0.012 for [Cu(dpmqn)(POP)]$^+$. The

reason for this can be explained by the steric effect of the CH_3 substituents in $[Cu(dpmqn)(POP)]^+$ preventing the excited state conformation changes from a tetrahedral to a flattened structure, which has a lower MLCT energy and a larger non-radiative rate constant. Whereas the emission quantum yields of both $[Cu(dpqn)(POP)]^+$ and $[Cu(dpmqn)(POP)]^+$ are modest in solution, these complexes are good emitters in the solid state. In a rigid PMMA matrix, relaxation caused by bond vibrations and rotations is restrained, leading to decrease in Stokes shift and increase in quantum yield and lifetime relative to those in solution. The quantum yield of 0.29 for $[Cu(dpmqn)(POP)]^+$ is remarkable but still smaller than that of 0.49 found for $[Cu(dmp)(POP)]^+$ under the same conditions.

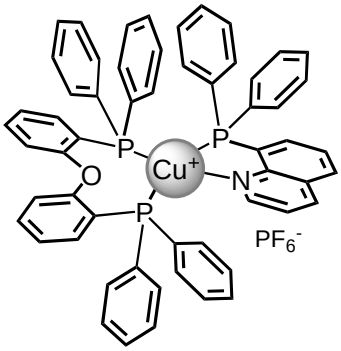

$[Cu(dpqn)(POP)](PF_6)$

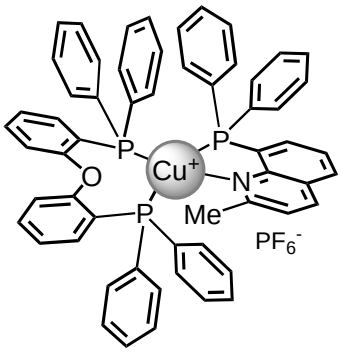

$[Cu(dpmqn)(POP)](PF_6)$

Phosphinediarylamido mononuclear and bis(phosphine)diarylamido dinuclear copper(I) complexes have been reported by Peters and co-workers.[33] These compounds are outstanding emitters both in solution and in the solid state.[33]

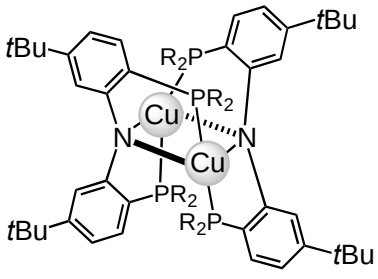

R = *i*Bu

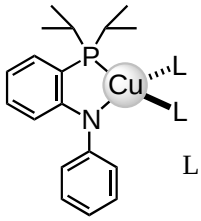

L = PPh_3 or dppe

The luminescence of these Cu(I) complexes arises from two excited states: a triplet and a singlet. Their excited singlet state is approximately 786 cm^{-1} above the triplet. At room

temperature, the levels are thermally equilibrated and emission from the singlet dominates. However the lifetime of the excited state remains long due to the equilibrium with the triplet level. In contrast, only emission from the triplet is observed at low temperature. The Stokes shift for these compounds is much smaller than those observed for classical Cu(I) phenanthroline complexes[33] and indicates less distortion in the excited state, thereby reducing non-radiative decay pathways.

The Cu(I) coordination chemistry of other P,N-ligands has been also investigated. Examples include 2-diphenylphosphino-pyridine (dpPy)[34] and 2-diphenylphosphino-1-methylimidazole (dpim).[35] These P,N-ligands are not chelates. They behave indeed as dinucleating bridging ligands. The outcome of the reactions depends on the ligand to Cu^{+} ratio and $[Cu_2(\mu\text{-}PN)_2]^{2+}$ and $[Cu_2(\mu\text{-}PN)_3]^{2+}$ have been reported. Whereas the Cu(I) complexes prepared from dpPy and dpim have been characterized in the solid state by X-ray crystal diffraction, solution studies revealed a equilibrium between several species. This has been particularly well investigated in the case of dpPy. Two isomeric forms of $[Cu_2(\mu\text{-}dpPy)_3]^{2+}$ differing from the relative orientation of the three bridging dpPy ligands can be obtained in the solid state depending on the crystallization conditions. The head-to-tail isomer is obtained when CH_3CN/Et_2O[34] and $CH_2Cl_2/EtOH$[34] are used for the recrystallization. In contrast, the head-to-head derivative crystallizes preferentially from $CH_2Cl_2/MeOH$.[34] In solution ligand association/dissociation take place and the distribution of complexes is profoundly affected by the nature of the solvent. Interesting emission properties in the solid state have been described qualitatively[34] for both isomeric forms of $[Cu_2(\mu\text{-}dpPy)_3]^{2+}$ but no quantitative data have been reported so far.

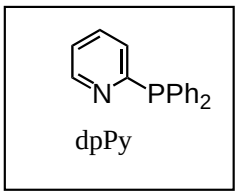

dpPy

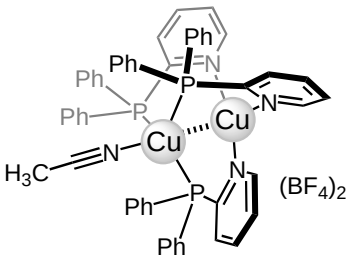

Head-to-Head

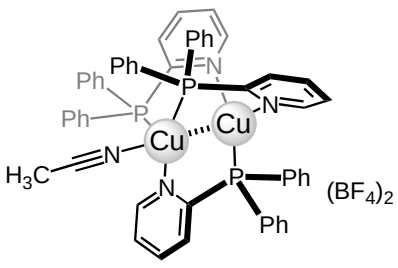

Head-to-Tail

As part of this research on Cu(I) derivatives prepared from P,N-ligands, we became interested in exploring in details the coordination chemistry of 2-diphenylphosphino-6-

methylpyridine (dpPyMe) with Cu(I) cations (Chapter 2). The additional methyl group in the P,N-ligand is expected to play an important role in the isomer distribution observed for $[Cu_2(\mu\text{-}dpPy)_3]^{2+}$*. At the same time, favorable steric factors may limit distortion in the excited state and high emission quantum yields can be expected.*

$[Cu(PP)_2]^+$ complexes obtained from bis-phosphine ligands have also been described.[36-37] Whereas these compounds have been generally prepared in the context of systematic structural studies to understand the coordination chemistry of PP ligands,[36] only a few reports describe their electronic properties.[37] The emission of $[Cu(dppb)_2]^+$ has been tentatively assigned to metal-to-ligand charge transfer (MLCT) excited states. Whereas the emission quantum yield of this compound is quite low in solution (0.0001%), it exhibits a bright luminescence in the solid state at room temperature as well as in rigid frozen CH_2Cl_2 solutions at 77 K. Indeed, under these conditions, geometric distorsions prompting non-radiative deactivation of the MLCT excited states are prevented. Complex $[Cu(dppb)_2]^+$ has been used for light emitting device fabrication. The electroluminescence spectra are red shifted and significantly broader when compared to the photoluminescence spectra recorded in CH_2Cl_2 solutions. As a result almost white light is produced by the device.[36]

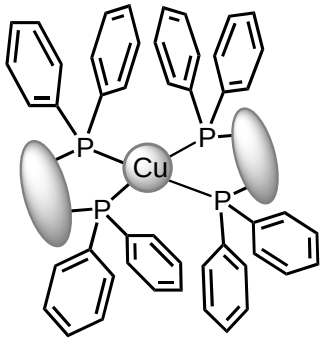

$[Cu(PP)_2]^+$

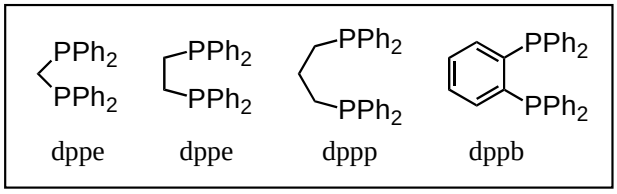

In conclusion of this literature survey on cationic Cu(I) complexes,[38] it appears that the rationalization of their electronic properties has made considerable progress in recent years. Additionally, efficient synthetic protocols have been reported and a wide range of Cu(I)-based structures synthesized. However, even if thermodynamically stable, Cu(I) complexes are also characterized by a kinetic instability and ligand exchange reactions are often observed in solution.[39] This is in particular the case for dinuclear Cu(I) complexes obtained from

dinucleating P,N-ligands as well as for heteroleptic $[Cu(NN)(PP)]^+$ derivatives. Despite remarkable luminescent properties, this equilibration between several species represents a major limitation for their applications. *The main goal of the present PhD thesis is to develop the appropriate ligand design principles to prevent the formation of several species in equilibrium. In the case of dinucleating P,N-ligands, the proposed strategy is based on the use of a ligand with additional substituents to shield the metal centers and thus to prevent nucleophilic attacks leading to ligand dissociation. In the case of the* $[Cu(NN)(PP)]^+$ *derivatives, the proposed synthetic strategy relies on the use of macrocyclic phenanthroline ligands preventing the formation of the corresponding homoleptic* $[Cu(NN)_2]^+$.

References

1) T. J. Meyer, *Pure Appl. Chem.* **1986**, *58*, 1193; A. Juris, V. Balzani, F. Barigelletti, S. Campagna, P. Belser, A. von Zelewsky, *Coord. Chem. Rev.* **1988**, *84*, 85.

2) V. Balzani, A. Juris, M. Venturi, S. Campagna and S. Serroni, *Chem. Rev.* **1996**, *96*, 759; J.-P. sauvage, J.-P. Collin, J.-C. Chambron, S. Guillerez, C. Coudret, V. Balzani, F. Barigelletti, L. de Cola, L. Flamigni, *Chem. Rev*. **1994**, *94*, 993.

3) A. Hagfeldt, M. Grätzel, *Acc. Chem. Res*. **2000**, *33*, 269.

4) M. G. Harrison, R. H. Friend, in *Electronic Materials: the Oligomer Approach* (K. Müllen and G. Wegner, Eds.), Wiley-VCH, **1998**, p. 515-558; K. Müllen, U. Scherf (Eds.), *Organic Light Emitting Devices*, Wiley-VCH, **2005**; E. Holder, B. M. W. Langeveld, U. S. Schubert, *Adv. Mater*. **2005**, *17*, 1109; P.-T. Chou, Y. Chi, *Chem. Eur. J*. **2007**, *13*, 380.

5) D. V. Scaltrito, D. W. Thompson, J. A. O'Callaghan, G. J. Meyer, *Coord. Chem. Rev*. **2000**, *208*, 243; N. Armaroli, *Chem. Soc. Rev*. **2001**, *30*, 113; N. Armaroli, G. Accorsi, F. Cardinali, A. Lisorti, *Top. Curr. Chem*. **2007**, *280*, 69; A. Lavie-Cambot, M. Cantuel, Y. Leydet, G. Jonusauskas, D. M. Bassani, N. D. McClenaghan, *Coord. Chem Rev*. **2008**, *252*, 2572.

6) P. J. Burke, D. R. McMillin, W. R. Robinson, *Inorg. Chem.* **1980**, *19*, 1211; R. Hamalainen, M. Ahlgren, U. Terpeinen, T. Raikas, *Cryst. Struct. Commun*. **1979**, *8*, 75; P. J. Burke, K. Henrick, D. R. McMillin, *Inorg. Chem.* **1982**, *21*, 1881; F. K. Klemens, C. E. Palmer, S. M. Rolland, P. E. Fanwick, D. R. McMillin, J.-P. Sauvage, *New J. Chem*. **1990**, *14*, 129; A. J. Pallenberg, K. S. Koenig, D. M. Barnhart, *Inorg. Chem*. 1995, 34, 2833; E. Gumienna-Kontecka, Y. Rio, C. Bourgogne, M. Elhabiri, R. Louis, A.-M. Albrecht-Gary, J.-F. Nierengarten, *Inorg. Chem*. **2004**, *43*, 3200; G. Accorsi, N. Armaroli, C. Duhayon, Alix Saquet, B. Delavaux-Nicot, R. Welter, O. Moudam, M. Holler, J.-F. Nierengarten, *Eur. J. Inorg. Chem*. **2010**, 164.

7) F. S. Stephens, P. A. Tucker, *J. Chem. Soc., Dalton Trans*. 1973, 2293; F. S. Stephens, *J. Chem. Soc., Dalton Trans*. **1972**, 1350; J. Kaiser, G. Brauer, F. A. Schroder, I. F. Taylor, S. E. Rasmussen, *J. Chem. Soc., Dalton Trans*. **1974**, 1490; W. D. Harrison, D. M. Kennedy, M. Power, R. Sheahan, B. J. Hathaway, *J. Chem. Soc., Dalton Trans*. **1981**, 1556; W. D. Harrison, B. J. Hathaway, D. Kennedy, *Acta Crystallogr., Sect. B*

1979, *35*, 2301; W. D. Harrison, B. J. Hathaway, *Acta Crystallogr., Sect. B* **1979**, *35*, 2910; R. J. Fereday, P. Hodgson, S. Tyagi, B. J. Hathaway, *J. Chem. Soc., Dalton Trans*. **1981**, 2070; O. P. Anderson, *Inorg. Chem*. **1975**, *14*, 730; D. Tran, B. W. Skelton, A. H. White, L. E. Laverman, P. C. Ford, *Inorg. Chem*. **1998**, *37*, 2505.

8) M. T. Miller, P. K. Gantzel, T. B. Karpishin, *Inorg. Chem*. **1998**, *37*, 2285.

9) B. R. James, J. P. Williams, *J. Chem. Soc*. **1961**, 2007; M. Ruthkosky, F. N. Castellano, G. J. Meyer, *Inorg. Chem*. **1996**, *35*, 6406; Y. Rio, G. Accorsi, N. Armaroli, D. Felder, E. Levillain, J.-F. Nierengarten, *Chem. Commun.* **2002**, 2830.

10) A. Livoreil, C. O. Dietrich-Buchecker, J.-P. Sauvage, *J. Am. Chem. Soc.* **1994**, *116*, 9399; A. Livoreil, J.-P. Sauvage, N. Armaroli, V. Balzani, L. Flamigni, B. Ventura, *J. Am. Chem. Soc.* **1997**, *119*, 12114; N. Armaroli, V. Balzani, J.-P. Collin, P. Gaviña, J.-P. Sauvage, B. Ventura, *J. Am. Chem. Soc.* **1999**, *121*, 4397.

11) For selected reviews, see: J.-P. Sauvage, *Acc. Chem. Res*., **1998**, *31*, 611; V. Balzani, M. Gomez-Lopez, J. F. Stoddart, *Acc. Chem. Res*. **1998**, *31*, 405; J.-P. Collin, C. Dietrich-Buchecker, P. Gavina, M. C. Jimenez-Molero, J.-P. Sauvage, *Acc. Chem. Res*. **2001**, *34*, 477; B. L. Feringa, *Acc. Chem. Res*., **2001**, *34*, 504; A. Harada, *Acc. Chem. Res*. **2001**, *34*, 456; C. S. Schalley, K. Beizai, F. Vögtle, *Acc. Chem. Res.* **2001**, *34*, 465; M. C. Jimenez-Molero, C. Dietrich-Buchecker, J.-P. Sauvage, *Chem. Commun*. **2003**, 1613; S. Saha, J. F. Stoddart, *Chem. Soc. Rev*. **2007**, *36*, 77; B. Champin, P. Mobian, J.-P. Sauvage, *Chem. Soc. Rev.* **2007**, *36*, 358; J. F. Stoddart, *Chem. Soc. Rev*. **2009**, *38*, 1802; J. D. Crowley, S. M. Goldup, A.-L. Lee, D. A. Leigh, R. T. McBurney, *Chem. Soc. Rev.* **2009**, *38*, 1530; S. Durot, F. Reviriego, J.-P. Sauvage, *Dalton Trans*. **2010**, *39*, 10557; R. S. Forgan, J.-P. Sauvage, J. F. Stoddart, *Chem. Rev*. **2011**, *111*, 5434; A. Coskun, M. Banaszak, R. D. Astumian, J. F. Stoddart, B. A. Grzybowski, *Chem. Soc. Rev*. **2012**, *41*, 19; A. C. Fahrenbach, C. J. Bruns, D. Cao, J. F. Stoddart, *Acc. Chem. Res*. **2012**, *45*, 1581.

12) M. T. Miller, P. K. Gantzel, T. B. Karpishin, *Inorg. Chem.* **1998**, *37*, 2285.

13) C. C. Phifer, D. R. McMillin, *Inorg. Chem.* **1986**, *25*, 1329; A. K. Ichinaga, J. R. Kirchhoff, D. R. McMillin, C. O. Dietrich-Buchecker, P. A. Marnot, J.-P. Sauvage, *Inorg. Chem.* **1987**, *26*, 4290; R. M. Everly and D. R. McMillin, *J. Phys. Chem.* **1991**, *95*, 9071; C. T. Cunningham, K. L. H. Cunningham, J. F. Michalec, D. R. McMillin, *Inorg. Chem.* **1999**, ***38***, 4388; M. T. Miller, P. K. Gantzel, T. B. Karpishin, *Inorg. Chem.* **1999**, *38*, 3414; M. T. Miller, T. B. Karpishin, *Inorg. Chem.* **1999**, *38*, 5246; M.

W. Blaskie, D. R. McMillin, *Inorg. Chem.* **1980**, *19*, 3519; R. M. Everly, D. R. McMillin, *Photochem. Photobiol.* **1989**, *6*, 711.

14) D. Felder, J.-F. Nierengarten, F. Barigelletti, B. Ventura, N. Armaroli, *J. Am. Chem. Soc.* **2001**, *123*, 6291; T. Gunaratne, M. A. J. Rodgers, D. Felder, J.-F. Nierengarten, G. Accorsi, N. Armaroli, *Chem. Commun*. **2003**, 3010.

15) O. Green, B. A. Gandhi, J. N. Burstyn, *Inorg. Chem.* **2009**, *48*, 5704.

16) P. Federlin, J.-M. Kern, A. Rastegar, C. O. Dietrich-Buchecker, P. A. Marnot, J.-P. Sauvage, *New J. Chem.* **1990**, *14*, 9.

17) J.-C. Chambron, A. Harriman, V. Heitz, J.-P. Sauvage, *J. Am. Chem. Soc*. **1993**, *115*, 6109; N. Armaroli, V. Balzani, F. Barigelletti, L. De Cola, L. Flamigni, J.-P. Sauvage, C. Hemmert, *J. Am. Chem. Soc.* **1994**, *116*, 5211; N. Armaroli, V. Balzani, L. De Cola, C. Hemmert, J.-P. Sauvage, *New J. Chem.* **1994**, *18*, 775; C. O. Dietrich-Buchecker, J.-P. Sauvage, N. Armaroli, P. Ceroni, V. Balzani, *Angew. Chem. Int. Ed. Engl.* **1996**, *35*, 1119; N. Armaroli, F. Diederich, C. O. Dietrich-Buchecker, L. Flamigni, G. Marconi, J.-F. Nierengarten, J.-P. Sauvage, *Chem. Eur. J.*, **1998**, *4*, 406; N. Armaroli, C. Boudon, D. Felder, J.-P. Gisselbrecht, M. Gross, G. Marconi, J.-F. Nicoud, J.-F. Nierengarten, V. Vicinelli, *Angew. Chem. Int. Ed. Engl.* **1999**, *38*, 3730; D. J. Cárdenas, J.-P. Collin, P. Gaviña, J.-P. Sauvage, A. De Cian, J. Fischer, N. Armaroli, L. Flamigni, V. Vicinelli, V. Balzani, *J. Am. Chem. Soc.* **1999**, *121*, 5481; N. Armaroli, G. Accorsi, J.-P. Gisselbrecht, M. Gross, J.-F. Eckert, J.-F. Nierengarten, *New J. Chem*. **2003**, *27*, 1470

18) Y. Rio, G. Enderlin, C. Bourgogne, J.-F. Nierengarten, J.-P. Gisselbrecht, M. Gross, G. Accorsi, N. Armaroli, *Inorg. Chem*. **2003**, *42*, 8783; F. Cardinali, H. Mamlouk, Y. Rio, N. Armaroli, J.-F. Nierengarten, *Chem. Commun*. **2004**, 1582; M. Holler, F. Cardinali, H. Mamlouk, J.-F. Nierengarten, J.-P. Gisselbrecht, M. Gross, Y. Rio, F. Barigelletti, N. Armaroli, *Tetrahedron* **2006**, *62*, 2060.

19) N. Alonso-Vante, J.-F. Nierengarten, J.-P. Sauvage, *J. Chem. Soc., Dalton Trans.* **1994**, 1649.

20) M. Grätzel, *Acc. Chem. Res*. **2009**, *42*, 1788.

21) T. Bessho, E. C. Constable, M. Grätzel, A. H. Redondo, C. E. Housecroft, W. Kylberg, M. K. Nazeeruddin, M. Neuburger, S. Schaffner, *Chem. Commun.* **2008**, 3717; C. L. Linfoot, P. Richardson, T. E. Hewat, O. Moudam, M. M. Forde, A. Collins, F. White, N. Robertson, *Dalton Trans*. **2010**, *39*, 8945.

22) M. T. Buckner, T. G. Matthews, F. E. Lytle, D. R. McMillin, J. Am. Chem. Soc. **1979**, *101*, 5846; R. A. Rader; D. R. McMillin, M. T. Buckner, T. G. Matthews, D. J. Casadonte, R. K. Lengel, S. B. Whittaker, L. M. Darmon, F. E. Lytle, *J. Am. Chem. Soc*. **1981**, *103*, 5906; A. A. Del Paggio, D. R. McMillin, *Inorg. Chem*. **1983**, *22*, 691; J. R. Kirchhoff, D. R. McMillin, W. R. Robinson, D. R. Powell, A. T. McKenzie, S. Chen, *Inorg. Chem*. **1985**, *24*, 3928; D. J. Casadonte, D. R. McMillin, *Inorg. Chem*. **1987**, *26*, 3950; C. E. A. Palmer, D. R. McMillin, *Inorg. Chem*. **1987**, *26*, 3837.

23) S. Sakaki, G. Koga, K. Ohkubo, *Inorg. Chem*. **1986**, *25*, 2330; S. Sakaki, G. Koga, S. Hinokuma, S. Hashimoto, K. Ohkubo, *Inorg. Chem*. **1987**, *26*, 1817.

24) D. G. Cuttell, S.-M. Kuang, P. E. Fanwick, D. R. McMillin, R. A. Walton, *J. Am. Chem. Soc*. **2002**, *124*, 6.

25) S.-M. Kuang, D. G. Cuttell, D. R. McMillin, P. E. Fanwick, R. A. Walton, *Inorg. Chem*. **2002**, *41*, 3313.

26) P. Coppens, *Chem. Commun*. **2003**, 1317; P. Coppens, I. I. Vorontsov, T. Graber, A Y. Kovalevsky, Y.-S. Chen, G. Wu, M. Gembicky, I. V. Novozhilova, *J. Am. Chem. Soc.* **2004**, *126*, 5980; K. Saito, T. Arai, N. Takahashi, T. Tsukuda, T. Tsubomura, *Dalton Trans*. **2006**, 4444.

27) N. Armaroli, G. Accorsi, G. Bergamini, P. Ceroni, M. Holler, O. Moudam, C. Duhayon, B. Delavaux-Nicot, J.-F. Nierengarten, *Inorg. Chim. Acta* **2007**, *360*, 1032; R. D. Costa, D. Tordera, E. Orti, H. Bolink, J. Schönle, S. Graber, C. E. Housecroft, E. C. Constable, J. A. Zampese, *J. Mater. Chem.* **2011**, *21*, 16108; T. MacCormick, W.-L. Jia, S. Wang, *Inorg. Chem*. **2006**, *45*, 147; H. Ge, W. Wei, P. Shuai, G. Lei, S. Qing, *J. Lumin.* **2011**, *131*, 238.

28) Q. Zhang, Q. Zhou, Y. Cheng, L. Wang, D. Ma, X. Jing, F. Wang, *Adv. Mater*. **2004**, *16*, 432-436; N. Armaroli, G. Accorsi, M. Holler, O. Moudam, J.-F. Nierengarten, Z. Zhou, R. T. Wegh, R. Welter, *Adv. Mater*. **2006**, *18*, 1313; Q. Zhang, Q. Zhou, Y. Cheng, L. Wang, D. Ma, X. Jing, F. Wang, *Adv. Funct. Mater.* **2006**, *16*, 1203.

29) O. Moudan, PhD thesis, University of Toulouse, **2007**.

30) T. Tsukada, C. Nishigata, K. Arai, T. Tsabomura, *Polyhedron* **2009**, *28*, 7.

31) C. Chen, K. Wang, P. Jiang, G. Song, H. Zhu, *Inorg. Chem. Commun*. **2012**, *17*, 116.

32) L. Qin, Q. Zhang, W. Sun, J. Wang, C. Lu, Y. Cheng, L. Wang, *Dalton Trans*. **2009**, 9388.

33) S. B. Harkins, J. C. Peters, *J. Am. Chem. Soc.* **2005**, *127*, 2030; A. J. M. Miller, J. L. Dempsey, J. C. Peters, *Inorg. Chem.* **2007**, *46*, 7244; J. C. Deaton, S. C. Switalski, D. Y. Kondakov, R. H. Young, T. D. Pawlik, D. J. Giesen, S. B. Harkins, A. J. M. Miller, S. F. Mickenberg, J. C. Peters, *J. Am. Chem. Soc*. **2010**, *132*, 9499.

34) E. Lastra, M. P. Gamasa, J. Gimeno, M. Lanfranchi, A. Tiripicchio, *J. Chem. Soc., Dalton Trans*. **1989**, 1499; J. S. Field, R. J. Haines, B. Warwick, M. M. Zulu, Polyhedron **1996**, *15*, 3741; A. Bakhoda, N. Safari, V. Amani, H. R. Khavasi, M. Gheidi, *Polyhedron* **2011**, *30*, 2950; Y.-J. Li, Z.-Y. Deng, X.-F. Xu, H.-B. Wu, Z.-X. Cao, Q.-M. Wang, *Chem. Commun*. **2011**, *47*, 9179; M. Maekawa, M. Munakata, S. Kitagawa, T. Yonazawa, *Bull. Chem. Soc. Jpn*. **1991**, *64*, 2286.

35) M. A. Jalil, T. Yamada, S. Fujinami, T. Honjo, H. Nishikawa, *Polyhedron* **2001**, *20*, 627.

36) P. Comba, C. Katsichtis, B. Nuber, H. Pritzkow, *Eur. J. Inorg. Chem*. **1999**, 777; J. R. Black, W. Levason, M. D. Spicer, M. Webster, *J. Chem. Soc., Dalton Trans.* **1993**, 3129; S. Kitagawa, M. Kondo, S. Kawata, S. Wada, M. Maekawa, M. Munakata, *Inorg. Chem*. **1995**, *34*, 1455; E. Szlyk, R. Kucharek, I. Szymanska, L. Pazderski, *Polyhedron* **2003**, *22*, 3389.

37) O. Moudam, A. Kaeser, B. Delavaux-Nicot, C. Duhayon, M. Holler, G. Accorsi, N. Armaroli, I. Séguy, J. Navarro, P. Destruel, J.-F. Nierengarten, *Chem. Commun*. **2007**, 3077.

38) Cationic Cu(I) complexes have been described in this section, it can be however noted that cluster compounds obtained from cuprous halide and various ligands present also interesting emission properties, see: C. L. Raston, A, H White, J. Chem. Soc., Dalton Trans. **1976**, 21, 2153; M. Vitale, P. C. Ford *Coord. Chem. Rev*. **2001**, *219*, 3; K. R. Kyle, C. K. Ryu, J. A. DiBenedetto, P. C. Ford, *J. Am. Chem. Soc*. **1991**, *113*, 2954; H. Araki, K. Tsuge, Y. Sasaki, S. Ishizaka, N. Kitamura, *Inorg. Chem*. **2005**, *44*, 9667.

39) E. Riesgo, Y.-Z. Hu, F. Bouvier, R. P. Thummel, *Inorg. Chem*. **2001**, *40*, 2541; I. Pianet, J.-M. Vincent, *Inorg. Chem*. **2004**, *43*, 2947; V. Hebbe-Viton, V. Desvergnes, J. J. Jodry, C. Dietrich-Buchecker, J.-P. Sauvage, J. Lacour, *Dalton Trans*. **2006**, 2058.

CHAPTER 1

Dinuclear Cu(I) Complexes Prepared From 2-Diphenylphosphino-6-Methylpyridine

1. Introduction

The design and the synthesis of P,N-ligands have focused enormous attention.[1-3] The interest in such ligands results mainly from their electronic asymmetry leading to coordination compounds perfectly suited for applications in catalysis.[1] The π-acceptor character of the phosphorus stabilizes metal centers in low oxidation states, while the nitrogen σ-donor facilitates oxidative addition reactions on the metallic center. The nitrogen donor is also often weakly coordinated to soft metal centers and thus easily provides open coordination sites.[1] The combination of these factors with specific steric effects has been often exploited in asymmetric catalysis, indeed numerous examples of optically pure P,N-ligands have been developed for such purposes.[1] Whereas catalytic systems based on P,N-ligands have been intensively investigated, such ligands have been by far less explored for the development of supramolecular assemblies[4] and phosphorescent materials.[5-7] The coordination chemistry of P,N-ligands is complicated and mixtures of complexes in equilibrium are sometimes obtained in solution.[3] It is likely that these considerations may have hampered interest in projects directed towards the preparation of luminescent metal complexes from P,N-ligands. In addition, the very low emission quantum yields described for Cu(I) complexes prepared from 8-diphenylphosphinoquinoline[8] or 4-diphenylphosphino-1,5-naphthyridine[9] ligands were not particularly encouraging. A few recent reports revealed however spectacular emission quantum yields for coordination compounds based on P,N-ligands.[6-7] Among them, the phosphinediarylamido mononuclear and bis(phosphine)diarylamido dinuclear copper(I) complexes reported by Peters and co-workers are outstanding emitters both in solution and in the solid state.[7] The luminescence of these Cu(I) complexes arises from two excited states: a triplet and a singlet. Their excited singlet state is approximately 786 cm^{-1} above the triplet. At room temperature, the levels are thermally equilibrated and emission from the singlet

dominates. However the lifetime of the excited state remains long due to the equilibrium with the triplet level. In contrast, only emission from the triplet is observed at low temperature. The Stokes shift for these compounds is much smaller than those observed for classical Cu(I) phenanthroline complexes[10] and indicates less distortion in the excited state, thereby reducing non-radiative decay pathways. The dinuclear Cu(I) complexes prepared from 2-diphenylphosphinopyridine (dpPy) also revealed interesting emission properties.[6] As shown in Figure 1, two isomeric forms of $[Cu_2(\mu\text{-dpPy})_3]^{2+}$ differing from the relative orientation of the 3 bridging dpPy ligands can be obtained in the solid state depending on the crystallization conditions.[6,11-13] The head-to-tail isomer is obtained when CH_3CN/Et_2O[11] and CH_2Cl_2/EtOH[6] are used for the recrystallization. In contrast, the head-to-head derivative crystallizes preferentially from CH_2Cl_2/MeOH.[6] In solution ligand association/dissociation take place and the distribution of complexes is profoundly affected by the nature of the solvent.

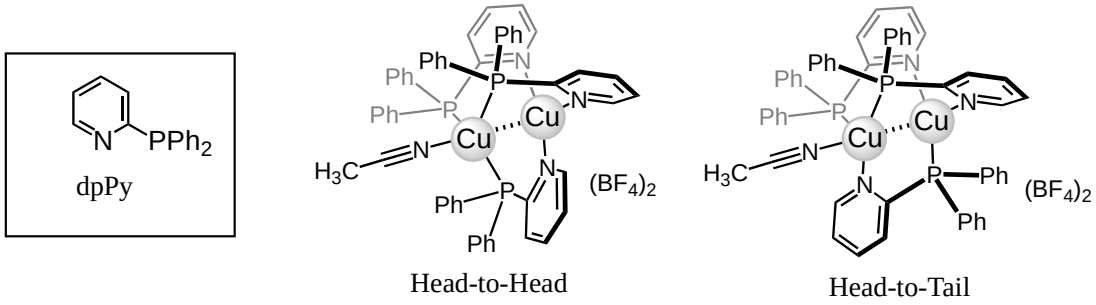

Figure 1. The two isomeric forms of $[Cu_2(\mu\text{-dpPy})_3]$ $(BF_4)_2$ obtained from the reaction of dpPy and $Cu(CH_3CN)_4BF_4$ in a 3:2 ratio.[6]

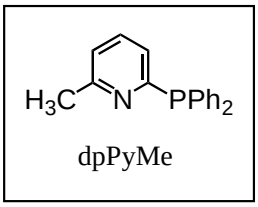

As part of this research, we became interested in exploring in details the coordination chemistry of 2-diphenylphosphino-6-methylpyridine (dpPyMe) with Cu(I) cations. The additional methyl group in the P,N-ligand is expected to play an important role in the photophysical properties of the resulting complexes as favorable steric factors may limit distortion in the excited state. On the other hand, steric factors may also affect the isomer distribution observed for $[Cu_2(\mu\text{-dpPy})_3]^{2+}$. Indeed, we found that only the head-to-head isomer is obtained both in solution and in the solid state for the analogous dinuclear complex prepared from dpPyMe.

2. Results and discussion

2.1. Synthesis and characterization

By analogy to the studies reported for the Cu(I) complexes obtained with dpPy,[11] the dpPyMe to Cu(I) ratio is expected to play an important role on the outcome of the reactions. Therefore, different stoichiometric conditions were systematically investigated. A first series of reactions were performed by mixing equimolar amounts of dpPyMe and $Cu(CH_3CN)_4BF_4$ in CH_2Cl_2. After 3 h, the solvents were evaporated. ^{1}H and ^{31}P NMR analysis of the crude product revealed that a dynamic mixture of several complexes was thus obtained. Crystallization by vapor diffusion of Et_2O into a CH_2Cl_2 solution of the reaction mixture gave a colorless crystalline solid. The X-ray crystal structure analysis revealed the formation of a dinuclear Cu(I) complex $[Cu_2(\mu\text{-dpPyMe})_2(CH_3CN)_2](BF_4)_2$ containing two P,N binucleating bridging ligands in a head-to-tail arrangement. Indeed, in the case of homodimetallic complexes prepared from dpPy, the head-to-tail arrangement is generally favored.[3] There are exceptions, in particular when the two metals are not in the same oxidation states.[14] In the case of Pt(II), the X-ray crystal structures of both possible isomers have been reported.[15] However, the head-to-head homobimetallic complex is the kinetic product of the reaction and it isomerizes slowly to the thermodynamic head-to-tail product.

In the structure of $[Cu_2(\mu\text{-dpPyMe})_2(CH_3CN)_2](BF_4)_2$, two conformers (**I** and **II**) are observed in the crystal. As shown in Figure 2, the main difference among them is the Cu-Cu distance: Cu(1)-Cu(1') = 2.6167(8) Å and Cu(2)-Cu(2') = 3.140(1) Å. A clear Cu-Cu interaction is thus observed in the case of **I**, whereas the two metal centers are not interacting significantly in the case of **II**. In the crystal lattice, the conformers are present in distinct layers and observation of the packing down crystallographic axis *b* reveals alternating layers of **I** and **II** (Figure 2B). For both conformers, the 8-membered metallacycle is centro-symmetric, centers of inversion being located in the middle of the cycles. The two metallacycle adopt a chair-like structure in which the two CH_3CN ligands are in axial positions and the two pyridine moieties in parallel planes (Figure 2C). The distances between the mean planes of the two pyridines are 0.678 Å for **I** and 1.959 Å for **II**. This substantial

difference results from the difference in the Cu-Cu distances in each conformer. For the same reason, significant differences are also observed for the N-Cu-N and N-Cu-P bond angles (Table 1).

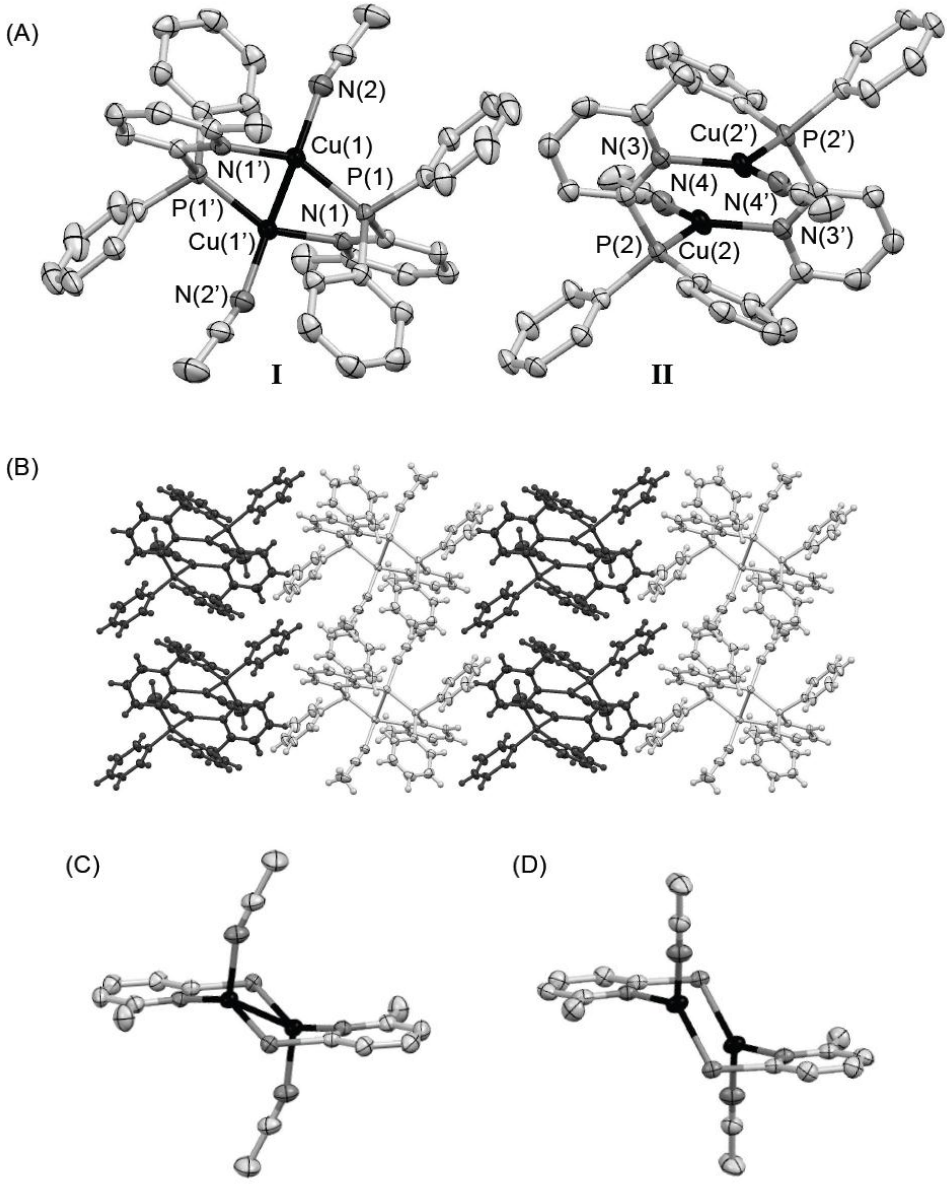

Figure 2. (A) X-ray crystal structure of $[Cu_2(\mu\text{-dpPyMe})_2(CH_3CN)_2](BF_4)_2$ (view down crystallographic axis *b*), two conformers (**I** and **II**) are observed in the crystal. (B) View of the packing down crystallographic axis *b* revealing alternating layers of the two conformers (**I**: pale gray, **II**: dark gray). Views of the chair-like conformations adopted by **I** (C) and **II** (D).

Table 1. Bond distances (Å) and bond angles (°) within the coordination sphere of the Cu^{+} cations in the X-ray crystal structure of $[Cu_2(\mu\text{-dpPyMe})_2(CH_3CN)_2](BF_4)_2$ (see Figure 2A for the numbering).

Selected bond lengths		Selected bond angles	
Cu(1)-P(1)	2.197(1)	P(1)-Cu(1)-N(1)	143.7(1)
Cu(1)-N(1)	1.985(4)	P(1)-Cu(1)-N(2)	108.3(1)
Cu(1)-N(2)	2.005(5)	N(1)-Cu(1)-N(2)	106.8(2)
Cu(2)-P(2)	2.199(1)	P(2)-Cu(2)-N(3)	126.2(1)
Cu(2)-N(3)	2.023(4)	P(2)-Cu(1)-N(4)	122.2(1)
Cu(2)-N(4)	1.951(4)	N(3)-Cu(2)-N(4)	109.9(1)

Whereas $[Cu_2(\mu\text{-dpPyMe})_2(CH_3CN)_2](BF_4)_2$ obtained in a pure form by recrystallization was perfectly stable in the solid state, it is important to highlight that equilibration between different complexes was observed as soon as the crystals are dissolved (even in a non-coordinating solvent such as CH_2Cl_2) as evidenced by the ^{1}H and ^{31}P NMR spectra recorded over a large range of temperatures (from -70°C to 25°C). This was also observed for the corresponding dpPy derivative.[11] However comparison with the NMR data reported in the literature[2,15] for $[Cu_2(\mu\text{-dpPy})_2(CH_3CN)_2](BF_4)_2$ revealed a completely different distribution of species in the case of dpPyMe. The ^{1}H NMR spectra recorded at various temperatures suggest the presence of at least two complexes, one being largely major (Figure 3). These are tentatively ascribed to the two possible isomers (head-to-tail and head-to-head) of $[Cu_2(\mu\text{-dpPyMe})_2(CH_3CN)_2](BF_4)_2$. Detailed analysis of the different species present in solution from the ^{1}H NMR spectra recorded at lower temperature was however made difficult due to coordination/decoordination of the CH_3CN ligands (Figure 3). It is rather difficult to clearly establish which isomer is favored in solution. The up-field shifted resonances for the pyridine resonances of the minor complex as well as its down-field shifted Py-CH_3 signal suggest the proximity of the aromatic groups of the second ligand and thus a head-to-tail structure. This is also suggested by the relative ^{31}P NMR chemical shifts of the two isomers (*vide supra*). As shown in Figure 3, the ^{31}P NMR spectra recorded at low temperature shows two sharp signals as well as two broader ones. This is in agreement with

the interpretation of the ^{1}H NMR data. The two sharp signals correspond likely to the head-to-tail and head-to-head isomers of $[Cu_2(\mu\text{-dpPyMe})_2(CH_3CN)_2](BF_4)_2$, the broad signals being tentatively attributed to the corresponding species with only one or no CH_3CN ligand. It is however not possible to exclude that the observed ^{31}P NMR resonances are due to other possible complexes formed from dpPyMe and Cu^{+}.

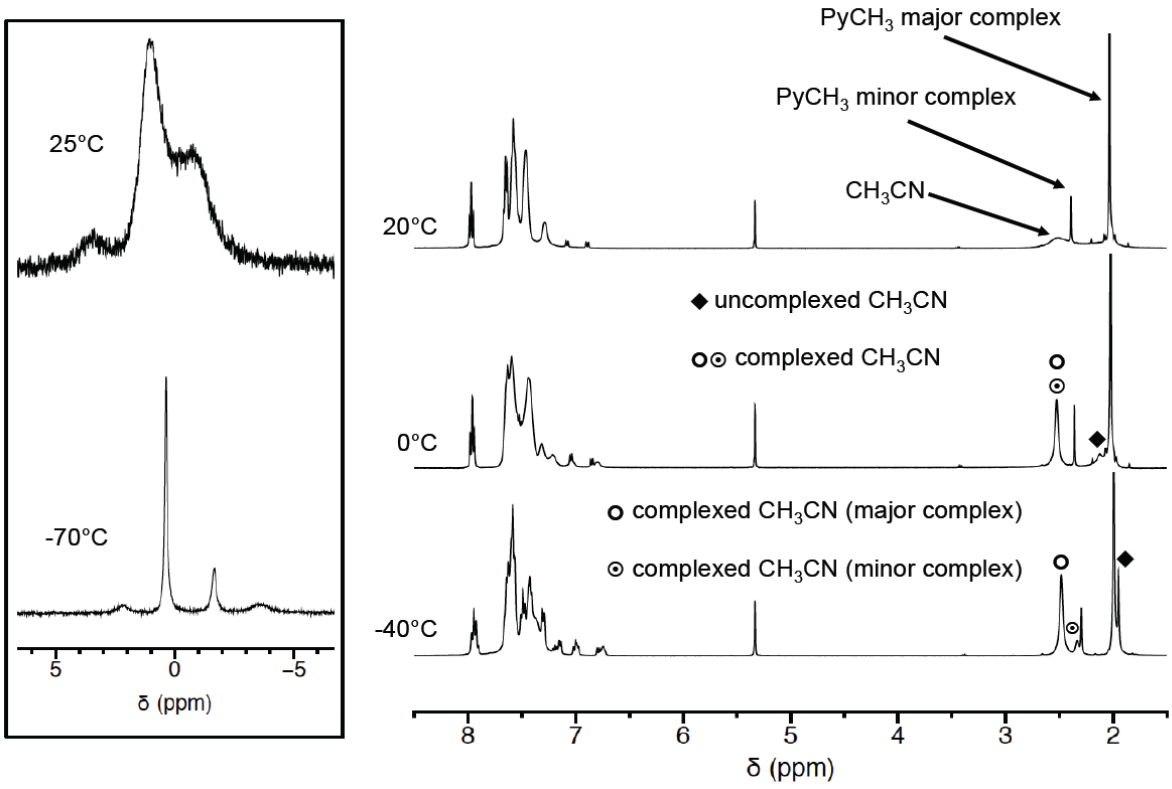

Figure 3. ^{1}H and ^{31}P NMR spectra (CD_2Cl_2) recorded upon dissolution of the crystallized sample of $[Cu_2(\mu\text{-dpPyMe})_2(CH_3CN)_2](BF_4)_2$. Variable temperature studies reveal the presence of several species in solution.

Analysis of the literature values for the ^{31}P NMR resonances of systems in which both head-to-head and head-to-tail isomers have been unambiguously characterized, it appears that the signal of the head-to-head complex is always significantly shifted down-field when compared to the corresponding head-to-tail derivative. Thus, the major signal may be ascribed to the head-to-head isomer. It appears that the minor isomer was preferentially crystallized from the starting mixture. It can also be noted that new crystallizations afforded systematically crystals

of the head-to-tail isomer. Whatever the solvents, we have never been able to obtain crystals of the head-to-head analogue. Clearly, the complex with the dpPyMe ligands in a head-to-tail arrangement is more prone to form crystals when compared to the other isomer, this does however not mean that this is the most favored species in solution. Indeed, crystallization of the minor complex drives the equilibrium in solution towards its formation and the most stable complex in solution is not necessarily the one obtained in the solid state. Due to the presence of different species in solution, complex $[Cu_2(\mu\text{-dpPyMe})_2(CH_3CN)_2](BF_4)_2$ was not further investigated.

A second series of reactions was then performed by mixing dpPyMe and $Cu(CH_3CN)_4BF_4$ in a 3:2 or a 4:2 molar ratio. After 3 h, ^{1}H and ^{31}P NMR analysis of the crude mixture of products revealed the same profile whatever the stoichiometry. Indeed, the spectra are also identical to the one recorded for the crude mixture obtained from the equimolar mixture of dpPyMe and $Cu(CH_3CN)_4BF_4$. These observations suggest the initial formation of a similar mixture of kinetic products in all the cases. The outcome of the crystallization results depends on the initial ratio of both components, *i.e*. dpPyMe and Cu^{+}, and is thermodynamically driven, at least for the 3:2 and 4:2 initial ratios. In both cases, the crystallization of the crude mixture gave the same compound. X-Ray crystal analysis of the crystals thus obtained shows the formation of a dinuclear Cu(I) complex $[Cu_2(\mu\text{-dpPyMe})_3(CH_3CN)](BF_4)_2$ (**1**) containing three bridging dpPyMe ligands in a head-to-head arrangement (Figure 4). The complex adopts a triple helical structure and is therefore chiral, both left- and right-handed helices are observed in the racemic crystal. This family of compounds represent actually the smallest known dinuclear triple helicates.[16] The two metal centers are in different coordination geometries, one being three- and the other four-coordinated. All the bond distances and bond angles (Table 2) are similar to the one reported for the analogous complex prepared from dpPy.[6] In **1**, Cu(2) forms a distorted tetrahedral array with three P atoms from the dpPyMe ligands and an additional N atom from an acetonitrile ligand. The other Cu atom, Cu(1), is in a distorted trigonal coordination geometry and accommodates the three pyridine subunits of the dpPyMe ligands. The Cu-Cu separation is 2.7520(6) Å which is slightly smaller than the sum of their van der Waals radius thus suggesting attractive cuprophilic interactions[17] that may also contribute to the overall stability of the system. View of the crystal structure down the Cu(1)-Cu(2) axis clearly reveals a

shielding of Cu(1) resulting from the presence of the methyl groups of the dpPyMe ligands (Figure 4D). This metal center is therefore protected against nucleophilic attacks, thus explaining the exceptional stability of the $[Cu_2(\mu\text{-dpPyMe})_3(CH_3CN)]^{2+}$ derivatives in solution (*vide supra*) when compared to the dpPy analogue lacking the CH_3 subunits. The triple helical structure of **1** is also stabilized by notable intramolecular π-π interactions between a phenyl moiety of each dpPyMe ligand and the pyridine ring of the neighboring dpPyMe subunit. These three interactions are highlighted in Figure 3C and the center-to-center distances between the aromatic rings ranges from 3.433 to 3.562 Å.

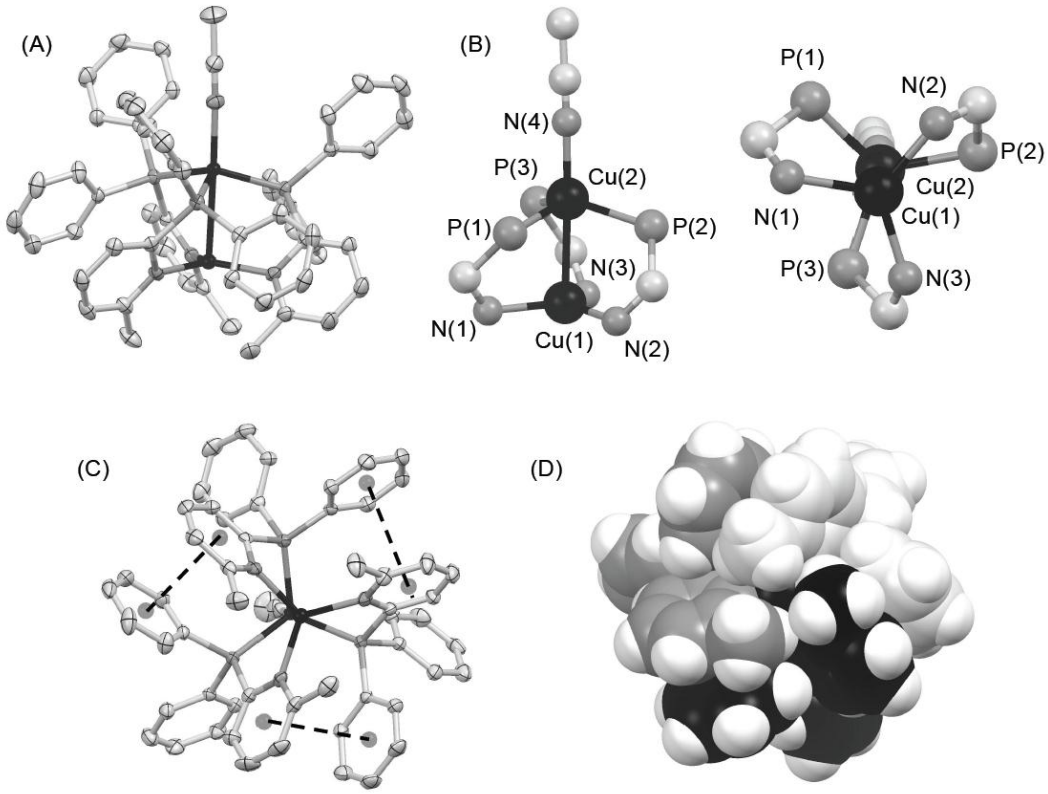

Figure 4. (A) ORTEP plot of the $[Cu_2(\mu\text{-dpPyMe})_3(CH_3CN)]^{2+}$ dication observed in the structure of **1**.$(CH_2Cl_2)_2$ (the H atoms are omitted for clarity, thermal ellipsoids are drawn at the 50% probability level). (B) Two views showing the details of the coordination sphere around the two metal centers. (C) View highlighting the interligand π-π interactions in the $[Cu_2(\mu\text{-dpPyMe})_3(CH_3CN)]^{2+}$ dication. (D) View along the Cu(1)-Cu(2) axis showing the shielding of Cu(1) due to the presence of the CH_3 groups.

Table 2. Bond distances (Å) and bond angles (°) within the coordination sphere of the $[Cu_2(\mu\text{-dpPyMe})_3(CH_3CN)]^{2+}$ dication in **1**.$(CH_2Cl_2)_2$ (see Figure 4B for the numbering).

Selected bond lengths		Selected bond angles	
Cu(1)-N(1)	2.051(3)	N(1)-Cu(1)-N(2)	119.2(1)
Cu(1)-N(2)	2.027(3)	N(1)-Cu(1)-N(3)	116.2(1)
Cu(1)-N(3)	2.028(3)	N(2)-Cu(1)-N(3)	122.5(1)
Cu(2)-P(1)	2.3257(9)	P(1)-Cu(2)-P(2)	113.39(4)
Cu(2)-P(2)	2.317(1)	P(1)-Cu(2)-P(3)	112.72(4)
Cu(2)-P(3)	2.332(1)	P(1)-Cu(2)-N(4)	103.3(1)
Cu(2)-N(4)	2.036(3)	P(2)-Cu(2)-P(3)	115.03(4)
		P(2)-Cu(2)-N(4)	106.8(1)
		P(3)-Cu(2)-N(4)	104.2(1)

The CH_3CN ligand in **1** is labile and was easily exchanged with other nitrile ligands (Scheme 1). Compound **1** was treated with a slight excess of the appropriate nitrile ligand (L2, L3, L4 or L6) in CH_2Cl_2 and extensively dried under high vacuum to eliminate CH_3CN. Complexes **2-3** and **6** were then obtained pure by recrystallization.

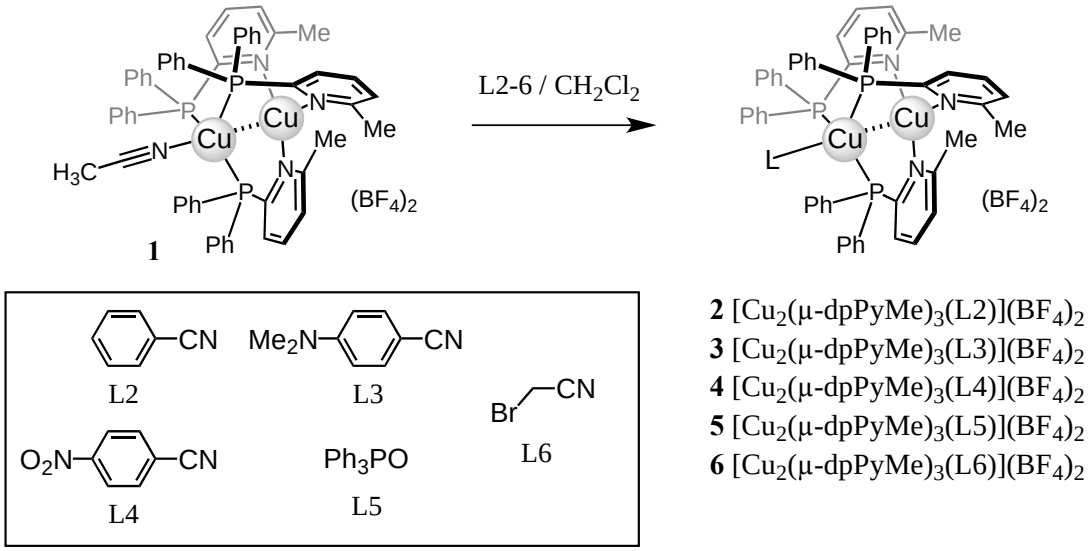

2 $[Cu_2(\mu\text{-dpPyMe})_3(L2)](BF_4)_2$
3 $[Cu_2(\mu\text{-dpPyMe})_3(L3)](BF_4)_2$
4 $[Cu_2(\mu\text{-dpPyMe})_3(L4)](BF_4)_2$
5 $[Cu_2(\mu\text{-dpPyMe})_3(L5)](BF_4)_2$
6 $[Cu_2(\mu\text{-dpPyMe})_3(L6)](BF_4)_2$

Scheme 1. Ligand exchange reactions.

CHAPTER 2

Dinuclear Cu^{I} complexes prepared from 2-diphenylphosphino-6-methylpyridine

The ligand exchange reaction was also attempted with triphenylphosphine. However oxidation of the phosphine ligand occurred during the ligand exchange process and the product obtained upon recrystallization was compound **5** incorporating a phenylphosphine oxide ligand. Compound **5** was also obtained by direct treatment of **1** with triphenylphosphine oxide.

X-ray quality crystals were obtained for compounds **2**, **4** and **5**. As shown in Figures 5 and 6, these dinuclear Cu(I) helical complexes are all characterized by a $[Cu_2(\mu\text{-dpPyMe})_3]^{2+}$ core unit containing three bridging dpPyMe ligands in a head-to-head arrangement. The bond distances and bond angles are similar to the one observed in the structure of compound **1**. The interligand π-π stacking interactions of the pyridine of each dpPyMe subunits with a phenyl group of a neighboring ligand seen for **1** are also systematically observed in the structures of **2**, **4** and **5**.

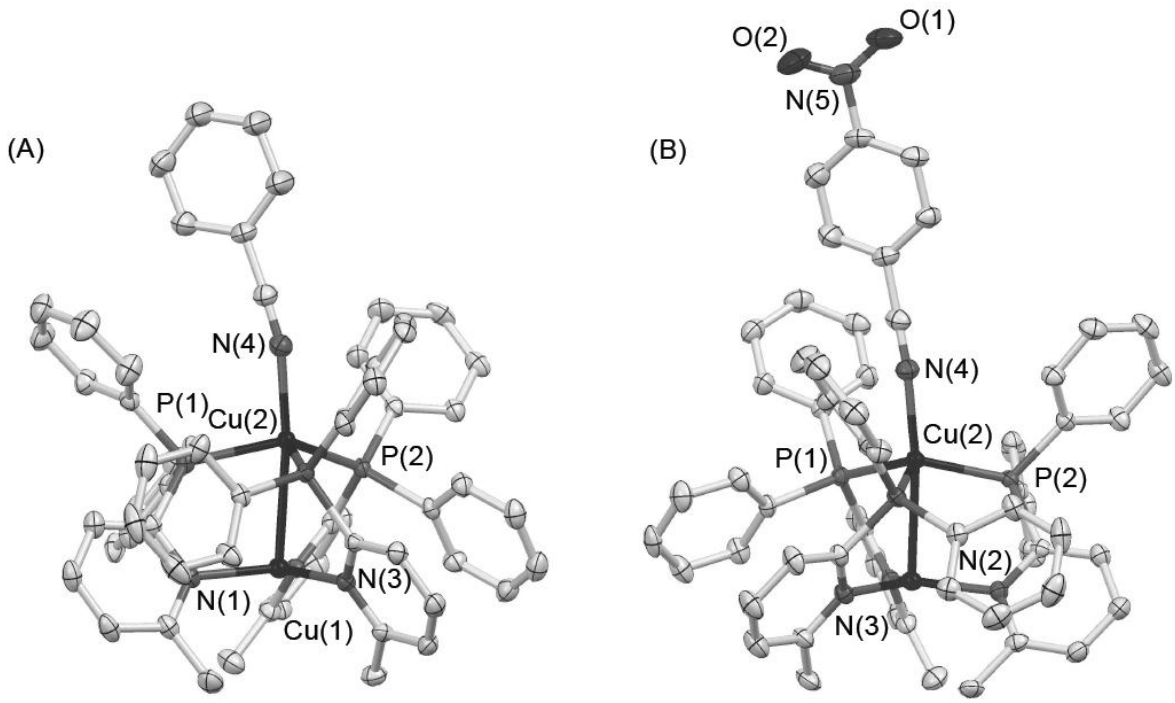

Figure 5. ORTEP plots of the $[Cu_2(\mu\text{-dpPyMe})_3(L)]^{2+}$ dications observed in the structures of **2**.CH_2Cl_2 (A) and **4**.CH_2Cl_2 (B). The H atoms are omitted for clarity, thermal ellipsoids are drawn at the 50% probability level. Selected bond lengths and bond angles for both structures are collected in Table 3.

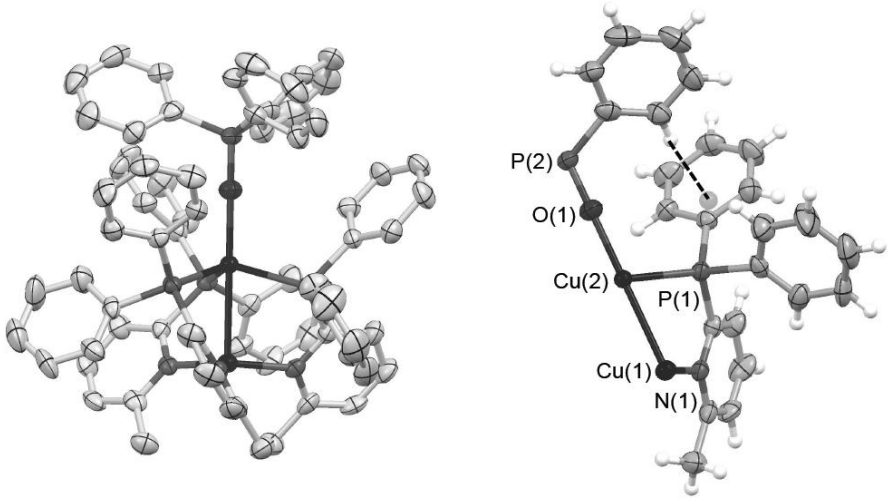

Figure 6. ORTEP plots of the $[Cu_2(\mu\text{-dpPyMe})_3(L)]^{2+}$ dication observed in the structure of **5**.$CHCl_3$ (the H atoms are omitted for clarity, thermal ellipsoids are drawn at the 50% probability level). Left: complete structure of the dication; right: asymmetric unit. An intramolecular C-H π interaction is highlighted (dashed line). Selected bond lengths: Cu(1)-N(1): 2.055(7), Cu(2)-P(1): 2.316(2), Cu(2)-O(1): 2.060(9) Å. Selected bond angles: N(1)-Cu(1)-N(1'): 119.6(3), P(1)-Cu(2)-P(1'): 114.44(9), P(1)-Cu(2)-O(2): 103.9(3).

Table 3. Bond distances and bond angles within the coordination sphere of the $[Cu_2(\mu\text{-dpPyMe})_3(L)]^{2+}$ dications in **2**.CH_2Cl_2 and **4**.CH_2Cl_2. (see Figure 5 for the numbering).

Selected bond lengths (Å)			Selected bond angles (°)		
	2	**4**		**2**	**4**
Cu(1)-N(1)	2.036(4)	2.034(3)	N(1)-Cu(1)-N(2)	119.0(2)	118.4(2)
Cu(1)-N(2)	2.025(4)	2.043(5)	N(1)-Cu(1)-N(3)	116.0(2)	121.6(2)
Cu(1)-N(3)	2.027(3)	2.044(6)	N(2)-Cu(1)-N(3)	123.1(1)	118.1(2)
Cu(2)-P(1)	2.328(1)	2.314(1)	P(1)-Cu(2)-P(2)	115.17(5)	113.05(5)
Cu(2)-P(2)	2.318(1)	2.310(1)	P(1)-Cu(2)-P(3)	111.75(4)	115.43(5)
Cu(2)-P(3)	2.316(1)	2.304(2)	P(1)-Cu(2)-N(4)	98.9(1)	106.4(1)
			P(2)-Cu(2)-P(3)	114.21(4)	114.80(5)
			P(2)-Cu(2)-N(4)	108.0(1)	97.2(1)
			P(3)-Cu(2)-N(4)	107.4(1)	107.8(1)

In the case of **5**, the two Cu atoms as well as the P and O atoms of the Ph_3PO ligands lie on a three-fold symmetry axis parallel to the *c* crystallographic axis. The four atoms adopt a perfectly linear arrangement with Cu(1)-Cu(2)-O(1) and Cu(2)-O(1)-P(2) angles of 180°. It can also be noted that **5** crystallizes in the form of conglomerates and only complexes with the same helicity are observed in the crystal lattice. Finally, a notable interligand CH/π interaction is observed. As shown in Figure 6, these interactions involve an aromatic CH group of the Ph_3PO ligand and one phenyl unit of the dpPyMe ligands. The hydrogen atom is located at 2.669 Å from the mean plane of the aromatic ring. This distance is within the typical range of the one usually observed of CH/π interactions.[18]

Compounds **1**-**6** were also characterized in solution. ^{1}H and ^{31}P NMR spectra recorded at different temperatures revealed a dynamic dissociation of the axial ligand (CH_3CN or L1-5) but no signals corresponding to head-to-tail isomers could be detected. This result is in sharp contrast with those obtained for the dpPy analogue of **1** for which different isomers are present in solution.[6,11-12] As seen in the X-ray crystal structures of **1**, **2**, **4** and **5**, the Cu(I) center coordinated by the three pyridine moieties is shielded by the three CH_3 groups. As a result, this particular metal center is protected towards nucleophilic attack and thus the ligand exchange allowing the isomerization is not possible anymore. As a typical example, the ^{1}H NMR spectra recorded at different temperature for compound **6** are shown in Figure 7. At room temperature, the ^{1}H NMR spectrum of **6** is characterized by three sets of signals in a typical pattern for a 2,6-disubstitued-pyridine bearing two different substituents and two broad singlet at δ = 2.45 and 3.78 ppm for the CH_3 groups of the dpPyMe ligands and the methylene group of 2-bromoacetonitrile, respectively. Interestingly, only three sets of signals are observed for the phenyl groups of the dpPyMe ligands at room temperature. By cooling the sample, a clear coalescence is observed at -10°C and the two phenyl groups of the three equivalent dpPyMe ligands give rise to a more complicated sets of signals at lower temperatures. The pairs of phenyl groups belonging to the same dpPyMe ligands are indeed diastereotopic in perfect agreement with the triple helical arrangement of the three P,N-ligands seen for dication $[Cu_2(\mu\text{-dpPyMe})_3]^{2+}$ in the X-ray crystal structures of **1**, **2**, **4** and **5**. At room temperature the two phenyl groups of each ligands exchange rapidly their position on the NMR timescale and therefore appear equivalent. In other words, these observations

suggest a fast dynamic racemization of compound **6** at room temperature. A similar behavior has been also observed for compounds **1**-**5**.

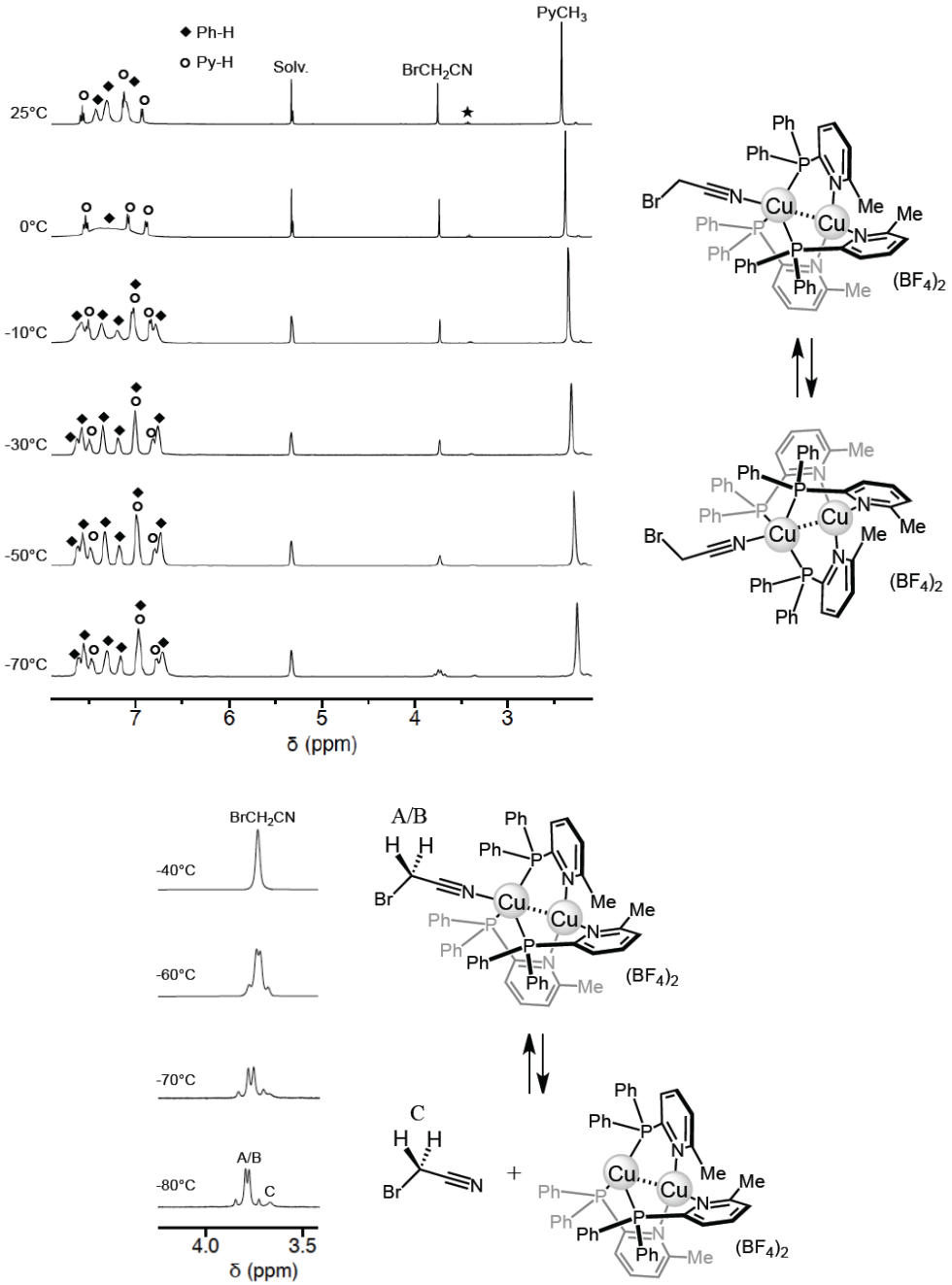

Figure 7. Top: ^{1}H NMR spectra of **6** recorded at different temperature in CD_2Cl_2 showing fast dynamic racemization on the NMR timescale at room temperature (* = Et_2O). Bottom: ^{1}H NMR resonance observed at different temperature for the axial $BrCH_2CN$ ligand revealing its fast coordination/decoordination at room temperature.

CHAPTER 2

Dinuclear Cu^{I} complexes prepared from 2-diphenylphosphino-6-methylpyridine

Close inspection of the ^{1}H NMR resonance of the methylene group of $BrCH_2CN$ shows a rapid coordination/decoordination of this axial ligand (Figure 7). At low temperature, the exchange is frozen and an AB system is observed for the CH_2 group of the coordinated $BrCH_2CN$ molecules. The diastereotopy of these protons results from the chirality of the $[Cu_2(\mu\text{-dpPyMe})_3]^{2+}$ core. This observation further supports a triple helical structure for **6** in solution. For compounds **1**-**5**, rapid exchange of the axial ligand was also observed. Finally, the ^{31}P NMR data of compounds **1**-**6** were also consistent with the proposed structures. As shown in Figure 8, the ^{31}P NMR spectrum of **6** revealed only a single resonance for the three equivalent P atoms. Cooling the sample to -70°C did not give rise to additional peaks and no P-Cu-P couplings were observed. This shows that the three P atoms are chemically and magnetically equivalent at all temperatures, thus it can be deduced that the compound remains intact in solution.

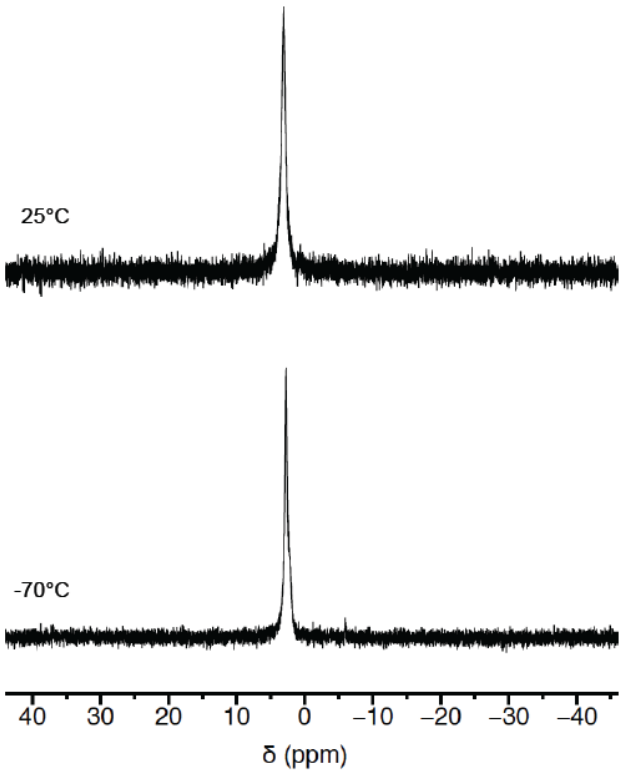

Figure 8. Top: ^{31}P NMR spectra of **6** recorded at different temperature in CD_2Cl_2.

2.2. Electrochemical properties

Béatrice Delavaux-Nicot (*Laboratoire de Chimie de Coordination du CNRS*, Toulouse France) has carried out the electrochemical investigations of the $[Cu_2(\mu\text{-dppyMe})_3L](BF_4)_2$ complexes.

The electrochemical properties of compounds **1-5**, dpPyMe and L3-5 were determined by cyclic voltammetry (CV) and Osteryoung Square Wave Voltammetry (OSWV). All the experiments were performed at room temperature in CH_2Cl_2 solutions containing tetra-*n*-butylammonium tetrafluoroborate (0.1 M) as supporting electrolyte, with a Pt wire as the working electrode and a saturated calomel electrode (SCE) as a reference. Potential data for all of the compounds are collected in Table 4. As a typical example, the OSWV and CV obtained for compound **2** are shown in Figure 9.

Table 4. Electrochemical data of the Cu(I) complexes determined by OSWV on a Pt working electrode in CH_2Cl_2 + 0.1 M $n Bu_4NBF_4$ at room temperature.[a,b]

	Oxidation		Reduction	
	E_1	E_2	E_1	E_1
dpPyMe	+1.39	+1.84	-1.59[c]	
1	+1.85		-1.68	-1.85
2	+1.92		-1.51	-1.61
L3	+1.33			
3	+1.44	+1.92	-1.62	
L4			-0.75	-1.49
4	+1.87		-0.72	-1.49
L5	+1.33			
5	+1.55	+1.82	-1.61	-1.89

[a] OSWVs were obtained using a sweep width of 20 mV, a frequency of 10 Hz, and a step potential of 5 mV. [b] Values in V *vs*. SCE. [c] Small amplitude signal.

For all the dinuclear complexes, an irreversible oxidation process is observed at +1.85 to +1.92 V *vs*. SCE. By analogy to previous work on $[Cu(NN)(PP)]^+$ derivatives,[19] the oxidation is centred on the metal but the process is irreversible due to the simultaneous oxidation of the

P-ligands which is associated with chemical reactions leading to the decomposition of the complexes.

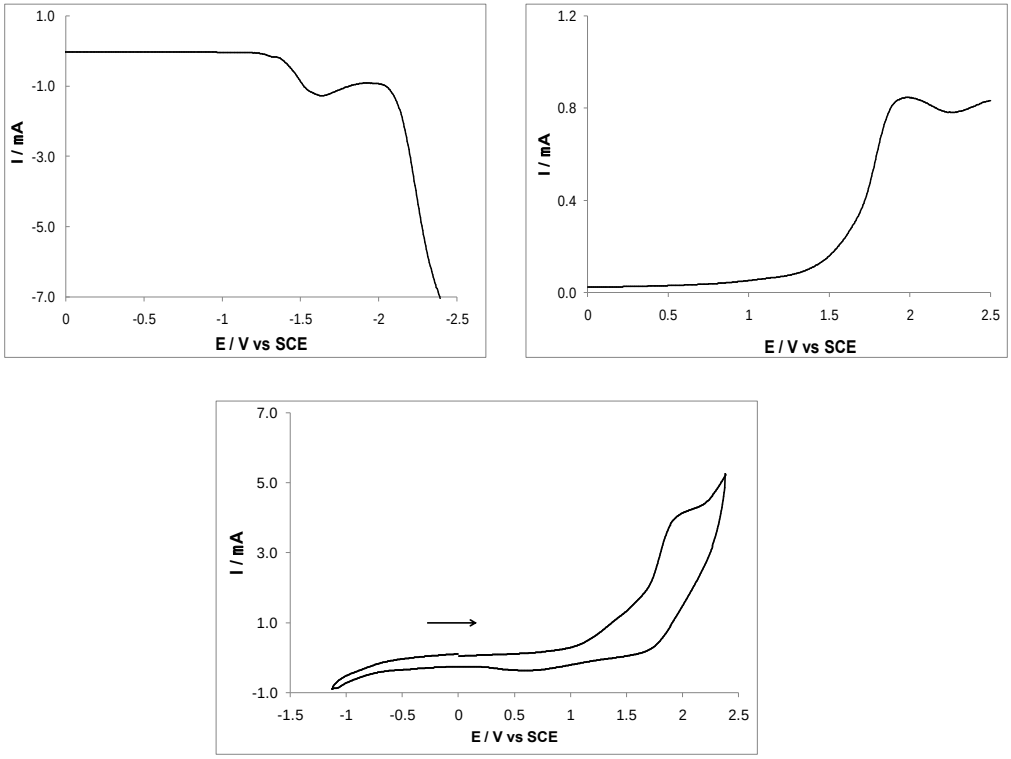

Figure 9. Top: OSWVs (cathodic and anodic scans) of compound **2** on a Pt electrode in CH_2Cl_2 + 0.1 M nBu$_4$NBF$_4$ at room temperature. Bottom: cyclic voltammogram showing the oxidation of **2** at v = 0.1 V.s^{-1} on a Pt electrode in CH_2Cl_2 + 0.1 M nBu$_4$NBF$_4$.

The exceptionally high redox potential for the oxidation of the Cu(I) centres in **1**-**5** suggests the inhibition of redox-induced distortion resulting from strong interligand interactions within the compact $[Cu_2(\mu\text{-dpPyMe})_3]^{2+}$ dicationic unit. Actually, the Cu(II)/Cu(I) redox potentials are very sensitive to steric effects and redox-induced changes of the coordination sphere around the copper centre are generally observed.[19] Steric factors that prevent these distortions upon oxidation will destabilize the highest oxidation state and the Cu(II)/Cu(I) redox potential is shifted to more positive potentials. In the particular case of **3**, the first oxidation process observed at +1.44 V *vs*. SCE is centred on the axial ligand. When compared to L3, the redox potential is shifted to more potential values (ΔE = 110 mV) thus showing an effective coordination of the nitrile unit onto the $[Cu_2(\mu\text{-dpPyMe})_3]^{2+}$ core. In the cathodic region, the

reductions observed for all the complexes are likely centered on the dpPyMe ligands except for **4**. In this case, the first reduction observed at -0.72 V *vs*. SCE involves its *p*-nitrobenzonitrile ligand. The corresponding oxidation is observed at -0.75 V *vs*. SCE for L4. The difference in redox potential (ΔE = 30 mV) between **4** and L4 suggests an effective axial coordination. When compared to **3**/L3, the potential shift resulting from the coordination to the Cu(I) centre is smaller in the case of **4**/L4. Indeed, L4 is expected to be a weaker ligand because of the electron withdrawing effect of the nitro group.

2.3. Photophysical properties

The photophysical properties of the $[Cu_2(\mu\text{-dppyMe})_3L](BF_4)_2$ derivatives have been investigated by Nicola Armaroli, John Mohanraj and Gianluca Accorsi (Bologna, Italy).

The electronic absorption spectra of complexes **1-5** and of the related ligands were recorded in CH_2Cl_2 (Figure 10). The spectral shapes of **1**, **2** and **5** are similar, whereas **3** and **4** show moderate changes due to the additional absorption features of ancillary chromophoric ligands L2 and L3. By comparison with the spectra of the ligands, the intense UV bands of **1-5** up to about 330 nm are attributable to ligand centered $\pi-\pi^*$ transition, whereas the weak, broad tails, in the range 330-380 nm, are tentatively assigned to MLCT transitions.[10] Such bands are significantly blue-shifted compared to other phosphorus (P) and nitrogen (N) based heteroleptic Cu(I) complexes.[20] This may be due to the effective coordination and electron withdrawing properties of P ligands, which stabilize the HOMO of complexes and consequently increases the energy gap with the LUMO.[21] In addition, the peculiar ligand structure assures tight packing of the complexes in the ground state and also possibly in the excited state; in fact, **1-5** exhibit exceptional stability over many days in CH_2Cl_2 solution.

At room temperature, all the complexes exhibit featureless, weak, bluish-green emission at any excitation wavelength in aerated CH_2Cl_2 (Figure 10). The photoluminescence quantum yield (PLQY) values and excited state lifetimes are gathered in Table 5; upon deoxygenating the samples, such values are substantially increased and are comparable with some other heteroleptic (N- and P-) Cu(I) complexes reported in the literature.[10] In line with previously reported Cu(I) luminescent complexes, the observed emission can be attributed to

metal-to-ligand-charge-transfer (MLCT) state(s), and this is supported by density functional theory calculations carried out on similar systems.[6] The strong sensitivity of the emission intensity to the presence oxygen, the μs-scale lifetime and the large shift between absorption and excitation maxima suggest a triplet nature for the emissive state.[10] Furthermore, the bi-exponential character of the luminescence decay (except for **4**) and the extended emission tail at longer wavelengths suggest the participation of multiple CT levels to the emission profiles.

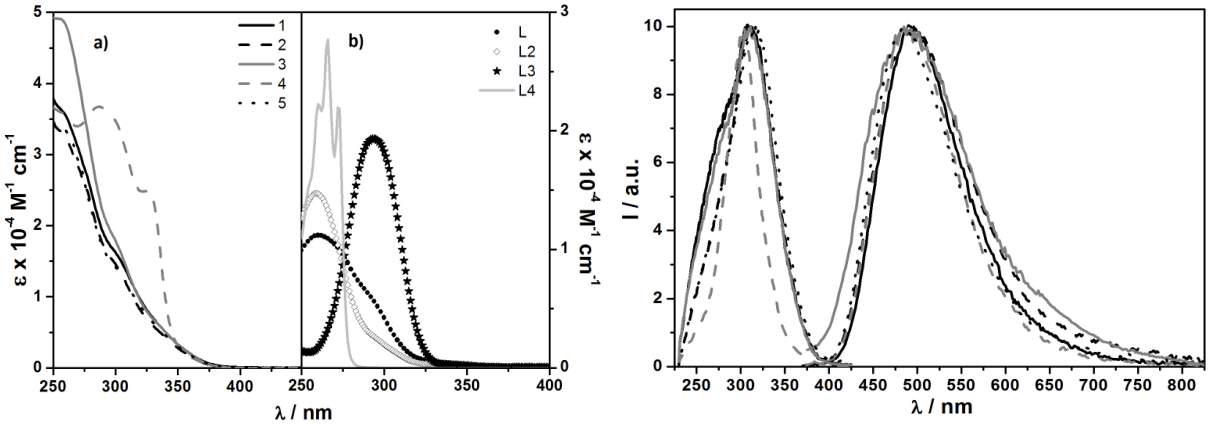

Figure 10. Left: electronic absorption spectra of (a) complexes **1-5** (solid-black, dashed-black, solid-grey, dashed-grey, dotted-black, respectively) and (b) ligands L (dots), L2 (squares), L3 (stars) and L4 (solid-grey) in CH_2Cl_2. Right: excitation and emission spectra of complexes **1-5** (solid-black, dashed-black, solid-grey, dashed-grey, dotted-black, respectively, uncorrected) in degassed CH_2Cl_2. Emission spectra are recorded upon exciting **1** and **3** at 320 nm, and **2**, **4** and **5** at 340 nm. Excitation spectra are collected at the respective emission maximum for each complex.

The long lifetime of the complexes **1**, **2**, **3** and **5** with high relative amplitude (Table 5) advocates the dominant contribution of a ^{3}MLCT state to the emission, although the trend is reversed in **4**. The absence of shoulders or well resolved emission bands suggest a minimal energy gap between non-degenerate MLCT levels. As a result, at room temperature, such levels are thermally equilibrated and this can explain the broad emission bands observed.

The excitation and emission spectra were also recorded in the solid state (KBr matrix). The excitation spectra of **1**, **2**, **4** and **5** are superimposed on each other, irrespective of the

ancillary ligand. This shows a virtually constant energy gap between the frontier orbitals, as also suggested by theoretical studies.[6] On the other hand, these complexes exhibit different emission maxima and, notably, emission quantum yield values as high as 46%, a remarkable finding for Cu(I) complexes. Excited state lifetimes are substantially longer than in CH_2Cl_2 solution but still biexponential (Table 5).

Table 5. Luminescence data of complexes **1-5**.

	CH_2Cl_2 solution (298 K)					Solid state (298 K)		
	Aerated			Deareted				
	Φ x 10^{-3}	τ [a] (µs)	λ_{max} (nm)	Φ	τ [a] (µs)	λ_{max} (nm)	Φ	τ [a] (µs)
1	2.3	0.32 (93) 0.03 (7)	490	0.028	11.7 (71) 1.5(29)	502	0.46	28 (50) 7 (50)
2	6.2	0.43 (88) 0.9 (12)	490	0.032	7.5 (63) 2 (37)	479	0.21	32 (71) 3 (29)
3	2.1	0.22 (78) 0.004 (22)	488	0.035	5.7 (100)	477	0.06	38 (73) 3.5 (27)
4	3.8	0.33 (91) 0.04 (9)	489	0.012	7 (23) 1.7 (77)	[b]	[b]	[b]
5	2.6	0.39 (87) 0.11 (13)	486	0.018	9 (85) 2 (15)	465	0.20	19 (77) 4 (23)

[a] The values in brackets are the relative weight of each component of the emission decay.

[b] Complex **4** shows multiple emission bands in the solid state.

3. Conclusion

A series of reactions have been performed by mixing dpPyMe and $Cu(CH_3CN)_4BF_4$ in different molar ratio. Whereas a similar kinetic mixture of complexes is obtained whatever the stoichiometry, the outcome of the crystallizations depends on the initial ration of both components. Starting from equimolar quantities of dpPyMe and Cu^{+}, a dinuclear Cu(I) complex with two P,N binucleating bridging ligands has been obtained. In contrast, by increasing the amount of dpPyMe, a dinuclear Cu(I) complex containing three bridging dpPyMe ligands in a head-to-head arrangement has been isolated. Both compounds are stable

in the solid state, however only $[Cu_2(\mu\text{-dpPyMe})_3(CH_3CN)](BF_4)_2$ remains intact in solution. The remarkable stability of this compound is ascribed to a steric effect resulting from the presence of the three CH_3 groups that are capable of protecting a metal center towards nucleophilic attack and thus the ligand exchange allowing the isomerization is not possible anymore. It has been also shown the axial CH_3CN ligand can be easily exchanged without disrupting the $[Cu_2(\mu\text{-dpPyMe})_3]^{2+}$ core. The electrochemical and photophysical properties of the complexes have been systematically investigated. The $[Cu_2(\mu\text{-dpPyMe})_3(L)](BF_4)_2$ derivatives are weak emitters in solution, however remarkable emission quantum yields have been found in a rigid matrix. In addition to their stability, the electronic properties of these compounds make them attractive candidates for light emitting applications. Further improvements of the emission properties can be expected by replacing the methyl groups of dpPyMe by larger substituents or by extending the conjugation of the π-system of the pyridine moiety.

4. Experimental section

General. Reagents were purchased as reagent grade and used without further purification. Acetonitrile (CH_3CN) was distilled over CaH_2 under Ar. Dichloromethane (CH_2Cl_2) was distilled over CaH_2 under Ar. All reactions were performed in standard glassware under an inert Ar atmosphere. Evaporation and concentration were done at water aspirator pressure and drying in vacuo at 10^{-2} Torr. Column chromatography: silica gel 60 (230-400 mesh, 0.040-0.063 mm) was purchased from E. Merck. Thin Layer Chromatography (TLC) was performed on aluminum sheets coated with silica gel 60 F_{254} purchased from E. Merck. NMR spectra were recorded on a Bruker AC 300 or AC 400 with solvent peaks as reference. Elemental analyses were carried out on a Perkin–Elmer 2400 B analyzer at the LCC Microanalytical Laboratory in Toulouse.

Electrochemistry. The electrochemical measurements were carried out with a potentiostat Autolab PGSTAT100. Experiments were performed at room temperature in a homemade airtight three–electrode cell connected to a vacuum/argon line. The reference electrode consisted of a saturated calomel electrode (SCE) separated from the solution by a bridge compartment. The counter electrode was a platinum wire of *ca*. 1 cm^2 apparent surface. The working electrode was a Pt microdisk (0.5 mm diameter). The supporting electrolyte nBu$_4$NBF$_4$ (Fluka, 99% electrochemical grade) was used as received and simply degassed under argon. Dichloromethane was freshly distilled over CaH_2 prior to use. The solutions used during the electrochemical studies were typically 10^{-3} M in compound and 0.1 M in supporting electrolyte. The solutions were degassed by bubbling argon before each series of measurements. The working electrode was polished with a polishing machine (Presi P230). Under these experimental conditions, Fc/Fc^+ is observed at +0.54 ± 0.01 V *vs*. SCE.

Photophysical studies. Dichloromethane (Carlo Erba, spectrofluorimetric grade) was used as solvent without further purification. Absorption spectra were recorded with a Perkin-Elmer Lambda 950 UV/vis/NIR spectrophotometer. For luminescence experiments, the solution samples were placed in fluorimetric 1 cm path cuvettes and, when necessary, the solution

were placed in a suitable cuvette and purged with argon to deoxygenate the solution; solid state measurements were carried out with discs, prepared by finely grinding the samples with (Sigma Aldrich, puriss) and pressed. Uncorrected emission spectra were obtained with an Edinburgh FLS920 spectrometer equipped with a peltier-cooled Hamamatsu R928 photomultiplayer tube (185–850 nm). An Edinburgh Xe900 450 W Xenon arc lamp was used as exciting light source. Corrected spectra were obtained via a calibration curve supplied with the instrument.

Luminescence quantum yields (Φ_{em}) in solution obtained from spectra on a wavelength scale [nm] were measured according to the approach described by Demas and Crosby[22] using air-equilibrated [Ru(bpy_3Cl_2 in water solution, Φ_{em} = 0.028% as standard.

The solid state Φ_{em} have been calculated by corrected emission spectra obtained from an apparatus consisting of barium sulfate coated integrating sphere (6 in.), with the same light source and detector stated above, following the procedure described by De Mello et al.[23]

Fluorescence lifetimes were measured with an IBH 5000F time-correlated single-photon counting spectrometer using pulsed NanoLED excitation sources at 331 nm. Analysis of the luminescence decay profiles against time was accomplished with the Decay Analysis Software DAS6 provided by the manufacturer.

Experimental uncertainties are estimated to be ± 8% for lifetime determinations, ± 20% for emission quantum yields, ± 2 nm and ± 5 nm for absorption and emission peaks respectively.

Reaction of dpPyMe with $Cu(CH_3CN)_4BF_4$

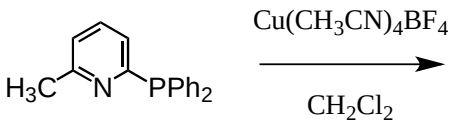

dpPyMe

A solution of $Cu(CH_3CN)_4BF_4$ (1 equiv., see Table 6) and dpPyMe (1, 1.5 or 2 equiv., see Table 6) in CH_2Cl_2 was stirred at room temperature. After 3 h, the solvent was evaporated and the resulting crude mixture analyzed by NMR (Figure 11).

Table 6. Quantities of reagents and volume of solvent used for the different reactions.

dpPyMe : Cu^{+} ratio	dpPyMe	$Cu(CH_3CN)_4BF_4$	CH_2Cl_2
2:2	50 mg (0.18 mmol)	56.7 mg (0.18 mmol)	10 mL
3:2	150 mg (0.54 mmol)	113.4 mg (0.36 mmol)	20 mL
4:2	50 mg (0.18 mmol)	28.4 mg (0.09 mmol)	10 mL

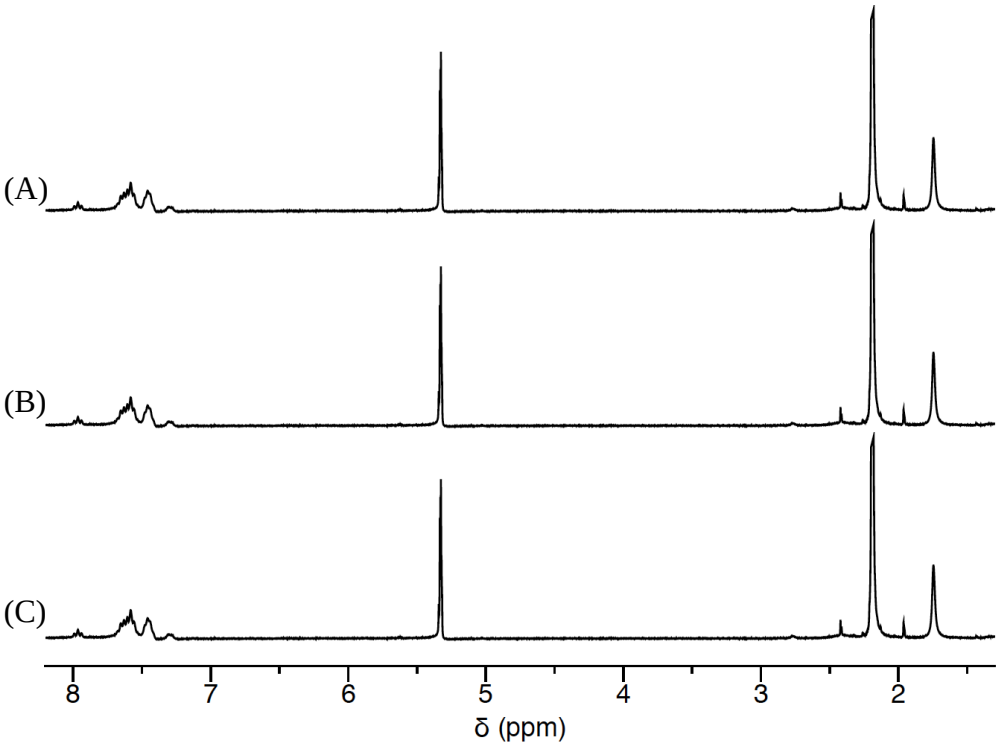

Figure 11. ^{1}H NMR (CD_2Cl_2) of the crude reaction mixtures obtained after evaporation. (A) dpPyMe (1 equiv.) and $Cu(CH_3CN)_4BF_4$ (1 equiv.), (B) dpPyMe (3 equiv.) and $Cu(CH_3CN)_4BF_4$ (2 equiv.), (C) dpPyMe (2 equiv.) and $Cu(CH_3CN)_4BF_4$ (1 equiv.).

$[Cu_2(\mu\text{-dpPyMe})_2(CH_3CN)_2](BF_4)_2$. A solution of $Cu(CH_3CN)_4BF_4$ (56.7 mg, 0.18 mmol) and dpPyMe (50 mg, 0.18 mmol) in CH_2Cl_2 was stirred at room temperature. After 3 h, the solvent was evaporated. Recrystallization by vapor diffusion of Et_2O into a CH_2Cl_2 solution

of the crude product gave $[Cu_2(\mu\text{-dpPyMe})_2(CH_3CN)_2](BF_4)_2$ (61 mg, 72%). Colorless crystals. Anal. Calcd for $C_{40}H_{38}N_4P_2Cu_2B_2F_8$: C, 51.25; H, 4.09; N, 5.98. Found: C, 51.37; H, 3.76; N, 5.51.

Compound **1**. A solution of $Cu(CH_3CN)_4BF_4$ (227 mg, 0.721 mmol) and dpPyMe (300 mg, 1.08 mmol) in CH_2Cl_2 (40 mL) was stirred at room temperature. After 3 h, the solvent was evaporated. Recrystallization by vapor diffusion of Et_2O into a CH_2Cl_2 solution of the crude product gave **1** (351 mg, 83%). Colorless crystals. ^{1}H-NMR (CD_2Cl_2, 300 MHz, 293 K): 7.56 (d, *J* = 8Hz, 4H), 7.42 (bm, 6H), 7.31 (bm, 11H), 7.10 (m,14H), 6.91 (d, *J* = 7Hz, 4H), 2.40(s, 9H), 1.92 (s, 3H). $^{31}P\{^{1}H\}$-NMR (CD_2Cl_2, 293 K, 162 MHz): 2.09. ESI-MS: 340.04 (97%, $[Cu(\mu\text{-dpPyMe})]^+$ calcd for $C_{18}H_{16}NPCu$), 617.17 (100%, $[Cu(\mu\text{-dpPyMe})_2]^+$ calcd for $C_{36}H_{32}N_2P_2Cu$), 894.29 (16%, $[Cu(\mu\text{-dpPyMe})_3]^+$ calcd for $C_{54}H_{48}N_3P_3Cu$) .Anal. Calcd for $C_{56}H_{47}N_4P_3Cu_2B_2F_8.1/2CH_2Cl_2$: C, 55.80; H, 4.31; N, 4.61. Found: C, 55.73; H, 4.40; N, 4.30.

Ligand exchange reactions

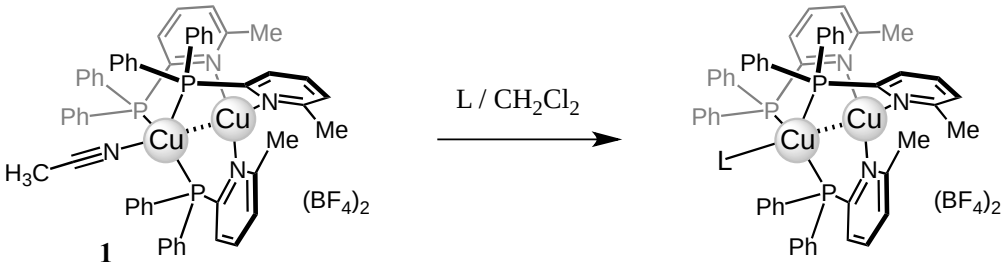

Compound **2**. A solution of **1** (150 mg, 0.128 mmol) and L2 (15 µL, 0.135 mmol) in CH_2Cl_2 (20 mL) was stirred at room temperature for 30 min. and evaporated to dryness. The resulting solid was dissolved in CH_2Cl_2 (20 mL) and the solution evaporated (3 X). The resulting solid was dried under high vacuum. Recrystallization by vapor diffusion of Et_2O into a CH_2Cl_2 solution of the crude product gave **2** (115 mg, 73%). Colorless crystals. ^{1}H-NMR (CD_2Cl_2, 300 MHz, 293 K): 7.73 (m, 1H), 7.61 (t, *J* = 7Hz, 4H),7.47 (m, 7H), 7.30 (m, 14H), 7.15 (m, 14H), 6.95 (d, *J* = 7Hz, 4H), 2.36 (s, 9H). $^{31}P\{^{1}H\}$-

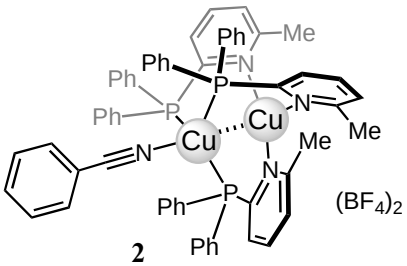

NMR (CD_2Cl_2, 293 K, 162 MHz): 4.22. ESI-MS: 340.04 (72%, $[Cu(\mu\text{-dpPyMe})]^+$ calcd for $C_{18}H_{16}NPCu$), 617.17 (100%, $[Cu(\mu\text{-dpPyMe})_2]^+$ calcd for $C_{36}H_{32}N_2P_2Cu$), 894.29 (50%, $[Cu(\mu\text{-dpPyMe})_3]^+$ calcd for $C_{54}H_{48}N_3P_3Cu$). Anal. Calcd for $C_{56}H_{47}N_4P_3Cu_2B_2F_8.1/2CH_2Cl_2$: C, 55.80; H, 4.31; N, 4.61. Found: C, 55.73; H, 4.40; N, 4.30.

Compound 3. A solution of **1** (150 mg, 0.128 mmol) and L3 (20 mg, 0.135 mmol) in CH_2Cl_2 (20 mL) was stirred at room temperature for 30 min. and evaporated to dryness. The resulting solid was dissolved in CH_2Cl_2 (20 mL) and the solution evaporated (3 X). The resulting solid was dried under high vacuum. Recrystallization by vapor diffusion of Et_2O into a CH_2Cl_2 solution of the crude product gave **3** (129 mg, 79%). Pale yellow crystals. ^{1}H-NMR (CD_2Cl_2, 300 MHz, 293 K): 7.55 (t, *J* = 7Hz, 7H), 7.37 (bm, 18H), 7.08 (d, *J* = 7Hz, 7H), 6.89 (t, *J* = 9Hz, 7H), 6.58 (d, *J* = 9Hz, 4H), 3.05 (s, 6H), 2.40 (s, 9H). ^{31}P{^{1}H}-NMR (CD_2Cl_2, 293 K, 162 MHz): 3.58. ESI-MS: 340.04 (100%, $[Cu(\mu\text{-dpPyMe})]^+$ calcd for $C_{18}H_{16}NPCu$), 617.17 (58%, $[Cu(\mu\text{-dpPyMe})_2]^+$ calcd for $C_{36}H_{32}N_2P_2Cu$), 894.29 (10%, $[Cu(\mu\text{-dpPyMe})_3]^+$ calcd for $C_{54}H_{48}N_3P_3Cu$). Anal. Calcd for $C_{63}H_{58}N_5P_3Cu_2B_2F_8$: C, 59.17; H, 4.57; N, 4.48. Found: C, 59.28; H, 4.62; N, 4.33.

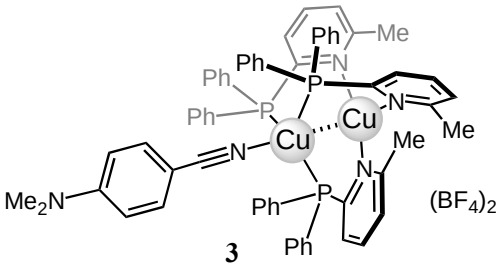

3

Compound 4. A solution of **1** (150 mg, 0.128 mmol) and L4 (20 mg, 0.135 mmol) in CH_2Cl_2 (20 mL) was stirred at room temperature for 30 min. and evaporated to dryness. The resulting solid was dissolved in CH_2Cl_2 (20 mL) and the solution evaporated (3 X). The resulting solid was dried under high vacuum. Recrystallization by vapor diffusion of Et_2O into a CH_2Cl_2 solution of the crude product gave **2** (159 mg, 97%). Yellow crystals. ^{1}H-NMR (CD_2Cl_2, 300 MHz, 293 K): 8.31 (d, *J* = 8Hz, 2H), 7.61 (m, 5H), 7.41 (m, 6H), 7.30 (m, 12H), 7.12 (m, 15H), 6.98 (d, *J* = 7Hz, 3H), 2.45 (s, 9H). ^{31}P{^{1}H}-NMR (CD_2Cl_2, 293 K, 162 MHz): 3.92. ESI-MS: 340.04 (100%, $[Cu(\mu\text{-dpPyMe})]^+$ calcd for $C_{18}H_{16}NPCu$), 617.17 (85%, $[Cu(\mu\text{-dpPyMe})_2]^+$ calcd for

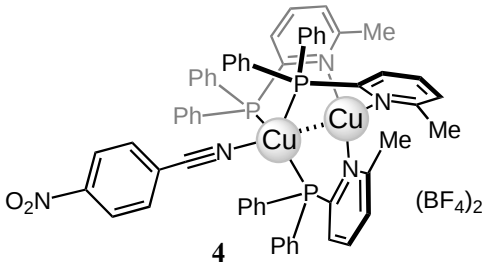

4

$C_{36}H_{32}N_2P_2Cu$), 894.29 (5%, $[Cu(\mu\text{-dpPyMe})_3]^+$ calcd for $C_{54}H_{48}N_3P_3Cu$). Anal. Calcd for $C_{61}H_{52}N_5O_2P_3Cu_2B_2F_8.CH_2Cl_2$: C, 54.53; H, 3.99; N, 5.13. Found: C, 54.73; H, 3.95; N, 5.24.

Compound **5**. A solution of **1** (150 mg, 0.128 mmol) and L5 (38 mg, 0.135 mmol) in CH_2Cl_2 (20 mL) was stirred at room temperature for 30 min. and evaporated to dryness. The resulting solid was dissolved in CH_2Cl_2 (20 mL) and the solution evaporated (3 X). The resulting solid was dried under high vacuum. Precipitation by addition of Et_2O into a CH_2Cl_2 solution of the crude product gave **5** (161 mg, 88%). Colorless crystals. ^{1}H-NMR (CD_2Cl_2, 300 MHz, 293 K): 7.64 (t, *J* = 7Hz, 4H), 7.50 (t, *J* = 7Hz, 5H), 7.28 (m, 18H), 7.06 (m, 12H), 6.90 (m, 12H), 6.71 (m, 9H), 2.39 (s, 9H). ^{31}P{^{1}H}-NMR (CD_2Cl_2, 293 K, 162 MHz): -0.58. ESI-MS: 340.05 (100%, $[Cu(\mu\text{-dpPyMe})]^+$ calcd for $C_{18}H_{16}NPCu$), 617.17 (65%, $[Cu(\mu\text{-dpPyMe})_2]^+$ calcd for $C_{36}H_{32}N_2P_2Cu$), 894.29 (25%, $[Cu(\mu\text{-dpPyMe})_3]^+$ calcd for $C_{54}H_{48}N_3P_3Cu$). Anal. Calcd for $C_{72}H_{63}N_3P_4OCu_2B_2F_8$: C, 61.29; H, 4.50; N, 2.98. Found: C, 61.12; H, 4.37; N, 2.99.

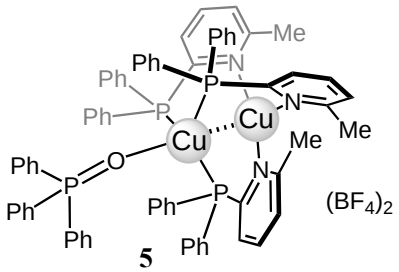

5

Compound **6**. A solution of **1** (150 mg, 0.128 mmol) and L6 (16 mL, 0.135 mmol) in CH_2Cl_2 (20 mL) was stirred at room temperature for 30 min. and evaporated to dryness. The resulting solid was dissolved in CH_2Cl_2 (20 mL) and the solution evaporated (3 X). The resulting solid was dried under high vacuum. Recrystallization by vapor diffusion of Et_2O into a CH_2Cl_2 solution of the crude product gave **2** (130 mg, 81%). Colorless crystals. ^{1}H-NMR (CD_2Cl_2, 300 MHz, 293 K): 7.62 (t, *J* = 7Hz, 3H), 7.44 (m, 6H), 7.31 (m, 12H), 7.18 (m, 4H), 7.10 (m, 11H), 6.98 (d, *J* = 7Hz, 3H), 3.78 (s, 2H), 2.45 (s, 9H). ^{31}P{^{1}H}-NMR (CD_2Cl_2, 293 K, 162 MHz): 3.10. ESI-MS: 340.05 (100%, $[Cu(\mu\text{-dpPyMe})]^+$ calcd for $C_{18}H_{16}NPCu$), 617.17 (55%, $[Cu(\mu\text{-dpPyMe})_2]^+$ calcd for $C_{36}H_{32}N_2P_2Cu$), 894.29 (15%, $[Cu(\mu\text{-dpPyMe})_3]^+$ calcd for $C_{54}H_{48}N_3P_3Cu$). Anal. Calcd for $C_{56}H_{46}BrN_4P_3Cu_2B_2F_8$: C, 53.87; H, 3.71; N, 4.49. Found: C, 53.59; H, 3.66; N, 4.34.

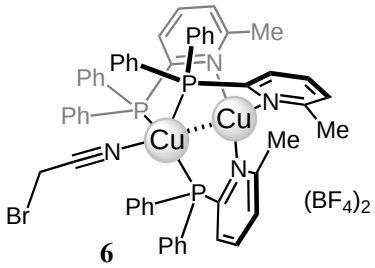

6

X-Ray crystal structures

(A) $[Cu_2(\mu\text{-dpPyMe})_2(CH_3CN)_2](BF_4)_2$. Crystals suitable for X-ray crystal-structure analysis were obtained by slow diffusion of Et_2O into a CH_2Cl_2 solution of the crude mixture obtained from dpPyMe (1 equiv.) and $Cu(CH_3CN)_4BF_4$ (1 equiv.). Data were collected at 173 K on a Bruker APEX-II CCD diffractometer (Mo-Kα radiation, λ = 0.71073 Å). The structure was solved by direct methods (SHELXS-97) and refined against F^2 using the SHELXL-97 software. The non-hydrogen atoms were refined anisotropically, using weighted full-matrix least-squares on F^2. The H-atoms were included in calculated positions and treated as ridig atoms using SHELXL default parameters. The crystallographic data are reported in Table 7.

(B) **1**.$(CH_2Cl_2)_2$. Crystals suitable for X-ray crystal-structure analysis were obtained by slow diffusion of Et_2O into a CH_2Cl_2 solution of **1**. Data were collected at 173 K on a Bruker APEX-II CCD diffractometer (Mo-Kα radiation, λ = 0.71073 Å). The structure was solved by direct methods (SHELXS-97) and refined against F^2 using the SHELXL-97 software. The non-hydrogen atoms were refined anisotropically, using weighted full-matrix least-squares on F^2. The H-atoms were included in calculated positions and treated as ridig atoms using SHELXL default parameters. The crystallographic data are reported in Table 7.

(C) **2**.CH_2Cl_2. Crystals suitable for X-ray crystal-structure analysis were obtained by slow diffusion of Et_2O into a CH_2Cl_2 solution of **2**. Data were collected at 173 K on a Bruker APEX-II CCD diffractometer (Mo-Kα radiation, λ = 0.71073 Å). The structure was solved by direct methods (SHELXS-97) and refined against F^2 using the SHELXL-97 software. The non-hydrogen atoms were refined anisotropically, using weighted full-matrix least-squares on F^2. The H-atoms were included in calculated positions and treated as ridig atoms using SHELXL default parameters. The crystallographic data are reported in Table 7.

(D) **4**.CH_2Cl_2. Crystals suitable for X-ray crystal-structure analysis were obtained by slow diffusion of Et_2O into a CH_2Cl_2 solution of **4**. Data were collected at 173 K on a Bruker APEX-II CCD diffractometer (Mo-Kα radiation, λ = 0.71073 Å). The structure was solved by direct methods (SHELXS-97) and refined against F^2 using the SHELXL-97 software. The non-hydrogen atoms were refined anisotropically, using weighted full-matrix least-squares on

F^2. The H-atoms were included in calculated positions and treated as ridig atoms using SHELXL default parameters. The crystallographic data are reported in Table 7.

(E) **5**.$CHCl_3$. Crystals suitable for X-ray crystal-structure analysis were obtained by slow diffusion of benzene into a $CHCl_3$ solution of **5**. Data were collected at 173 K on a Bruker APEX-II CCD diffractometer (Mo-Kα radiation, λ = 0.71073 Å). The structure was solved by direct methods (SHELXS-97) and refined against F^2 using the SHELXL-97 software. The non-hydrogen atoms were refined anisotropically, using weighted full-matrix least-squares on F^2. The H-atoms were included in calculated positions and treated as ridig atoms using SHELXL default parameters. The crystallographic data are reported in Table 7.

Table 7A. Crystallographic and structure refinement data for (A) $[Cu_2(\mu\text{-dpPyMe})_2(CH_3CN)_2](BF_4)_2$, (B) **1**.$(CH_2Cl_2)_2$ and (C) **2**.CH_2Cl_2.

	(A)	(B)	(C)
Chemical formula	$C_{40}H_{38}Cu_2N_4P_2(BF_4)_2$	$C_{56}H_{51}Cu_2N_4P_3B_2F_8(CH_2Cl_2)_2$	$C_{61}H_{53}Cu_2N_4P_3B_2F_8CH_2Cl_2$
M (g/mol)	937.38	1343.47	1320.61
Crystal system	Triclinic	Monoclinic	Triclinic
Space group	P -1	P 2_1/C	P -1
a (Å)	8.9862(2)	20.8139(5)	12.7009(2)
b (Å)	10.7970(3)	12.7855(4)	15.6490(5)
c (Å)	21.5188(9)	21.9411(5)	17.2354(4)
α (°)	92.257(2)	90	78.8930(10)
β (°)	90.900(2)	94.614(2)	68.421(2)
γ (°)	91.758(2)	90	67.333(2)
V ($Å^3$)	2084.94(11)	5820.0(3)	2934.32(12)
Z	2	4	2
F(000)	952	2736	1348
Reflections collected	21396	32994	29406
θ range for data collection (°)	1.89-27.52	1.84-27.44	1.27-27.49
Independent reflections	9535	13271	13426
Independent reflections having I > 2σ(I)	6578	8524	10293
Number of parameters	515	734	724
$R_1(F^2)$	0.0692	0.0599	0.0695
$wR_2(F^2)$	0.1779	0.1274	0.1855

CHAPTER 2

Dinuclear Cu^{I} complexes prepared from 2-diphenylphosphino-6-methylpyridine

Table 7B. Crystallographic and structure refinement data for (D) **4**.$(CH_2Cl_2)_2$ and (E) **5**.$CHCl_3$.

	(D)	(E)
Chemical formula	$C_{61}H_{52}Cu_2N_5O_2P_3B_2F_8CH_2Cl_2$	$C_{72}H_{63}Cu_2N_3OP_4B_2F_8CHCl_3$
M (g/mol)	1365.61	1530.20
Crystal system	Triclinic	Hexagonal
Space group	P -1	P 63
a (Å)	12.6676(4)	13.2812(3)
b (Å)	15.8009(5)	13.2812(3)
c (Å)	17.5506(5)	22.1734(8)
α (°)	88.648(2)	90
β (°)	69.2410(10)	90
γ (°)	66.797(2)	120
V ($Å^3$)	1991.51(16)	3387.17(16)
Z	2	2
F(000)	1392	1564
Reflections collected	28573	18349
θ range for data collection (°)	1.25-27.49	1.77-27.47
Independent reflections	13684	4398
Independent reflections having I > 2σ(I)	9687	3410
Number of parameters	772	279
$R_1(F^2)$	0.0744	0.0783
$wR_2(F^2)$	0.1980	0.2102

5. References

1) For selected reviews, see: a) H. A. McManus, P. J. Guiry, *Chem. Rev*. **2004**, *104*, 4151; b) G. Helmchen, A. Pfaltz, *Acc. Chem. Res*. **2000**, *33*, 336; c) F. Speiser, P. Braunstein, L. Saussine, *Acc. Chem. Res*. **2005**, *38*, 784; d) P. J. Guiry, C. P. Saunders, *Adv. Synth. Catal*. **2004**, *346*, 497.

2) G. R. Newkome, *Chem. Rev*. **1993**, *93*, 2067.

3) S. Maggini, *Coord. Chem. Rev*. **2009**, *253*, 1793.

4) a) N. G. Gianneschi, M. S. Masar III, C. A. Mirkin, *Acc. Chem. Res*. **2005**, *38*, 825; b)

5) a) Q.-M. Wang, Y.-A. Lee, O. Crespo, J. Deaton, C. Tang, H. J. Gysling, M. C. Gimeno, C. Larraz, M. D. Villacampa, A. Laguna, R. Eisenberg, *J. Am. Chem. Soc.* **2004**, *126*, 9488; b) V. W.-W. Yam, K.-L. Yu, E. C.-C. Cheng, P. K.-Y. Yeung, K.-K. Cheung, N. Zhu, *Chem. Eur. J*. **2002**, *8*, 4121; c) L. Qin, Q. Zhang, W. Sun, J. Wang, C. Lu, Y. Cheng, L. Wang, *Dalton Trans*. **2009**, 9388;

6) Y.-J. Li, Z.-Y. Deng, X.-F. Xu, H.-B. Wu, Z.-X. Cao, Q.-M. Wang, *Chem. Commun*. **2011**, *47*, 9179.

7) a) S. B. Harkins, J. C. Peters, *J. Am. Chem. Soc.* **2005**, *127*, 2030; b) A. J. M. Miller, J. L. Dempsey, J. C. Peters, *Inorg. Chem.* **2007**, *46*, 7244; c) J. C. Deaton, S. C. Switalski, D. Y. Kondakov, R. H. Young, T. D. Pawlik, D. J. Giesen, S. B. Harkins, A. J. M. Miller, S. F. Mickenberg, J. C. Peters, *J. Am. Chem. Soc*. **2010**, *132*, 9499.

8) T. Tsukada, C. Nishigata, K. Arai, T. Tsabomura, *Polyhedron* **2009**, *28*, 7.

9) C. Chen, K. Wang, P. Jiang, G. Song, H. Zhu, *Inorg. Chem. Commun*. **2012**, *17*, 116.

10) a) D. V. Scaltrito, D. W. Thompson, J. A. O'Callaghan, G. J. Meyer, *Coord. Chem. Rev*. **2000**, *208*, 243; b) N. Armaroli, *Chem. Soc. Rev.* **2001**, *30*, 113; c) N. Armaroli, G. Accorsi, F. Cardinali, A. Listorti, *Top. Curr. Chem.* **2007**, *280*, 69; d) A. Lavie-Cambot, M. Cantuel, Y. Leydet, G. Jonusauskas, D. M. Bassani, N. D. McClenaghan, *Coord. Chem Rev*. **2008**, *252*, 2572; e) A. Barbieri, G. Accorsi, N. Armaroli, *Chem. Commun.* **2008**, 2185.

11) E. Lastra, M. P. Gamasa, J. Gimeno, M. Lanfranchi, A. Tiripicchio, *J. Chem. Soc., Dalton Trans*. **1989**, 1499.

12) a) M. Maekawa, M. Munakata, S. Kitagawa, T. Yonazawa, *Bull. Chem. Soc. Jpn*. **1991**, *64*, 2286; b) M. A. Jalil, T. Yamada, S. Fujinami, T. Honjo, H. Nishikawa, *Polyhedron* **2001**, *20*, 627; c) J. S. Field, R. J. Haines, B. Warwick, M. M. Zulu, Polyhedron **1996**, *15*, 3741; d) A. Bakhoda, N. Safari, V. Amani, H. R. Khavasi, M. Gheidi, *Polyhedron* **2011**, *30*, 2950.

13) a) W.-H. Chan, S.-M. Peng, C.-M. Che, *Dalton Trans*. **1998**, 2867; b) M. A. Jalil, T. Yamada, S. Fujinami, T. Honjo, H. Nishikawa, *Polyhedron* **2001**, *20*, 627.

14) Z. Z. Zhang, H. K. Wang, Z. Xi, X. K. Yao, R. J. Wang, *J. Organomet. Chem*. **1989**, *376*, 123.

15) a) J. P. Farr, F. E. Wood, A. L. Balch, *Inorg. Chem.* **1983**, *22*, 3387 ; b) M. M. J. P. Farr, Olmstead, A. L. Balch, *J. Am. Chem. Soc.* **1980**, *102*, 6654, c) A. Maisonnat, J. P. Farr, A. L. Balch, *Inorg. Chim. Acta* **1981**, *53*, L217.

16) For reviews, see: E. C. Constable, *Tetrahedron* **1992**, *48*, 10013; C. Piguet, G. Bernardinelli, G. Hopfgartner, *Chem. Rev*. **1997**, *97*, 2005; M. Albrecht, *Chem. Rev*. **2001**, *101*, 3457.

17) S. Sculfort, P. Braunstein, *Chem. Soc. Rev*. **2011**, *40*, 2741.

18) N. Nishio, M. Hirota, Y. Umezawa, *The CH/π interaction: Evidence, Nature and Consequences* Wiley-VCH: New York, **1998**.

19) N. Armaroli, G. Accorsi, G. Bergamini, P. Ceroni, M. Holler, O. Moudam, C. Duhayon, B. Delavaux-Nicot, J.-F. Nierengarten, *Inorg. Chim. Acta* **2007**, *360*, 1032.

20) a) D. G. Cuttell, S.-M. Kuang, P. E. Fanwick, D. R. McMillin, R. A. Walton, *J. Am. Chem. Soc.* **2002**, *124*, 6; b) S.-M. Kuang, D. G. Cuttell, D. R. McMillin, P. E. Fanwick, R. A. Walton, *Inorg. Chem*. **2002**, *41*, 3313.

21) D. Felder, J. F. Nierengarten, F. Barigelletti, B. Ventura, N. Armaroli, *J. Am. Chem. Soc.* **2001**, *123*, 6291.

22) G. A. Crosby, J. N. *J.* Demas, *Phys. Chem.* **1971**, *75*, 991.

23) J. C. de Mello, H. F. Wittmann, R. H. Friend, *Adv. Mater*. **1997**, *9*, 230.

Heteroleptic Cu(I) Complexes Prepared From Phenanthroline and Bis-Phosphine Ligands

1. Introduction

Cu(I) complexes prepared from phosphines and ligands such as 2,2'-bipyridine (bipy) or 1,10-phenanthroline (phen) have been investigated in details more then 30 years ago.[1,2] Initially, such systems generally prepared with PPh_3 as the P-ligands looked promising because they exhibit long lifetimes in the solid state as well as in frozen solution.[1] They also display interesting photochemical properties in relation to light-induced electron transfer.[2] However, detailed studies have shown that exciplex quenching is important even for compounds incorporating bulky phosphines such as PPh_3.[1] Moreover, the speciation of these compounds was hard to control even in non-coordinating solvents such as CH_2Cl_2.[1] McMillin and co-workers have also reported mixed-ligand Cu(I) complexes prepared from 1,10-phenanthroline derivatives and bis[2-(diphenylphosphino)-phenyl]ether (POP).[3,4] Not only ligand dissociation is essentially suppressed for the complexes prepared from this particular chelating bis-phosphine ligand,[4] but these compounds are also characterized by remarkably high emission quantum yields from their long lived metal-to-ligand charge transfer (MLCT) excited state. Following this key finding, numerous examples of related heteroleptic Cu(I) complexes have been prepared from bis-phosphine and aromatic diimine ligands.[6-9] Their outstanding emission properties have been exploited to produce efficient light emitting devices thus showing that inexpensive and earth-abundant Cu(I) is an attractive alternative to noble metal ions for such applications.[6-7] As part of this research, our group has investigated the preparation of heteroleptic Cu(I) complexes combining various phenanthroline derivatives (NN) with different bis-phosphine ligands (PP).[8,10-12] During the course of these studies, it was found that an equilibrium between the homoleptic and the heteroleptic complexes is sometimes observed in solution. This represents actually a major limitation for the preparation of stable $[Cu(NN)(PP)]^+$ derivatives.[13] We became thus interested in a deeper understanding of the structural parameters influencing the stability of these compounds and decided to systematically reinvestigate their preparation. This knowledge is indeed essential to produce

new stable materials. At the same time, systematic investigations of the electronic properties of the prepared $[Cu(NN)(PP)]^+$ derivatives have been performed to elucidate the key parameters allowing to obtain new luminescent materials.

2. Results and discussion

2.1. Synthesis and characterization

Starting from the library of phenanthroline derivatives and PP ligands depicted in Figure 1, the possibility to prepare heteroleptic $[Cu(NN)(PP)]^+$ derivatives was systematically investigated. The six selected bis-phosphine ligands (dppm, dppe, dppp, dppb, dppFc and POP) are all commercially available as well as 1,10-phenanthroline (**phen**), neocuproine (2,9-dimethyl-1,10-phenanthroline, **dmp**) and bathophenanthroline (4,7-diphenyl-1,10-phenanthroline, **Bphen**). 2,9-Diphenethyl-1,10-phenanthroline[14] (**dpep**) and 2,9-diphenyl-1,10-phenanthroline[8,15] (**dpp**) were prepared according to reported procedures.

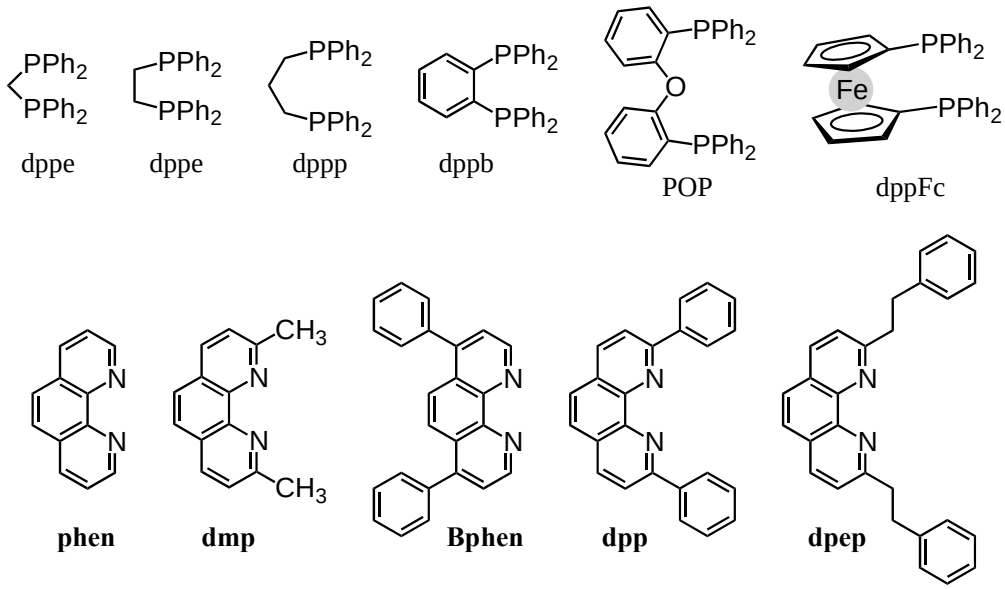

Figure 1. The library of NN and PP ligands used for the preparation of heteroleptic $[Cu(NN)(PP)]^+$ derivatives.

2,9-Unsubstituted-1,10-phenanthroline derivatives (phen and Bphen). The treatment of **phen** with an equimolar amount of the appropriate bis-phosphine ligand (dppe, dppp, dppb, POP or dppFc) and $Cu(CH_3CN)_4BF_4$ in CH_2Cl_2/CH_3CN gave the corresponding [Cu(**phen**)(PP)]BF_4 derivatives (Scheme 1). ^{1}H NMR analysis of the crude mixtures thus obtained indicated the formation of a single complex in all the cases. The heteroleptic complexes were then isolated in a pure form by recrystallization in CH_2Cl_2/Et_2O. Similar results were obtained when **Bphen** was used as the NN ligand, the [Cu(**Bphen**)(PP)]BF_4 complexes were thus prepared in excellent isolated yields.

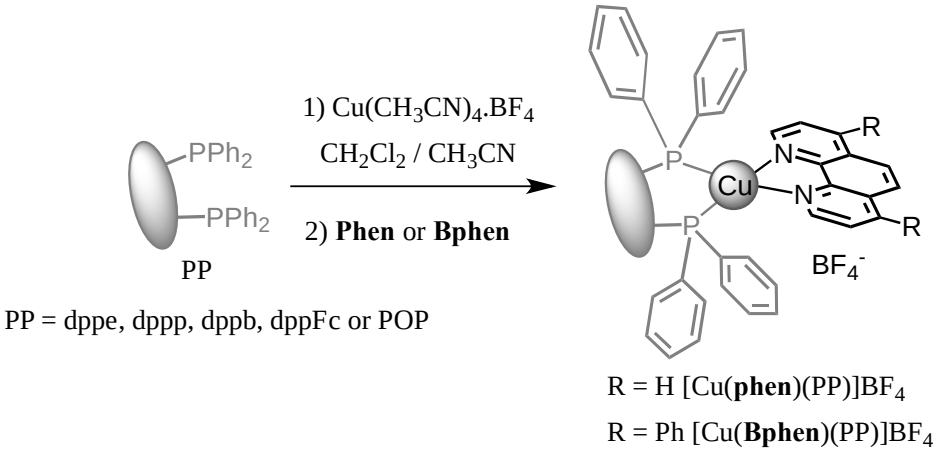

Scheme 1. Preparation of heteroleptic $[Cu(NN)(PP)]^+$ derivatives from **phen** and **Bphen**.

The [Cu(**phen**)(PP)]BF_4 and [Cu(**Bphen**)(PP)]BF_4 complexes were characterized by ^{1}H-, ^{13}C- and ^{31}P NMR spectroscopy, mass spectrometry and elemental analysis. Typical examples of ^{1}H and ^{31}P NMR spectra are shown in Figure 2. For all the compounds, the ^{31}P NMR spectrum recorded at room temperature revealed a single resonance for the two equivalent P atoms of the chelating PP ligand. Cooling the samples to -60°C did not give rise to significant changes and no additional signals could be detected. The ^{1}H NMR spectra were also consistent with the proposed structures. Analysis of the integration of the ^{1}H NMR spectra revealed that, in all the cases, both PP and NN ligands are present in a 1:1 ratio. As shown in Figure 2, a slight line broadening is observed for the ^{1}H NMR resonance of the phenanthroline proton H(2) of all the complexes, this effect is most likely due to the proximity of the quadrupolar $^{63/65}$Cu nuclei.[16] In contrast, all the other signals in the ^{1}H NMR

spectra of complexes [Cu(NN)(PP)]BF_4 (NN = **phen** or **Bphen**) are well resolved and show no signs of broadening.

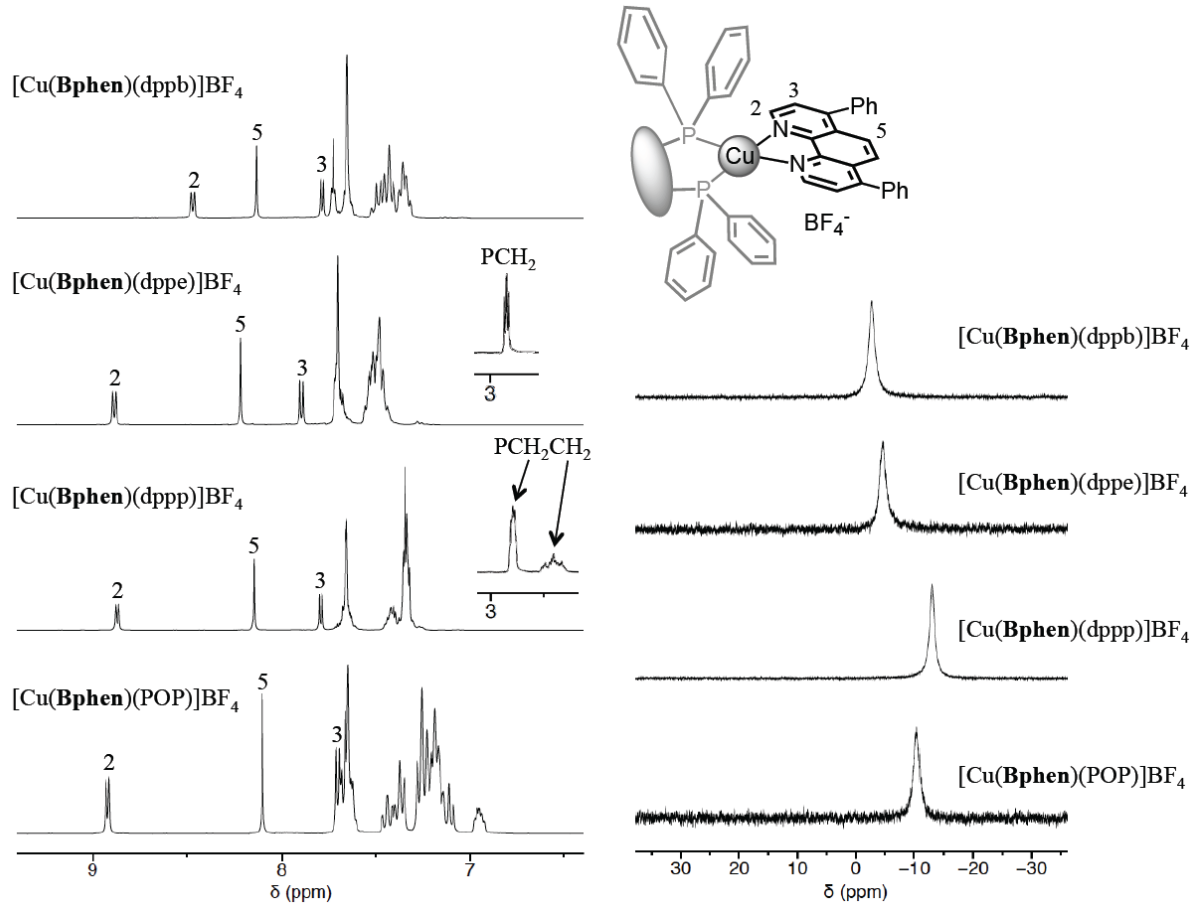

Figure 2. ^{1}H (left) and ^{31}P (right) NMR spectra of [Cu(**Bphen**)(PP)]$^{+}$ (PP = dppb, dppe, dppp and POP) recorded in CD_2Cl_2 at room temperature.

It can also be noted that the signal of proton H(2) is shielded in [Cu(**Bphen**)(PP)]BF_4 when compared to the corresponding signal in **Bphen** as a result of the ring current effect of the phenyl groups of the PP ligand on this particular proton. The shielding ranges from 0.4 to 0.9 ppm, the most important one being observed with dppb. Actually, the bite angles being different for each of the chelating PP ligands, the relative orientation of the phenyl groups is not the same in the various complexes and thus the effect on the chemical shift of H(2) is specific for each PP ligand. Importantly, the NMR spectra indicate also that there is no significant ligand exchange in solution leading to the formation of the corresponding homoleptic species. Finally, the structure of all the complexes was confirmed by FAB mass

spectrometry. For all the compounds, the mass spectrum displays a singly charged ion peak assigned to $[Cu(NN)(PP)]^+$. Other minor peaks corresponding to $[Cu(NN)]^+$ and $[Cu(PP)]^+$ are also systematically observed in the mass spectra.

X-ray quality crystals of [Cu(**phen**)(dppb)]BF_4 were obtained by vapor diffusion of Et_2O into a CH_2Cl_2 solution of the complex. As shown in Figure 3, the copper atom is in a highly distorted tetrahedral environment in which both the phenanthroline and the dppb are chelating ligands. The distorsion mainly arises from the restricted chelate bite angles of both ligands (P(1)-Cu(1)-P(2): 88.11(3) and N(1)-Cu(1)-N(2): 81.9(1)°). The angle between the planes P(1)-Cu(1)-P(2) and (N1)-Cu(1)-(N2) is 85.6° and the bridging phenyl ring of dppb is tilted by *ca*. 31.6° with respect to the P(1)-Cu(1)-P(2) plane.

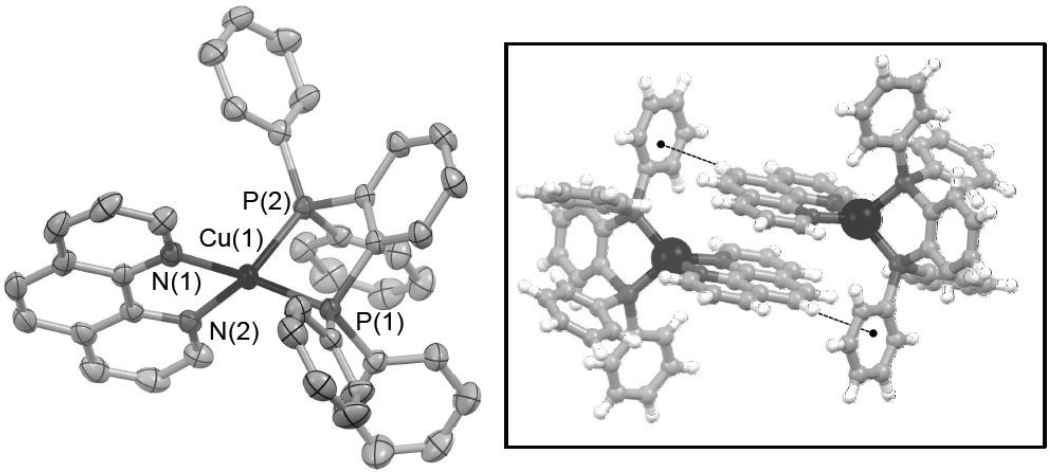

Figure 3. ORTEP plot of the structure of [Cu(**phen**)(dppb)]BF_4 (the H atoms and the counteranion are omitted for clarity, thermal ellipsoids are drawn at the 50% probability level). The inset shows the pairwise stacking of the phenanthroline ligand of neighboring $[Cu(\textbf{phen})(dppb)]^+$ cations. Selected bond lengths: Cu(1)-P(1): 2.2382(9), Cu(1)-P(2): 2.2487(9), Cu(1)-N(1): 2.040(3), Cu(1)-N(2): 2.049(3) Å; selected bond angles: P(1)-Cu(1)-P(2): 88.11(3), P(1)-Cu(1)-N(1): 124.61(8) , P(1)-Cu(1)-N(2): 129.37(8), P(2)-Cu(1)-N(1): 120.88(7), P(2)-Cu(1)-N(2): 116.11(7), N(1)-Cu(1)-N(2): 81.9(1)°.

Inspection of the crystal packing reveals a dimeric arrangement of the $[Cu(\textbf{phen})(dppb)]^+$ cations in which the phenanthroline ligands partially overlay one another, the average distance between the mean planes of the two phenanthroline ligands being *ca*. 3.5 Å. (Figure

3). A similar arrangement has been already reported for the X-ray crystal structures of [Cu(**phen**)(POP)]BF_4[3] and [Cu(**phen**)(dppFc)]BF_4.[10] In all the cases, the components of the pair are related to one another through a center of inversion that is located between the planes of the phenanthroline rings. As shown in Figure 3, two notable C–H/π intermolecular interactions are also observed between neighbouring [Cu(**phen**)(dppb)]$^+$ cations. These interactions involve one hydrogen atom of the phenanthroline unit and a phenyl group of the dppb ligand belonging to the neighbouring cations. These phenanthroline hydrogen atoms are located at 2.8 Å from the center of their neighbouring phenyl ring.

In the particular case of dppm, the reaction with an equimolar amount of $Cu(CH_3CN)_4BF_4$ and **phen** in CH_2Cl_2/CH_3CN gave the dinuclear complex [Cu_2(**phen**)$_2$(μ-dppm)$_2$]$(BF_4)_2$ (Scheme 2). Similarly, [Cu_2(**Bphen**)$_2$(μ-dppm)$_2$]$(BF_4)_2$ was obtained when the reaction was performed with **Bphen**. Indeed, dppm can chelate metals but the four-membered ring in such complexes is strained and the ligand has a greater tendency to act either as a monodentate ligand or as a bridging bidentate ligand.[17] Whereas a few examples of Cu(I) complexes in which dppm is a chelate ligand have been reported,[11] dinuclear Cu(I) complexes with two bridging dppm ligands are by far more common.[18,19] It is also interesting to note that the chelating tendency of the $Ph_2P(CH_2)_nPPh_2$ ligands observed for n = 2 and 3 in the particular case of these Cu(I) complexes decreases when the chain length further increases. Effectively, dinuclear complexes have been reported for 1,4-bis(diphenylphosphino)butane (n = 4).[5]

The dinuclear complexes were characterized by NMR spectroscopy, mass spectrometry and elemental analysis. The ^{1}H and ^{31}P NMR spectra of [Cu_2(**Bphen**)$_2$(μ-dppm)$_2$]$(BF_4)_2$ recorded in CD_2Cl_2 at room temperature are depicted in Figure 4. In addition to the signals corresponding to phenyl groups of the dppm moieties, the ^{1}H NMR spectrum of [Cu_2(**phen**)$_2$(μ-dppm)$_2$]$(BF_4)_2$ is characterized by four sets of signals in a typical pattern for a 4,7-diphenyl-1,10-phenanthroline and a broad singlet at δ = 3.88 ppm for the dppm ligands. The ^{31}P NMR of this compound gave a broad singlet signal at room temperature (δ = -6.62 ppm, $\Delta\nu_{1/2}$ = 216 Hz). Cooling the sample to 200 K did not give rise to additional peaks and no couplings were observed (*e.g.* $^2J_{P–C–P}$ or $^2J_{P–Cu–P}$) at all temperatures. This shows that the four P atoms are chemically and magnetically equivalent, thus it can be deduced that the compound remains intact in solution.

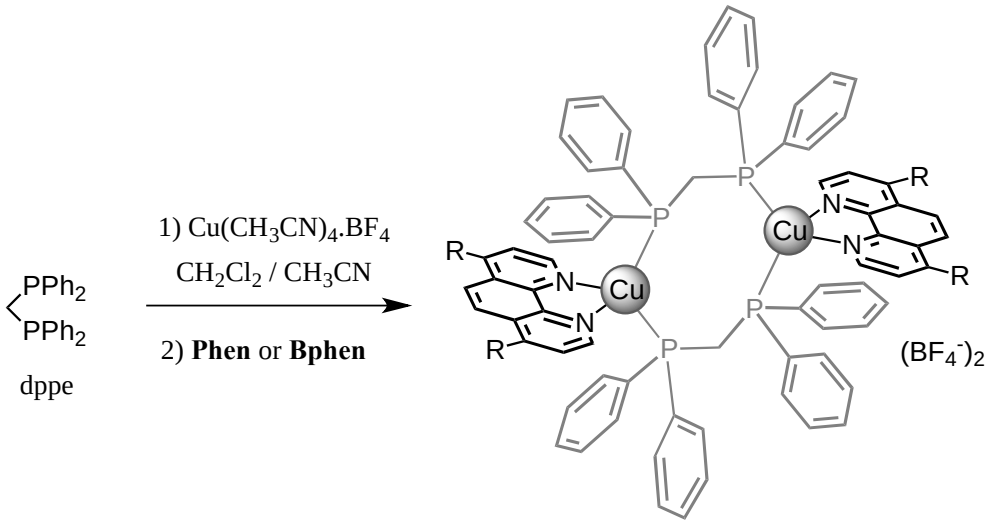

Scheme 2. Preparation of $[Cu_2(\mathbf{phen})_2(\mu\text{-dppm})_2](BF_4)_2$ and $[Cu_2(\mathbf{Bphen})_2(\mu\text{-dppm})_2](BF_4)_2$.

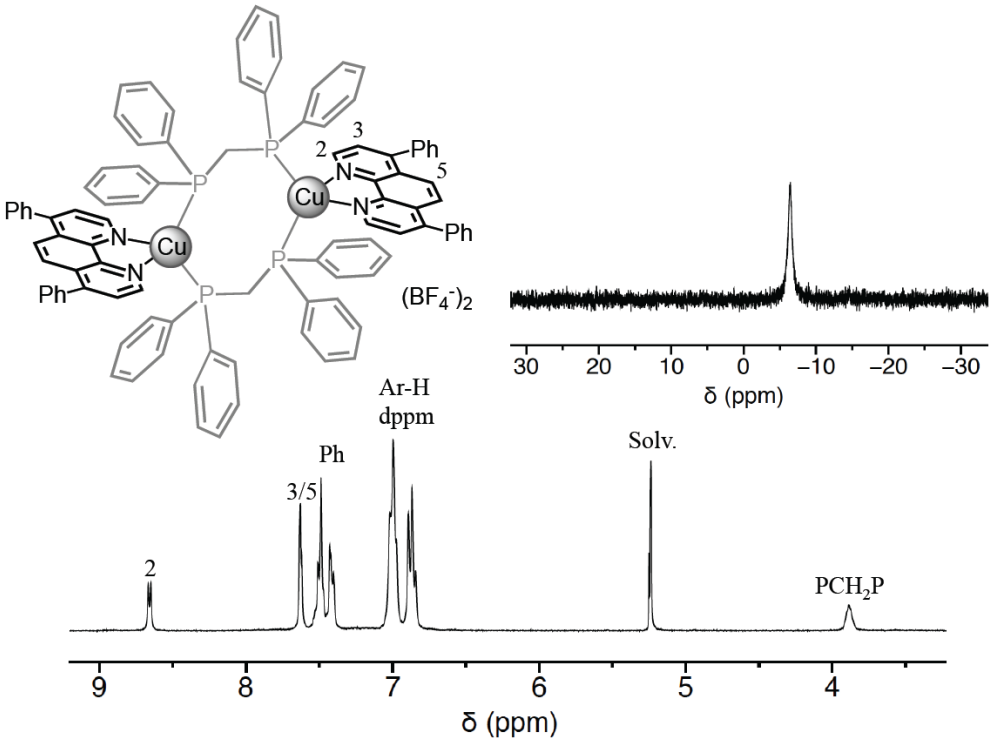

Figure 4. ^{1}H (bottom) and ^{31}P (top right) NMR spectra of $[Cu_2(\mathbf{Bphen})_2(\mu\text{-dppm})_2](BF_4)_2$ recorded in CD_2Cl_2 at room temperature.

CHAPTER 3

Heteroleptic Cu(I) complexes prepared from phenanthroline and bis-phosphine ligands

For $[Cu_2(\mathbf{Bphen})_2(\mu\text{-dppm})_2](BF_4)_2$, crystals suitable for X-ray crystal-structure analysis were obtained by slow diffusion of Et_2O into a CH_2Cl_2 solution of the complex. Two views of the $[Cu_2(\mathbf{Bphen})_2(\mu\text{-dppm})_2]^{2+}$ dication are shown in Figure 5. Selected bond lengths and angles are summarized in Table 1. The two dppm moieties are bridging two $[Cu(\mathbf{Bphen})]^+$ cations thus forming a eight-membered $Cu_2P_4C_2$ metallacycle. With a Cu(1)-Cu(2) distance of 4.464 Å, there are no Cu-Cu interactions in $[Cu_2(\mathbf{Bphen})_2(\mu\text{-dppm})_2]^{2+}$. Notable intramolecular π-π interactions involve two phenyl rings within both of the dppm ligands. The average distance between the mean planes of the aromatic rings is *ca*. 3.6 Å in both cases. In addition, two intramolecular face-to-face π-π interactions are also observed between both phenanthroline ligands and a phenyl unit of one of their neighboring PPh_2 moieties. The establishment of these interactions is at the origin of the particularly large P-Cu-P angles. As a result, the metallacycle adopts a peculiar folded conformation and both phenanthrolines are not anymore in a relative face-to-face orientation as typically observed in the X-ray crystal structures of related compounds.[19]

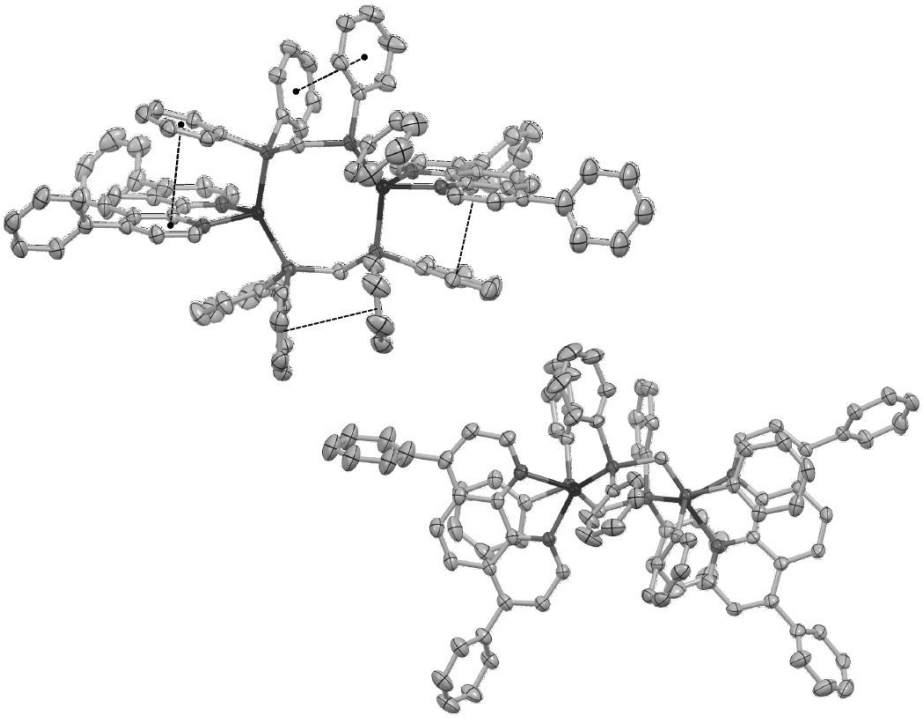

Figure 5A. Two views of the structure of $[Cu_2(\mathbf{Bphen})_2(\mu\text{-dppm})_2](BF_4)_2.CH_2Cl_2$ (the H atoms, the counteranions and the CH_2Cl_2 molecule are omitted for clarity, thermal ellipsoids of the ORTEP plot are drawn at the 50% probability level).

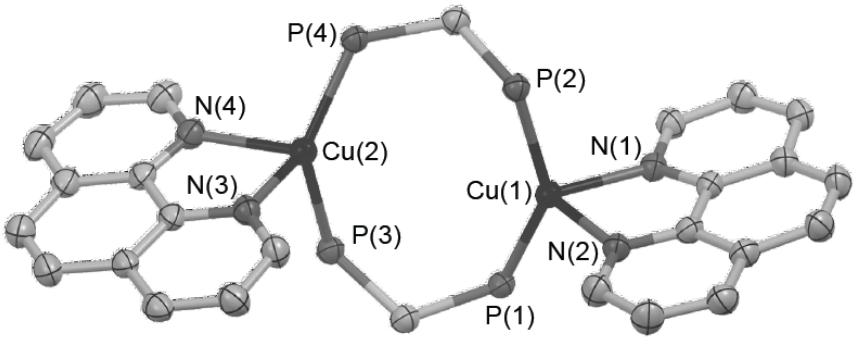

Figure 5B. Details of the coordination sphere around the Cu(I) cations in the structure of $[Cu_2(\mathbf{Bphen})_2(\mu\text{-dppm})_2](BF_4)_2.CH_2Cl_2$.

Table 1. Bond distances (Å) and bond angles (°) within the coordination sphere of $[Cu_2(\mathbf{Bphen})_2(dppm)_2](BF_4)_2.CH_2Cl_2$ (see Figure 5B for the numbering).

Selected bond lengths		Selected bond angles	
Cu(1)-P(1)	2.2182(7)	P(1)-Cu(1)-P(2)	141.34(3)
Cu(1)-P(2)	2.2368(8)	P(1)-Cu(1)-N(1)	105.86(7)
Cu(1)-N(1)	2.091(2)	P(1)-Cu(1)-N(2)	108.25(7)
Cu(1)-N(2)	2.081(3)	P(2)-Cu(1)-N(1)	103.49(7)
Cu(2)-P(3)	2.2844(7)	P(2)-Cu(1)-N(2)	101.25(7)
Cu(2)-P(4)	2.2296(8)	N(1)-Cu(1)-N(2)	79.70(9)
Cu(2)-N(3)	2.081(3)	P(3)-Cu(2)-P(4)	134.83(3)
Cu(2)-N(4)	2.130(2)	P(3)-Cu(2)-N(3)	97.69(7)
		P(3)-Cu(2)-N(4)	98.25(7)
		P(4)-Cu(2)-N(3)	122.56(7)
		P(4)-Cu(2)-N(4)	108.03(7)
		N(3)-Cu(2)-N(4)	79.10(9)

CHAPTER 3

Heteroleptic Cu(I) complexes prepared from phenanthroline and bis-phosphine ligands

2,9-Disubstituted-1,10-phenanthroline derivatives (dmp, dpep and dpp). The reaction of **dmp, dpep** and **dpp** with the PP ligands and $Cu(CH_3CN)_4BF_4$ was systematically investigated. A solution of the appropriate bis-phosphine ligand (1 equiv.) and $Cu(CH_3CN)_4BF_4$ (1 equiv.) in CH_2Cl_2/CH_3CN was stirred for 0.5 h, then **dmp, dpep** or **dpp** (1 equiv.) was added. After 1 h, the solvents were evaporated. The products were analyzed as received by ^1H NMR. The relative proportion of the different possible complexes, i.e. $[Cu(NN)(PP)]BF_4$, $[Cu(NN)_2]BF_4$ and $[Cu(PP)_2]BF_4$, was deduced from the comparison with the ^1H NMR spectrum of the corresponding $[Cu(NN)_2]BF_4$ derivative recorded in the same solvent. The results are summarized in Table 2 and typical ^1H NMR spectra are depicted in Figure 6.

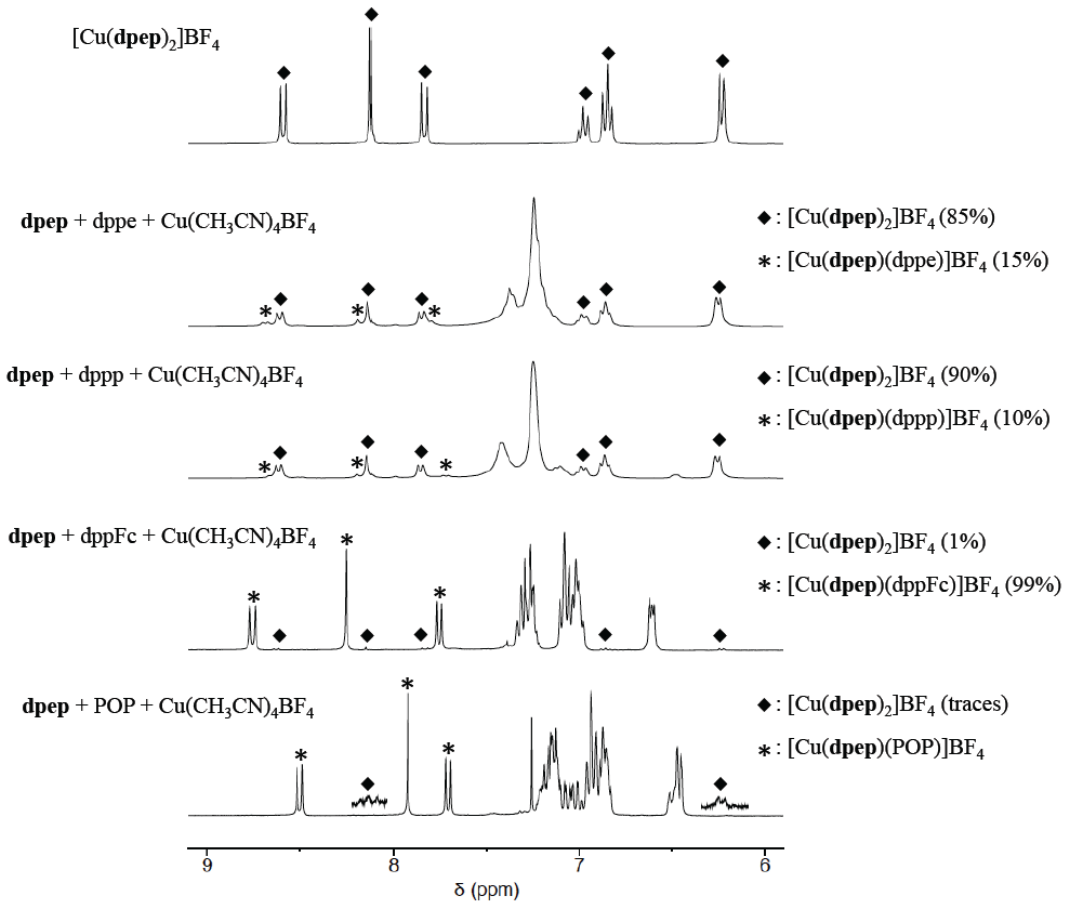

Figure 6. Aromatic region of the ^1H NMR spectra of the crude products obtained after the treatment of various PP ligands with $Cu(CH_3CN)_4BF_4$ and **dpep**. For comparison purposes, the ^1H NMR spectrum of $[Cu(\mathbf{dpep})_2]BF_4$ (top) is also represented.

Whereas the heteroleptic $[Cu(NN)(PP)]^+$ complexes were the only reaction products whatever the PP ligand when starting from 2,9-unsubstituted-1,10-phenanthrolines, the situation became completely different when 2,9-substituted-1,10-phenanthroline derivatives were used as starting material. Effectively, when using **dmp** and **dpep** as reagents, a mixture of $[Cu(NN)(PP)]BF_4$, $[Cu(NN)_2]BF_4$ and $[Cu(PP)_2]BF_4$, was always obtained and their relative proportion found to be highly dependent on the bis-phosphine ligand (Table 2). In contrast, homoleptic complexes were obtained as the only detectable products when **dpp** was used as NN ligand. Obviously, steric effects resulting from the presence of the bulky phenyl rings on the **dpp** ligand destabilize the heteroleptic $[Cu(\mathbf{dpp})(PP)]^+$ complexes. In addition to the remarkable thermodynamic stability of $[Cu(\mathbf{dpp})_2]BF_4$,[20] this negative steric effect drives the dynamic complexation scenario towards the formation of homoleptic complexes almost exclusively.

Table 2. Proportion of heteroleptic complex obtained upon reaction of the various PP ligands with $Cu(CH_3CN)_4BF_4$ and **dmp**, **dpep** or **dpp** as deduced from the integration of the ^1H NMR spectra of the crude product mixture.

	dmp	**dpep**	**dpp**
dppm	70%	10%	traces
dppe	80%	15%	traces
dppp	80%	10%	traces
dppb	65%	5%	traces
dppFc	> 99%	> 99%	traces
POP	> 99.5%	> 99.5%	traces

dppFc and POP. $[Cu(\mathbf{dmp})(dppFc)]BF_4$,[10] $[Cu(\mathbf{dmp})(POP)]BF_4$,[3,4] $[Cu(\mathbf{dpep})(dppFc)]BF_4$[10] and $[Cu(\mathbf{dpep})(POP)]BF_4$[8] were obtained pure by vapor diffusion of Et_2O into a CH_2Cl_2 solution of the corresponding reaction mixture. The four compounds have been already reported in the literature and X-ray crystal structures of three of them are known. Values of 113.18, 116.44 and 117.98° have been reported for the P-Cu-P bond angles of

[Cu(**dmp**)(dppFc)]BF_4,[10] [Cu(**dmp**)(POP)]BF_4,[3,4] and [Cu(**dpep**)(POP)]BF_4,[8] respectively. ^1H and ^{31}P NMR analysis of the recrystallized samples recorded in CD_2Cl_2 revealed that the heteroleptic complex was the largely major species present in solution (> 99%). However, traces of [Cu(**dmp**)$_2$]BF_4[21] or [Cu(**dpep**)$_2$]BF_4[15] were always detected in the ^1H NMR, thus showing that ligand exchange reactions take place to a minor extend for the heteroleptic complexes prepared from 2,9-disubstituted-1,10-phenanthroline and dppFc or POP.

dppm, dppe, dppp, dppb. Some of the heteroleptic complexes were obtained pure as crystalline solids by vapor diffusion of Et_2O into a CH_2Cl_2 solution of the corresponding reaction mixture. This was the case for [Cu_2(**dmp**)$_2$(μ-dppm)$_2$]$(BF_4)_2$, [Cu(**dmp**)(dppe)]BF_4, [Cu(**dmp**)(dppp)]BF_4 and [Cu(**dmp**)(dppb)]BF_4. All attempts to obtain the other heteroleptic complexes in a pure form by recrystallization of the crude product mixture failed. Indeed, slow diffusion of Et_2O into a CH_2Cl_2 solution of the mixture of complexes yielded either only orange-red crystals of [Cu(NN)$_2$]BF_4 or a mixture of orange-red and yellow crystals corresponding to [Cu(NN)$_2$]BF_4 and [Cu(NN)(PP)]BF_4, respectively.

X-ray quality crystals were obtained for both [Cu(**dmp**)(dppe)]BF_4 and [Cu(**dmp**)(dppp)]BF_4. Their X-ray crystal structures are depicted in Figure 7. Selected bond lengths and angles are summarized in Table 3.

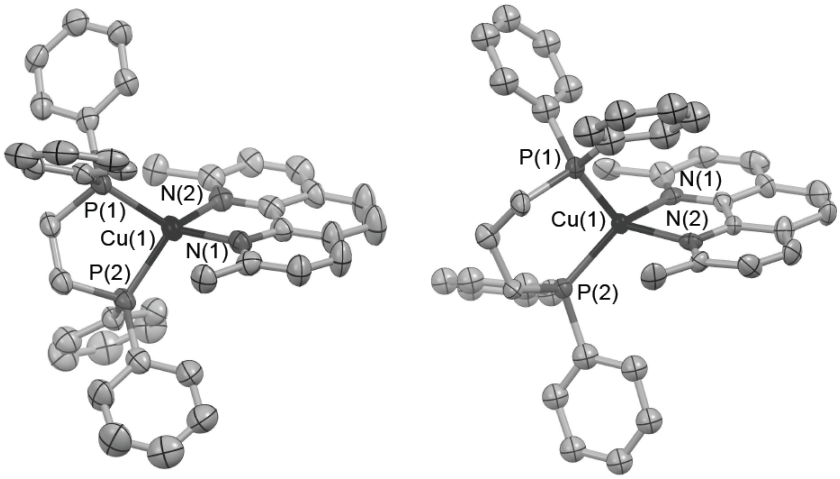

Figure 7. ORTEP plot of the structures of [Cu(**dmp**)(dppe)]BF_4.Et_2O (left) and [Cu(**dmp**)(dppp)]BF_4 (right). The H atoms, the solvent in the case of dppe, and the counteranion are omitted for clarity, thermal ellipsoids are drawn at the 50% probability level.

The structures of the [Cu(**dmp**)(dppe)]$^+$ and [Cu(**dmp**)(dppp)]$^+$ cations are similar to the one described for the X-ray crystal structures of the corresponding PF_6^- salts.[5] Whereas no particular differences in bond lengths are observed for [Cu(**dmp**)(dppe)]BF_4 and [Cu(**dmp**)(dppp)]BF_4, the bond angles around the Cu(I) cation are significantly different as a result of the P-Cu-P angles imposed by the different number of methylene units between the two P atoms in both complexes. It can be noted that the PPh_2 groups do not significantly interact with the **dmp** ligand, however in both cases, they are sterically close to the methyl groups which is located in between two phenyl groups. The closest C-H to phenyl distances ranges from 2.54 to 2.85 Å for [Cu(**dmp**)(dppe)]BF_4. Values ranging from 2.85 to 3.30 Å are seen for [Cu(**dmp**)(dppe)]BF_4. These observations explain well the observed destabilization of heteroleptic complexes prepared from 2,9-disubstituted-1,10-phenanthroline ligands (*vide infra*).

Table 3. Bond distances and bond angles within the coordination sphere of [Cu(**dmp**)(PP)]BF_4 (PP = dppe and dppp, see Figure 7 for the numbering).

Selected bond lengths (Å)			Selected bond angles (°)		
	PP = dppe	PP = dppp		PP = dppe	PP = dppp
Cu(1)-P(1)	2.265(2)	2.269(3)	P(1)-Cu(1)-P(2)	91.56(7)	104.2(1)
Cu(1)-P(2)	2.274(2)	2.258(3)	P(1)-Cu(1)-N(1)	132.0(2)	121.8(2)
Cu(1)-N(1)	2.058(6)	2.089(8)	P(1)-Cu(1)-N(2)	119.7(2)	108.1(2)
Cu(1)-N(2)	2.055(6)	2.087(9)	P(2)-Cu(1)-N(1)	114.5(2)	120.8(2)
			P(2)-Cu(1)-N(2)	120.3(2)	119.8(4)
			N(1)-Cu(1)-N(2)	82.2(2)	81.4(3)

Whereas all the **dmp** containing heteroleptic complexes obtained in a pure form by recrystallization were perfectly stable in the solid state, ***it is important to highlight that equilibration between the homoleptic and heteroleptic complexes was observed as soon as the crystals are dissolved*** (even in a non-coordinating solvent such as CH_2Cl_2). Indeed, the heteroleptic/homoleptic ratio deduced from the ^{1}H NMR spectrum is exactly the same as the one observed in the crude mixture (Table 2). These observations show that ligand exchange reactions are taking place in solution for all these compounds. In other words, there is a dynamic equilibrium between the heteroleptic complexes and the corresponding homoleptic

species in solution (Figure 8). Indeed all the species present in the solutions were clearly identified by ^{1}H and ^{31}P NMR spectroscopy as well as by FAB mass spectrometry.

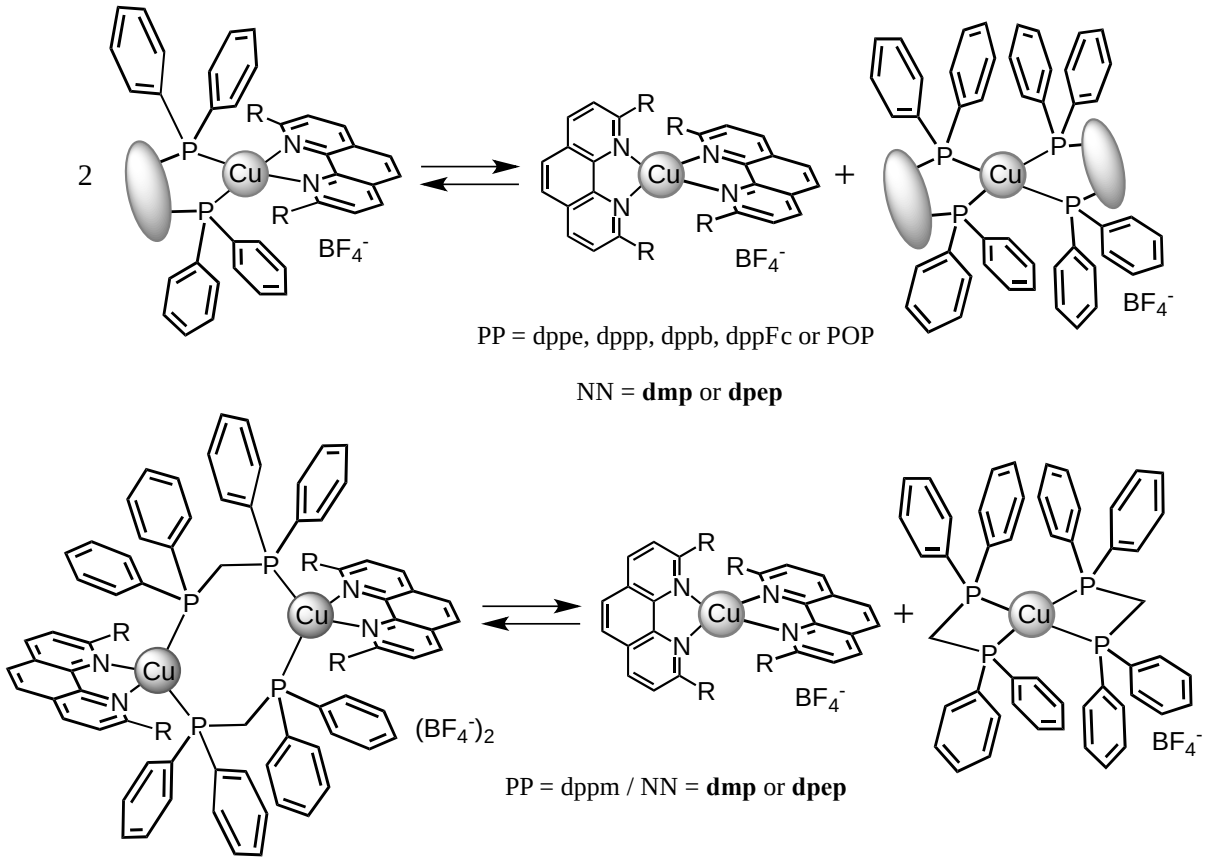

Figure 8. Dynamic equilibrium evidenced in solution between the heteroleptic complexes and their corresponding homoleptic species.

The typical resonances of both [Cu(**dmp**)(PP)]$^{+}$ and [Cu(**dmp**)$_2$]$^{+}$ derivatives were clearly recognized in the ^{1}H NMR spectra of the dynamic mixtures, but typical resonances of [Cu(PP)$_2$]BF$_4$ were not always easily distinguishable (Figure 9). The presence of the homoleptic complex [Cu(PP)$_2$]BF$_4$ was however unambiguously demonstrated by ^{31}P NMR spectroscopy (Figure 10). [Cu(dppm)$_2$]BF$_4$,[11] [Cu(dppe)$_2$]BF$_4$,[22] [Cu(dppp)$_2$]BF$_4$[22] and [Cu(dppb)$_2$]BF$_4$[11] are all known compounds and their ^{31}P NMR spectra are described in the literature. For all the systems, the diagnostic signals of both homoleptic and heteroleptic complexes were clearly observed at room temperature (Figure 10) except in the case of dppe. Actually, the ^{31}P NMR signal of [Cu(dppe)$_2$]BF$_4$ is particularly broad at room temperature[22]

preventing its observation under these conditions. As reported in the literature, lowering the temperature led to a significant decrease of $\Delta\nu_{1/2}$ and the characteristic signal observed at δ = +7.8 ppm confirmed the presence of $[Cu(dppe)_2]BF_4$ in solution.

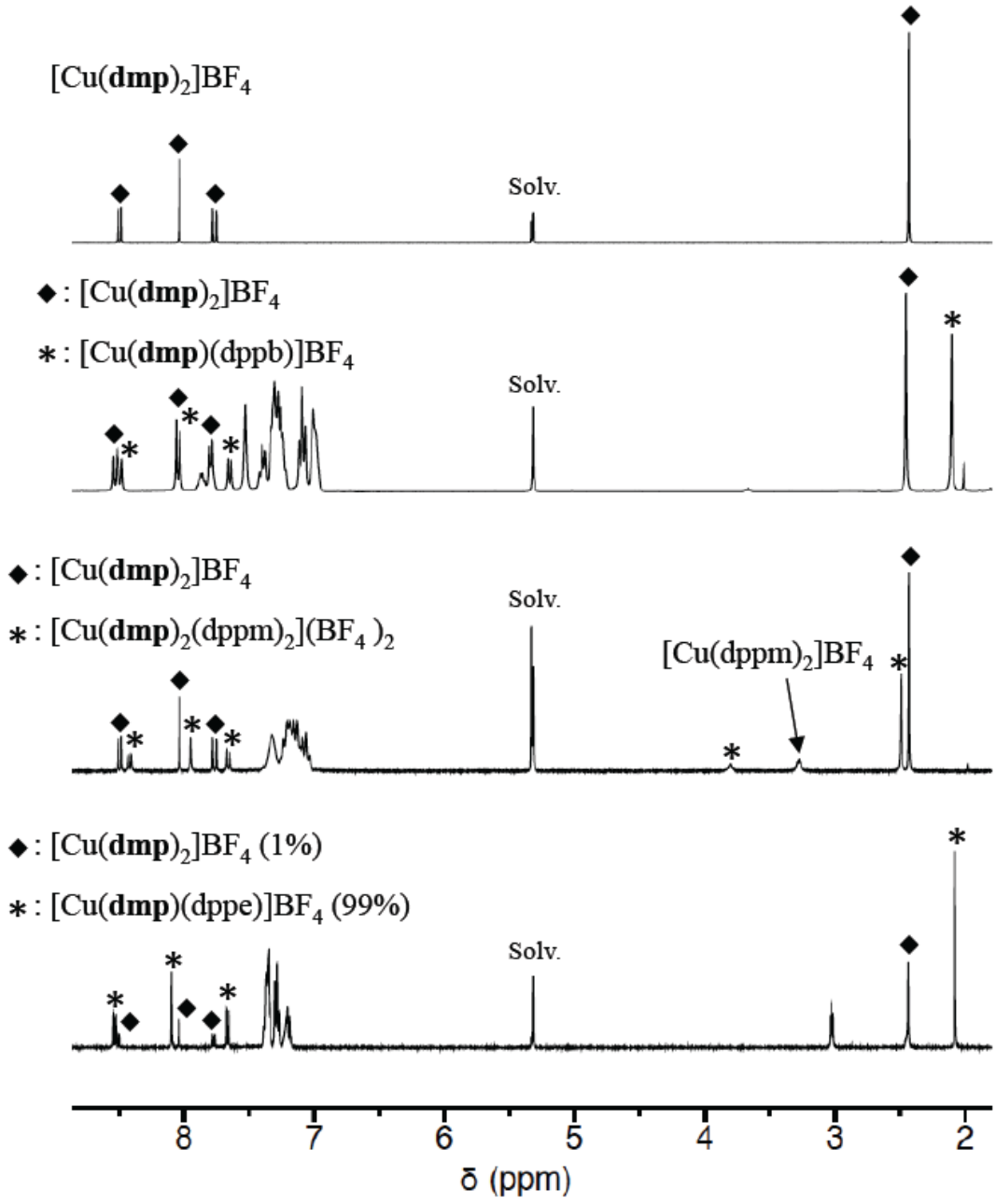

Figure 9. ^{1}H NMR (CD_2Cl_2) recorded upon dissolution of recrystallized samples of $[Cu_2(\mathbf{dmp})_2(\mu\text{-dppm})_2](BF_4)_2$, $[Cu(\mathbf{dmp})(dppe)]BF_4$, and $[Cu(\mathbf{dmp})(dppb)]BF_4$. In all the cases, ligand exchange reactions take place and the typical resonances of $[Cu(\mathbf{dmp})_2]BF_4$ are clearly observed. For comparison purposes, the ^{1}H NMR spectrum of $[Cu(\mathbf{dmp})_2]BF_4$ (top) is also represented.

It can also be noted that the ^{31}P NMR resonance of $[Cu(dppp)_2]BF_4$ is not well resolved and appears complicated at room temperature. Detailed variable temperature NMR studies have been reported for this compound[22] and the complicated ^{31}P NMR pattern of $[Cu(dppp)_2](BF_4)$ explained by a slow conformational exchange (ring inversion) on the NMR timescale. Indeed, at low temperature the phosphorus atoms of $[Cu(dppp)_2]BF_4$ are non equivalent as a result of a frozen chair conformation of the CuP2C3 six-membered rings.

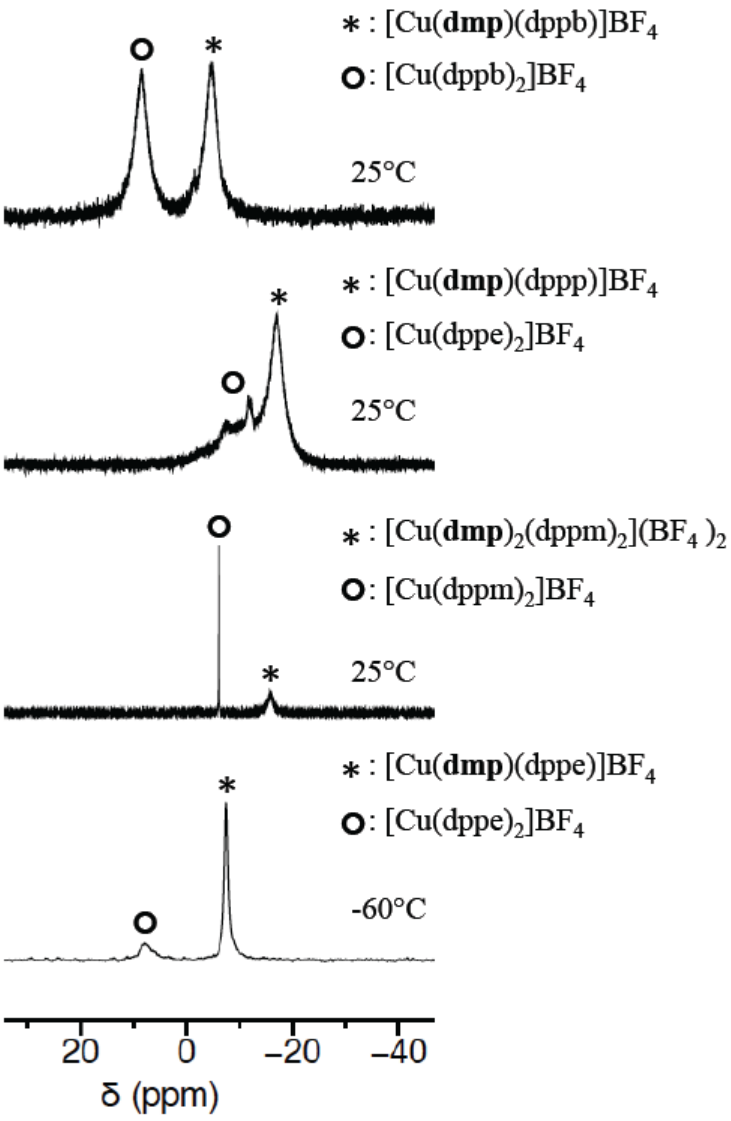

Figure 10. ^{31}P NMR (CD_2Cl_2) recorded upon dissolution of recrystallized samples of [Cu(**dmp**)(dppb)]BF_4, [Cu(**dmp**)(dppp)]BF_4, [Cu_2(**dmp**)$_2$(μ-dppm)$_2$]$(BF_4)_2$, and [Cu(**dmp**)(dppe)]BF_4. In all the cases, ligand exchange reactions take place and the typical resonances of $[Cu(PP)_2]BF_4$ are clearly observed.

CHAPTER 3

Heteroleptic Cu(I) complexes prepared from phenanthroline and bis-phosphine ligands

It is well known that thermodynamically stable copper(I) complexes are also kinetically labile and fast ligand exchange is often observed in solution at ambient temperature.[23] This is also clearly observed for the Cu(I) complexes prepared from bis-phosphines and phenanthroline ligands. In this particular case, whatever the ratio of homoleptic and heteroleptic complexes in solution, all ligands and metal binding sites are utilized to generate coordinatively saturated complexes. Therefore the equilibrium between the different complexes must be mainly governed by the relative thermodynamic stability of the different possible complexes.[24] On the one hand, homoleptic $[Cu(NN)_2]^+$ complexes prepared from 2,9-disustituted-1,10-phenanthroline ligands are particularly stable (log β = 10-12),[20] they have thus *a priori* tendency to drive the equilibrium towards the formation of the homoleptic complexes. In contrast, this is not the case for the Cu(I) complexes obtained from 2,9-unsubstituted-1,10-phenanthrolines. The corresponding $[Cu(NN)_2]^+$ complexes are actually less stable and therefore unable to significantly compete with the formation of $[Cu(NN)(PP)]^+$. On the other hand, subtle steric effects may also contribute to stabilize/destabilize both $[Cu(PP)_2]^+$ and $[Cu(NN)(PP)]^+$ derivatives. Actually, the differences in behavior observed for the various bis-phosphine ligands maybe explained by the differences in bite angles for the different chelating P-ligands. When this angle is small enough (dppe, dppp and dppb), the Cu(I) center can easily accommodate two ligands to form a stable homoleptic complex.[11,22] In contrast, steric factors resulting from the wider P-Cu-P angle for the other bis-phosphines (dppFc and POP) may substantially destabilize the $[Cu(PP)_2]^+$ derivative. This is clearly seen in the case of $[Cu(POP)_2]^+$ for which a X-ray crystal structure could be obtained (Figure 13).[25] The Cu(I) cation is effectively too small to accommodate two POP ligands in a tetrahedral coordination geometry. Only one POP ligand is chelating the metal while the other one is acting as a monodentate ligand. As a result the Cu(I) cation is in a distorted trigonal coordination geometry.

The homoleptic Cu(I) complex prepared from dppFc has been characterized in solution by Long and co-workers but no X-ray crystal structure has been published for this compound.[26] We decided to prepare this compound from dppFc and $Cu(CH_3CN)_4BF_4$. As reported by Long and co-workers, the resulting complex displays broadened ^1H and ^{31}P NMR features at room temperature suggesting dissociative processes in solution. Crystals were obtained by slow diffusion of Et_2O into a CH_2Cl_2 solution of the crude mixture of complexes.

Surprisingly, their X-ray crystal structure analysis revealed the formation of a dinuclear Cu(I) complex (Figure 14). Each metal center is chelated by a dppFc ligand and the two $[Cu(dppFc)]^+$ subunits are connected by an additional bridging dppFc ligand. ^1H and ^{31}P NMR spectra recorded upon dissolution of the recrystallized sample are different when compared to the crude mixture. This is consistent with a different ligand to metal ratio in solution. However, as in the case of the crude mixture, the NMR data suggest the presence of several species in solution. Being out of the scope of the present investigation, this system was not further investigated.

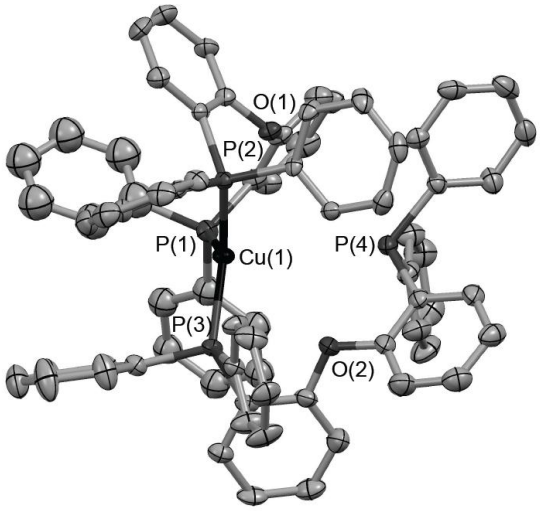

Figure 13. ORTEP plot of the structure of $[Cu(POP)_2]BF_4$. The H atoms and the counteranion are omitted for clarity, thermal ellipsoids are drawn at the 50% probability level. Selected bond lengths: Cu(1)-P(1): 2.273(1), Cu(1)-P(2): 2.261(1), Cu(1)-P(3): 2.263(1) Å; selected bond angles: P(1)-Cu(1)-P(2): 114.03(6), P(1)-Cu(1)-P(3): 121.49(6) , P(2)-Cu(1)-P(3): 121.90(6)°. P(4) is at a non bonding distance from the Cu center (3.96 Å).

The X-ray crystal structure analysis of the homoleptic Cu(I) complexes prepared from dppFc and POP revealed that the Cu(I) cation is too small to accommodate two ligands in a distorted tetrahedral coordination geometry. Indeed, the large P-Cu-P angle prevents the formation of a tetra-coordinated complex in both cases. As mentioned above, these homoleptic complexes are thus destabilized and this effect contributes to favor the formation of the $[Cu(NN)(PP)]^+$ derivatives.

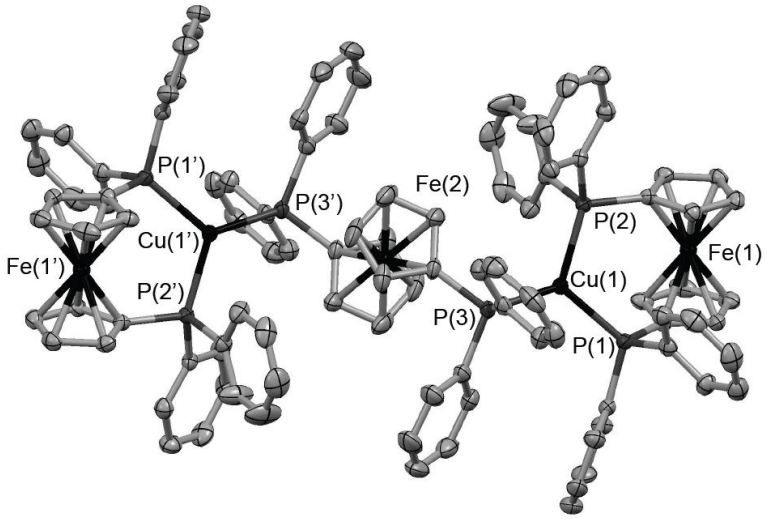

Figure 14. ORTEP plot of the structure of $[Cu_2(dppFc)_3](BF_4)_2.(H_2O)_2.CH_2Cl_2$. The H atoms, the solvent molecules and the counteranions are omitted for clarity, thermal ellipsoids are drawn at the 50% probability level. Selected bond lengths: Cu(1)-P(1): 2.264(1), Cu(1)-P(2): 2.274(1), Cu(1)-P(3): 2.248(2) Å; selected bond angles: P(1)-Cu(1)-P(2): 111.75(5), P(1)-Cu(1)-P(3): 122.48(5) , P(2)-Cu(1)-P(3): 125.02(5)°.

Finally, the difference in bite angle for the various chelating P-ligands may also affect the stability of $[Cu(NN)(PP)]^+$. Indeed, when the phenanthroline ligand is substituted in its 2 and 9 positions, negative steric effects may contribute to destabilize the heteroleptic complex. This view is indeed supported by the X-ray crystal structures of [Cu(**dmp**)(dppe)]BF_4 and [Cu(**dmp**)(dppp)]BF_4 in which the methyl groups of the **dmp** ligand are close to the phenyl units of the PPh_2 moieties. In the case of dppb, the P-Cu-P angle is in the same range and similar steric effects are expected. These observations explain also well the further destabilization observed for the corresponding heteroleptic complexes prepared from **dpep**. Steric hindrance may also limit the stability of the dinuclear Cu(I) complexes obtained from dppm and 2,9-disubstituted-1,10-phenanthrolines. For all these P-ligands, steric effects are involved in the destabilization of the heteroleptic complexes and thus contribute, at least in part, to displace the dynamic mixture towards the homoleptic species. In contrast, for dppFc and POP, the P-Cu-P angle is wider (113-118°) and the wrapping of the phenanthroline ligand is more effective in $[Cu(NN)(PP)]^+$. As a result, the orientation of the phenyl groups of the two PPh_2 subunits is different and negative steric effects are limited. In addition to the

destabilization of the homoleptic Cu(I) complexes of dppFc and POP (*vide supra*), this limited steric hindrance drive the system towards the almost exclusive formation of the heteroleptic complexes.

2.2. Electrochemical properties

Béatrice Delavaux-Nicot (*Laboratoire de Chimie de Coordination du CNRS*, Toulouse France) has carried out the electrochemical investigations of the stable heteroleptic [Cu(NN)(PP)]BF_4 complexes reported in the previous section. The electrochemical properties of the [Cu(NN)(dppFc)]BF_4 derivatives have been already reported in details[10] and have not been further investigated.

The electrochemical properties of the Cu(I) complexes were determined by cyclic voltammetry (CV) and Osteryoung Square Wave Voltammetry (OSWV). All the experiments were performed at room temperature in CH_2Cl_2 solutions containing tetra-*n*-butylammonium tetrafluoroborate (0.1 M) as supporting electrolyte, with a Pt wire as the working electrode and a saturated calomel electrode (SCE) as a reference. Potential data for all of the compounds are collected in Table 4. As typical examples, the cyclic voltammograms obtained from [Cu(**phen**)(dppp)]BF_4, [Cu(**phen**)(dppb)]BF_4 and [Cu(**Bphen**)(dppp)]BF_4 are shown in Figure 15. All the mononuclear complexes present a reversible one-electron transfer process both in the cathodic and in the anodic region. By analogy to previous work,[3,10,12] the first oxidation process is centred on the metal while the first reduction involves the phenanthroline ligand. A second oxidation is also observed for all the compounds. This process is irreversible and ascribed to the oxidation of the P-ligands. As reported earlier,[10] chemical reactions leading to the decomposition of the complexes are associated with this second oxidation. As a result, the first oxidation remains effectively reversible as long as the highest potential values in the CV do not reach that of the second oxidation. The electrochemical behaviour of the dinuclear complexes [Cu_2(**phen**)$_2$(μ-dppm)$_2$]$(BF_4)_2$ and [Cu_2(**Bphen**)$_2$(μ-dppm)$_2$]$(BF_4)_2$ is similar and the oxidation of the two metal centers occurs at the same potential. Interestingly, the heteroleptic complexes with POP and dppm ligands present Cu(I) oxidation at more positive potentials when compared to the other derivatives (ΔE = 0.2 to 0.35 V for POP and dppm, respectively). The Cu(II)/Cu(I) redox potentials is indeed very sensitive to steric effects. It is well established that a distortion of the pseudo-tetrahedral coordination sphere

around the copper occurs upon oxidation to form a flattened structure with a distorted square planar coordination geometry more appropriate for Cu(II) cations.[27] Steric factors that will prevent this distortion will destabilize the highest oxidation state and the Cu(II)/Cu(I) redox potential will be shifted to more positive potentials. For both dppm and POP derivatives, interligand interactions may inhibit more efficiently the redox-induced flattening distortion when compared to all the others. However, it is also believed that the P-Cu-P angle imposed by the P-ligand may play a significant role in the oxidation-induced distortion. When this angle is close to 90°, the ideal value for a square planar coordination geometry, the distortion is facilitated. This is the case for dppe, dppp and dppb for which the P-Cu-P angle range from 88 to 104°. In contrast, the wider P-Cu-P angles of the dppm (*ca*. 141°) and POP (*ca*. 116°) derivatives disfavour the distortion upon oxidation of the metal center. This interpretation explains well the more important potential shift observed for the dppm derivatives. The slight potential shift when going from the dppe (P-Cu-P of *ca*. 91°) to the dppp (P-Cu-P of *ca*. 104°) derivatives also supports this view.

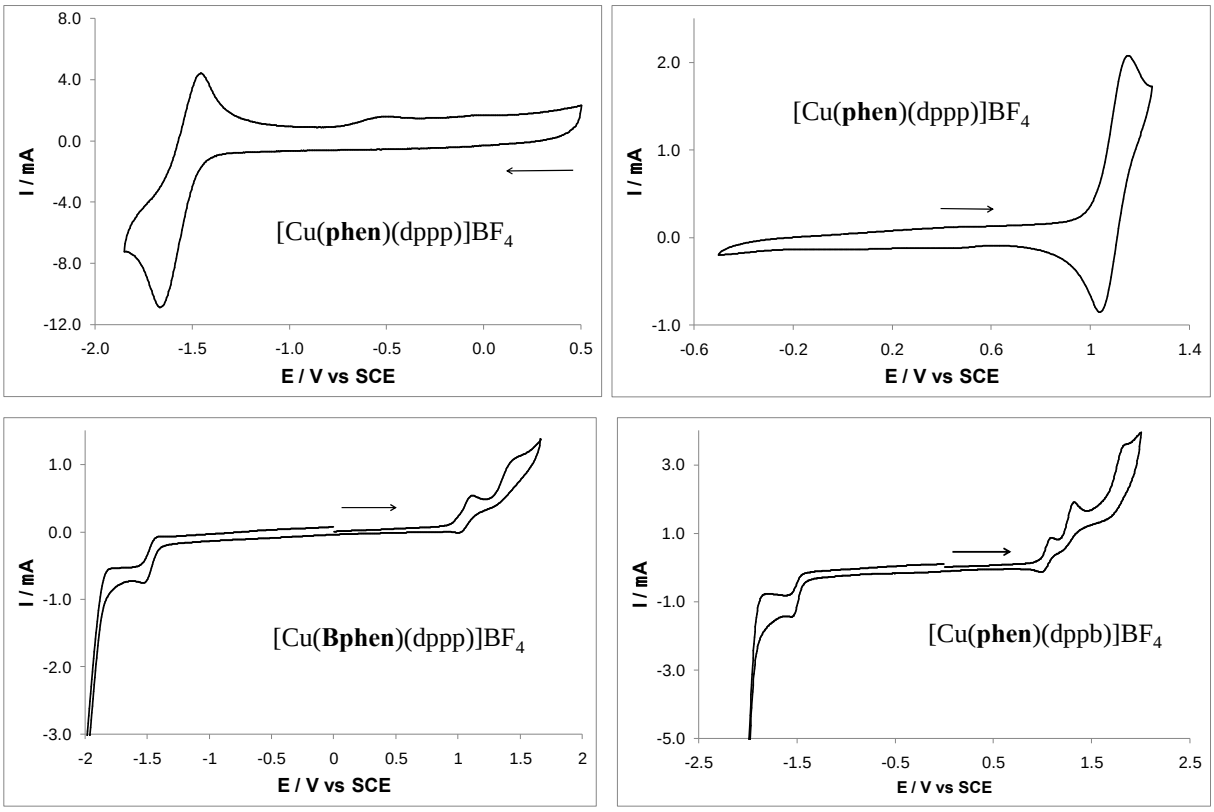

Figure 15. Typical examples of cyclic voltammograms on a Pt electrode in CH_2Cl_2 + 0.1 M nBu_4NBF_4 (top left: v = 20 Vs^{-1}, top right: v = 10 Vs^{-1}, bottom left: v = 0.1 Vs^{-1}, bottom right: v = 0.1 Vs^{-1}).

Table 4. Electrochemical data of the Cu(I) complexes determined by OSWV on a Pt working electrode in CH_2Cl_2 + 0.1 M nBu_4NBF_4 at room temperature.[a,b]

	Oxidation		Reduction
	E_1	E_2	E_1
$[Cu_2(\mathbf{phen})_2(\mu\text{-dppm})_2](BF_4)_2$	+1.46	%[c]	-1.33
$[Cu_2(\mathbf{Bphen})_2(\mu\text{-dppm})_2](BF_4)_2$	+1.45	%[c]	-1.30
$[Cu(\mathbf{phen})(dppe)]BF_4$	+1.07	+1.24	-1.51
$[Cu(\mathbf{Bphen})(dppe)]BF_4$	+1.04	+1.28	-1.45
$[Cu(\mathbf{phen})(dppp)]BF_4$	+1.09	+1.36	-1.53
$[Cu(\mathbf{Bphen})(dppp)]BF_4$	+1.08	+1.41	-1.47
$[Cu(\mathbf{phen})(dppb)]BF_4$	+1.07	+1.30	-1.48
$[Cu(\mathbf{Bphen})(dppb)]BF_4$	+1.06	+1.34	-1.44
$[Cu(\mathbf{phen})(POP)]BF_4$	+1.31	%[c]	-1.56
$[Cu(\mathbf{Bphen})(POP)]BF_4$	+1.31	%[c]	-1.51

[a] OSWVs were obtained using a sweep width of 20 mV, a frequency of 10 Hz, and a step potential of 5 mV.

[b] Values in V *vs*. SCE.

[c] The second oxidation is broad and not well-defined for these compounds

3. Conclusion

The systematic investigations done with the library of phenanthroline and bis-phosphine ligands shown in Figure 1 revealed several important trends: (i) whatever the bis-phosphine ligand, stable heteroleptic complexes are obtained from 1,10-phenanthroline; (ii) 4,7-substituents on the phenanthroline ligand (**Bphen**) have no particular influence on the formation of the heteroleptic complexes; (iii) heteroleptic complexes obtained from **dmp** are stable in the solid state but a dynamic ligand exchange reaction is systematically observed in solution and the homoleptic/heteroleptic ratio is highly dependent on the bis-phosphine ligand; (iv) by increasing the size of the 2,9-substituents, e.g. when going from **dmp** to **dpep**, the heteroleptic complexes are further destabilized and the homoleptic complexes are favored

except in the cases of dppFc and POP for which the heteroleptic complexes are still almost exclusively obtained, (v) by further increasing the size of the 2,9-substituents, e.g. when going from **dpep** to **dpp**, only homoleptic complexes were obtained whatever the bis-phosphine ligand as a result of steric hindrance, (vi) the difference in behavior of the various bis-phosphine ligands has been explained by their different chelate bite angles influencing the stability of both $[Cu(NN)(PP)]^+$ and $[Cu(PP)_2]^+$, the remarkable stability of the dppFc and POP containing heteroleptic derivatives results from a substantial destabilization of both $[Cu(dppFc)_2]^+$ and $[Cu(POP)_2]^+$ species as well as from a favorable orientation of the aromatic groups of the PPh_2 moieties limiting steric hindrance effects when the phenanthroline ligand is substituted in its 2 and 9 positions.

Detailed analysis revealed that the dynamic equilibrium resulting from ligand exchange reactions is mainly influenced by the relative thermodynamic stability of the different possible complexes. The exceptionally high thermodynamic stability of the homoleptic $[Cu(NN)_2]^+$ complexes tends to drive the equilibrium towards the formation of the homoleptic complexes, this is particularly the case when steric hindrance effects destabilize the $[Cu(NN)(PP)]^+$ derivatives prepared from 2,9-disubstituted-1,10-phenanthroline ligands. This effect is however in part counter-balanced by a substantial destabilization of the $[Cu(PP)_2]^+$ derivatives in the case of POP and dppFc. With these particular chelating P-ligands, stable $[Cu(NN)(PP)]^+$ derivatives are obtained even from 1,10-phenanthroline ligands bearing substituents of a reasonable size. The electrochemical properties of this series of complexes have been investigated. It appears the P-Cu-P angle has a dramatic influence on the oxidation-induced distortion of the complexes. When this angle is significantly different from the ideal 90° for a square planar coordination geometry for the oxidized species as in the case of dppm and POP, the Cu(II) complexes are significantly destabilized and the Cu(II)/Cu(I) redox potential shifted to higher potentials.

The photophysical properties of the stable heteroleptic complexes reported in this section are underway in the group of Nicola Armaroli (Bologna, Italy). Only partial results are currently available and it was not possible to rationalize the data at this stage.

CHAPTER 3

Heteroleptic Cu(I) complexes prepared from phenanthroline and bis-phosphine ligands

4. Experimental section

General. Reagents were purchased as reagent grade and used without further purification. Compounds **dpep**,[15] **dpp**,[14] [Cu(**dpep**)$_2$]BF$_4$[15] and [Cu(**dmp**)$_2$]BF$_4$[21] were prepared according to previously reported procedures. Acetonitrile (CH_3CN) was distilled over CaH_2 under Ar. Dichloromethane (CH_2Cl_2) was distilled over CaH_2 under Ar. All reactions were performed in standard glassware under an inert Ar atmosphere. Evaporation and concentration were done at water aspirator pressure and drying in vacuo at 10^{-2} Torr. Column chromatography: silica gel 60 (230-400 mesh, 0.040-0.063 mm) was purchased from E. Merck. Thin Layer Chromatography (TLC) was performed on aluminum sheets coated with silica gel 60 F_{254} purchased from E. Merck. NMR spectra were recorded on a Bruker AC 300 or AC 400 with solvent peaks as reference. Elemental analyses were carried out on a Perkin–Elmer 2400 B analyzer at the LCC Microanalytical Laboratory in Toulouse. Mass spectra were obtained at the *Service Commun de Spectrométrie de Masse de l'Université Paul Sabatier et du CNRS de Toulouse*. Fast atom bombardment (FAB) spectra were performed on a Nermag R 10-10H spectrometer. A 9 kV xenon atom beam was used to desorb samples from the 3-nitrobenzyl alcohol matrix.

Electrochemistry. The electrochemical measurements were carried out with a potentiostat Autolab PGSTAT100. Experiments were performed at room temperature in a homemade airtight three–electrode cell connected to a vacuum/argon line. The reference electrode consisted of a saturated calomel electrode (SCE) separated from the solution by a bridge compartment. The counter electrode was a platinum wire of *ca*. 1 cm^2 apparent surface. The working electrode was a Pt microdisk (0.5 mm diameter). The supporting electrolyte *n*Bu$_4$NBF$_4$ (Fluka, 99% electrochemical grade) was used as received and simply degassed under argon. Dichloromethane was freshly distilled over CaH_2 prior to use. The solutions used during the electrochemical studies were typically 10^{-3} M in compound and 0.1 M in supporting electrolyte. Before each measurement, the solutions were degassed by bubbling Ar and the working electrode was polished with a polishing machine (Presi P230). Under these experimental conditions, Fc/Fc^+ is observed at +0.54 ± 0.01 V *vs*. SCE.

General procedure for the preparation of [Cu(phen)(PP)]BF_4 and [Cu(Bphen)(PP)]BF_4

A solution of the appropriate bis-phosphine ligand (1 equiv.) and $Cu(CH_3CN)_4BF_4$ (1 equiv.) in a 7:3 CH_2Cl_2/CH_3CN mixture was stirred for 0.5 h, then **phen** or **Bphen**(1 equiv.) was added. After 1 h, the solvents were evaporated. The heteroleptic complexes were then obtained pure as crystalline solids by slow diffusion of Et_2O into a CH_2Cl_2 solution of the crude product.

[Cu(**phen**)(dppe)]BF_4. This compound was thus obtained in 86 % yield as a yellow crystalline solid. ^{1}H-NMR (CD_2Cl_2, 300 MHz, 293 K): 8.76 (d, J = 4Hz, 2H), 8.67 (d, J = 8 Hz, 2H), 8.17 (s, 2H), 7.90 (dd, J = 8Hz, J = 4Hz, 2H), 7.39 (m, 20H), 2.76 (t, J = 6Hz, 4H). ^{31}P{^{1}H}-NMR (CD_2Cl_2, 293 K, 162 MHz): -4.80. ^{13}C {^{1}H}-NMR (CD_2Cl_2, 298 K, 75 MHz): 150.9, 144.7, 138.6, 133.1, 132.9 (t, J_{PC} = 8Hz, 8C), 132.8, 132.6, 131.4, 130.7, 130.1 (t, J_{PC} = 4Hz, 8C), 128.2, 125.9, 26.4 (t, J_{PC} = 19Hz, 2C). Anal. Calcd for $C_{38}H_{32}N_2P_2CuBF_4$: C, 62.61; H, 4.42; N, 3.84. Found: C, 62.72; H, 4.56; N, 3.80. FAB-MS: 641.0 ([M - BF_4]$^+$, calcd for $C_{38}H_{32}N_2P_2Cu$: 641.13).

[Cu(**phen**)(dppp)]BF_4. This compound was thus obtained in 62 % yield as a yellow crystalline solid. ^{1}H-NMR (CD_2Cl_2, 300 MHz, 293 K): 8.77 (d, J = 4Hz, 2H), 8.60 (d, J = 8 Hz, 2H), 8.12 (s, 2H), 7.83 (dd, J = 8Hz, J = 4Hz, 2H), 7.36 (m, 4H), 7.24 (m, 16H), 2.71 (m, 4H), 2.34 (m, 2H). ^{31}P{^{1}H}-NMR (CD_2Cl_2, 293 K, 162 MHz): -13.39. ^{13}C{^{1}H}-NMR (CD_2Cl_2, 298 K, 75 MHz): 150.8, 144.4, 138.3, 134.2 (t, J_{PC} = 16Hz, 4C), 132.7(t, J_{PC} = 8Hz, 8C), 130.9, 130.6, 129.7 (t, J_{PC} = 5Hz, 8C), 128.2, 125.8, 29.5 (t, J_{PC} = 8Hz, 2C), 20.6 (t, J_{PC} = 4Hz, 1C). Anal. Calcd for $C_{39}H_{34}N_2P_2CuBF_4.CH_2Cl_2$: C, 58.03; H, 4.38; N, 3.38. Found: C, 57.94; H, 4.75; N, 3.11. FAB-MS: 655 ([M - BF_4]$^+$, calcd for $C_{39}H_{34}N_2P_2Cu$: 655.15).

[Cu(**phen**)(dppb)]BF_4. This compound was thus obtained in 93 % yield as a yellow crystalline solid. ^{1}H-NMR (CD_2Cl_2, 300 MHz, 293 K): 8.59 (d, J = 8 Hz, 2H), 8.35 (d, J = 4 Hz, 2H), 8.09(s, 2H), 7.79 (dd, J = 8Hz, J = 5Hz, 2H), 7.66 (m, 4H), 7.44 (m, 4H), 7.35 (m, 8H), 7.25(m, 8H). ^{31}P{^{1}H}-NMR (CD_2Cl_2, 293 K, 162 MHz): -2.94.^{13}C{^{1}H}-NMR (CD_2Cl_2, 298 K, 75 MHz): 150.7, 144.6, 142.0, 138.5, 135.7 (t, J_{PC} = 4Hz, 2C), 133.5 (t, J_{PC} = 8Hz,

8C), 133.1, 132.9, 132.6, 132.3, 131.1, 130.5, 129.9 (t, J_{PC} = 5Hz, 8C), 128.1, 125.8. Anal. Calcd for $C_{42}H_{32}N_2P_2CuBF_4$: C, 59.92; H, 3.97; N, 3.25. Found: C, 60.01; H, 3.99; N, 3.01. FAB-MS: 689 ([M - BF_4]$^+$, calcd for $C_{42}H_{32}N_2P_2Cu$: 689.13).

[Cu(**phen**)(dppFc)]BF_4. This compound was thus obtained in 75% yield as an orange crystalline solid. The analytical data were identical to those described in the literature.[10]

[Cu(**phen**)(POP)]BF_4. This compound was thus obtained in 95 % yield as a yellow crystalline solid. The analytical data were identical to those described in the literature.[3,4]

[Cu_2(**phen**)$_2$(μ-dppm)$_2$]$(BF_4)_2$. This compound was thus obtained in 87% yield as a yellow crystalline solid. ^{1}H-NMR (CD_2Cl_2, 300 MHz, 293 K): 8.68 (d, J = 4Hz, 4H), 8.24 (d, J = 8 Hz, 4H), 7.77 (m, 4H), 7.69 (s, 4H), 7.07-6.87 (m, 40H), 3.88 (m, 4H). ^{31}P{^{1}H}-NMR (CD_2Cl_2, 293 K, 162 MHz): -6.62. Anal. Calcd for $C_{74}H_{60}N_4P_4Cu_2B_2F_8$: C, 62.16; H, 4.23; N, 3.92. Found: C, 62.43; H, 4.55; N, 3.92.

[Cu(**Bphen**)(dppe)]BF_4. This compound was thus obtained in 61% yield as a yellow crystalline solid. ^{1}H-NMR (CD_2Cl_2, 300 MHz, 293 K): 8.86 (d, J = 5Hz, 2H), 8.19 (s, 2H), 7.87 (d, J = 5Hz, 2H), 7.68 (m, 10H), 7.53-7.41 (m, 20H), 2.83 (t, J = 6Hz, 4H). ^{31}P{^{1}H}-NMR (CD_2Cl_2, 293 K, 162 MHz): -4.44. ^{13}C {^{1}H}-NMR (CD_2Cl_2, 298 K, 75MHz): 151.2, 150.5, 145.4 (t, J_{PC} = 2Hz, 4C), 137.0, 133.0 (t, J_{PC} = 8Hz, 8C), 132.9, 132.7, 131.4, 130.4, 130.3, 130.1 (t, J_{PC} = 5Hz, 8C), 129.8, 128.5, 126.1, 125.9, 26.4 (t, J_{PC} = 19Hz, 2C). Anal. Calcd for $C_{50}H_{40}N_2P_2CuBF_4$: C, 68.15; H, 4.57; N, 3.18. Found: C, 68.32; H, 4.35; N, 3.34. FAB-MS: 793 ([M - BF_4]$^+$, calcd for $C_{50}H_{40}N_2P_2Cu$: 793.2).

[Cu(**Bphen**)(dppp)]BF_4. This compound was thus obtained in 65% yield as a yellow crystalline solid. ^{1}H-NMR (CD_2Cl_2, 300 MHz, 293 K): 8.84 (d, J = 5Hz, 2H), 8.12 (s, 2H), 7.77 (d, J = 5Hz, 2H), 7.63 (m, 10H), 7.41-7.29 (m, 20H), 2.77 (m, 4H), 2.38 (m, 2H). ^{31}P{^{1}H}-NMR (CD_2Cl_2, 293 K, 162 MHz): -13.03. ^{13}C {^{1}H}-NMR (CD_2Cl_2, 298 K, 75MHz): 150.9, 150.4, 145.1 (t, J_{PC} = 2Hz, 4C), 137.0, 134.3 (t, J_{PC} = 16Hz, 4C), 132.8 (t, J_{PC} = 8Hz, 8C), 130.9, 130.4, 130.3, 129.8, 129.7, 129.73, 129.6, 128.4, 126, 125.8, 29.5 (t, J_{PC} = 8Hz, 2C), 20.6 (t, J_{PC} = 2Hz,1C) Anal. Calcd for $C_{51}H_{42}N_2P_2CuBF_4$: C, 68.43; H, 4.73; N, 3.13.

Found: C, 68.12; H, 4.90; N, 2.99. FAB-MS: 807 ([M - BF_4]$^+$, calcd for $C_{51}H_{42}N_2P_2Cu$: 807.21).

[Cu(**Bphen**)(dppb)]BF_4. This compound was thus obtained in 90% yield as a yellow crystalline solid. ^{1}H-NMR (CD_2Cl_2, 300 MHz, 293 K): 8.44 (d, *J* = 5Hz, 2H), 8.11 (s, 2H), 7.76 (d, *J* = 5Hz, 2H), 7.70 (m, 4H), 7.63 (m, 10H), 7.49-7.29 (m, 20H). ^{31}P{^{1}H}-NMR (CD_2Cl_2, 293 K, 162 MHz): -2.71. ^{13}C{^{1}H}-NMR (CD_2Cl_2, 298 K, 75 MHz): 151.1, 150.2, 145.2 (t, J_{PC} = 2Hz, 4C), 142.1 (t, J_{PC} = 35Hz, 2C), 136.9, 135.7 (t, J_{PC} = 4Hz, 2C), 133.5 (t, J_{PC} = 8Hz, 8C), 133.2, 132.9, 132.7, 132.4, 131.1, 130.4, 130.3, 129.9, 129.92, 129.8, 129.81, 128.3, 126.0, 125.8. Anal. Calcd for $C_{54}H_{40}N_2P_2CuBF_4.H_2O$: C, 68.47; H, 4.47; N, 2.96. Found: C, 68.12; H, 4.71; N, 3.07. FAB-MS: 841 ([M - BF_4]$^+$, calcd for $C_{54}H_{40}N_2P_2Cu$: 841.2).

[Cu(**Bphen**)(dppFc)]BF_4. This compound was thus obtained in 70% yield as an orange crystalline solid. ^{1}H-NMR (CD_2Cl_2, 300 MHz, 293 K): 8.83 (d, *J* = 5Hz, 2H), 8.09 (s, 2H), 7.67-7.58 (m, 12H), 7.33 (m, 20H), 4.59 (m, 4H), 4.45 (m, 4H). ^{31}P{^{1}H}-NMR (CD_2Cl_2, 293 K, 162 MHz): -8.70. ^{13}C{^{1}H}-NMR (CD_2Cl_2, 298 K, 100 MHz): 150.9, 150.4,144.8 (t, J_{PC} = 2Hz, 4C), 137.0, 134.4, 134.1, 133.9, 133.8 (t, J_{PC} = 8Hz, 8C), 131, 130.4, 130.3, 129.8, 129.5 (t, J_{PC} = 5Hz, 8C), 128.4, 126.0, 125.8, 75.44, 75.4 (t, J_{PC} = 5Hz, 2C), 75.2, 74.9, 73.7 (t, J_{PC} = 2Hz, 2C).

[Cu(**Bphen**)(POP)]BF_4. This compound was thus obtained in 92% yield as a yellow crystalline solid. The analytical data were identical to those described in the literature.[28]

[Cu_2(**Bphen**)$_2$(μ-dppm)$_2$](BF_4)$_2$. This compound was thus obtained in 48% yield as a yellow crystalline solid. ^{1}H-NMR (CD_2Cl_2, 300 MHz, 293 K): 8.75 (d, *J* = 5Hz, 4H), 7.72 (m, 8H), 7.58 (m, 13H), 7.51 (m, 7H), 7.09 (m, 25H), 6.96 (m, 15H), 3.98 (m, 4H). ^{31}P{^{1}H}-NMR (CD_2Cl_2, 293 K, 162 MHz): -6.45. ^{13}C{^{1}H}-NMR (CD_2Cl_2, 298 K, 75 MHz): 151.1, 150.1, 144.2, 137.3, 133.7, 133.3, 130.5, 130.4, 129.9, 129.7, 129.1, 127.5, 126.2, 124.9, 66.5, 27.3, 15.9. Anal. Calcd for $C_{98}H_{76}N_4P_4Cu_2B_2F_8.CH_2Cl_2$: C, 65.36; H, 4.32; N, 3.08. Found: C, 65.20; H, 4.01; N, 3.25.

CHAPTER 3

Heteroleptic Cu(I) complexes prepared from phenanthroline and bis-phosphine ligands

General procedure for the preparation of $[Cu(dmp)(PP)]BF_4$ and $[Cu(dpep)(PP)]BF_4$

A solution of the appropriate bis-phosphine ligand (1 equiv.) and $Cu(CH_3CN)_4BF_4$ (1 equiv.) in a 7:3 CH_2Cl_2/CH_3CN mixture was stirred for 0.5 h, then **dmp** or **dpep** (1 equiv.) was added. After 1 h, the solvents were evaporated. The products were analyzed as received by ^1H NMR. The relative proportion of the different possible complexes, i.e. $[Cu(NN)(PP)]BF_4$, $[Cu(NN)_2]BF_4$ and $[Cu(NN)_2]BF_4$, was deduced from the comparison with the ^1H NMR spectrum of the corresponding $[Cu(NN)_2]BF_4$ derivative recorded in the same solvent. Some of the heteroleptic complexes were obtained pure as crystalline solids by vapor diffusion of Et_2O into a CH_2Cl_2 solution of the corresponding reaction mixture. This was the case for $[Cu_2(\mathbf{dmp})_2(\mu\text{-dppm})_2](BF_4)_2$, $[Cu(\mathbf{dmp})(dppe)]BF_4$, $[Cu(\mathbf{dmp})(dppp)]BF_4$, $[Cu(\mathbf{dmp})(dppb)]BF_4$, $[Cu(\mathbf{dmp})(dppFc)]BF_4$, $[Cu(\mathbf{dmp})(POP)]BF_4$, $[Cu(\mathbf{dpep})(dppFc)]BF_4$, and $[Cu(\mathbf{dpep})(POP)]BF_4$. All attempts to obtain the other heteroleptic complexes in a pure form by recrystallization of the crude product mixture failed. Indeed, slow diffusion of Et_2O into a CH_2Cl_2 solution of the mixture of complexes yielded either only orange-red crystals of $[Cu(NN)_2]BF_4$ or a mixture of orange-red and yellow crystals corresponding to $[Cu(NN)_2]BF_4$ and $[Cu(NN)(PP)]BF_4$, respectively.

$[Cu_2(\mathbf{dmp})_2(\mu\text{-dppm})_2](BF_4)_2$. This compound was thus obtained in 52% yield as a yellow crystalline solid. As soon as dissolved in CH_2Cl_2, ligand exchange took place and analysis of the ^1H NMR spectrum revealed the presence of different species in solution: $[Cu_2(\mathbf{dmp})_2(\mu\text{-dppm})_2](BF_4)_2$ (70%), $[Cu(\mathbf{dmp})_2]BF_4$[21] (30%) and $[Cu(dppm)_2]BF_4$ (30%).[11] The presence of $[Cu(dppm)_2]BF_4$ was confirmed by its ^{31}P NMR resonance observed at δ = -6.03 ppm, the additional peak observed in the ^{31}P NMR spectrum at δ = -15.67 ppm is assigned to $[Cu_2(\mathbf{dmp})_2(\mu\text{-dppm})_2](BF_4)_2$.

$[Cu(\mathbf{dmp})(dppe)]BF_4$. This compound was thus obtained in 69% yield as a yellow crystalline solid. As soon as dissolved in CH_2Cl_2, ligand exchange took place and analysis of the ^1H NMR spectrum revealed the presence of different species in solution: $[Cu(\mathbf{dmp})(dppe)]BF_4$ (80%), $[Cu(\mathbf{dmp})_2]BF_4$[21] (20%) and $[Cu(dppe)_2]BF_4$ (20%).[22] The presence of $[Cu(dppe)_2]BF_4$ was confirmed by its broad ^{31}P NMR resonance observed at δ = 7.80 ppm (207 K), the additional peak observed in the ^{31}P NMR spectrum at δ = -7.53 ppm is assigned

to [Cu(**dmp**)(dppe)]BF_4. FAB-MS: 859.8 ([$Cu(dppe)_2$]$^+$, 33%), 669.7 (Cu[(dppe)(**dmp**)]$^+$, 100%), 479.5 ([Cu(**dmp**)]$_2^+$, 40%), 461.5 ([Cu(dppe)]$^+$, 63%), 271.4 ([Cu(**dmp**)]$^+$, 3%).

[Cu(**dmp**)(dppp)]BF_4. This compound was thus obtained in 76% yield as a yellow crystalline solid. As soon as dissolved in CH_2Cl_2, ligand exchange took place and analysis of the ^{1}H NMR spectrum revealed the presence of different species in solution: [Cu(**dmp**)(dppp)]BF_4 (80%), [Cu(**dmp**)$_2$]BF_4[21] (20%) and [Cu(dppp)$_2$]BF_4 (20%).[22] The presence of [Cu(dppp)$_2$]BF_4 was confirmed by its broad ^{31}P NMR resonance centered at δ = -10 ppm, the additional peak observed in the ^{31}P NMR spectrum at δ = -17.01 ppm is assigned to [Cu(**dmp**)(dppp)]BF_4.

[Cu(**dmp**)(dppb)]BF_4. This compound was thus obtained in 45% yield as a yellow crystalline solid. As soon as dissolved in CH_2Cl_2, ligand exchange took place and analysis of the ^{1}H NMR spectrum revealed the presence of different species in solution: [Cu(**dmp**)(dppb)]BF_4 (65%), [Cu(**dmp**)$_2$]BF_4[21] (35%) and [Cu(dppp)$_2$]BF_4 (35%).[11] The presence of [Cu(dppb)$_2$]BF_4 was confirmed by its ^{31}P NMR resonance observed at δ = 8.42 ppm, the additional peak observed in the ^{31}P NMR spectrum at δ = -4.64 ppm is assigned to [Cu(**dmp**)(dppb)]BF_4.

[Cu(**dmp**)(dppFc)]BF_4. This compound was thus obtained in 90% yield as a yellow crystalline solid. The analytical data were identical to those described in the literature.[10]

[Cu(**dmp**)(POP)]BF_4. This compound was thus obtained in 70% yield as a yellow crystalline solid. The analytical data were identical to those described in the literature.[3,4,10]

[Cu(**dpep**)(dppFc)]BF_4. This compound was thus obtained in 71% yield as a yellow crystalline solid. The analytical data were identical to those described in the literature.[10]

[Cu(**dpep**)(POP)]BF_4. This compound was thus obtained in 86% yield as a yellow crystalline solid. The analytical data were identical to those described in the literature.[8]

CHAPTER 3

Heteroleptic Cu(I) complexes prepared from phenanthroline and bis-phosphine ligands

Preparation of $[Cu(POP)_2]BF_4$

A mixture of $Cu(CH_3CN)BF_4$ (0.05 g, 0.16 mmol) and POP (0.171 g, 0.32 mmol) in CH_2Cl_2 (10 mL) was stirred for 1 h at room temperature. The resulting solution was concentrated to ca. 5 mL. Crystals of $[Cu(POP)_2]BF_4$ were obtained by vapor diffusion of *n*-Hexane into this CH_2Cl_2 solution. Compound $[Cu(POP)_2]BF_4$ was thus obtained in 68% yield as colorless crystals. ^{1}H-NMR (CD_2Cl_2, 300 MHz, 293 K): 6.49 (d, J = 4 Hz, 2H), 6.76-6.83 (m, 10H), 7.00 (t, J = 8 Hz, 10H), 7.18 (td, J = 8 and 2 Hz, 2H), 7.26 (t, J = 7 Hz, 4H). ^{31}P{^{1}H}-NMR (CD_2Cl_2, 293 K, 121.5 MHz): -13.57. ^{13}C{^{31}P}{^{1}H}-NMR (CD_2Cl_2, 298 K, 75.5 MHz): 119.6, 125.0, 129.0, 130.5, 131.5, 132.4, 134.1, 134.7, 158.5. Anal. Calcd for $C_{72}H_{56}O_2P_4CuBF_4$: C, 70.45; H, 4.6. Found: C, 70.13; H, 4.44. FAB-MS: 1139.7 (17%, $[Cu(POP)_2]^+$), 601.3 (100%, $[Cu(POP)]^+$).

Preparation of the homoleptic complex from dppFc

A mixture of $Cu(CNCH_3)BF_4$ (0.03 g, 0.09 mmol) and DPPF (0.100 g, 0.18 mmol) in CH_2Cl_2 (10 mL) was stirred for 1 h at room temperature. The resulting solution was evaporated to yield an orange powder in quantitative yield. The product was analyzed as received. ^{1}H-NMR (CD_2Cl_2, 300 MHz, 298 K): 4.01 (br, 4H), 4.27 (br, 4H), 7.26-7.30 (m, 16H), 7.41-7.47 (m, 4H). ^{31}P{^{1}H}-NMR (CD_2Cl_2, 298 K, 121.5 MHz): -9.33. Anal. Calcd for $C_{68}H_{56}P_4Fe_2CuBF_4 \cdot 0.5CH_2Cl_2$: C, 63.21; H, 4.41. Found: C, 63.54; H, 3.99. As described in the literature for the corresponding PF_6 salt,[26] the broad signals of the ^{1}H-NMR spectra suggest a dynamic equilibrium between different species. This was confirmed by variable temperature ^{1}H and ^{31}P NMR studies in the case of the PF_6 salt.[26] Recrystallization by slow diffusion of *n*-Hexane into a CH_2Cl_2 solution of the crude product yielded dark orange crystals (65 mg). X-ray crystal structure analysis revealed the crystallization of $[Cu_2(dppFc)(dppFc)_2](BF_4)_2$. The ^{1}H and ^{31}P NMR spectra recorded upon dissolution of these crystals in CD_2Cl_2 are complex and consistent with the presence of different species in solution. This compound has not been further investigated.

X-ray crystal structures

(A) [Cu(**phen**)(dppb)]BF_4. Crystals suitable for X-ray crystal-structure analysis were obtained by slow diffusion of Et_2O into a CH_2Cl_2 solution of [Cu(**phen**)(dppb)]BF_4. Data were collected at 173 K on a Bruker APEX-II CCD diffractometer (Mo-Kα radiation, λ = 0.71073 Å). The structure was solved by direct methods (SHELXS-97) and refined against F^2 using the SHELXL-97 software. The non-hydrogen atoms were refined anisotropically, using weighted full-matrix least-squares on F^2. The H-atoms were included in calculated positions and treated as ridig atoms using SHELXL default parameters. The crystallographic data are reported in Table 5.

(B) [Cu_2(**Bphen**)$_2$(μ-dppm)$_2$]$(BF_4)_2$.CH_2Cl_2. Crystals suitable for X-ray crystal-structure analysis were obtained by slow diffusion of Et_2O into a CH_2Cl_2 solution of [Cu_2(**Bphen**)$_2$(μ-dppm)$_2$]$(BF_4)_2$. Data were collected at 173 K on a Bruker APEX-II CCD diffractometer (Mo-Kα radiation, λ = 0.71073 Å). The structure was solved by direct methods (SHELXS-97) and refined against F^2 using the SHELXL-97 software. The non-hydrogen atoms were refined anisotropically, using weighted full-matrix least-squares on F^2. The H-atoms were included in calculated positions and treated as ridig atoms using SHELXL default parameters. The crystallographic data are reported in Table 5.

(C) [Cu(**dmp**)(dppe)]BF_4.Et_2O. Crystals suitable for X-ray crystal-structure analysis were obtained by slow diffusion of Et_2O into a CH_2Cl_2 solution of [Cu(**dmp**)(dppe)]BF_4. Data were collected at 180 K on a Stoe IPDS diffractometer (Mo-Kα radiation, λ = 0.71073 Å). The structure was solved by direct methods (SHELXS-97) and refined against F^2 using the SHELXL-97 software. The non-hydrogen atoms were refined anisotropically, using weighted full-matrix least-squares on F^2. The H-atoms were included in calculated positions and treated as ridig atoms using SHELXL default parameters. The crystallographic data are reported in Table 5.

(D) [Cu(**dmp**)(dppp)]BF_4. Crystals suitable for X-ray crystal-structure analysis were obtained by slow diffusion of Et_2O into a CH_2Cl_2 solution of [Cu(**dmp**)(dppp)]BF_4. Data were collected at at 180 K on a Stoe IPDS diffractometer (Mo-Kα radiation, λ = 0.71073 Å). The

structure was solved by direct methods (SHELXS-97) and refined against F^2 using the SHELXL-97 software. The non-hydrogen atoms were refined anisotropically, using weighted full-matrix least-squares on F^2. The H-atoms were included in calculated positions and treated as ridig atoms using SHELXL default parameters. The crystallographic data are reported in Table 5.

(E) $[Cu(POP)_2]BF_4$. Crystals suitable for X-ray crystal-structure analysis were obtained by slow diffusion of *n*-Hexane into a CH_2Cl_2 solution of $[Cu(POP)_2]BF_4$. Data were collected at 173 K on a Bruker APEX-II CCD diffractometer (Mo-Kα radiation, λ = 0.71073 Å). The structure was solved by direct methods (SHELXS-97) and refined against F^2 using the SHELXL-97 software. The non-hydrogen atoms were refined anisotropically, using weighted full-matrix least-squares on F^2. The H-atoms were included in calculated positions and treated as ridig atoms using SHELXL default parameters. The crystallographic data are reported in Table 5.

(F) $[Cu_2(\mu\text{-dppFc})(dppFc)_2](BF_4)_2.(CH_2Cl_2)(H_2O)_2$. Crystals suitable for X-ray crystal-structure analysis were obtained by slow diffusion of *n*-Hexane into a CH_2Cl_2 solution of dppFc (2 equiv.) and $Cu(CH_3CN)_4BF_4$ (1 equiv.). Data were collected at 180 K on an Oxford XCALIBUR diffractometer (Mo-Kα radiation, λ = 0.71073 Å). The structure was solved by direct methods (SHELXS-97) and refined against F^2 using the SHELXL-97 software. The non-hydrogen atoms were refined anisotropically, using weighted full-matrix least-squares on F^2. The H-atoms were included in calculated positions and treated as ridig atoms using SHELXL default parameters. The crystallographic data are reported in Table 5.

Table 5A. Crystallographic and structure refinement data for (A) [Cu(**phen**)(dppb)]BF_4, (B) [Cu_2(**Bphen**)$_2$(μ-dppm)$_2$](BF_4)$_2$.CH_2Cl_2 and (C) [Cu(**dmp**)(dppe)]BF_4.Et_2O.

	(A)	(B)	(C)
Chemical formula	$C_{42}H_{32}CuN_2P_2BF_4$	$C_{98}H_{76}Cu_2N_4P_4B_2F_8CH_2Cl_2$	$C_{40}H_{36}CuN_2BF_4.C_4H_{10}O$
M (g/mol)	776.99	1819.13	831.16
Crystal system	Orthorombic	Monoclinic	Tetragonal
Space group	P bca	P_21/c	I_41/a
a (Å)	17.5517(4)	14.8569(1)	21.129(3)
b (Å)	19.0568(3)	26.6640(2)	21.129(3)
c (Å)	21.3477(5)	25.5647(2)	36.050(7)
α (°)	90	90	90
β (°)	90	106.834(1)	90
γ (°)	90	90	90
V (Å^3)	7140.4(3)	9693.33(12)	16093(4)
Z	8	4	16
F(000)	3184	3736	6912
Reflections collected	49313	151203	53093
θ range for data collection (°)	1.84-27.48	1.13-27.49	2.228-26.006
Independent reflections	8188	22231	7839
Independent reflections having I > 2σ(I)	5244	16541	4496
Number of parameters	469	1060	447
$R_1(F^2)$	0.0516	0.0601	0.0925
$wR_2(F^2)$	0.1363	0.1728	0.1070

CHAPTER 3

Heteroleptic Cu(I) complexes prepared from phenanthroline and bis-phosphine ligands

Table 5B. Crystallographic and structure refinement data for (D) [Cu(**dmp**)(dppp)]BF_4, (E) [Cu(POP)$_2$]BF_4 and (F) [Cu_2(μ-dppFc)(dppFc)$_2$]$(BF_4)_2$.$(CH_2Cl_2)(H_2O)_2$.

	(D)	(E)	(F)
Chemical formula	$C_{41}H_{38}CuN_2P_2BF_4$	$C_{72}H_{56}CuO_2P_4BF_4$	$C_{103}H_{86}Cu_2Fe_2B_2F_8.(H_2O)_2.CH_2Cl_2$
M (g/mol)	771.06	1227.48	1040.40
Crystal system	Monoclinic	Orthorombic	Monoclinic
Space group	P1c1	Pbcn	$C_12/c1$
a (Å)	10.450(2)	20.0837(6)	32.6110(16)
b (Å)	16.194(3)	24.4373(7)	14.7493(7)
c (Å)	10.998(2)	24.7392(8)	25.9505(14)
α (°)	90	90	90
β (°)	100.97(3)	90	128.807(8)
γ (°)	90	90	90
V (Å^3)	1827.2(6)	12141.8(6)	9726.7(14)
Z	2	8	4
F(000)	796	5072	4248
Reflections collected	12142	16153	46659
θ range for data collection (°)	2.267-26.006	2.612-29.082	2.762-29.085
Independent reflections	6545	8956	13000
Independent reflections having I > 2σ(I)	3601	6792	5898
Number of parameters	298	656	584
$R_1(F^2)$	0.0671	0.0679	0.0473
$wR_2(F^2)$	0.0788	1.1238	0.0538

5. References

1) a) M. T. Buckner, T. G. Matthews, F. E. Lytle, D. R. McMillin, J. Am. Chem. Soc. **1979**, *101*, 5846; b) R. A. Rader; D. R. McMillin, M. T. Buckner, T. G. Matthews, D. J. Casadonte, R. K. Lengel, S. B. Whittaker, L. M. Darmon, F. E. Lytle, *J. Am. Chem. Soc.* **1981**, *103*, 5906; c) A. A. Del Paggio, D. R. McMillin, *Inorg. Chem.* **1983**, *22*, 691; d) J. R. Kirchhoff, D. R. McMillin, W. R. Robinson, D. R. Powell, A. T. McKenzie, S. Chen, *Inorg. Chem.* **1985**, *24*, 3928; e) D. J. Casadonte, D. R. McMillin, *Inorg. Chem.* **1987**, *26*, 3950; f) C. E. A. Palmer, D. R. McMillin, *Inorg. Chem.* **1987**, *26*, 3837.

2) a) S. Sakaki, G. Koga, K. Ohkubo, *Inorg. Chem.* **1986**, *25*, 2330; b) S. Sakaki, G. Koga, S. Hinokuma, S. Hashimoto, K. Ohkubo, *Inorg. Chem.* **1987**, *26*, 1817.

3) D. G. Cuttell, S.-M. Kuang, P. E. Fanwick, D. R. McMillin, R. A. Walton, *J. Am. Chem. Soc.* **2002**, *124*, 6.

4) S.-M. Kuang, D. G. Cuttell, D. R. McMillin, P. E. Fanwick, R. A. Walton, *Inorg. Chem.* **2002**, *41*, 3313.

5) a) P. Coppens, *Chem. Commun*. **2003**, 1317; b) P. Coppens, I. I. Vorontsov, T. Graber, A Y. Kovalevsky, Y.-S. Chen, G. Wu, M. Gembicky, I. V. Novozhilova, *J. Am. Chem. Soc.* **2004**, *126*, 5980; c) K. Saito, T. Arai, N. Takahashi, T. Tsukuda, T. Tsubomura, *Dalton Trans*. **2006**, 4444.

6) R. D. Costa, D. Tordera, E. Orti, H. Bolink, J. Schönle, S. Graber, C. E. Housecroft, E. C. Constable, J. A. Zampese, *J. Mater. Chem.* **2011**, *21*, 16108.

7) a) C. L. Linfoot, P. Richardson, T. E. Hewat, O. Moudam, M. M. Forde, A. Collins, F. White, N. Robertson, *Dalton Trans*. **2010**, *39*, 8945; b) Q. Zhang, Q. Zhou, Y. Cheng, L. Wang, D. Ma, X. Jing, F. Wang, *Adv. Mater.* **2004**, *16*, 432-436; c) Q. Zhang, Q. Zhou, Y. Cheng, L. Wang, D. Ma, X. Jing, F. Wang, *Adv. Funct. Mater.* **2006**, *16*, 1203; d) T. MacCormick, W.-L. Jia, S. Wang, *Inorg. Chem*. **2006**, *45*, 147-155; e) H. Ge, W. Wei, P. Shuai, G. Lei, S. Qing, *J. Lumin.* **2011**, *131*, 238.

8) N. Armaroli, G. Accorsi, M. Holler, O. Moudam, J.-F. Nierengarten, Z. Zhou, R. T. Wegh, R. Welter, *Adv. Mater*. **2006**, *18*, 1313.

9) L. Yang, J.-K. Feng, A.-M. Ren, M. Zhang, Y.-G. Ma, X.-D. Liu, *Eur. J. Inorg. Chem*. **2005**, 1867.

10) N. Armaroli, G. Accorsi, G. Bergamini, P. Ceroni, M. Holler, O. Moudam, C. Duhayon, B. Delavaux-Nicot, J.-F. Nierengarten, *Inorg. Chim. Acta* **2007**, *360*, 1032.

11) O. Moudam, A. Kaeser, B. Delavaux-Nicot, C. Duhayon, M. Holler, G. Accorsi, N. Armaroli, I. Séguy, J. Navarro, P. Destruel, J.-F. Nierengarten, *Chem. Commun*. **2007**, 3077.

12) A. Listorti, G. Accorsi, Y. Rio, N. Armaroli, O. Moudam, A. Gégout, B. Delavaux-Nicot, M. Holler, J.-F. Nierengarten, *Inorg. Chem* **2008**, *47*, 6254

13) M. Mohankumar, M. Holler, J.-F. Nierngarten, J.-P. Sauvage, *Chem. Eur. J*. **2012**, *18*, 12192.

14) C. O. Dietrich-Buchecker, P. A. Marnot, J.-P. Sauvage, *Tetrahedron Lett*. **1982**, *23*, 5291.

15) E. Gumienna-Kontecka, Y. Rio, C. Bourgogne, M. Elhabiri, R. Louis, A.-M. Albrecht-Gary, J.-F. Nierengarten, *Inorg. Chem*. **2004**, *43*, 3200;

16) R. M. Gschwind, *Chem. Rev*. **2008**, *108*, 3029.

17) a) R. J. Puddephatt, *Chem. Soc. Rev*. **1983**, *12*, 99; b) B. Chaudret, B. Delavaux, R. Poilblanc, *Coord. Chem. Rev*. **1988**, *86*, 191.

18) a) P. D. Harvey, M. Drouin, T. Zhang, *Inorg. Chem*. **1997**, *36*, 4998; b) J. K. Bera, M. Nethaji, A. C. Samuelson, *Inorg. Chem*. **1999**, *38*, 218; c) T. C. Deivaraj, J. J. Vittal, *J. Chem. Soc., Dalton Trans*. **2001**, 322; d) R.-N. Yang, Y.-A. Sun, Y.-M. Hou, X-Y. Hu, D.-M. Jin, *Inorg. Chim. Acta* **2000**, *304*, 1; e) Y. Ruina, L. Kunhua, H. Yimin, W. Dongmei, J. Douman, *Polyhedron* **1997**, **16**, 4033; f) R. Yang, Y. Liu, D. Jin, *J. Coord. Chem*. **2002**, *55*, 179.

19) Y.-Q. Wei, K.-C. Wu, B.-T. Zhuang, Z.-F. Zhou, *J. Coord. Chem*. **2006**, *59*, 713.

20) a) B. R. James, R. J. P. Williams, *J. Chem. Soc*. **1961**, 2007, b) F. A. Arnaud-Neu, E. Marques, M.-J. Schwing-Weill, C. O. Dietrich-Buchecker, J.-P. Sauvage, J. Weiss, *New J. Chem*. **1988**, *12*, 15.

21) D. R. McMillin, M. T. Buckner, B. T. Ahn, *Inorg. Chem*. **1977**, *16*, 943.

22) P. Comba, C. Katsichtis, B. Nuber, H. Pritzkow, *Eur. J. Inorg. Chem*. **1999**, 777.

23) a) E. Riesgo, Y.-Z. Hu, F. Bouvier, R. P. Thummel, *Inorg. Chem*. **2001**, *40*, 2541; b) I. Pianet, J.-M. Vincent, *Inorg. Chem*. **2004**, *43*, 2947; c) V. Hebbe-Viton, V. Desvergnes, J. J. Jodry, C. Dietrich-Buchecker, J.-P. Sauvage, J. Lacour, *Dalton Trans*. **2006**, 2058.

24) S. De, K. Mahata, M. Schmittel, *Chem. Soc. Rev*. **2010**, *39*, 1555.

25) A. Kaeser, PhD thesis, Toulouse (France), **2008**.

26) N. Long, J. Martin, G. Opromolla, A. J. P. White, D. J. Williams, P. Zanello, *J. Chem. Soc., Dalton Trans*. **1999**, 1981.

27) a) P. Federlin, J.-M. Kern, A. Rastegar, C. . Dietrich-Buchecker, P. A. Marnot, J.-P. Sauvage, *New J. Chem*. **1990**, *14*, 9; b) M. Ruthkosky, F. N. Castellano, G. J. Meyer, *Inorg. Chem*. **1996**, *35*, 6406; c) Y. Rio, G. Accorsi, N. Armaroli, D. Felder, E. Levillain, J.-F. Nierengarten, *Chem. Commun*. **2002**, 280.

28) Z. Kong, W. Li, G. Che, B. Chu, D. Bi, L. Han, and L. Chen, *Appl. Phy. Lett.* **2006,** *89*, 161112.

CHAPTER 3

Heteroleptic Cu(I) complexes prepared from phenanthroline and bis-phosphine ligands

Macrocyclic Phenanthroline Ligands for the Preparation of Heteroleptic Cu(I) Complexes

The work described in this chapter was done in collaboration with Prof. Jean-Pierre Sauvage (University of Strasbourg). Our stimulating scientific discussions as well as his continuous support and interest in this work are gratefully acknowledged.

1. Introduction

Bis-phenanthroline copper(I) complexes are thermodynamically stable compounds (log β = 10–12),[1] but they are also kinetically labile and fast ligand exchange is observed in solution at ambient temperature.[2] Therefore, the dynamic coordination of two distinct phenanthroline ligands around a Cu(I) cation is rather difficult to control. To date, two strategies have been reported for the selective synthesis of stable heteroleptic bis-phenanthroline copper(I) complexes.[3] The first one is based on *topological constraints*, the second on *steric constraints*. In both cases, maximum site occupancy is the key principle that allows the control on the dynamic heteroleptic complexation scenario.[3] This principle implies that all ligands and metal binding sites are utilized to generate coordinatively saturated complexes. Therefore, the maximum site occupancy requires a perfect match between the number of ligands and the coordination number of the metal ions used.[3,4] If the match is not perfect either by stoichiometry or design, coordinatively frustrated metal ligand assemblies will be left over.

Topological constraints. The approach using topological constraints has been reported in 1983 by Sauvage and co-workers.[5] As shown in Figure 1, the reaction of a macrocyclic phenanthroline ligand (**M30**) with an open chain phenanthroline derivative (**L**) in presence of Cu(I) cations gave exclusively the heteroleptic complex $[Cu(\mathbf{M30})(\mathbf{L})]^{+}$.

CHAPTER 4

Macrocyclic phenanthroline ligands for the preparation of heteroleptic Cu^{I} complexes

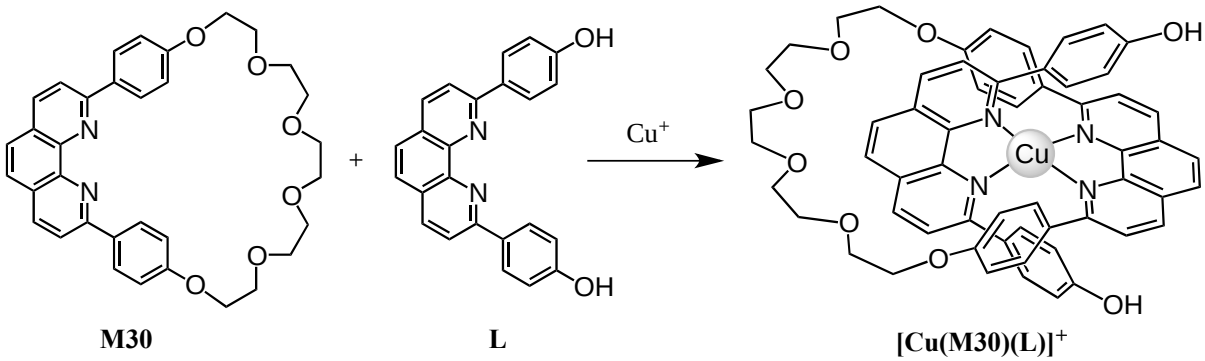

Figure 1. Approach developed by Sauvage for the quantitative preparation of heteroleptic bis-phenanthroline Cu(I) complexes.

Owing to the macrocyclic nature of ligand **M30**, the formation of the homoleptic complex $[Cu(\mathbf{M30})_2]^+$ is impossible, whereas the formation of $[Cu(\mathbf{M30})(\mathbf{L})]^+$ is not sterically prevented. The other competing reaction, *i.e.* the formation of the homoleptic complex $[Cu(\mathbf{L})_2]^+$, is unlikely due to maximum site occupancy problems. This is readily demonstrated by considering an equimolar mixture of **M30**, **L** and Cu(I) leading to the formation of $[Cu(\mathbf{L})_2]^+$:

$$2\,\mathbf{M30} + 2\,\mathbf{L} + 2\,Cu^+ \longrightarrow [Cu(\mathbf{L})_2]^+ + [Cu(\mathbf{M30})]^+ + \mathbf{M30}$$

Quantitative formation of $[Cu(\mathbf{L})_2]^+$ would leave behind the coordinatively frustrated entities $[Cu(\mathbf{M30})]^+$ and uncomplexed **M30**. This frustration drives the setting towards the clean formation of the heteroleptic complex. The discovery of this principle has been a major step towards the development of the field of mechanically interlocked molecules.[6] Indeed, Cu(I) complexed pseudo-rotaxane such as $[Cu(\mathbf{M30})(\mathbf{L})]^+$ have been extensively used for the preparation of numerous rotaxanes, catenanes and molecular machines.[6,7]

Steric constraints. Schmittel and co-workers have reported in 1997 another principle for the exclusive synthesis of mononuclear heteroleptic complexes.[8] The concept is based on the steric obstruction of homoleptic metal complexes by using the bulky 2,9-dimesityl-1,10-phenanthroline ligand (Figure 2). Hence, in the presence of an unhindered counterpart, for example 1,10-phenanthroline, quantitative heteroleptic complex formation has been observed.

The generality of this approach has been of utmost help to fabricate a large variety of sophisticated heteroleptic multi-component supramolecular architectures. Examples include ring-in-ring structures,[9] nanoboxes,[10] grids,[11] nanobaskets,[12] racks,[13] rectangles,[14] and tweezers.[15]

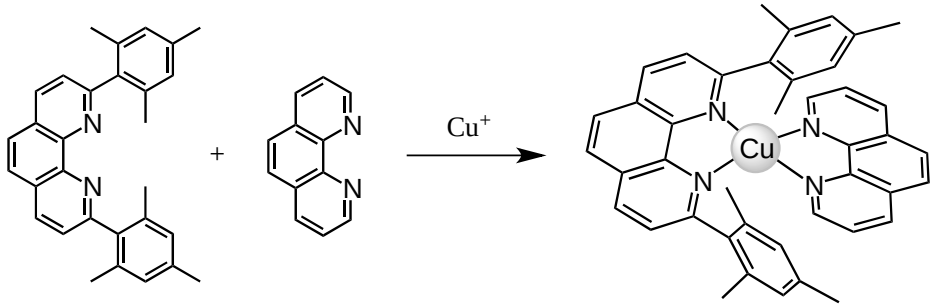

Figure 2. Approach developed by Schmittel for the quantitative preparation of heteroleptic bis-phenanthroline Cu(I) complexes.

As described in the previous chapter, the major limitation for the preparation of stable $[Cu(phen)(PP)]^+$ derivatives results from the exceptionally high thermodynamic stability of the corresponding homoleptic $[Cu(phen)_2]^+$ complexes. Based on the strategies developed for the formation of stable coordination compounds consisting of two distinct phenanthroline ligands around a Cu(I) cation, it appears clear that the use of a phenanthroline ligand for which the formation of a homoleptic Cu(I) complex is not possible would be an efficient synthetic approach for the preparation of stable $[Cu(phen)(PP)]^+$ derivatives. The strategy based on the steric obstruction of homoleptic metal complexes by using 1,10-phenanthroline derivatives with bulky 2,9-substituent is however not attractive for this purpose. Indeed, steric effects resulting from the bulky diphenylphosphino subunits of the PP ligands are expected to prevent the formation of the $[Cu(phen)(PP)]^+$ derivatives. In contrast, the formation of stable heteroleptic complexes can be anticipated by applying the approach based on topological constraints. Therefore, we have decided to incorporate the 2,9-disubstituted-1,10-phenanthroline subunit in a macrocyclic structure (Figure 3). In such a case, the formation of homoleptic complexes from the macrocyclic phenanthroline ligand being impossible, the maximum site occupancy principle should in principle favor the formation of stable heteroleptic Cu(I)-complexed pseudo-rotaxanes.

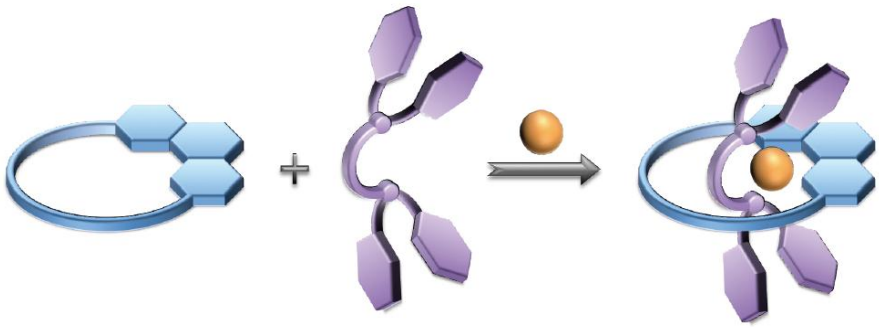

Figure 3. Proposed concept for the preparation of stable $[Cu(phen)(PP)]^{+}$ derivatives based on the approach using topological constraints developed by Sauvage.

2. Results and discussion

2.1. Preliminary investigations

To validate the proposed concept for the synthesis of stable $[Cu(phen)(PP)]^{+}$ derivatives, we first used the classical macrocyclic phenanthroline ligand **M30** developed in the Sauvage group. This ligand was kindly provided by Jean-Pierre Sauvage. Preliminary experiments were done with two bis-phosphine ligands, namely POP and dppp.

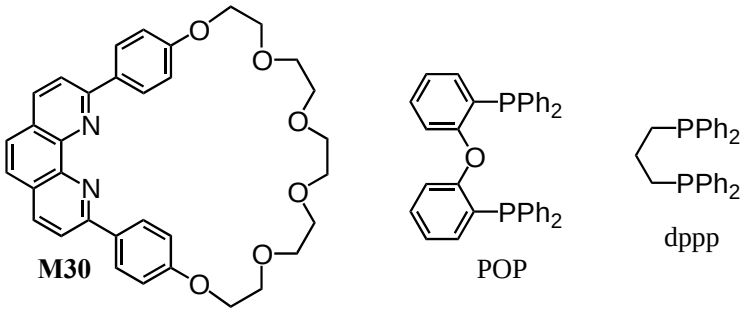

POP (1 equiv.) was added to a solution of $Cu(CH_3CN)_4BF_4$ (1 equiv.) and **M30** (1 equiv.) in CH_2Cl_2/CH_3CN. After 1 h, the solvents were evaporated. The heteroleptic complex

[Cu(**M30**)(POP)]BF_4 was then obtained by recrystallization in CH_2Cl_2/Et_2O. The ^{1}H and ^{31}P NMR spectra of the Cu(I) complex thus obtained are depicted in Figure 4.

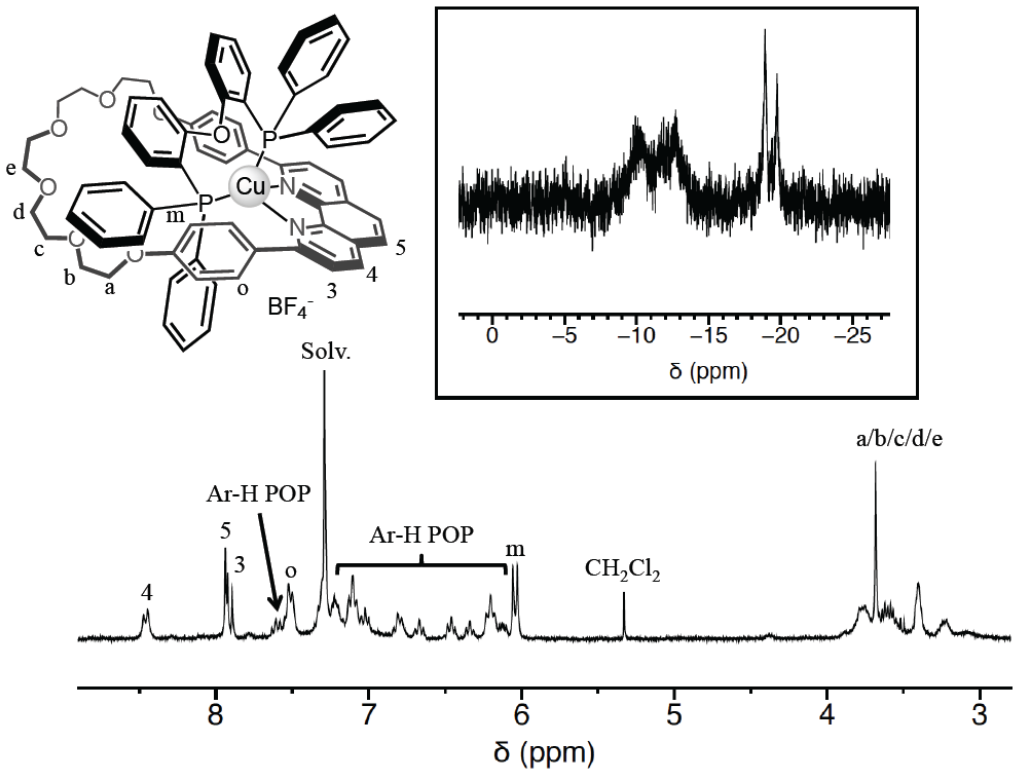

Figure 4. ^{1}H and ^{31}P NMR spectra ($CDCl_3$) of [Cu(**M30**)(POP)]BF_4.

Analysis of the integration of the ^{1}H NMR spectrum reveals that the isolated Cu(I) complex incorporates both POP and **M30** in a 1:1 ratio. However, the spectrum is not consistent with a symmetric pseudo-rotaxane structure resulting from the complete threading of the POP ligand through the macrocycle. Indeed, the series of signals attributed to the protons of the POP ligand are more complex than the one typically observed for classical [Cu(phen)(POP)]BF_4 derivatives. In addition, the signals observed for the pentaethylene glycol subunit of **M30** are more complicated than the ones expected for a [Cu(**M30**)(POP)]BF_4 pseudo-rotaxane with a C_{2v} symmetrical structure. Indeed, the CH_2 groups are diastereotopic suggesting that the isolated heteroleptic Cu(I) complex is chiral. As shown in Figure 4, these observations may be explained by a partially threaded POP ligand. Indeed, the diphenylphosphino moieties of POP is too bulky to pass through the 30-membered ring of **M30** and thus the formation of an ideal

pseudo-rotaxane is prevented. This view is further supported by the ^{31}P NMR spectra of [Cu(**M30**)(POP)]BF_4. Fortunately, crystals suitable for X-ray crystal structure analysis of [Cu(**M30**)(POP)]BF_4 could be obtained. As anticipated from the NMR data, the POP ligand is only partially threaded through the **M30** ligand (Figure 5). The macrocycle adopts a basket type conformation to accommodate one phenyl group of the POP ligand, all the other aromatic rings of the POP moiety being located on one side of the mean plane of the **M30** macrocycle.

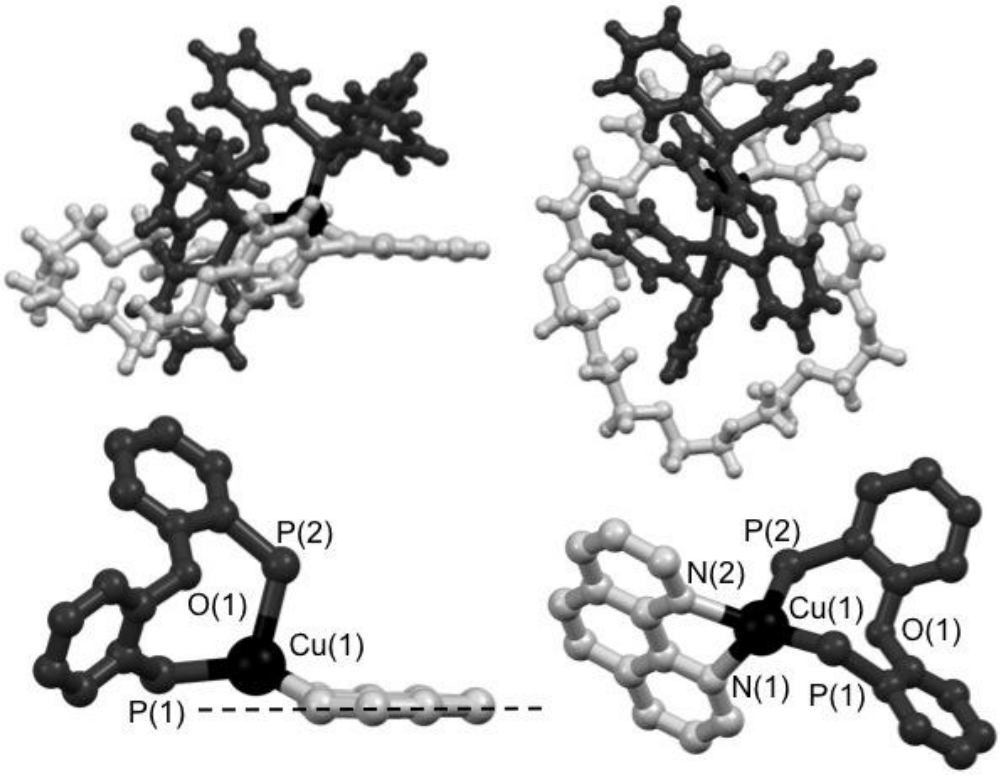

Figure 5. Top and side views of the X-ray crystal structure of [Cu(**M30**)(POP)]BF_4 (**M30**: pale gray, POP: dark gray, Cu: black, the counteranion is omitted) and details of the coordination sphere around the Cu(I) cation.

As a result of this peculiar conformation, the coordination sphere around the Cu(I) cation is highly distorted with P–Cu–P and N–Cu–N bond angles of 109.0(1) and 78.2(3)°, respectively (see Table 1). It can be noted that the POP ligand is bound to the metal only

through its pair of P donor atoms, the ether O atom being at a non-bonding distance from the Cu center (3.300(7) Å). The partial threading of the POP unit induces an important rocking of the POP ligand (*ca*. 37.3°) and the Cu(I) atom is located 0.737 Å over the mean plane of the phenanthroline moiety. These distortions induce (i) a slight decrease of the N(1)–Cu(1)–N(2) angle concomitant with an increase of the Cu-N bond lengths and (ii) a lengthening of the Cu(1)-P(2) bond when compared to the Cu(1)-P(1) bond (see Table 1). Indeed, the Cu(1)-P(2) bond distance (2.394(3) Å) is significantly longer when compared to the one typically observed for Cu-P distances in analogous complexes (in general in the 2.2 to 2.3 Å range).[16] This may explain the broadening observed for the signal of one P atom in the ^{31}P NMR spectra of [Cu(**M30**)(POP)]BF_4 (Figure 4). Indeed, a dynamic coordination/decoordination of this particular P atom is possible in solution. The slight broadening of some signals in the ^{1}H NMR spectra of [Cu(**M30**)(POP)]BF_4 may also be explained by this fast dynamic exchange between tri- and tetra-coordinated species. Finally, it can be added that this compound is not very stable and decomposes slowly. This is not too surprising as the Cu(I) cation is not in a favorable coordination environment as a result of steric effects.

Table 1. Bond distances (Å) and bond angles (°) within the coordination sphere of [Cu(**M30**)(POP)]BF_4 (see Figure 5 for the numbering).

Selected bond lengths		Selected bond angles	
Cu(1)-P(1)	2.265(2)	P(1)-Cu(1)-P(2)	109.0(1)
Cu(1)-P(2)	2.394(3)	P(1)-Cu(1)-N(1)	128.7(2)
Cu(1)-N(1)	2.094(8)	P(1)-Cu(1)-N(2)	131.1(2)
Cu(1)-N(2)	2.199(7)	P(2)-Cu(1)-N(1)	100.5(2)
		P(2)-Cu(1)-N(2)	102.8(2)
		N(1)-Cu(1)-N(2)	78.2(3)

The preparation of a Cu(I) complexed pseudo-rotaxane was also attempted by adding successively $Cu(CH_3CN)_4BF_4$ (1 equiv.) and dppp (1 equiv.) to a solution of **M30** (1 equiv.) in CH_2Cl_2/CH_3CN. After 1 h, the solvents were evaporated. Recrystallization by slow diffusion of Et_2O into a CH_2Cl_2 solution of the crude product gave yellow crystals. The ^{1}H

and ^{31}P NMR spectra of the product thus obtained are shown in Figure 6. Integration of the ^{1}H NMR spectrum revealed that the isolated Cu(I) complex combines one dppp subunit with two equivalent **M30** ligands. Clearly, this complex is neither a C_{2v} symmetrical pseudo-rotaxane or a partially threaded [Cu(**M30**)(dppp)]BF_4 compound similar to the one obtained when POP was used as the PP ligand. Given the high symmetry of the isolated compound, a possible structure is a dinuclear Cu(I) complex in which two equivalent $[Cu(\mathbf{M30})]^{+}$ moieties are connected by a bridging PP ligand (μ-dppp). The two Cu(I) cations are thus in a distorted trigonal coordination geometry.

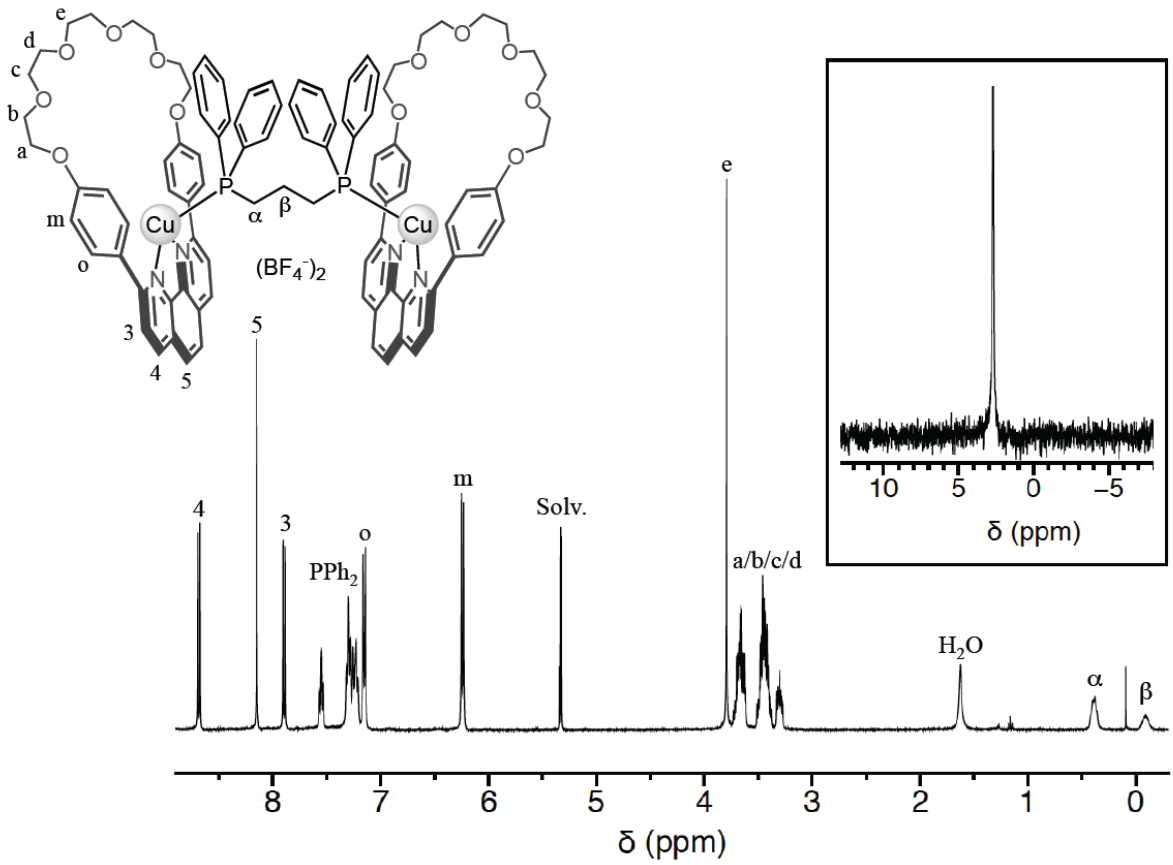

Figure 6. ^{1}H and ^{31}P NMR spectra (CD_2Cl_2) of $[Cu_2(\mathbf{M30})_2(\mu\text{-dppp})](BF_4)_2$.

The ^{31}P NMR spectrum showing that the two P atoms of the bridging ligand are equivalent is in agreement with the proposed $[Cu_2(\mathbf{M30})_2(\mu\text{-dppp})](BF_4)_2$ structure. Importantly, the P atoms of the μ-dppp ligand are observed at δ = 2.3 ppm. For $[Cu(phen)(dppp)]^{+}$ complexes with a chelating dppp unit, the resonance of the P atoms is typically observed around δ = -18

ppm. Actually, similar down-field shifts have been reported when going from a bridging μ-dppp ligand in $[Ag_2(phen)_2(\mu\text{-dppp})](BF_4)_2$ to a chelating one in $[Ag(phen)(dppp)]BF_4$.[17,18] Finally, electrospray mass spectrometry provided definitive evidence for the formation of $[Cu_2(\mathbf{M30})_2(\mu\text{-dppp})](BF_4)_2$ in spite of a high degree of fragmentation. The spectrum is dominated by peaks at m/z = 475.1 (99%), 567.2 (100%) and 629.2 (95%) corresponding to $[dppp + Cu]^+$, $[\mathbf{M30} + H]^+$, and $[\mathbf{M30} + Cu]^+$, respectively. Peaks of lower intensity are also observed at m/z = 1041.3 (10%) and 1759.5 (3%). These peaks are attributed to $[Cu(\mathbf{M30})(dppp)]^+$ and $[Cu_2(\mathbf{M30})_2(\mu\text{-dppp})(BF_4)]^+$, respectively.

The observed formation of $[Cu_2(\mathbf{M30})_2(\mu\text{-dppp})](BF_4)_2$ results from two constraints: (i) the formation of the homoleptic complex $[Cu(\mathbf{M30})_2]^+$ is impossible and (ii) the bulky PPh_2 moieties prevent the threading process of the dppp ligand leading to Cu(I)-complexed pseudo-rotaxanes. The formation of a distorted tetrahedral complex with a partially threaded chelating dppp ligand as in the case of POP is also not favorable. Actually, whereas POP is in general a chelating ligand, dinuclear complexes with bridging dppp ligands are common. In the particular case of dppp, the only way for the system to fulfill the maximum site occupancy principle is to adopt a dynamic heteroleptic complexation scenario in which the Cu(I) cations are in a distorted trigonal coordination geometry. In this way, the maximum of ligands are used and all the metal binding sites are utilized to generate trigonal complexes. This view was further confirmed by performing the reaction under stoichiometric conditions, *i.e.* **M30** (2 equiv.), dppp (1 equiv.) and $Cu(CH_3CN)_4BF_4$ (2 equiv.). Indeed, a perfect match between the number of ligands and the coordination number of the Cu(I) cations allowed the quantitative self-assembly of $[Cu_2(\mathbf{M30})_2(\mu\text{-dppp})](BF_4)_2$ as deduced from the ^1H NMR spectrum of the crude reaction mixture.

These preliminary investigations revealed that the bulky PPh_2 subunits of the bisphosphine ligands prevent the threading through the macrocyclic ligand **M30** and the preparation of Cu(I) complexed pseudo-rotaxanes is not possible. The combination of this steric constraint with the topological one resulting from the macrocyclic structure of **M30** plays a major role in the self-assembly process. The outcome depends actually on the adaptive capabilities of the PP ligand. In the case of POP which is a chelating ligand by nature, the PP ligand forces the system to adopt a sterically congested structure with a highly distorted tetrahedral coordination geometry around the Cu(I) cation. As a result, the metal is poorly stabilized in $[Cu(\mathbf{M30})(POP)]BF_4$ and slow decomposition is observed in solution. In

contrast, in the case of dppp, the bis-phosphine ligand is answering to both the steric and topological constraints by adopting a non-chelating coordination mode to generate $[Cu_2(\mathbf{M30})_2(\mu\text{-dppp})](BF_4)_2$. With the two metal centers in a trigonal coordination geometry protected by the phenyl moieties of both dppp and **M30**, the system prevents negative steric congestion effects and is thus stable. Whereas the results are of interest from the coordination chemistry point of view, **M30** is not the appropriate building block to validate the proposed concept for the formation of stable Cu(I) complexed pseudo-rotaxane. In order to prepare successfully such compounds, the design of new macrocyclic ligands is necessary.

2.2. First generation of Cu(I) pseudo-rotaxanes

Based on the results described in the previous section, we have designed a new macrocyclic phenanthroline ligand with a larger ring size. We have also decided to use a 2,9-diphenethyl-1,10-phenanthroline moiety rather then a 2,9-diphenyl-1,10-phenanthroline one in order to introduce some flexibility and thus to facilitate the threading process. The proposed retrosynthetic analysis of the designed macrocyclic ligand is shown in Figure 7.

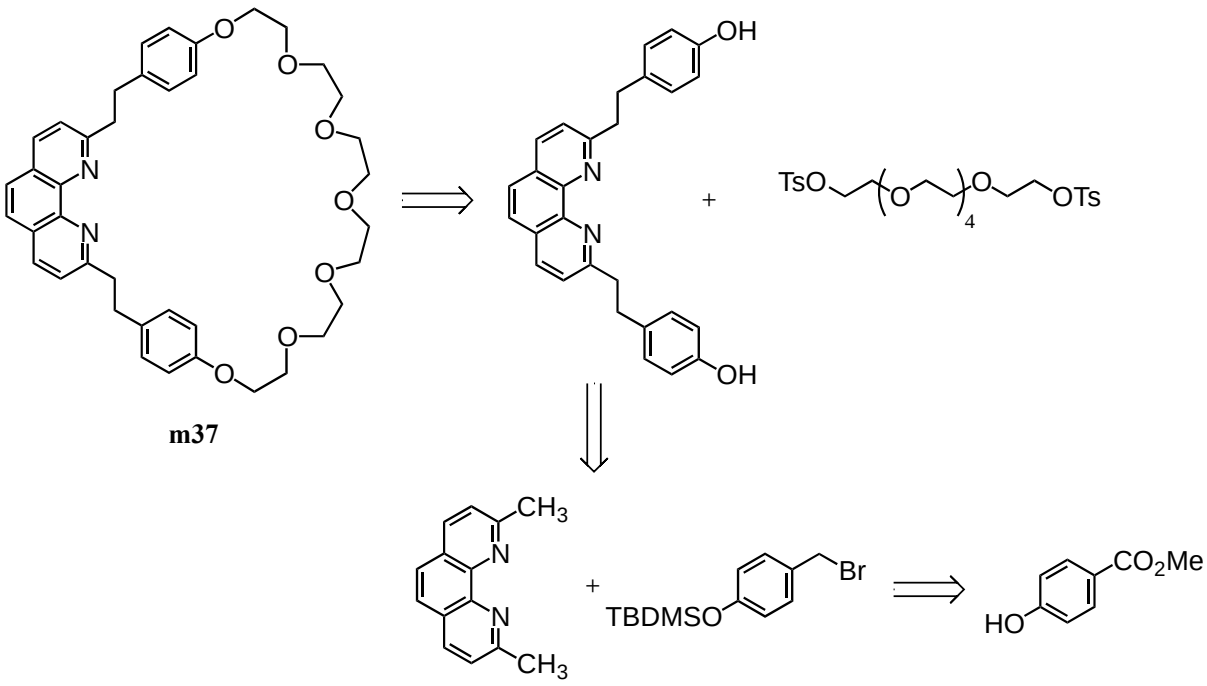

Figure 7. Structure of **m37** and the proposed retrosynthetic scheme for its synthesis.

Macrocycle **m37** may be prepared from the reaction of hexaethylene glycol ditosylate with a 2,9-diphenethyl-1,10-phenanthroline derivative bearing two phenol functions. The later compound may be obtained from an alkylation reaction of the dicarbanionic species derived from 2,9-dimethyl-1,10-phenanthroline with a benzylic bromide bearing a protected phenol function. The benzylic bromide building block may be obtained in tree steps from methyl 4-hydroxybenzoate.

The preparation of *p*-[(*tert*-butyldimethylsilyl)oxy]benzyl bromide (**4**) is depicted in Scheme 1. The phenol function of methyl 4-hydroxybenzoate (**1**) was protected as a *tert*-butyldimethylsilyl (TBDMS) ether by treatment with TBDMSCl in the presence of imidazole. $LiAlH_4$ reduction of **2** and reaction of the resulting benzylic alcohol **3** with TMSBr in $CHCl_3$ afforded **4**. It is worth noting that the choice of the appropriate conditions for the preparation of the benzylic bromide was the key to this synthesis.[19] Actually, this intermediate was found to be unstable. Under bromination conditions using TMSBr, no chromatographic purification step was required as the volatile by-products are eliminated by simple evaporation and the impurities precipitated from a hexane solution of the crude product.

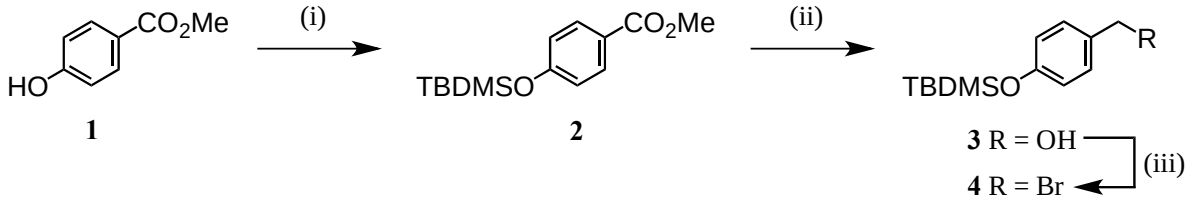

1 **2**

Scheme 1. Reagents and conditions: (i) TBDMSCl, Imidazole, DMF (98%); (ii) $LiAlH_4$, THF (98%); (iii) TMSBr, $CHCl_3$ (72%)

As shown in Scheme 2, treatment of 2,9-dimethyl-1,10-phenanthroline (**5**) with LDA (2 equiv.) at –78°C followed by reaction of the resulting dicarbanion with *p*-[(*tert*-butyldimethylsilyl)oxy]benzyl bromide (**4**) gave **6** in a moderate yield (38%). Actually, as typically observed for such reactions,[20] products of mono-alkylation were also formed in the reaction, making the purification of **6** particularly difficult.

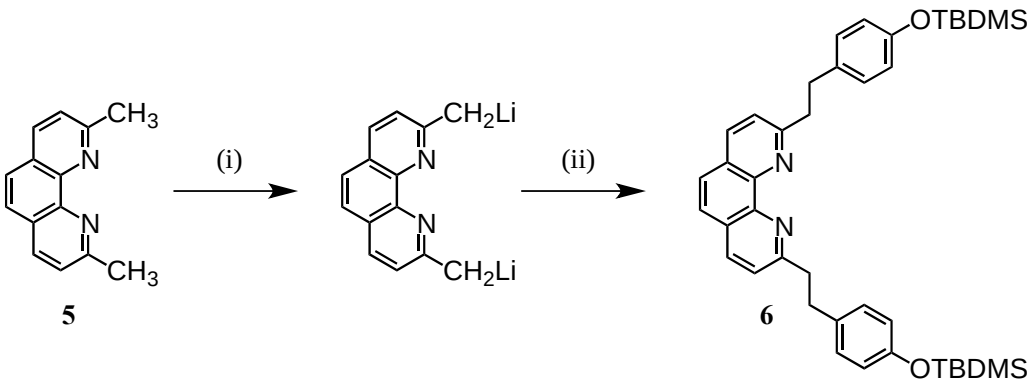

Scheme 2. Reagents and conditions: (i) LDA, THF, (ii) **4**, THF (38%).

The synthesis of the macrocyclic phenanthroline ligand **m37** is depicted in Scheme 3. Building block **8** was prepared from hexaethylene glycol (**7**) according to a reported procedure.[21] The macrocyclization reaction leading to **m37** was achieved by treatment of compound **6** with bis-tosylate **8** in the presence of CsF in CH_3CN.[22] Under these conditions, cleavage of the TBDMS protecting groups was achieved *in situ* to generate the corresponding bis-phenolate intermediate, thus avoiding the preparation of desilylated **6**[20a] which is highly insoluble in common organic solvents and difficult to handle. The reaction of the bis-phenolate intermediate thus generated with bis-tosylate **8** then gave **m37**. This macrocycle with a ring size of 37 atoms was isolated in 18% yield.

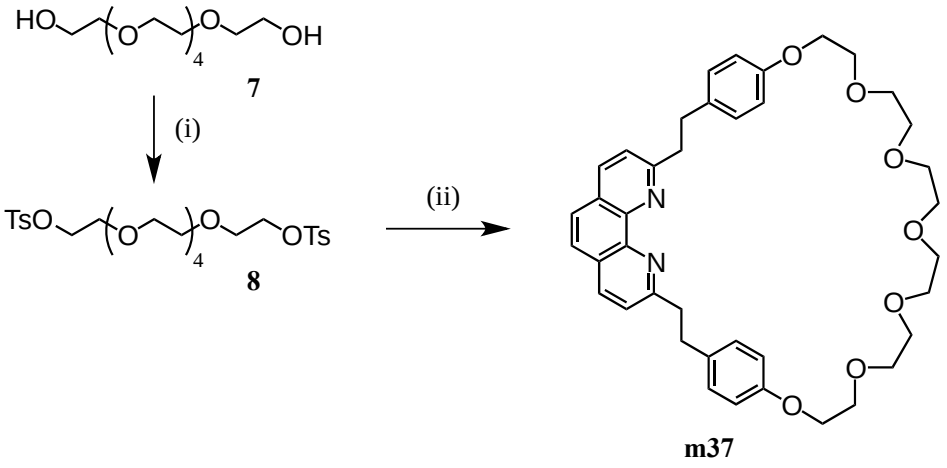

Scheme 3. Reagents and conditions: (i) TsCl, pyridine, DMAP, CH_2Cl_2 (86%); (ii) **6**, CH_3CN, CsF (18%)

The ^{1}H NMR spectrum of macrocycle **m37** is depicted in Figure 7. In addition to the signals corresponding to hexaethylene glycol moiety, the ^{1}H-NMR spectrum of **m37** is characterized by two sets of doublets and a singlet in a typical pattern for a 2,9-disubstituted-1,10-phenanthroline; an AA'XX' system for the *p*-disubstituted phenyl ring and an A_2X_2 system for the CH_2CH_2 linker. The proposed macrocyclic structure is supported by the symmetry of the compound deduced from the NMR spectrum and the hexaethylene glycol to phenanthroline ratio deduced from the integration. The structure of **m37** was also confirmed by MALDI-TOF mass spectrometry showing the expected molecular ion peak at *m/z* 667.3 (MH^+, calcd for $C_{40}H_{47}N_2O_7$: 667.338).

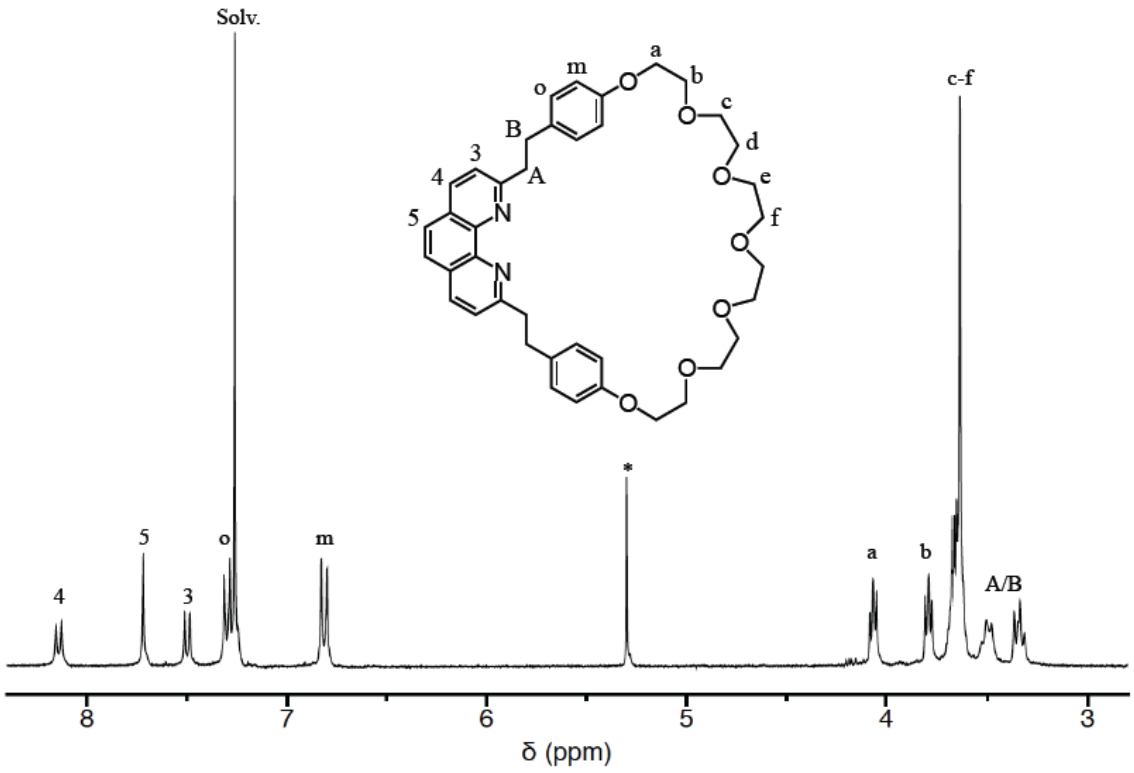

Figure 7. ^{1}H NMR spectrum ($CDCl_3$, 300 MHz) of **m37** (* = CH_2Cl_2).

$Cu(CH_3CN)_4BF_4$ (1 equiv.) and the appropriate bis-phosphine ligand (1 equiv.) were successively added to a solution of **m37** (1 equiv.) in CH_2Cl_2/CH_3CN (Scheme 4). After 1 h, the solvents were evaporated and the ^{1}H NMR analysis (CD_2Cl_2) of the crude products revealed the almost quantitative formation of a single product (POP and dppFc) or of a largely major compound (dppe and dppp).

The four [Cu(**m37**)(PP)]BF_4 pseudo-rotaxanes were then recrystallized (CH_2Cl_2/Et_2O) and fully characterized. Their structure was confirmed by electrospray mass spectrometry. For all the compounds, the mass spectrum displays a singly charged ion peak assigned to [Cu(**m37**)(PP)]$^+$. These heteroleptic complexes are remarkably stable in CH_2Cl_2 solutions and no detectable ligand exchange reactions could be detected. The UV/vis absorption spectra of [Cu(**m37**)(PP)]BF_4 recorded in CH_2Cl_2 show the diagnostic MLCT band of [Cu(phen)(PP)]BF_4 derivatives in the 380-420 nm region.[23] Finally, the NMR data were in full agreement with the proposed structures. As a typical example, the ^{1}H NMR of [Cu(**m37**)(dppe)]BF_4 is depicted in Figure 8.

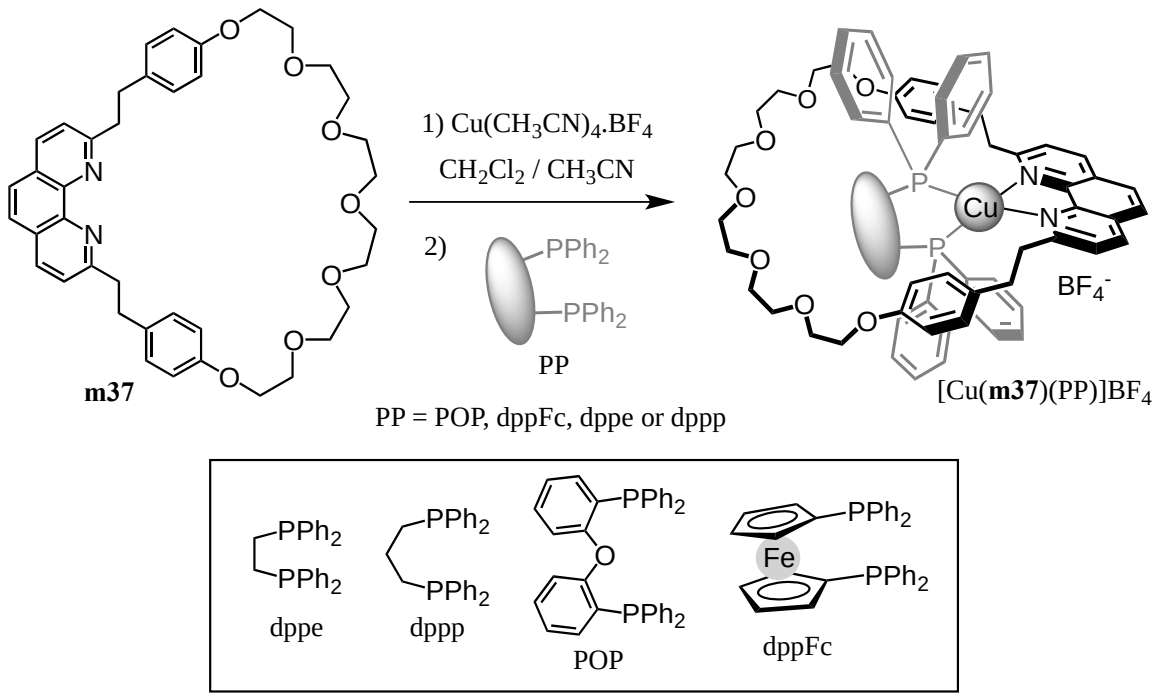

Scheme 4. Preparation of pseudo-rotaxanes [Cu(**m37**)(PP)]BF_4 from **m37** and various bis-diphenyphosphino-bridged ligands (dppe: 59%, dppp: 61%, POP: 85%, dppFc: 81%).

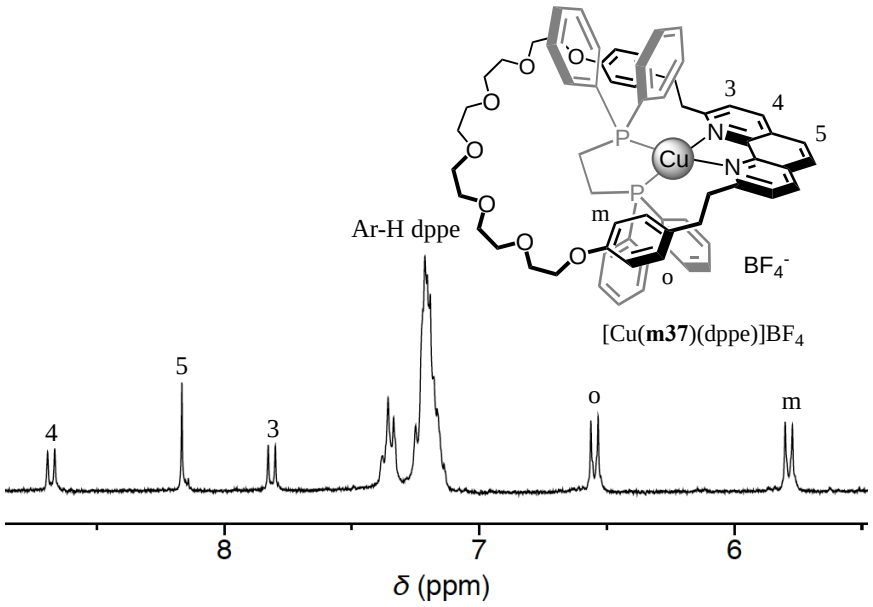

Figure 8. Aromatic region of the ^{1}H NMR spectrum (CD_2Cl_2, 300 MHz) of [Cu(**m37**)(dppe)]BF_4.

Remarkably, the signals of the *p*-disustituted phenyl rings of the **m37** ligand (H-o and H-m) are shielded of 0.75 (H-o) and 1.02 (H-m) ppm in the ^{1}H-NMR spectrum of [Cu(**m37**)(dppe)]BF_4 when compared to the corresponding signals in the spectrum of **m37**. This dramatic up-field shift originates from the ring current effect of the phenyl subunits of the dppe ligand located close to the phenethyl groups of **m37**. This view is also supported by the 2D NOESY spectrum of [Cu(**m37**)(dppe)]BF_4 recorded in CD_2Cl_2. Effectively, correlation peaks are observed between the Ar-H protons of the dppe moiety and the Ph-CH_2 of the **m37** ligand. The latter observations clearly reveal that the phenethyl moieties of **m37** and the PPh_2 subunits of dppe are spatially close in perfect agreement with the proposed pseudo-rotaxane structure. Similar observations have been also made with the three other [Cu(**m37**)(PP)]BF_4 derivatives thus showing the formation of pseudo-rotaxanes in all the cases. Therefore, the Cu^{I}-mediated threading of all the bis-phosphine ligands through the **m37** macrocycle was effective.

The X-ray crystal structure analysis of [Cu(**m37**)(POP)]BF_4 unambiguously proved the threading of the POP moiety through the macrocyclic phenanthroline ligand (Figure 9). Although the resolution of the structure is only moderate because of the disorder in the

hexaethylene glycol chain subunit of the **m37** ligand and the inclusion of unresolved solvent molecules (CH_2Cl_2), the identity of the Cu^{I}-complexed pseudo-rotaxane is in no doubt.

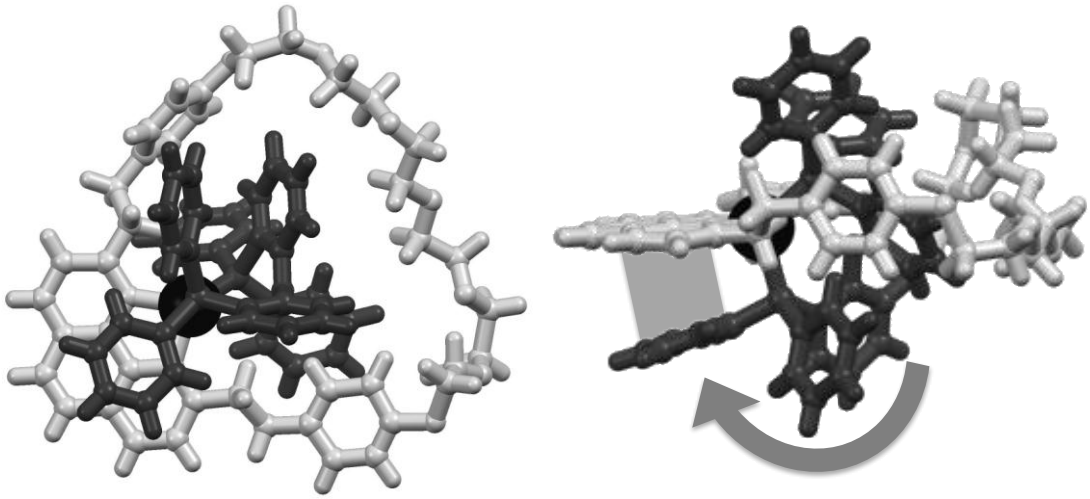

Figure 9. Top and side views of the X-ray crystal structure of [Cu(**m37**)(POP)]BF_4 (**m37**: pale gray, POP: dark gray, Cu: black), the counteranion is omitted. The rocking of the POP ligand allowing the establishment of an intramolecular π-π interaction between a phenyl ring of the POP ligand and the phenanthroline moiety of **m37** is highlighted (right).

The Cu^{I} center with the POP ligand and the 2,9-diphenethyl-1,10-phenanthroline subunit are well resolved. Several interesting details were revealed. The copper atom is in a distorted tetrahedral environment in which both the phenanthroline and the POP moieties are chelating ligands. It can be noted that the ether O atom of the POP subunit is at a non-bonding distance from the Cu^{I} center (> 3.25 Å). The distorted tetrahedral coordination mainly arises from the restricted bite angle of the phenanthroline ligand N(1)–Cu–N(2) (81.9(2)°), whereas the corresponding bis-phosphine bite angle P(1)–Cu–P(2) is 117.43(6)°. Finally, the intramolecular face-to-face π-π interaction between one phenyl ring of the POP ligand and the phenanthroline moiety of **m37** induces a significant rocking of the POP ligand (*ca*. 17.5°).

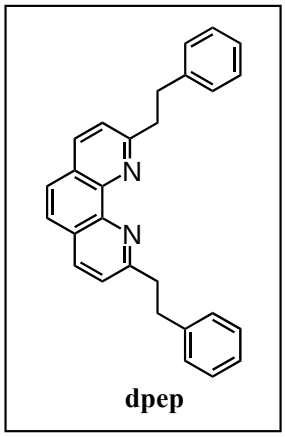

dpep

In order to highlight the influence of the macrocyclic structure of **m37** on the stability of the heteroleptic Cu^{I} complexes, the present results have to be compared to the one obtained with the corresponding acyclic derivatives prepared from 2,9-diphenethyl-1,10-phenanthroline (**dpep**). As described in chapter 3, [Cu(**dpep**)(PP)]BF_4 was the major reaction product and only traces of the homoleptic complexes were detected for both dppFc and POP. In contrast, when starting from dppe and dppp, the reaction with $Cu(CH_3CN)_4BF_4$ and **dpep** led to only small amounts of [Cu(**dpep**)(PP)]BF_4 (*ca*. 10-15%) and the formation of the homoleptic complexes was largely preferred. When compared to the efficient synthesis of the [Cu(**m37**)(PP)]BF_4 derivatives from **m37** and their good stability in solution whatever the nature of the PP ligand, the results obtained with the acyclic phenanthroline ligand **dpep** are very different, in particular when using dppe or dppp as starting material. In the case of **dpep**, the outcome of the reaction with $Cu(CH_3CN)_4BF_4$ and the various PP ligands is driven by the relative thermodynamic stability[1] of the [Cu(**dpep**)(PP)]BF_4 and [Cu(**dpep**)$_2$]BF_4 species. Given the fact that the thermodynamic stability of [Cu(**dpep**)$_2$]BF_4 must be very high, the preparation of stable heteroleptic [Cu(**dpep**)(PP)]BF_4 complexes is not possible with all the PP ligands. In the case of **m37**, the formation of the homoleptic bis-phenanthroline Cu^{I} complex being prevented by the macrocyclic nature of the phenanthroline ligand, the formation of heteroleptic complexes becomes thermodynamically favorable. In fact, if a certain proportion of the homoleptic complex $[Cu(PP)_2]BF_4$ would be formed, the stoichiometry of the reaction would necessarily imply the formation of an equivalent proportion of uncomplexed ring, which is highly unfavorable from a thermodynamic viewpoint. In other words, the maximum site occupancy principle favors the formation of stable heteroleptic Cu(I)-complexed pseudo-rotaxanes whatever the PP ligand.

2.3. Second generation of Cu(I) pseudo-rotaxanes

In the previous section, we have shown that the formation of stable heteroleptic Cu(I) complexes combining phenanthroline and bisphosphine ligands is possible by applying a

synthetic approach based on topological constraints. The preparation of these complexes is however limited by the synthesis of the macrocyclic phenanthroline derivative. In particular, the macrocyclization reaction leading to **m37** in a moderate yield (18%) is the main limiting step. With the aim to improve the synthesis of the macrocyclic phenanthroline derivative, we became interested in a synthetic approach using a ring closing metathesis (RCM) reaction to generate the macrocycle. Indeed, spectacular results have been reported in the literature for macrocyclization under reaction conditions using the Grubbs catalyst.[24-26] Among the numerous examples, the preparation of catenanes and molecular knots from Cu(I) bis-phenanthroline precursors can be highlighted.[26]

The synthesis of macrocycle **m30** is depicted in Scheme 5. Compound **9** was prepared in three steps from ethylene glycol according to a reported procedure.[27] Phenanthroline **10** was obtained in 41% yield from the reaction of the dicarbanion derived from neocuproine (**5**) with bromide **9** in THF.

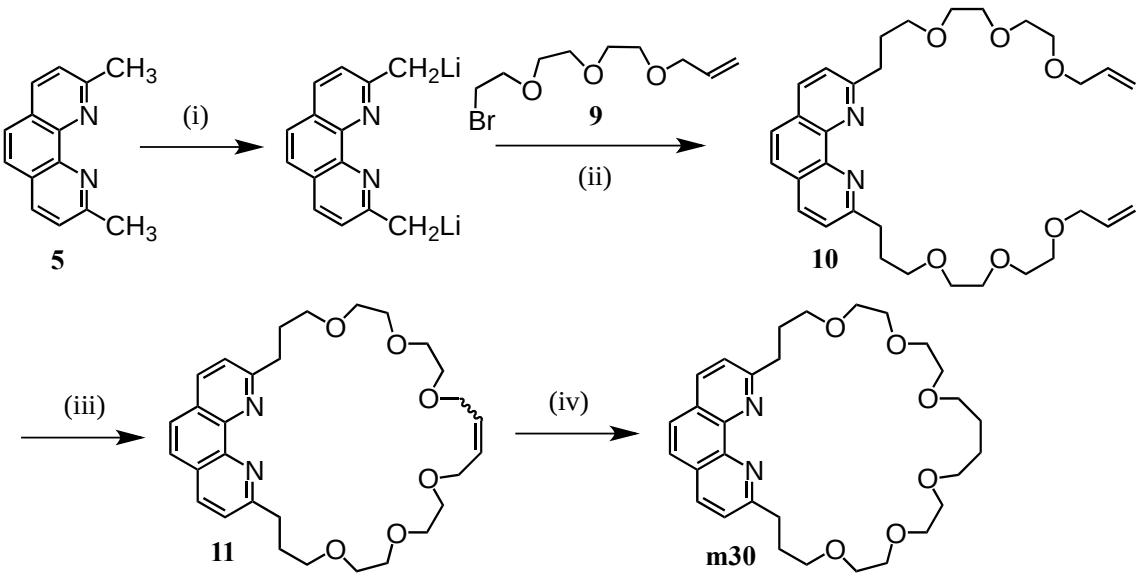

Scheme 5. Reagents and conditions: (i) LDA, THF, (ii) **9**, THF (41%); (iii) first generation Grubbs' catalysts, CH_2Cl_2 (86%); (iv) H_2, Pd/C, THF (60%).

The macrocyclization was then performed under RCM reaction conditions using the first generation Grubbs' catalyst. Importantly, the coordinating phenanthroline moiety does not interact with the ruthenium catalyst and macrocycle **11** was thus prepared in a remarkable

86% isolated yield. Close inspection of the ^{1}H NMR of **11** revealed that this compound was obtained as an *E*/*Z* isomeric mixture, one isomer being largely major (*ca*. 90%). Finally, hydrogenation of the carbon-carbon double bond was carried out using Pd/C. Compound **m30** was isolated in 60% yield. This moderate yield is due to the formation of secondary products resulting from a partial reduction of the phenanthroline moiety under these conditions. An improvement of this step is possible by using the Crabtree's iridium catalyst.[28] As described in the literature for the reduction of related phenanthroline derivatives,[26b] almost quantitative reduction of the carbon-carbon double bond was possible under these experimental conditions. However, this particular catalyst being particularly expensive, these conditions were not used when the synthesis was performed on a large scale.

The preparation of Cu(I) complexed pseudo-rotaxanes from **m30** was achieved by adding successively $Cu(CH_3CN)_4BF_4$ (1 equiv.) and the appropriate bis-phosphine ligand (1 equiv.) to a solution of **m30** (1 equiv.) in CH_2Cl_2/CH_3CN (Scheme 6). The resulting [Cu(**m30**)(PP)]BF_4 complexes were then isolated in a pure form by recrystallization (Et_2O/CH_2Cl_2).

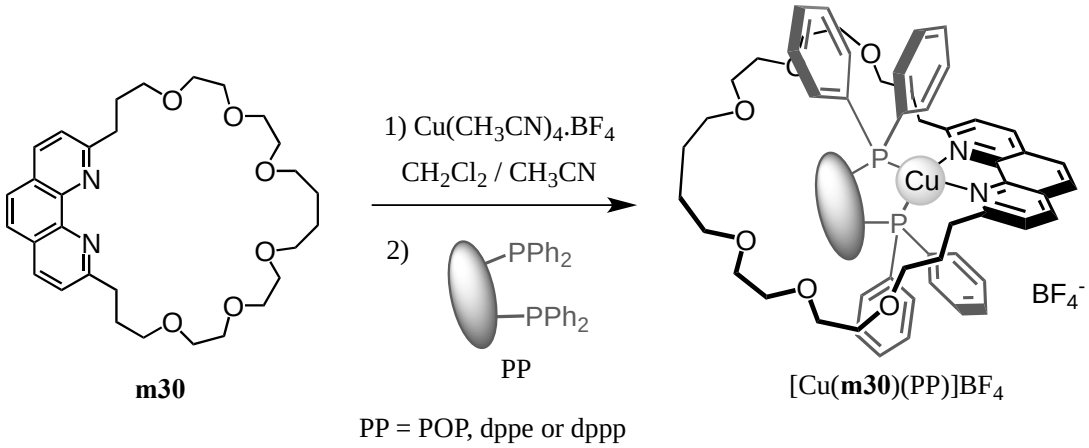

Scheme 6. Preparation of pseudo-rotaxanes [Cu(**m30**)(PP)]BF_4 from **m30** and various bis-phosphine ligands (dppe: 63%, dppp: 77%, POP: 75%).

In order to fully explore the possible synthetic pathways leading to pseudo-rotaxanes [Cu(**m30**)(PP)]BF_4, we became also interested in performing the RCM reaction from the Cu(I)-complexed acyclic precursors [Cu(**10**)(PP)]BF_4. In this respect, the preparation of the

acyclic derivatives was attempted from ligand **10** and the three PP ligands (dppe, dppp and POP). A solution of the appropriate bis-phosphine ligand (1 equiv.) and $Cu(CH_3CN)_4BF_4$ (1 equiv.) in CH_2Cl_2/CH_3CN was stirred for 0.5 h, then **10** (1 equiv.) was added. After 1 h, the solvents were evaporated. The products were analyzed as received by ^1H NMR. The relative proportion of the different possible complexes, *i.e.* $[Cu(\mathbf{10})(PP)]BF_4$, $[Cu(\mathbf{10})_2]BF_4$ and $[Cu(PP)_2]BF_4$, was deduced from the comparison with the ^1H NMR spectrum of $[Cu(\mathbf{L})_2]BF_4$ recorded in the same solvent. In the case of both dppe and dppp, the reaction with $Cu(CH_3CN)_4BF_4$ and **10** led to only small amounts of the desired acyclic precursors $[Cu(\mathbf{10})(PP)]BF_4$ (*ca*. 10%) and the formation of the homoleptic complexes is largely preferred. In contrast, when starting from POP, $[Cu(\mathbf{10})(POP)]BF_4$ was the only reaction product and no traces of the corresponding homoleptic complexes could be detected (Scheme 7).

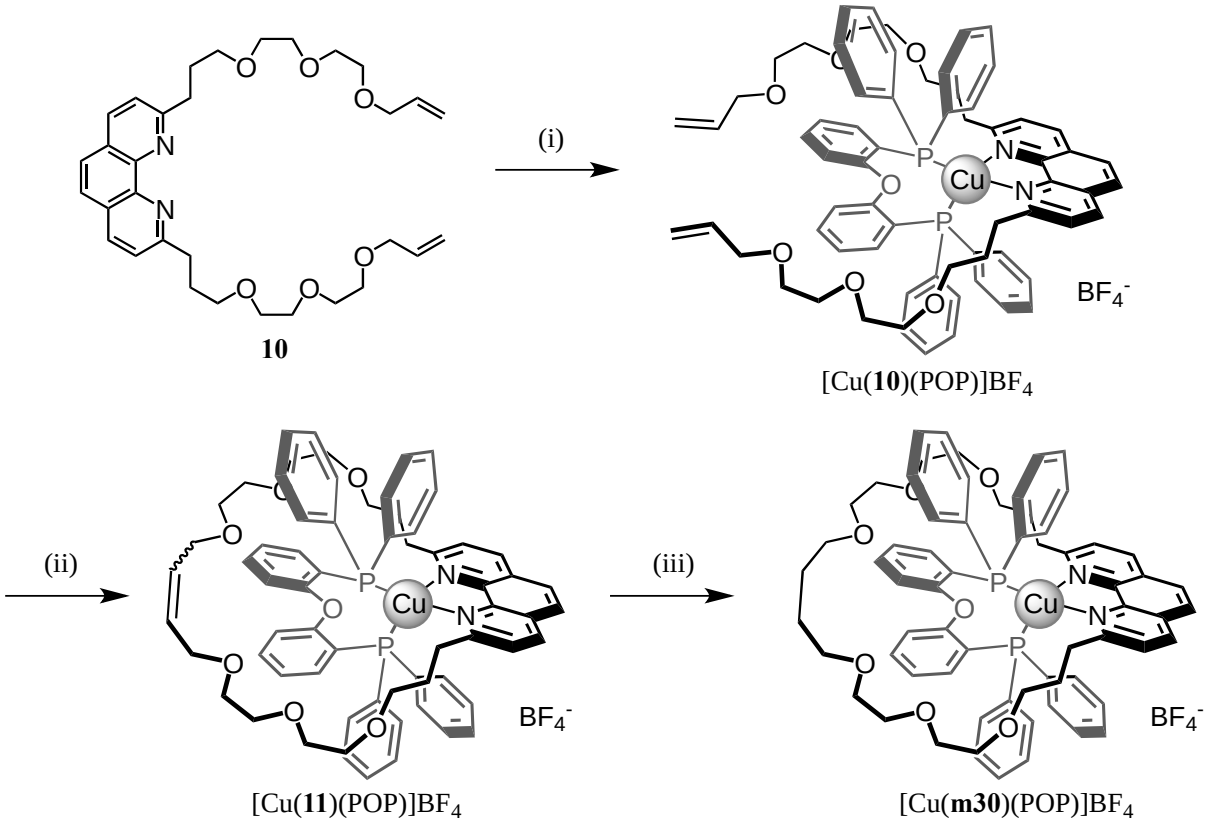

Scheme 7. Reagents and conditions: (i) POP, $Cu(CH_3CN)_4BF_4$, CH_2Cl_2, CH_3CN (85%); (ii) second generation Grubbs' catalysts, CH_2Cl_2 (36%); (iii) H_2, Pd/C, THF (40%).

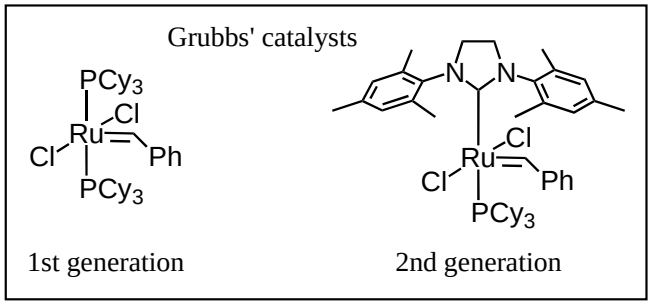

The first attempted cyclisation reactions of precursor [Cu(**10**)(POP)]BF_4 were performed under RCM conditions using the Grubbs' first generation catalyst in CH_2Cl_2. Under these conditions, no reaction was observed with 5 mol% of the ruthenium benzylidene catalyst. By using a larger amount of catalyst (30 mol%), the reaction started but consumption of the starting material stopped rapidly and no further reaction could be observed upon addition of new portions of catalyst to the reaction mixture. The desired Cu(I) complexed macrocyle was obtained at best in 5% yield under these conditions. The reaction conditions could be significantly improved by using the Grubbs' second generation catalyst. In this case, [Cu(**10**)(POP)]BF_4 could be converted more efficiently into [Cu(**11**)(POP)]BF_4. However, as in the previous case, consumption of the reagents stopped after a few hours of reaction and it was impossible to reach completion. Based on TLC and on the recovered starting material after column chromatography, *ca*. 20% of the reagent was not converted. Compound [Cu(**11**)(POP)]BF_4 was isolated by column chromatography on SiO_2 in 36% yield. This moderate yield is mainly due to difficulties encountered during the purification. Effectively, partial decomposition of the complex was observed on SiO_2. Actually, part of the compound remained adsorbed on SiO_2 all along the column (this was easily observed due to the yellow color of the compound) and could not be eluted anymore.

Both the first and second generation Grubbs' catalysts are generally tolerant to a wide range of functional groups, it is however known that none of them are suitable for olefin metathesis reactions involving free phosphine substrates.[29] Actually, the presence of free phosphine ligands disfavors the equilibrium for olefin binding to the catalyst in the first step of a dissociative mechanism for the RCM.[29] Indeed, competition between the better donating phosphine ligand and the olefin leads to inhibition of the catalyst.[29] This effect is only partially prevented by the coordination of the phosphine ligand to the Cu(I) cation in the case of reagent [Cu(**10**)(POP)]BF_4. Actually, copper(I) complexes being kinetically labile and thus allowing ligand exchange reactions in solution, the observed loss of activity for the RCM reaction maybe explained by the slow release of small amounts of free phosphine in the reaction mixture. The improved yield obtained with the Grubbs' second generation catalyst

results from a kinetic effect, the RCM reaction being much faster with this catalyst than with the first generation one. Finally, Pd-catalyzed hydrogenation of the carbon-carbon double bond of [Cu(**11**)(POP)]BF_4 gave [Cu(**m30**)(POP)]BF_4 in 40% yield. As in the previous step, the moderate yield is mainly due to difficulties encountered during the purification.

Pseudo-rotaxanes [Cu(**m30**)(PP)]BF_4 (PP = dppe, dppp and POP) were characterized by NMR spectroscopy and electrospray mass spectrometry. Crystals suitable for X-ray analysis were obtained for both [Cu(**m30**)(dppe)]BF_4 and [Cu(**m30**)(POP)]BF_4. As shown in Figure 10, the X-ray crystal structure analysis of [Cu(**m30**)(dppe)]BF_4 reveals a perfect threading of the dppe moiety through the macrocyclic phenanthroline ligand. The two diphenylphosphino subunits are effectively located at opposite sides from the mean plane of the **m30** macrocycle as suggested by the symmetry deduced from the NMR data of [Cu(**m30**)(dppe)]BF_4. It can be noted that due to some rotational freedom, one of the phenyl group of the dppe ligand is disordered. However, only one of the two possible orientations in the crystal lattice is shown in Figure 10 for the sake of clarity.

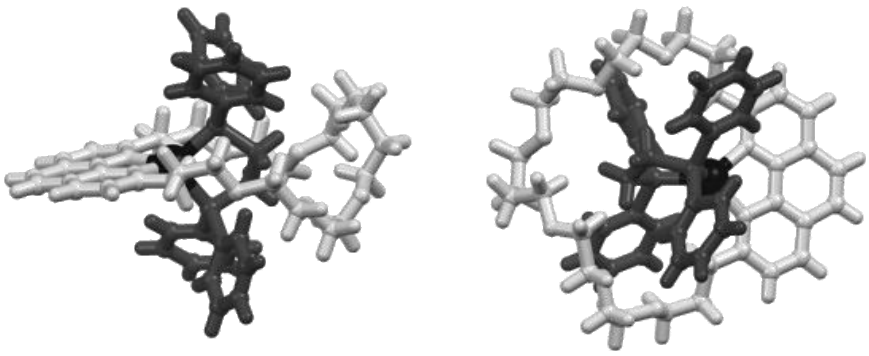

Figure 10. Top and side views of the X-ray crystal structure of [Cu(**m30**)(dppe)]BF_4 (**m30**: pale gray, dppe: dark gray, Cu: black, the counteranion is omitted).

As typically seen for $[Cu(phen)(PP)]^+$ complexes, packing induced distortions from an idealized pseudotetrahedral geometry are observed.[16,23] Close inspection of the crystal packing reveals a dimeric arrangement of the $[Cu(\mathbf{m30})(dppe)]^+$ cations in which two C–H/π intermolecular interactions are clearly established (Figure 11). These interactions involving

one hydrogen atom of a phenyl unit of the dppe ligand and the phenanthroline belonging to an adjacent molecule induce a slight rocking (*ca.* 10°) of the dppe ligand.

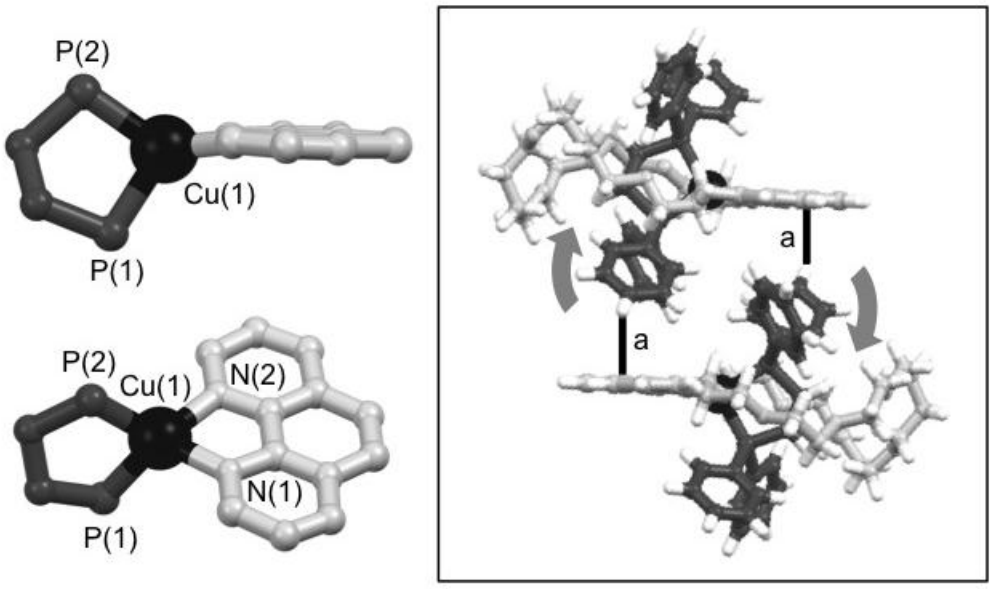

Figure 11. Details of the coordination sphere around the Cu(I) cation in the X-ray crystal structure of [Cu(**m30**)(dppe)]BF_4 (**m30**: pale gray, dppe: dark gray, Cu: black). Selected bond lengths: Cu(1)-P(1): 2.268(4), Cu(1)-P(2): 2.247(1), Cu(1)-N(1): 2.062(4), Cu(1)-N(2): 2.054(4) Å; selected bond angles: P(1)-Cu(1)-P(2): 92.42(5), P(1)-Cu(1)-N(1): 114.9(1), P(1)-Cu(1)-N(2): 121.8.1(1), P(2)-Cu(1)-N(1): 125.0(1), P(2)-Cu(1)-N(2): 124.2(1), N(1)-Cu(1)-N(2): 81.8(1)°. Inset: crystal packing showing the dimeric arrangment of the [Cu(**m30**)(dppe)]$^+$ cations in the crystal lattice (a = 2.857 Å).

Whereas the C_{2v} symmetrical pseudo-rotaxane structure deduced from the NMR data was confirmed by the X-ray crystal structure analysis of [Cu(**m30**)(dppe)]BF_4, the structure of the Cu(I) complex prepared from POP revealed only a partial threading of the PP ligand through **m30** (Figure 12). Actually, one phenyl group of the POP ligand is located within the cavity of the macrocyclic ligand whereas all the others are located on the same side of **m30**. This peculiar conformation results from the complete folding of macrocycle **m30**. It does however not induce significant distortions of the coordination geometry around the Cu(I) center in [Cu(**m30**)(POP)]BF_4. Indeed, the Cu-P and Cu-N distances as well as the bond P-

Cu-P, P-Cu-N and N-Cu-N bond angles are within the normal range when compared to known structures of $[Cu(phen)(POP)]^{+}$ complexes.[16,23]

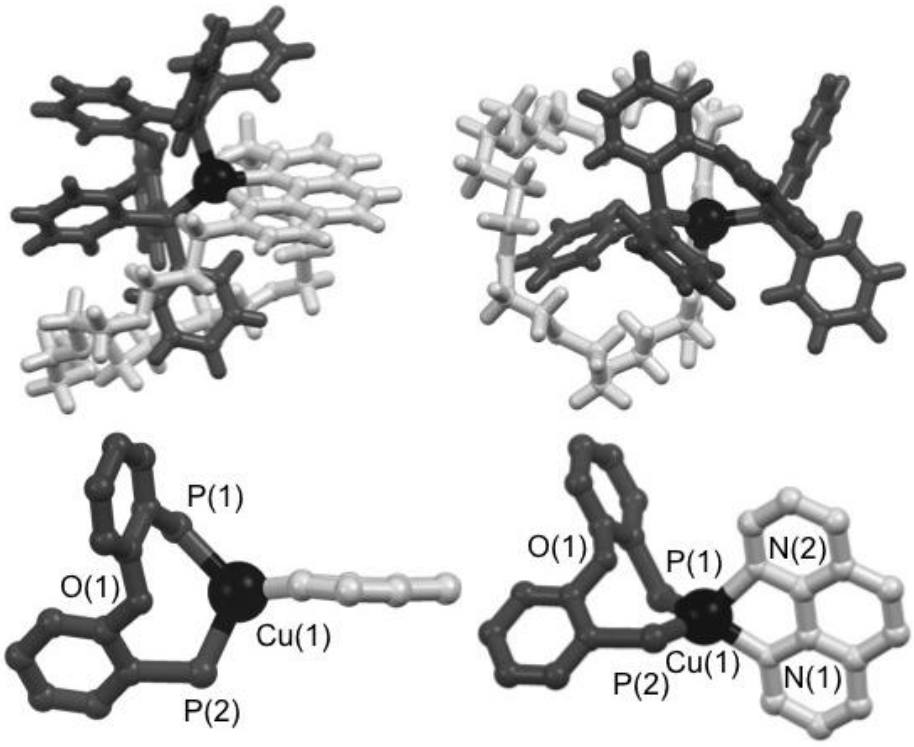

Figure 12. Top and side views of the X-ray crystal structure of [Cu(**m30**)(POP)]BF_4 (**m30**: pale gray, POP: dark gray, Cu: black, the counteranion is omitted) and details of the coordination sphere around the Cu(I) cation. Selected bond lengths: Cu(1)-P(1): 2.287(1), Cu(1)-P(2): 2.288(1), Cu(1)-N(1): 2.095(5), Cu(1)-N(2): 1.140(4); selected bond angles: P(1)-Cu(1)-P(2): 111.9(1), P(1)-Cu(1)-N(1):115.0(1) , P(1)-Cu(1)-N(2): 121.0(1), P(2)-Cu(1)-N(1): 119.2(1), P(2)-Cu(1)-N(2): 106.5(1), N(1)-Cu(1)-N(2): 79.8(2)°.

The ^{31}P NMR spectrum of [Cu(**m30**)(POP)]BF_4 recorded at room temperature shows a single resonance at δ = -13.57 ppm and suggests that the two P atoms of the POP moiety are equivalent. The latter observation is apparently in contradiction with the solid state structure of [Cu(**m30**)(POP)]BF_4 for which the two P atoms are different. Indeed, the four phenyl groups of the POP ligand may exchange their position inside and outside the cavity of **m30** in solution. In other words, the chain of the **m30** ligand is flexible enough to allow a fast

dynamic exchange between different conformers on the NMR timescale. As a result, the two P atoms appear as equivalent in the ^{31}P NMR spectrum recorded at room temperature. In order to confirm this hypothesis, ^{31}P NMR spectra were recorded at different temperatures. As shown in Figure 13, by cooling the solution to -40°C, the exchange between different conformers becomes slow on the NMR timescale, as attested by the two sets of doublets (^{2}J = 115 Hz) observed for the P atoms of the POP ligand. This is in perfect agreement with the partially threaded conformation observed in the X-ray crystal structure.

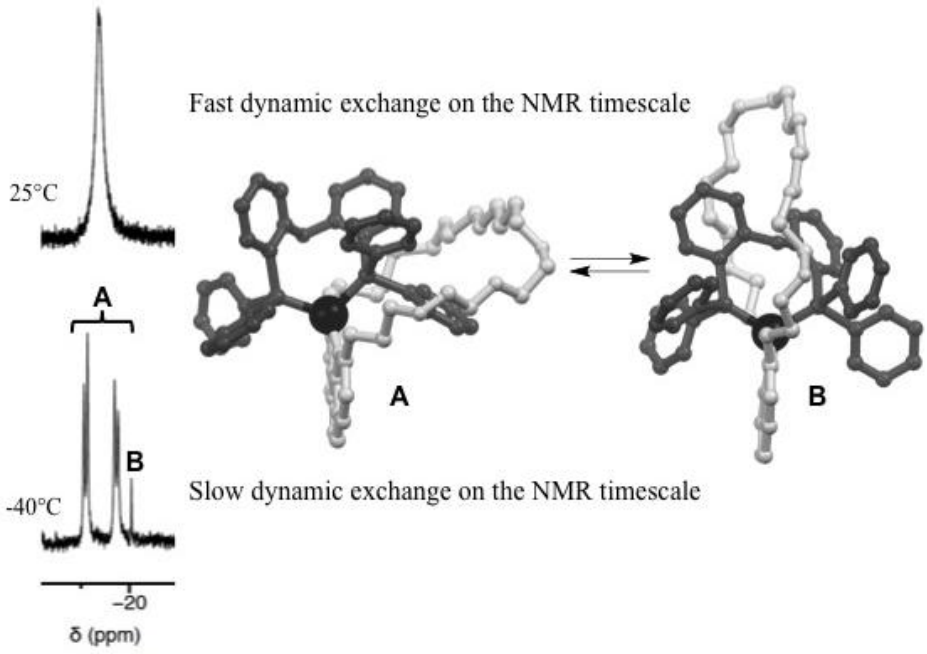

Figure 13. ^{31}P NMR spectra (CD_2Cl_2, 162 MHz) of [Cu(**m30**)(POP)]BF_4 recorded at different temperatures revealing a dynamic exchange between different topomers, *i.e.* topomerization.

Interestingly, a singlet is also observed at δ = -20.4 ppm. The latter is attributed to a C_{2v} symmetrical conformer (**B**) in which the POP ligand is fully threaded through the macrocycle. The minor population of this particular conformer suggests that it might be destabilized by steric congestion when the large phenyloxyphenyl bridging unit of the POP ligand is located within the cavity of **m30**. Indeed, the flexible **m30** macrocycle adopts preferentially a folded conformation in order to minimize steric congestion, the partially threaded conformer is thus energetically favored and its population largely major in solution. This view was fully

supported by computational studies. The molecular geometry was optimized at the PM6 semi-empirical level for both conformers **A** and **B** (Figure 14). The calculated energy difference between these two conformers is significant (~ 5.2 kcal mol^{-1}) and explains the preferential population of the **A** conformers in good agreement with the low temperature ^{31}P NMR spectrum. The energy barrier for the exchange between the **A** and **B** conformers must be low thus allowing a fast dynamic exchange at room temperature. In this way, each of the four phenyl rings of the POP ligand is alternatively located inside or outside the cavity of the **m30** macrocycle, the exchange taking place through the less energetically favored conformer (**B**).

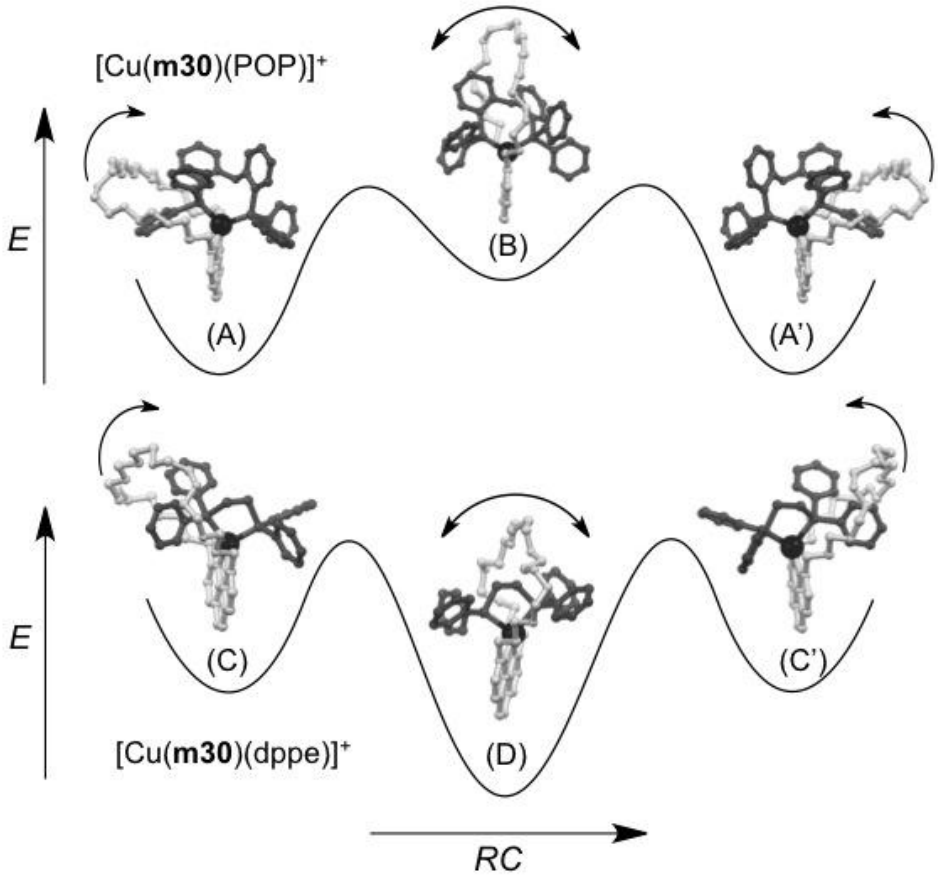

Figure 14. Calculated structures of the different topomers of [Cu(**m30**)(POP)]$^{+}$ (top) and [Cu(**m30**)(dppe)]$^{+}$ (bottom); **m30**: pale gray, PP ligand: dark gray, Cu: black, the H atoms have been omitted for clarity. A potential energy diagram is proposed to explain the dynamic exchange between topomers, *i.e.* topomerization, evidenced for [Cu(**m30**)(POP)]BF_4 by the variable temperature ^{31}P and ^{1}H NMR studies. In the case of [Cu(**m30**)(dppe)]BF_4, only topomer **D** was detected and no dynamic exchange could be evidenced.

It is also worth noting that conformer **A** is chiral and the dynamic molecular motions of the flexible chain of **m30** are responsible of a dynamic racemization, *i.e.* a fast exchange between **A** and **A'** (Figure 14). This was clearly evidenced from the ^{1}H-NMR spectra recorded over a large range of temperatures (from -80°C to 100°C, Figure 15).

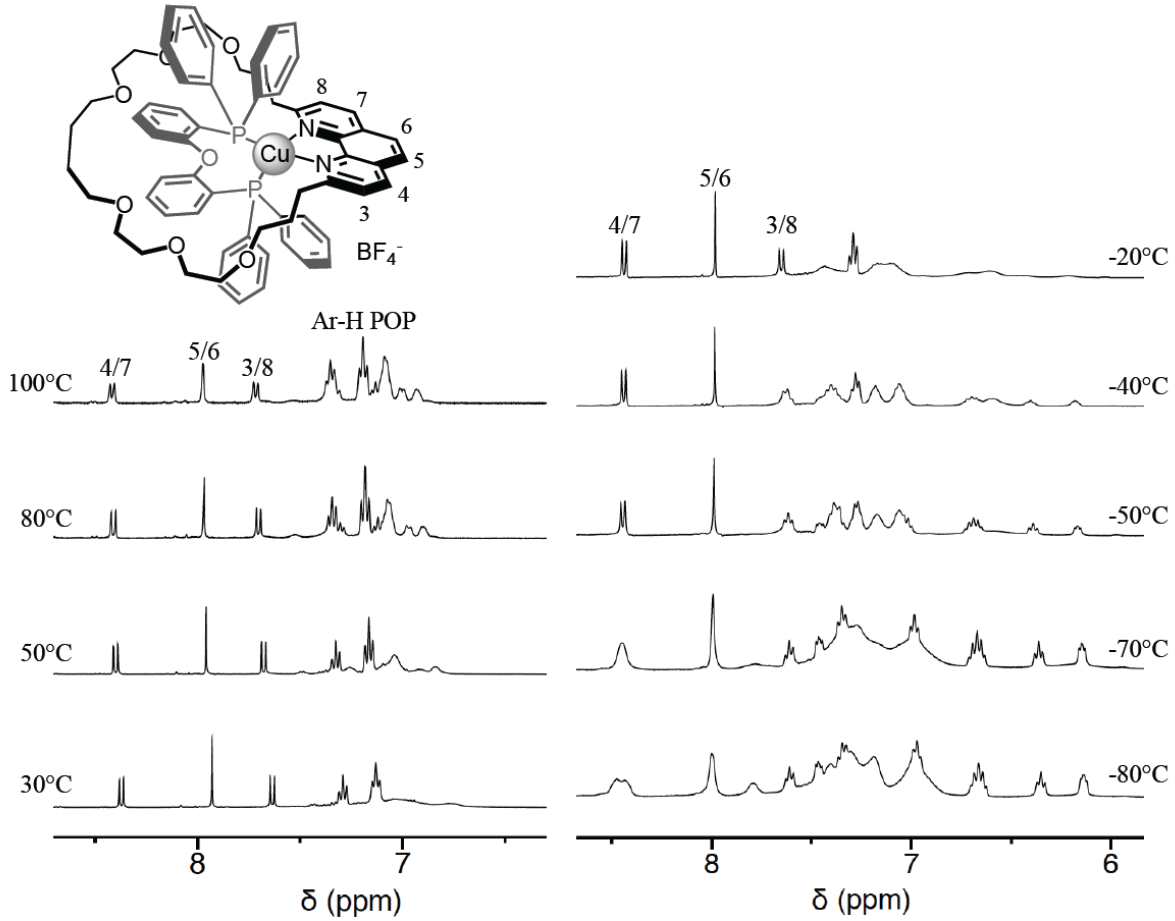

Figure 15. ^{1}H NMR spectra of [Cu(**m30**)(POP)]BF_4 recorded at different temperatures in $CDCl_2CDCl_2$ (left) and CD_2Cl_2 (right).

At high temperatures, two doublets are seen for the phenanthroline protons H(3-8) and H(4-7). Indeed, the exchange between the different conformers is fast on the NMR timescale under these conditions and both pairs of protons [H(3)-H(7) and H(4)-H(8)] appear equivalent in the ^{1}H-NMR spectrum. By cooling the solution, the NMR study revealed a clear coalescence and a reversible splitting of these peaks. Indeed, the exchange of conformers becomes slow on the

NMR timescale at low temperature and four sets of signals are observed for the phenanthroline protons H(3), H(4), H(7) and H(8) at -80°C. In other words, these pairs of protons are diastereotopic under these conditions due to the preferential chiral conformation adopted by [Cu(**m30**)(POP)]$^{+}$. The topological constraints resulting from the macrocyclic structure of the phenanthroline ligand are responsible for this particularly original dynamic conformational exchange. By analogy to the dynamics of an ensemble of protein conformations in which a topomeric set of structures is obtainable from a specific structure through local backbone folding transformations that do not disrupt the covalent bonding of the peptide backbone,[30] we thus propose to name these particular conformers in equilibrium ***topomers***, *i.e.* conformers having different topographies.

Variable temperature NMR studies were also carried out with [Cu(**m30**)(dppe)]BF_4. In this case, no dynamic exchange between topomers could be evidenced. Whatever the temperature, a single resonance is observed at δ = -6.87 ppm in the ^{31}P NMR spectrum. The C_{2v} symmetrical topomer is this time largely preferred and the partially threaded one could not be detected. These observations are in full agreement with the X-ray crystal structure of [Cu(**m30**)(dppe)]BF_4. When compared to POP, the bridging unit of dppe is smaller and does not generate particular steric congestions, thus the threaded topomer is not destabilized. Actually, computational studies revealed a significant energy difference between the fully (**D**) and partially threaded (**C**) topomers (~ 6.1 kcal mol^{-1}, see Figure 14). There is a clear energy penalty for the folding of the macrocycle. Indeed, in the case of POP, the fact that topomer **A** is favored shows that the steric congestion in fully threaded **B** must be relatively important.

3. Conclusion

We have demonstrated that the formation of stable heteroleptic [Cu(phen)(PP)]$^{+}$ complexes is possible by applying a synthetic approach based on topological constraints. For this purpose, the 2,9-disubstituted-1,10-phenanthroline subunit has been incorporated in a macrocyclic structure. In this way, the formation of homoleptic [Cu(phen)$_2$]$^{+}$ is prevented and the maximum site occupancy principle favors the formation of stable heteroleptic Cu(I)-complexed pseudo-rotaxanes. This is the case when the macrocycle is large and flexible enough (**m30** and **m37**) to allow the threading of the bulky diphenylphosphino moieties of the

PP building block. In contrast, when the phenanthroline-containing macrocycle (**M30**) is not large and flexible enough to allow the threading of the PP ligand, the combination of this steric constraint with the topological one resulting from the macrocyclic structure of the phenanthroline ligand plays a major role in the self-assembly process. The outcome depends actually on the adaptive capabilities of the PP ligand. Finally, we have shown that Cu(I) complexed pseudo-rotaxanes can be also prepared from the corresponding acyclic heteroleptic $[Cu(phen)(PP)]^{+}$ derivative by using a ring closing metathesis reaction. This result paves the way towards the preparation of new families of real rotaxanes by using precursors affording smaller macrocycles or by incorporating bis-phosphines with substituted phenyl groups. Upon RCM followed by demetallation, unprecedented rotaxane ligands containing both phenanthroline and bis-phosphine chelating subunits could be obtained (Figure 16). In addition to the synthetic challenge, systematic investigations of the coordination chemistry of such ligands are attractive future research avenues for preparation of unusual transition metal complexes with original electronic properties.

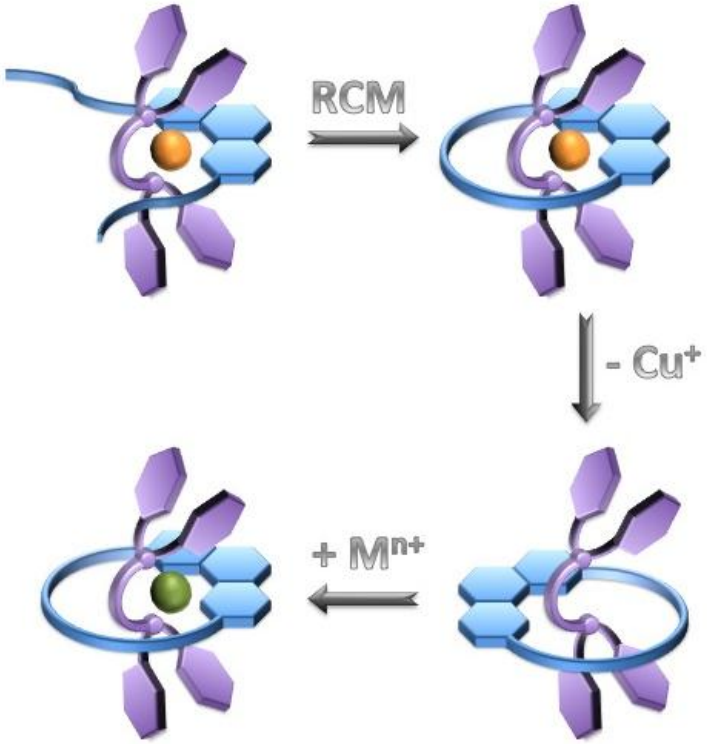

Figure 16. Proposed synthetic strategy for the preparation of rotaxane ligands containing both phenanthroline and bis-phosphine chelating subunits.

CHAPTER 4

Macrocyclic phenanthroline ligands for the preparation of heteroleptic Cu^{I} complexes

The photophysical properties of the heteroleptic complexes described in this chapter are underway in the group of Nicola Armaroli (CNR, Bologna, Italy) and are not available at this stage. It can however be pointed out that qualitative measurements performed in our group revealed a particularly strong emission for some of the pseudo-rotaxanes.

4. Experimental section

General. Reagents were purchased as reagent grade and used without further purification. Acetonitrile (CH_3CN) was distilled over CaH_2 under Ar. Dichloromethane (CH_2Cl_2) was distilled over CaH_2 under Ar. Tetrahydrofuran (THF) was distilled over Na under Ar. All reactions were performed in standard glassware under an inert Ar atmosphere. Evaporation and concentration were done at water aspirator pressure and drying in vacuo at 10^{-2} Torr. Column chromatography: silica gel 60 (230-400 mesh, 0.040-0.063 mm) was purchased from E. Merck. Thin Layer Chromatography (TLC) was performed on aluminum sheets coated with silica gel 60 F_{254} purchased from E. Merck. IR spectra (cm^{-1}) were recorded on a Perkin–Elmer Spectrum One Spectrophotometer. NMR spectra were recorded on a Bruker AC200 or AC 300 or AC 400 with solvent peaks as reference. The ^{1}H signals were assigned by 2D experiments (COSY and ROESY). MALDI-TOF-mass spectra were carried out on a Bruker BIFLEX™ matrix-assisted laser desorption time-of-flight mass spectrometer. ESI-MS mass spectra were carried out on a Bruker MicroTOF spectrometer.

Compound [Cu(M30)(POP)]BF_4

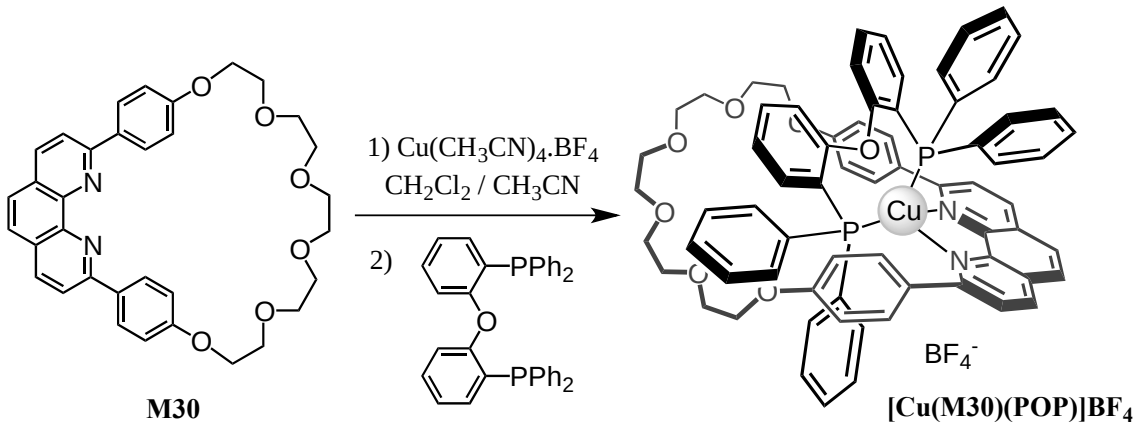

M30 **[Cu(M30)(POP)]BF_4**

A solution of **M30** (32 mg, 0.056 mmol) and $Cu(CH_3CN)_4BF_4$ (18 mg, 0.056 mmol) in a 7:3 CH_2Cl_2/CH_3CN mixture (10 mL) was stirred for 0.5 h, then POP (30 mg, 0.056 mmol) was added. After 1 h, the solvents were evaporated. Recrystallization by slow diffusion of Et_2O into a CH_2Cl_2 solution of the crude product gave [Cu(**M30**)(POP)]BF_4 (30 mg, 42% yield) as orange crystals. ^{1}H NMR (CD_2Cl_2, 300 MHz): 8.43 (d, J = 8Hz, 2H), 7.91 (s, 2H), 7.88 (d, J =

8Hz, 2H), 7.58 (m, 1H), 7.48 (m, 4H), 7.19 (m, 4H), 7.03 (m, 8H), 6.71 (m, 5H), 6.43 (m, 2H), 6.31 (m, 2H), 6.17 (m, 4H), 6.12 (m, 2H), 6.01 (d, *J* = 8Hz, 4H), 3.65 (m, 12H), 3.37 (m, 4H), 3.19 (m, 4H).

Crystals suitable for X-ray crystal-structure analysis were obtained by slow diffusion of Et_2O into a CH_2Cl_2 solution of **[Cu(M30)(POP)]BF_4**. Data were collected at 173 K on a Bruker APEX-II CCD diffractometer (Mo-Kα radiation, λ = 0.71073 Å). The structure was solved by direct methods (SHELXS-97) and refined against F^2 using the SHELXL-97 software. The non-hydrogen atoms were refined anisotropically, using weighted full-matrix least-squares on F^2. The H-atoms were included in calculated positions and treated as ridig atoms using SHELXL default parameters. Crystallographic data: formula: $C_{70}H_{62}CuN_2O_7P_2.BF_4$ (M = 1255.51 g.mol^{-1}); yellow crystal, 0.20 × 0.10 × 0.12 mm; crystal system: monoclinic, space group $P2_1/c$; *a* = 13.292(5) Å; *b* = 28.770(5) Å; *c* = 19.994(5) Å; *β* = 128.310(15)°; V = 5999(3) Å^3; Z = 4; F(000) = 2608; a total of 59051 reflections collected; 1.69° < θ < 28.02°, 14418 independent reflections with 7128 having I > 2σ(I); 544 parameters; Final results : $R_1(F^2)$ = 0.1655; $wR_2(F^2)$ = 0.2409, Goof = 1.181.

Compound $[Cu_2(M30)_2(dppp)](BF_4)_2$

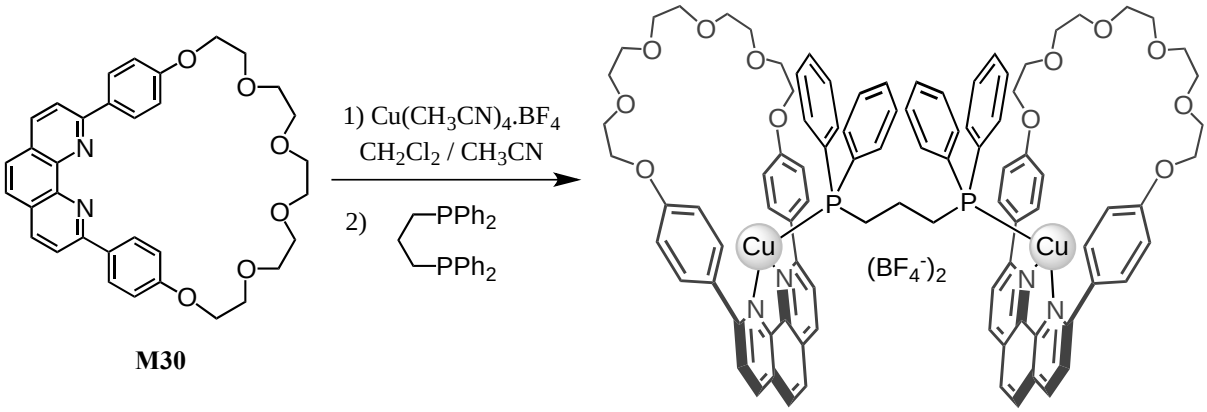

A solution of **M30** (70 mg, 0.124 mmol) and $Cu(CH_3CN)_4BF_4$ (39 mg, 0.124 mmol) in a 7:3 CH_2Cl_2/CH_3CN mixture (20 mL) was stirred for 0.5 h, then dppp (26 mg, 0.062 mmol) was added. After 1 h, the solvents were evaporated. Recrystallization by slow diffusion of Et_2O into a CH_2Cl_2 solution of the crude product gave $[Cu_2(\mathbf{M30})_2(dppp)](BF_4)_2$ (92 mg, 81%) as

yellow crystals. ^{1}H NMR (CD_2Cl_2, 400 MHz): 8.69 (d, *J* = 8Hz, 4H), 8.15 (s, 4H), 7.89 (d, *J* = 8Hz, 4H), 7.55 (t, *J* = 7Hz, 4H), 7.26 (m, 16H), 7.15 (d, *J* = 8Hz, 8H), 6.24 (d, *J* = 8Hz, 8H), 3.79 (s, 8H), 3.66 (m, 12H), 3.46 (m, 16H), 3.32 (m, 4H), 0.38 (m, 4H), -0.09 (m, 2H). $^{31}P\{^{1}H\}$ NMR (CD_2Cl_2, 162 MHz): 2.69. ES-MS: 1759.5 (3%, $[Cu_2(\mathbf{M30})_2(dppp)(BF_4)]^+$), 1041.3 (10%, $[Cu(\mathbf{M30})(dppp)]^+$), 629.2 (95%, $[\mathbf{M30} + Cu]^+$), 567.2 (100%, $[\mathbf{M30} + H]^+$), 475.1 (99%, $[dppp + Cu]^+$).

Compound 2

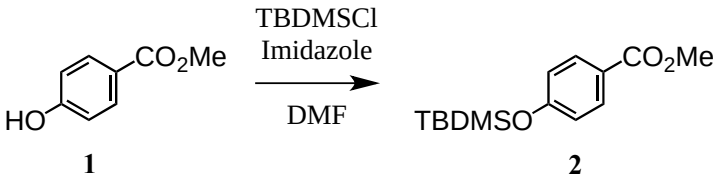

1 **2**

A mixture of TBDMSCl (10.40 g, 69 mmol), imidazole (8.95 g, 131 mmol) and **1** (10.00 g, 66 mmol) in DMF (200 mL) was stirred at 0°C for 4 h, then at room temperature for 24 h and evaporated. The residue was taken up with Et_2O, washed with brine, dried ($MgSO_4$), filtered and evaporated. Column chromatography on SiO_2 (CH_2Cl_2) yielded **2** (17.24 g, 98%) as a colorless oil. ^{1}H NMR ($CDCl_3$, 200 MHz): 7.94 (d, *J* = 8 Hz, 2 H), 6.85 (d, *J* = 8 Hz, 2 H), 3.88 (s, 3H), 0.99 (s, 9 H), 0.23 (s, 6 H). ^{13}C NMR ($CDCl_3$, 50 MHz): 166.7, 159.5, 131.4, 123.1, 117.7, 51.7, 25.5, 18.1. Elemental analysis calcd for $C_{14}H_{22}O_3Si$: C 63.12, H 8.32; found C 62.92, H 8.40.

Compound 3

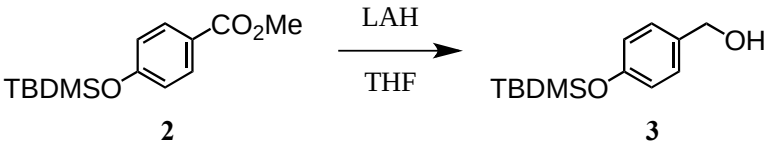

2 **3**

A 1 M $LiAlH_4$ solution in dry THF (54 mL, 54 mmol) was added dropwise to a stirred solution of **2** (10.00 g, 38 mmol) in dry THF (150 mL) at 0°C. The resulting mixture was stirred for 5 h at 0°C, then MeOH and H_2O were carefully added. The resulting mixture was filtered (Celite) and evaporated. Column chromatography on SiO_2 (CH_2Cl_2) yielded **3** (8.80 g,

98%) as a colorless oil. ^{1}H NMR ($CDCl_3$, 200 MHz): 7.22 (d, *J* = 8 Hz, 2 H), 6.83 (d, *J* = 8 Hz, 2 H), 4.59 (broad s, 2H), 0.99 (s, 9 H), 0.23 (s, 6 H). ^{13}C NMR ($CDCl_3$, 50 MHz): 155.0, 133.7, 128.4, 119.9, 64.5, 25.5, 18.1. Elemental analysis calcd for $C_{13}H_{22}O_2Si$: C 65.50, H 9.30; found C 65.66, H 9.41.

Compound 4

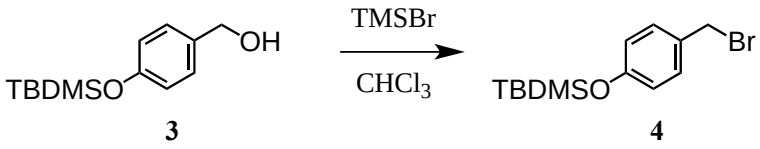

3 **4**

TMSBr (4.1 mL) was added to a stirred solution of **3** (5.00 g, 21 mmol) in $CHCl_3$ (50 mL) at 0°C. After 1 h, the mixture was allowed to warm to room temperature (within 1 h), then stirred for 1 h, filtered and evaporated. The resulting oil was dissolved in hexane (100 mL) and placed in the freezer overnight. The solution was filtered to remove the precipitate and evaporated to give **4** (4.60 g, 72%) as a colorless oil that was used as received in the next step. ^{1}H NMR ($CDCl_3$, 200 MHz): 7.26 (d, *J* = 8 Hz, 2 H), 6.80 (d, *J* = 8 Hz, 2 H), 4.99 (s, 2H), 0.99 (s, 9 H), 0.21 (s, 6 H).

Compound 6

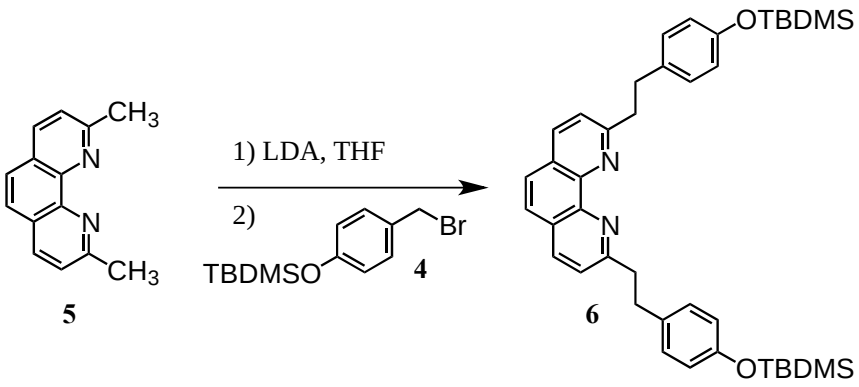

5 **4** **6**

A 2 M solution of LDA in THF (9.2 mL, 18.4 mmol) was added slowly to a solution of **5** (1.90 g, 9 mmol) in anhydrous THF (60 mL) at -78°C under Ar. After 3 h, a solution of **4** (6.10 g, 20 mmol) in THF (10 mL) was added dropwise. The resulting mixture was stirred 2 h at -78°C, then 15 h at room temperature. The solution was then poured into ice water (150

mL). The mixture was extracted with CH_2Cl_2 (3 x 100 mL) and the combined organic layers were dried ($MgSO_4$), filtered and evaporated. Column chromatography (SiO_2, CH_2Cl_2/2% MeOH) yielded **5** (2.30 g, 38%) as a colorless glassy product. ^{1}H NMR ($CDCl_3$, 200 MHz): 8.13 (d, J = 8 Hz, 2H), 7.72 (s, 2H), 7.45 (d, J = 8 Hz, 2H), 7.19 (d, J = 8 Hz, 4H), 6.78 (d, J = 8 Hz, 4H), 3.52 (m, 4H), 3.25 (m, 4H), 0.99 (s, 18H), 0.20 (s, 12H). ^{13}C NMR ($CDCl_3$, 50 MHz): 161.7, 153.5, 145.3, 135.9, 134.3, 129.2, 126.9, 125.3, 122.5, 119.7, 41.0, 34.6, 25.5,17.9. Elemental analysis calcd for $C_{40}H_{52}O_2Si_2N_2$: C 74.03, H 8.08; N 4.32; found C 73.76, H 8.17, N 4.20.

Compound 8

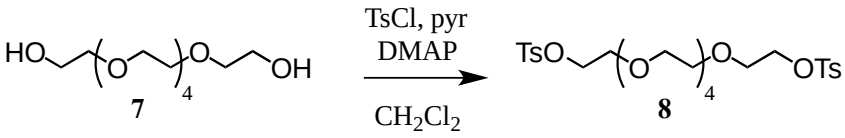

This compound was prepared according to a reported procedure.[21] A mixture of **7** (5 g, 17.71 mmol), TsCl (8.10 g, 42.5 mmol), DMAP (1.08 g, 8.86 mmol) and pyridine (3 mL, 37.19 mmol) in CH_2Cl_2 (30 mL) was stirred at 0^0 C for 72h. Then the reaction mixture was concentrated and the residue was taken up in CH_2Cl_2/H_2O. The organic layer was dried ($MgSO_4$), filtered and evaporated. Column chromatography on SiO_2 (CH_2Cl_2/10% EtOAc) gave **8** (6.8 g, 65%) as a colorless oil. The analytical data were identical to those described in the literature.

Macrocycle m37

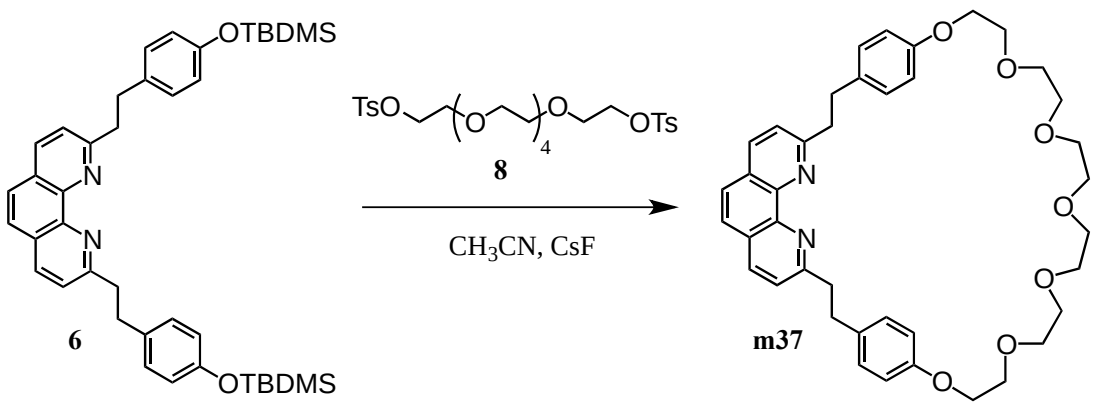

A solution of **6** (1.710 g, 2.63 mmol) and **8** (1.252 g, 2.63 mmol) in CH_3CN (200 mL) was added dropwise over 12 hours to a stirred suspension of CsF (2.395 g, 15.72 mmol) in CH_3CN (400 mL) heated at 60°C. The resulting mixture was then refluxed for 48 h and concentrated. The residue was taken up in CH_2Cl_2/H_2O. The organic layer was dried ($MgSO_4$), filtered and evaporated. Repeated column chromatography on SiO_2 (CH_2Cl_2/1 to 2% MeOH) yielded **m37** (300 mg, 18%) as a colorless glassy product. ^1H NMR ($CDCl_3$, 300 MHz): 8.14 (d, *J* = 7 Hz, 2H), 7.72 (s, 2H), 7.50 (d, *J* = 7 Hz, 2H), 7.30 (d, *J* = 7 Hz, 4H), 6.81 (d, *J* = 7 Hz, 4H), 4.07 (t, *J* = 6 Hz, 4H), 3.79 (t, *J* = 6 Hz, 4H), 3.64 (m, 16H), 3.52 (m, 4H), 3.35 (m, 4H). ^{13}C {^1H} NMR (CD_2Cl_2, 75 MHz): 162.3, 157.8, 146.3, 136.9, 135.1, 130.4, 128.0, 126.3, 123.4, 115.3, 71.6, 71.4, 71.3 (2C), 70.4, 68.3, 41.5, 34.9. MALDI-TOF MS: 667.3 (MH^+, calcd for $C_{40}H_{47}N_2O_7$: 667.338). Elemental analysis calcd for $C_{40}H_{46}N_2O_7$: C 72.05, H 6.95, N 4.20; found: C 71.88, H 6.99, N 4.33.

General procedure for the preparation of pseudo-rotaxanes [Cu(m37)(PP)]BF_4

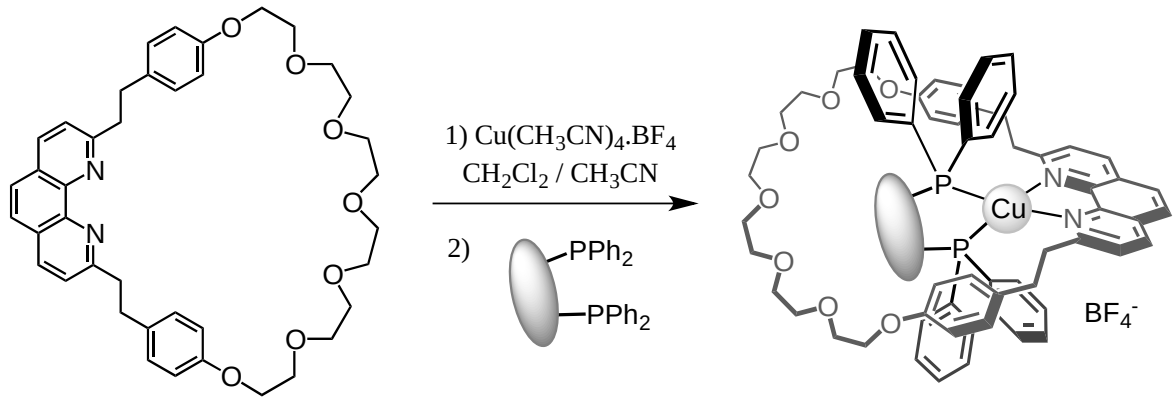

m37 **[Cu(m37)(PP)]BF_4**

A solution of **m37** (1 equiv.) and $Cu(CH_3CN)_4BF_4$ (1 equiv.) in a 7:3 CH_2Cl_2/CH_3CN mixture was stirred for 0.5 h, then the appropriate bis-phosphine ligand (1 equiv.) was added. After 1 h, the solvents were evaporated. The product was then purified as outlined in the following text.

Pseudo-rotaxane [Cu(m37)(POP)]BF_4

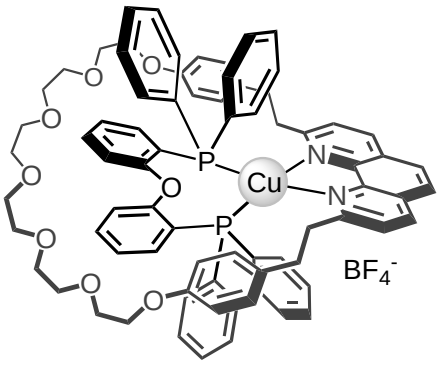

This compound was prepared from **m37** (80 mg, 0.12 mmol), $Cu(CH_3CN)_4BF_4$ (38 mg, 0.12 mmol) and POP (65 mg, 0.12 mmol) in CH_2Cl_2/CH_3CN (7:3, 10 mL). Recrystallization by slow diffusion of Et_2O into a CH_2Cl_2 solution of the crude product gave [Cu(**m37**)(POP)]BF_4 (140 mg, 85%) as yellow crystals. ^{1}H NMR (CD_2Cl_2, 300 MHz): 8.43 (d, *J* = 7 Hz, 2H), 7.88 (s, 2H), 7.72 (d, *J* = 7 Hz, 2H), 7.21 (m, 6H), 7.08 (m, 4H), 7.00 (m, 8H), 6.83 (m, 8H), 6.65 (d, *J* = 7 Hz, 4H), 6.50 (d, *J* = 7 Hz, 2H), 6.18 (d, 4H), 4.17 (m, 4H), 3.85 (m, 4H), 3.70 (m, 4H), 3.62 (m, 4H), 3.51 (m, 8H), 3.12 (m, 4H), 2.73 (m, 4H). ^{31}P {^{1}H} NMR (CD_2Cl_2, 162 MHz): -13.94. ES-MS: 1267.42 ($[M - BF_4]^+$, calc. for $C_{76}H_{74}N_2O_8P_2Cu$: 1267.422). Elemental analysis calcd for $C_{76}H_{74}BCuF_4N_2O_8P_2.CH_2Cl_2$: C 64.20, H 5.32, N 1.94; found: C 64.45, H 5.56, N 1.45.

Crystals suitable for X-ray crystal-structure analysis were obtained by slow diffusion of Et_2O into a CH_2Cl_2 solution of **[Cu(m37)(POP)]BF_4**. Data were collected at 173 K on a Bruker APEX-II CCD diffractometer (Mo-Kα radiation, λ = 0.71073 Å). The structure was solved by direct methods (SHELXS-97) and refined against F^2 using the SHELXL-97 software. The non-hydrogen atoms were refined anisotropically, using weighted full-matrix least-squares on F^2. The H-atoms were included in calculated positions and treated as ridig atoms using SHELXL default parameters. It can be noted that the residual electronic density corresponding to a non-resolved CH_2Cl_2 molecule has been squeezed. Crystallographic data: formula: $C_{76}H_{74}CuN_2O_8P_2.BF_4$ (M = 1355.66 g.mol^{-1}); yellow crystal, 0.4 × 0.2 × 0.15 mm; crystal system: monoclinic, space group $P2_1/c$; *a* = 12.6921(8) Å; *b* = 22.5455(15) Å; *c* = 27.1848(18) Å; *β* = 102.440(2)°; V = 7596.3(9) Å^3; Z = 4; F(000) = 2832; a total of 59051 reflections collected; 1.78° < θ < 29.03°, 20168 independent reflections with 8887 having I > 2σ(I); 745 parameters; Final results : $R_1(F^2)$ = 0.1412; $wR_2(F^2)$ = 0.3802, Goof = 1.210.

CHAPTER 4

Macrocyclic phenanthroline ligands for the preparation of heteroleptic Cu^{I} complexes

Pseudo-rotaxane [Cu(m37)(dppFc)]BF_4

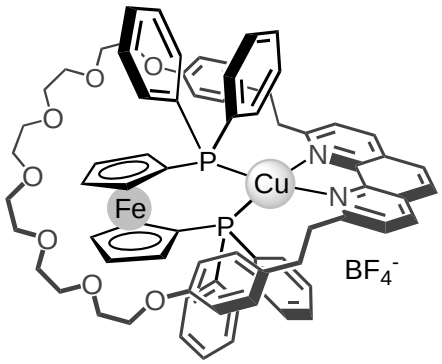

This compound was prepared from **m37** (52 mg, 0.08 mmol), $Cu(CH_3CN)_4BF_4$ (24 mg, 0.08 mmol) and dppFc (43 mg, 0.08 mmol) in CH_2Cl_2/CH_3CN (7:3, 10 mL). Recrystallization by slow diffusion of Et_2O into a CH_2Cl_2 solution of the crude product gave [Cu(**m37**)(dppFc)]BF_4 (87 mg, 81%) as dark orange crystals. ^{1}H NMR (CD_2Cl_2, 300 MHz): 8.66 (d, *J* = 7 Hz, 2H), 8.17 (s, 2H), 7.72 (d, *J* = 7 Hz, 2H), 7.35 (m, 4H), 7.14 (m, 8H), 6.98 (m, 8H), 6.69 (d, *J* = 7 Hz, 4H), 6.22 (d, *J* = 7 Hz, 4H), 4.54 (s, 4H), 4.14 (m, 4H), 4.09 (m, 4H), 3.85 (m, 4H), 3.73 (m, 16H), 2.63 (m, 4H), 2.45 (m, 4H). ^{31}P {^{1}H} NMR (CD_2Cl_2, 162 MHz): -12.22. ES-MS: 1283.40 ($[M - BF_4]^+$, calcd for $C_{74}H_{74}N_2P_2FeCuO_7$: 1283.362). Elemental analysis calcd for $C_{74}H_{74}BCuF_4FeN_2O_7P_2.H_2O$: C 63.96, H 5.51, N 2.02; found: C 63.87, H 5.81, N 1.94.

Pseudo-rotaxane [Cu(m37)(dppe)]BF_4

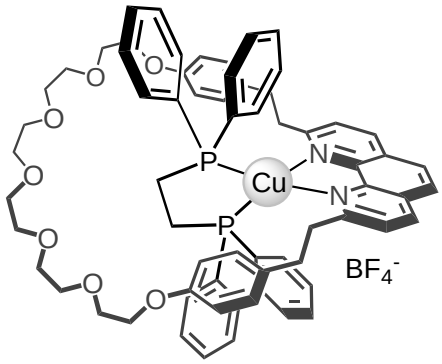

This compound was prepared from **m37** (70 mg, 0.10 mmol), $Cu(CH_3CN)_4BF_4$ (33 mg, 0.10 mmol) and dppe (41 mg, 0.10 mmol) in CH_2Cl_2/CH_3CN (7:3, 10 mL). Column chromatography (SiO_2, CH_2Cl_2/1% MeOH) followed by recrystallization (slow diffusion of Et_2O into a CH_2Cl_2 solution of the product) gave [Cu(**m37**)(dppe)]BF_4 (75 mg, 59%) as yellow crystals. ^{1}H NMR (CD_2Cl_2, 300 MHz): 8.68 (d, *J* = 7 Hz, 2H), 8.17 (s, 2H), 7.81 (d, *J* = 7 Hz, 2H), 7.35-7.20 (m, 20H), 6.55 (d, *J* = 7 Hz, 4H), 5.79 (d, *J* = 7 Hz, 4H), 4.13 (m, 4H), 3.84 (m, 4H), 3.72 (m, 12H); 2.64-2.53 (m, 10H), 2.44 (m, 4H). ^{31}P{^{1}H} NMR (CD_2Cl_2, 162 MHz): -7.66. ES-MS: 1127.39 ($[M - BF_4]^+$, calcd for $C_{66}H_{70}N_2P_2CuO_7$: 1127.395). Elemental analysis calcd for $C_{66}H_{70}BCuF_4N_2O_7P_2.H_2O$: C 64.26, H 5.88, N 2.27; found: C 64.66, H 5.49, N 1.91.

Pseudo-rotaxane [Cu(m37)(dppp)]BF_4

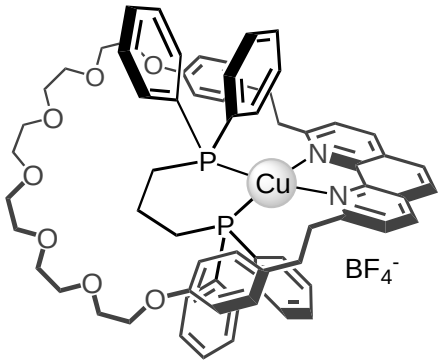

This compound was prepared from **m37** (56 mg, 0.08 mmol), $Cu(CH_3CN)_4BF_4$ (26 mg, 0.08 mmol) and dppp (34 mg, 0.08 mmol) in CH_2Cl_2/CH_3CN (7:3, 10 mL). Column chromatography (SiO_2, CH_2Cl_2/1% MeOH) followed by recrystallization (slow diffusion of Et_2O into a CH_2Cl_2 solution of the product) gave [Cu(**m37**)(dppp)]BF_4 (63 mg, 61% yield) as yellow crystals. ^{1}H NMR (CD_2Cl_2, 300 MHz): 8.66 (d, *J* = 7 Hz, 2H), 8.17 (s, 2H), 7.74 (d, *J* = 7 Hz, 2H), 7.38-6.96 (m, 20H), 6.67 (d, *J* = 7 Hz, 4H), 6.07 (d, *J* = 7 Hz, 4H), 4.15 (m, 4H), 3.83 (m, 4H), 3.67 (m, 16H), 2.60 (m, 4H), 2.51 (m, 4H), 2.33 (m, 6H). $^{31}P\{^1H\}$ NMR (CD_2Cl_2, 162 MHz): -18.05. ES-MS: 1141.41 ($[M - BF_4]^+$, calcd for $C_{67}H_{72}CuN_2O_7P_2$: 1141.411). Elemental analysis calcd for $C_{67}H_{72}BCuF_4N_2O_7P_2.H_2O$: C 64.50, H 5.98, N 2.25; found: C 64.78, H 6.25, N 2.19.

Compound 9

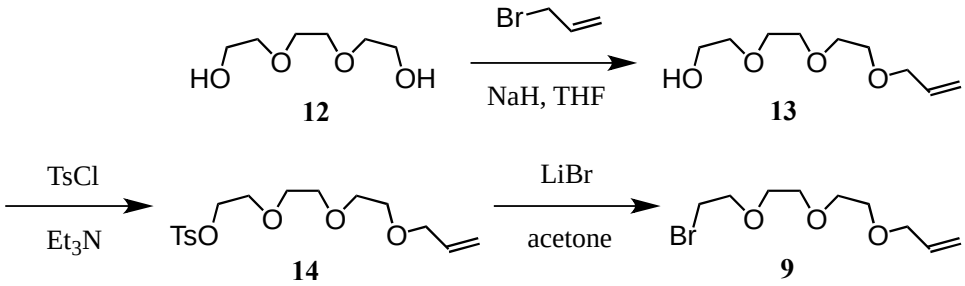

This compound was prepared in three steps according to a reported procedure.[27]

*Compound **13***. NaH (3.2 g, 80 mmol) was added portion wise to a solution of **12** (20.5 mL, 150 mmol) in dry THF (50 mL) at room temperature. After 15 minutes, allyl bromide (4.32 ml, 50 mmol) was added and the resulting mixture stirred at room temperature for 1h. H_2O (5 mL) was added and the solvent removed under vacuum. The residue was taken up in CH_2Cl_2/H_2O. The organic layer was washed with saturated brine, dried over $MgSO_4$, filtered and evaporated. The yellow oily crude product was further purified by column

chromatography on SiO_2 (cyclohexane/ethyl acetate: 2/3) to give **2** (6.84 g, 71%). The analytical data were identical to those described in the literature.

*Compound **14***. A solution of **2** (6.84 g, 35.96 mmol) in distilled triethyl amine (90 mL) was cooled to 0^0 C. Then tosyl chloride (10.29 g, 53.9 mmol) was added to the medium and the resulting mixture was stirred at room temperature for 24h. The reaction mixture was poured into ice and the aqueous phase extracted with ethyl acetate. The combined organic layers were washed with a 2% aqueous AcOH solution and H_2O. The organic layer was then dried over $MgSO_4$, filtered and evaporated to give a yellow oil. Column chromatography on SiO_2 (Cyclohexane/Ethyl acetate 1:1) gave **3** (10 g, 80%) as a colorless oil. The analytical data were identical to those described in the literature.

*Compound **9***. A mixture of **3** (8 g, 23.23 mmol) and LiBr (6.05 g, 69.68 mmol) in acetone (150 mL) was refluxed for 24h. The solvent was removed under vacuum and the residue taken up in CH_2Cl_2/H_2O. The organic layer was dried ($MgSO_4$), filtered and evaporated. Column chromatography on SiO_2 (Cyclohexane / Ethyl acetate 1:1) gave **4** (5 g, 85%) as a pale yellow oil. The analytical data were identical to those described in the literature.

Compound 10

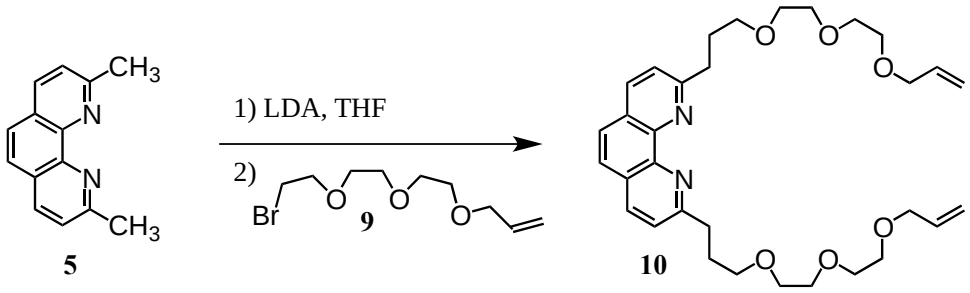

A 2 M solution of LDA in THF (9 mL, 18 mmol) was added slowly to a stirred solution of **5** (1.87 g, 8.97 mmol) in anhydrous THF (50 mL) at -78 °C under Ar. After 4 h, a solution of **9** (5.0 g, 19.75 mmol) in THF (10 mL) was added dropwise. The resulting mixture was stirred for 2 h at -78°C, then for 16 h at room temperature. The solution was then poured into ice water (150 mL). The mixture was extracted with CH_2Cl_2 (3 x 100 mL) and the combined organic layers were dried ($MgSO_4$), filtered and evaporated. Column chromatography (SiO_2,

CH_2Cl_2/1 to 2% MeOH) gave **10** (2.02 g, 41% yield) as a pale yellow glassy product. ^1H NMR (CD_2Cl_2, 400 MHz): 8.15 (d, *J* = 8 Hz, 2H), 7.72 (s, 2H), 7.54 (d, *J* = 8Hz, 2H), 5.91 (m, 2H), 5.29-5.13 (m, 4H), 3.99-3.97 (m, 4H), 3.63-3.55 (m, 20H), 3.20 (m, 4H), 2.17 (m, 4H). ^{13}C {^1H} NMR (CD_2Cl_2, 75 MHz): 163.0, 146.4, 136.9, 135.9, 127.9, 126.3, 123.4, 117.1, 72.8, 71.4, 71.3, 71.1, 70.4, 36.6, 30.9. MALDI-TOF MS: 553.12 (MH^+, calcd for $C_{32}H_{45}N_2O_6$: 553.32).

Compound 11

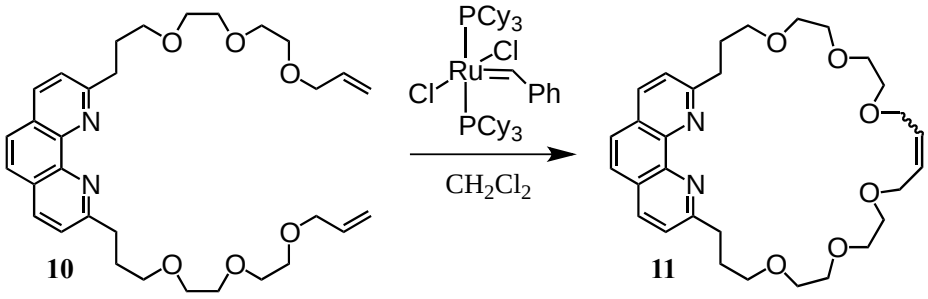

Grubb's 1st generation catalyst (5 mol%) was added to a 0.01M solution of **10** (600 mg, 1.086 mmol) in CH_2Cl_2. After 6h at room temperature, an additional portion of catalyst (5 mol%) was added. After 6 h, the solvent was removed under vacuum. Column chromatography on SiO_2 (CH_2Cl_2/1 to 3% MeOH) gave **11** (490 mg, 86% yield) as a pale yellow glassy product. ^1H NMR ($CDCl_3$, 300 MHz): 8.12 (d, *J* = 8Hz, 2H), 7.68 (s, 2H), 7.49 (d, *J* = 8Hz, 2H), 5.79 (m, 2H), 4.02 (m, 4H), 3.70-3.55 (m, 20H), 3.26 (m, 4H), 2.24 (m, 4H). MALDI-TOF MS: 525.11 (MH^+, calcd for $C_{30}H_{41}N_2O_6$: 525.29).

Compound m30

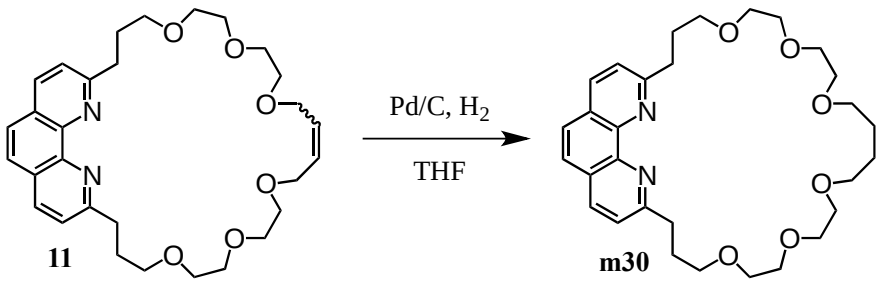

A mixture of **11** (550 mg, 1.05 mmol) and Pd/C (10 wt. % loading, 55 mg) in THF (50 mL) was stirred at room temperature under positive H_2 atmosphere. After 4 h, the mixture was filtered (celite) and evaporated. Column chromatography on SiO_2 (CH_2Cl_2/1 to 3% MeOH) gave **3** (330 mg, 60% yield) as a colorless glassy product. ^1H NMR (CD_2Cl_2, 300 MHz): 8.17 (d, *J*=8Hz, 2H), 7.73 (s, 2H), 7.53 (d, *J*=8Hz, 2H), 3.67-3.58 (m, 16H), 3.53 (m, 4H), 3.45 (m, 4H), 3.21 (m, 4H), 2.18 (m, 4H), 1.61 (m, 4H). ^{13}C {^1H} NMR (CD_2Cl_2, 75 MHz): 163.1, 146.4, 136.9, 127.9, 126.2, 123.3, 71.7, 71.6, 71.5, 71.4, 71.2, 70.9, 36.7, 30.9, 27.2. MALDI-TOF MS: 527.15 (MH^+, calcd for $C_{30}H_{43}N_2O_6$: 527.31).

General procedure for the preparation of pseudo-rotaxanes [Cu(m30)(PP)]BF_4

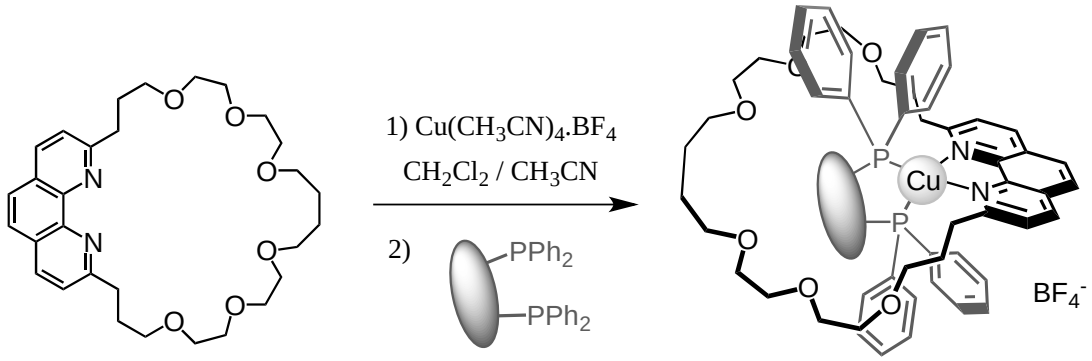

m30 [Cu(**m30**)(PP)]BF_4

A solution of **m30** (1 equiv.) and $Cu(CH_3CN)_4BF_4$ (1 equiv.) in a 7:3 CH_2Cl_2/CH_3CN mixture was stirred for 0.5 h, then the appropriate bis-phosphine ligand (1 equiv.) was added. After 1 h, the solvents were evaporated. The product was then purified as outlined in the following text.

Pseudo-rotaxane [Cu(m30)(dppe)]BF_4

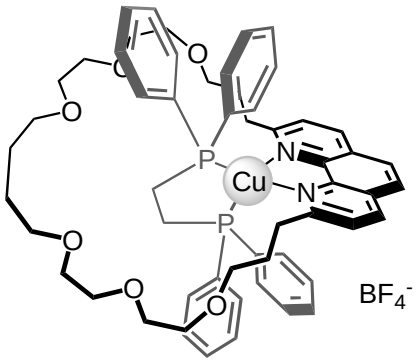

A solution of **m30** (70 mg, 0.133 mmol) and $Cu(CH_3CN)_4BF_4$ (42 mg, 0.133 mmol) in CH_2Cl_2/CH_3CN (7 : 3, 10 mL) mixture was stirred for 0.5 h, then dppe (53 mg, 0.133 mmol) was added. After 1 h, the solvents were evaporated. Recrystallization by slow diffusion of Et_2O into a CH_2Cl_2 solution of the crude product gave [Cu(**m30**)(dppe)]BF_4 (90 mg, 63%) as orange

crystals. ^{1}H NMR (CD_2Cl_2, 300 MHz): 8.57 (d, *J* = 7Hz, 2H), 8.09 (s, 2H), 7.68 (d, *J* = 7Hz, 2H), 7.30 (m, 20H), 3.54 (m, 16H), 3.25 (m, 10H), 2.82 (m, 4H), 2.48 (m, 4H), 1.72 (m, 4H), 1.39 (m, 2H). ^{31}P {^{1}H} NMR (CD_2Cl_2, 162 MHz): -6.87. MALDI-TOF MS: 987.2 (MH^+, calcd for $C_{56}H_{67}N_2P_2CuO_6$: 987.37).

Crystals suitable for X-ray crystal-structure analysis were obtained by slow diffusion of Et_2O into a CH_2Cl_2 solution of [Cu(**m30**)(dppe)]BF_4. Data were collected at 173 K on a Bruker APEX-II CCD diffractometer (Mo-Kα radiation, λ = 0.71073 Å). The structure was solved by direct methods (SHELXS-97) and refined against F^2 using the SHELXL-97 software. The non-hydrogen atoms were refined anisotropically, using weighted full-matrix least-squares on F^2. The H-atoms were included in calculated positions and treated as ridig atoms using SHELXL default parameters. Crystallographic data: formula: $C_{56}H_{66}CuN_2O_6P_2.BF_4$ (M = 1075.40 $g.mol^{-1}$); yellow crystal, 0.50 × 0.25 × 0.15 mm; crystal system: triclinic, space group P-1; *a* = 11.7950(7) Å; *b* = 13.2034(7) Å; *c* = 19.7058(11) Å; *α* = 106.642(1)°; *β* = 106.201(1)°; *γ* = 91.402(1); V = 2805.3(3) $Å^3$; Z = 2; F(000) = 1128; a total of 36543 reflections collected; 2.24° < θ < 28.09°, 13553 independent reflections with 8630 having I > 2σ(I); 553 parameters; Final results : $R_1(F^2)$ = 0.0905; $wR_2(F^2)$ = 0.2668, Goof = 1.102.

Pseudo-rotaxane [Cu(m30)(dppp)]BF_4

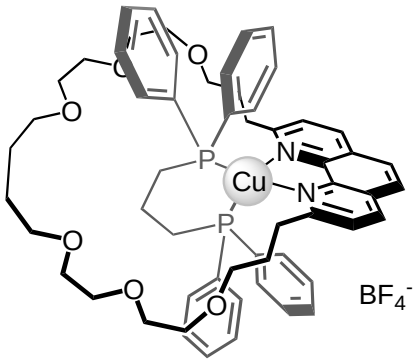

A solution of **m30** (60 mg, 0.114 mmol) and $Cu(CH_3CN)_4BF_4$ (36 mg, 0.114 mmol) in CH_2Cl_2/CH_3CN (7:3, 10 mL) mixture was stirred for 0.5 h, then dppp (47 mg, 0.114 mmol) was added. After 1 h, the solvents were evaporated. Recrystallization by slow diffusion of Et_2O into a CH_2Cl_2 solution of the crude product gave [Cu(**m30**)(dppp)]BF_4 (95 mg, 77%) as orange powder. ^{1}H NMR (CD_2Cl_2, 300 MHz): 8.53 (d, *J* = 8Hz, 2H), 8.09 (s, 2H), 7.62 (d, *J* = 8Hz, 2H), 7.16 (m, 20H), 3.61-3.37 (m, 20H), 2.96 (m, 4H), 2.59 (m, 4H), 1.66 (m, 4H), 1.27 (m, 10H). ^{31}P {^{1}H} NMR (CD_2Cl_2, 162 MHz): -16.43. ES-MS: 1001.39 ($[M - BF_4]^+$, calcd for $C_{57}H_{68}N_2P_2CuO_6$: 1001.38).

CHAPTER 4

Macrocyclic phenanthroline ligands for the preparation of heteroleptic Cu^{I} complexes

Pseudo-rotaxane [Cu(m30)(POP)]BF_4

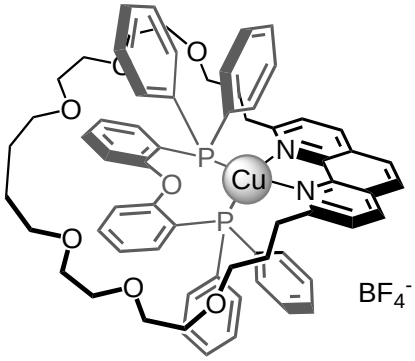

A solution of **m30** (110 mg, 0.208 mmol) and $Cu(CH_3CN)_4BF_4$ (66 mg, 0.208 mmol) in CH_2Cl_2/CH_3CN (7:3, 10 mL) mixture was stirred for 0.5 h, then POP (113 mg, 0.208 mmol) was added. After 1 h, the solvents were evaporated. Column chromatography (SiO_2, CH_2Cl_2/1% MeOH) followed by recrystallization (slow diffusion of Et_2O into a CH_2Cl_2 solution of the product) gave [Cu(**m30**)(POP)]BF_4 (191 mg, 75% yield) as yellow crystals. ^{1}H NMR (CD_2Cl_2, 300 MHz): 8.43 (d, *J* = 8Hz, 2H), 7.98 (s, 2H), 7.68 (d, *J* = 8Hz, 2H), 7.31 (m, 6H), 7.15 (m, 8H), 7.05-6.82 (m, 14H), 3.15-3.07 (m, 20H), 2.92 (t, *J* = 6Hz, 4H), 2.67 (t, *J* = 6Hz, 4H), 1.32 (m, 8H). ^{13}C {^{1}H} NMR (CD_2Cl_2, 75 MHz): 164.4, 144.1, 144.0, 143.9, 138.3, 134.4, 134.3, 132.7, 130.9, 129.7, 129.6, 129.5, 128.7, 127.0, 125.4, 71.6, 71.2, 70.9, 70.8, 70.7, 70.4, 38.8, 29.6, 27.2. ^{31}P {^{1}H} NMR (CD_2Cl_2, 162 MHz): -13.57. ES-MS: 1127.39 ([M - BF_4]$^+$, calcd for $C_{66}H_{70}N_2P_2CuO_7$: 1127.40).

Crystals suitable for X-ray crystal-structure analysis were obtained by slow diffusion of Et_2O into a CH_2Cl_2 solution of [Cu(**m30**)(POP)]BF_4. Data were collected at 173 K on a Bruker APEX-II CCD diffractometer (Mo-Kα radiation, λ = 0.71073 Å). The structure was solved by direct methods (SHELXS-97) and refined against F^2 using the SHELXL-97 software. The non-hydrogen atoms were refined anisotropically, using weighted full-matrix least-squares on F^2. The H-atoms were included in calculated positions and treated as ridig atoms using SHELXL default parameters. Crystallographic data: formula: $C_{66}H_{70}CuN_2O_7P_2.BF_4$ (M = 1215.53 g.mol^{-1}); yellow crystal, 0.30 × 0.25 × 0.20 mm; crystal system: triclinic, space group P-1; *a* = 13.6380(5) Å; *b* = 14.9380(5) Å; *c* = 15.6669(6) Å; α = 78.733(1)°; β = 72.898(1)°; γ = 83.964(1); V = 2988.29(19) Å^3; Z = 2; F(000) = 1272; a total of 47180 reflections collected; 2.04° < θ < 30.09°, 14418 independent reflections with 17435 having I > 2σ(I); 634 parameters; Final results : $R_1(F^2)$ = 0.1250; $wR_2(F^2)$ = 0.3530, Goof = 1.484.

Compound [Cu(10)(POP)]BF_4

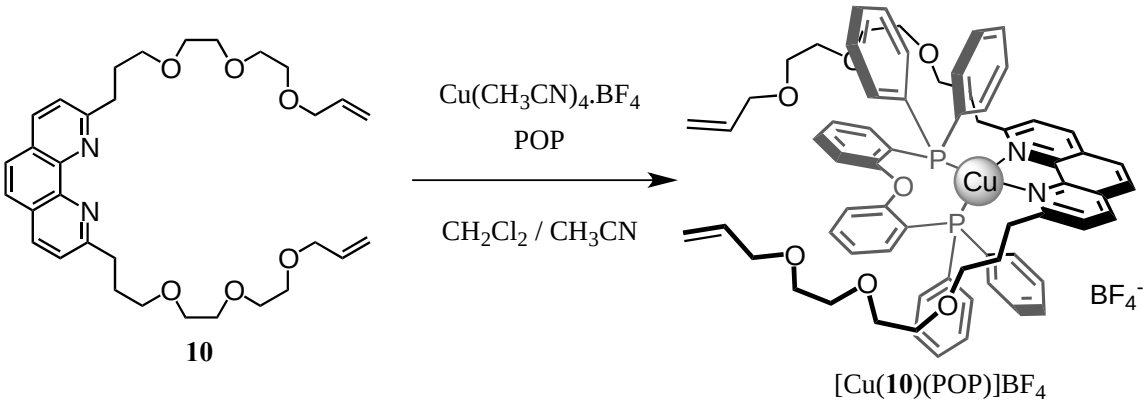

10 [Cu(**10**)(POP)]BF_4

A solution of POP (292 mg, 0.543 mmol) and $Cu(CH_3CN)_4BF_4$ (171 mg, 0.543 mmol) in CH_2Cl_2 (50 mL) was stirred for 0.5 h, then **10** (300 mg, 0.543 mmol) was added. After 1 h, the solvents were evaporated. The residue was dissolved in a minimum of CH_2Cl_2 and the Cu(I) complex precipitated by addition of Et_2O. Filtration yielded [Cu(**10**)(POP)]BF_4 (575 mg, 85% yield) as an orange powder. ^{1}H NMR (CD_2Cl_2, 400 MHz): 8.44 (d, *J* = 8Hz, 2H), 7.92 (s, 2H), 7.70 (d, *J* = 8Hz, 2H), 7.33-6.99 (m, 28H), 5.91 (m, 2H), 5.30-5.14 (m, 4H), 3.99 (m, 4H), 3.56 (s, 8H), 3.48 (t, *J* = 4Hz, 4H), 3.32 (t, *J* = 4Hz, 4H), 2.93 (m, 4H), 2.77 (m, 4H), 1.46 (m, 4H).

Pseudo-rotaxane [Cu(11)(POP)]BF_4

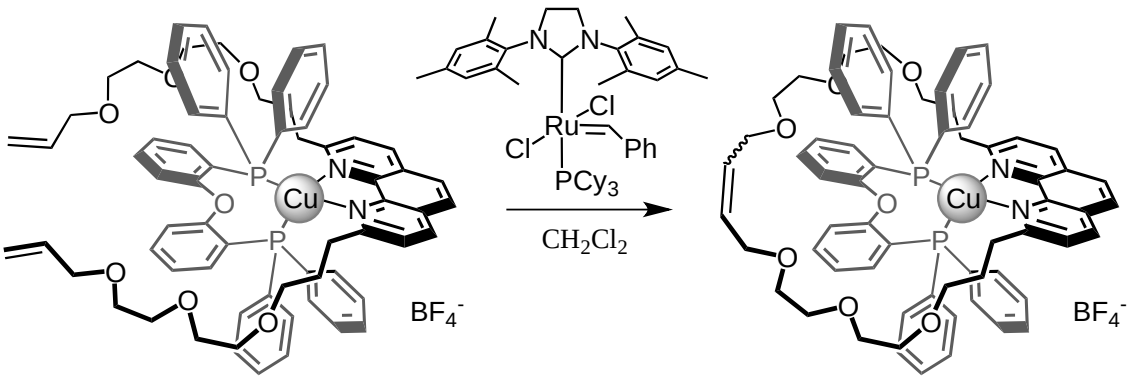

[Cu(**10**)(POP)]BF_4 [Cu(**11**)(POP)]BF_4

Grubb's 2nd generation catalyst (5 mol%) was added to a 0.005 M solution of [Cu(**10**)(POP)]BF_4 (575 mg, 0.463 mmol) in CH_2Cl_2. After 6h at room temperature, an

additional portion of catalyst (5 mol%) was added. After 6 h, the solvent was removed under vacuum. Column chromatography on SiO_2 (CH_2Cl_2/1 to 4% MeOH) gave [Cu(**11**)(POP)]BF_4 (200 mg, 36% yield) as pale yellow solid. ^{1}H NMR ($CDCl_3$, 300 MHz): 8.48 (d, *J* = 8Hz, 2H), 8.01 (s, 2H), 7.68 (d, *J* = 8Hz, 2H), 7.29 (m, 6H), 7.14 (m, 8H), 7.05-6.78 (m, 14H), 5.49 (m, 2H), 3.67 (m, 4H), 3.21-3.10 (m, 14H), 2.90 (m, 4H), 2.68 (m, 4H), 1.32 (m, 6H).

Pseudo-rotaxane [Cu(m30)(POP)]BF_4

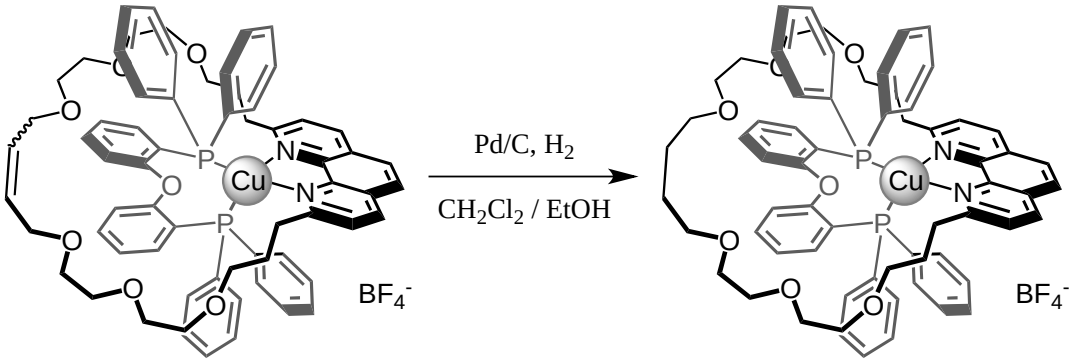

[Cu(**11**)(POP)]BF_4 [Cu(**m30**)(POP)]BF_4

A mixture of [Cu(**11**)(POP)]BF_4 (200 mg, 0.164 mmol) and Pd/C (10 wt. % loading, 20 mg) in CH_2Cl_2/EtOH (1:1) (30 mL) was stirred at room temperature under positive H_2 atmosphere. After 4 h, the mixture was filtered (celite) and evaporated. Column chromatography on SiO_2 gave [Cu(**m30**)(POP)]BF_4 (80 mg, 40% yield) as yellow powder.

Computational studies

The molecular modeling was performed with *Spartan'10* Macintosh Parallel Edition (Wavefunction Inc., USA) at the semi-empirical PM6 level.

For both [Cu(**m30**)(dppe)]$^+$ and [Cu(**m30**)(POP)]$^+$, the molecular geometry was optimized for the two possible conformers:

- **A** and **B** for [Cu(**m30**)(POP)]$^+$
- **C** and **D** for [Cu(**m30**)(dppe)]$^+$

The calculated structures (**m30**: pale gray, PP ligand: dark gray, Cu: black, the H atoms have been omitted for clarity) and the corresponding heats of formation are indicated bellow.

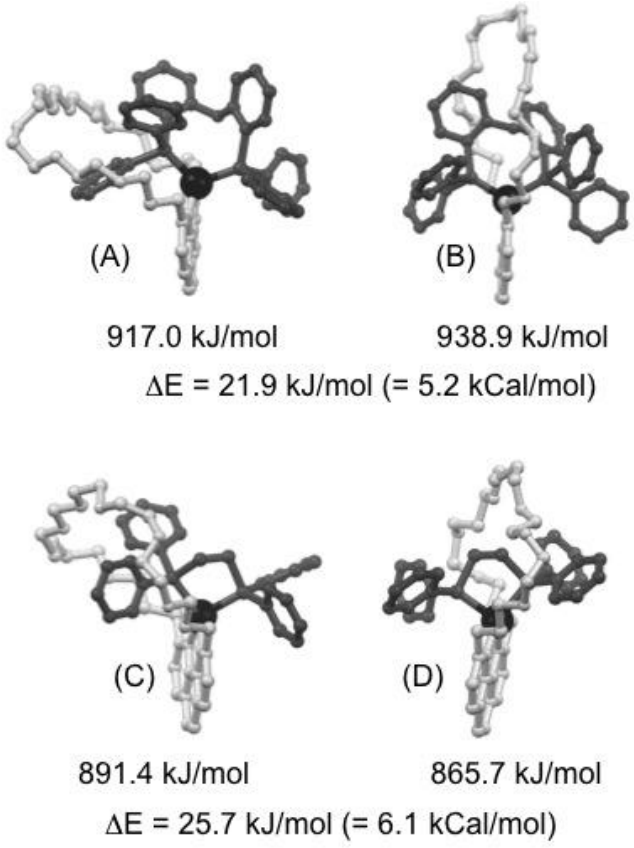

5. References

1) a) B. R. James, R. J. P. Williams, *J. Chem. Soc.* **1961**, 2007, b) F. A. Arnaud-Neu, E. Marques, M.-J. Schwing-Weill, C. O. Dietrich-Buchecker, J.-P. Sauvage, J. Weiss, *New J. Chem*. **1988**, *12*, 15.

2) a) E. Riesgo, Y.-Z. Hu, F. Bouvier, R. P. Thummel, *Inorg. Chem*. **2001**, *40*, 2541; b) I. Pianet, J.-M. Vincent, *Inorg. Chem.* **2004**, *43*, 2947; c) V. Hebbe-Viton, V. Desvergnes, J. J. Jodry, C. Dietrich-Buchecker, J.-P. Sauvage, J. Lacour, *Dalton Trans*. **2006**, 2058.

3) For a review on metal-coordination-driven dynamic heteroleptic architectures, see: S. De, K. Mahata, M. Schmittel, *Chem. Soc. Rev*. **2010**, *39*, 1555.

4) a) M. Albrecht, *Chem. Rev*. **2001**, *101*, 3457; b) G. F. Swiegers, T. J. Malefetse, *Coord. Chem. Rev*. **2002**, *225*, 91. c) B. H. Northrop, Y.-R. Zheng, K.-W. Chi, P. J. Stang, *Acc. Chem. Res*., **2009**, *42*, 1554; d) R. Chakrabarty, P. S. Mukherjee, P. J. Stang, *Chem. Rev.*, **2011**, *111*, 6810; e) P. J. Stang, B. Olenyuk, *Acc. Chem. Res.*, **1997,** *30*, 502; f) M. Fujita, K. Ogura, *Coord. Chem. Rev.*, **1996**, *148*, 249; g) M. Fujita, *Chem. Soc. Rev*., **1998**, *27*, 417; h) M. Fujita, *Acc. Chem. Res*., **1999**, *32*, 53; i) M. Fujita, M. Tominaga, A. Hori, B. Therrien, *Acc. Chem. Res*., **2005**, *38*, 371.

5) a) C. O. Dietrich-Buchecker, J.-P. Sauvage, J.-P. Kintzinger, *Tet. Lett.*,**1983**, *24*, 5095; b) C. O. Dietrich-Buchecker, J.-P. Sauvage, *Tet. Lett*., **1983**, *24*, 5091; c) C. O. Dietrich-Buchecker, J.-P. Sauvage, J.-M. Kern, *J. Am. Chem. Soc*., **1984**, *106*, 3043; d) C. O. Dietrich-Buchecker, J.-P. Sauvage, *Tetrahedron.*,**1990**, *46*, 503;

6) For selected reviews, see: a) P. C. Haussman, J. F Stoddart, *The Chemical Record*., **2009**, *9*, 136; b) R. S. Forgan, J.-P. Sauvage, J. F. Stoddart, *Chem. Rev.*, **2011**, *111*, 5434; c) S. Saha, J. F. Stoddart, *Chem. Soc. Rev*., **2007**, *36*, 77; d) D. B. Amabilino, J. F. Stoddart, *Chem. Rev.*, **1995**, *95*, 2725; e) F. M. Raymo, J. F.Stoddart, *Chem. Rev.*, **1999,** *99*, 1643; f) V.Balzani, M. G. Lopez, J. F. Stoddart, *Acc. Chem. Res.*,**1998,** *31*, 405; g) A. R. Pease, J. O. Jeppesen, J. F. Stoddart, Y. Luo, C. P. Collier, J. R. Heath, *Acc. Chem. Res*., **2001**, *34*, 433; h) W.R. Dichtel, O. S. Miljanic, W. Zhang, J. M. Spruell, K. Patel, I. Aprahamian, J. R. Heath, J. F. Stoddart, *Acc. Chem. Res*., **2008**, *41***,** 1750; i) A. C. Fahrenbach, C. J. Bruns, D. Cao, J. F. Stoddart, *Acc. Chem. Res*., **2012**, *45*, 1581; j) J. E. Beves, B. A. Blight, C. J. Campbell, D. A. Leigh and R. T.

McBurney *Angew. Chem. Int. Ed*., **2011**, *50*, 9260; k) J.-F. Ayme, J. E. Beves, C. J. Campbell, D. A. Leigh, *Chem. Soc. Rev.*, **2012**, *ASAP*; l) J. D. Crowley, S. M. Goldup, A.-L. Lee, D. A. Leigh, R. T. McBurney, *Chem. Soc. Rev*., **2009**, *38*, 1530; m) S. Anderson, H. L. Anderson, J. K. M . Sanders, *Acc. Chem. Res*., **1993,** *26*, 469; n) R. Jager, F. Vögtle, *Angew. Chem. Int. Ed. Engl.*, **1997**, *36*, 930; o) T. J. Hubin, D. H. Busch, *Coord. Chem. Rev*., **2000**, *200-202*, 5; p) V. Balzani, A. Credi, S. Silvi and M. Venturi, *Chem. Soc. Rev.*, **2006**, *35*, 1135.

7) a) C. Dietrich-Buchecker and J.-P. Sauvage, *Chem. Rev.*, **1987**, *87*, 795; b) B. Champin, P. Mobian and J.-P. Sauvage, *Chem. Soc. Rev.*, **2007**, *36*, 358; c) J.-P. Sauvage, *Acc. Chem. Res*. **1998**, *31*, 611; d) J.-P.Collin, J.-P. Sauvage, *Chem. Lett.*, **2005** , *34*, 742; e) J.-P. Collin, V. Heitz, S. Bonnet, J.-P. Sauvage, *Inorg. Chem. Comm.*, **2005**, *8*, 1063; f) F. Durola1, J.-P. Sauvage, O. S.Wenger, *Coord. Chem. Rev* **2010**, *254*, 1748; g) M.-J. Blanco, M. C. Jiménez, J.-C. Chambron, V. Heitz, M. Linke, J.-P. Sauvage, *Chem. Soc. Rev.*, **1999**, *28*, 293; h) C. Dietrich-Buchecker, M. C. J.-Molero, V. Sartor, J.-P. Sauvage, *Pure Appl. Chem.*, **2003**, *75*, 1383; i) C. Dietrich-Buchecker, G. Rapenne, J.-P. Sauvage, *Co.ord. Chem. Rev.*, **1999**, *185*, 167; j) J.-P. Collin, C. Dietrich-Buchecker, P. Gavina, M. C. J.-Molero, J.-P. Sauvage, *Acc. Chem. Res*., **2001,** *34*, 477; k) J.-P. Sauvage, *Acc. Chem. Res.*, **1990,** *23*,319.

8) M. Schmittel, A. Ganz, *Chem. Commun*. **1997**, 999.

9) M. Schmittel, A. Ganz, D. Fenske, *Org. Lett*. **2002**, *4*, 2289.

10) M. Schmittel, H. Ammon, V. Kalsani, A. Wiegrefe, C. Michel, *Chem. Commun*. **2002**, 2566.

11) M. Schmittel, V. Kalsani, D. Fenske, A. Wiegrefe, *Chem. Commun*. **2004**, 490.

12) V. Kalsani, H. Amon, F. Jäckel, J. P. Rabe, M. Schmittel, *Chem. Eur. J*. **2004**, *10*, 5481.

13) V. Kalsani, H. Bodenstedt, D. Fenske, M. Schmittel, *Eur. J. Inorg. Chem*. **2005**, 1841.

14) R. S. K. Kishore, V. Kalsani, M. Schmittel, *Chem. Commun*. **2006**, 3690.

15) R. S. K. Kishore, T. Paululat, M. Schmittel, *Chem. Eur. J*. **2006**, 12, 8136.

16) N. Armaroli, G. Accorsi, G. Bergamini, P. Ceroni, M. Holler, O. Moudam, C. Duhayon, B. Delavaux-Nicot, J.-F. Nierengarten, *Inorg. Chim. Acta* **2007**, *360*, 1032 and references therein.

17) A. Kaeser, PhD thesis, University of Toulouse (France), **2008**.

18) a) P. Coppens, I. Vorontsov, T. Graber, A. Kovalevsky, Y. Chen, G. Wu, M. Gembicky, I. Novozhilova, *J. Am. Chem. Soc.* **2004**, *126*, 5980. B) P. Coppens, *Chem. Commun.* **2003**, 1317.

19) a) M. Gutiérrez-Nava, H. Nierengarten, P. Masson, A. Van Dorsselaer, J.-F. Nierengarten, *Tetrahedron Lett.* **2003**, *44*, 3043; b) A. Gégout, T. M. Figueira-Duarte, J.-F. Nierengarten, A. Listorti, N. Armaroli, *Synlett*. **2006**, 3095.

20) a) E. Gumienna-Kontecka, Y. Rio, C. Bourgogne, M. Elhabiri, R. Louis, A.-M. Albrecht-Gary, J.-F. Nierengarten, *Inorg. Chem.* **2004**, *43*, 3200; b) G. Accorsi, N. Armaroli, C. Duhayon, Alix Saquet, B. Delavaux-Nicot, R. Welter, O. Moudam, M. Holler, J.-F. Nierengarten, *Eur. J. Inorg. Chem*. **2010**, 164.

21) W. Raßthofer, W. Wehner and F. Vögtle ; *J. Lieb. Ann. Chem.*, **1976**, *5*, 916.

22) D. N. Reinhoudt, F. de Jong, H. P. M. Tomassen, *Tetrahedron Lett*. **1979**, *20*, 2067.

23) a) D. G. Cuttell, S.-M. Kuang, P. E. Fanwick, D. R. McMillin, R. A. Walton, *J. Am. Chem. Soc.* **2002**, *124*, 6; b) S.-M. Kuang, D. G. Cuttell, D. R. McMillin, P. E. Fanwick, R. A. Walton, *Inorg. Chem*. **2002**, *41*, 3313; c) L. Yang, J.-K. Feng, A.-M. Ren, M. Zhang, Y.-G. Ma, X.-D. Liu, *Eur. J. Inorg. Chem*. **2005**, 1867; d) C. L. Linfoot, P. Richardson, T. E. Hewat, O. Moudam, M. M. Forde, A. Collins, F. White, N. Robertson, *Dalton Trans*. **2010**, *39*, 8945; e) Q. Zhang, Q. Zhou, Y. Cheng, L. Wang, D. Ma, X. Jing, F. Wang, *Adv. Mater.* **2004**, *16*, 432; f) Q. Zhang, Q. Zhou, Y. Cheng, L. Wang, D. Ma, X. Jing, F. Wang, *Adv. Funct. Mater.* **2006**, *16*, 1203-1208; g) N. Armaroli, G. Accorsi, M. Holler, O. Moudam, J.-F. Nierengarten, Z. Zhou, R. T. Wegh, R. Welter, *Adv. Mater*. **2006**, *18*, 1313; h) T. MacCormick, W.-L. Jia, S. Wang, *Inorg. Chem*. **2006**, *45*, 147; i) H. Ge, W. Wei, P. Shuai, G. Lei, S. Qing, *J. Lumin.* **2011**, *131*, 238; j) R. D. Costa, D. Tordera, E. Orti, H. Bolink, J. Schönle, S. Graber, C. E. Housecroft, E. C. Constable, J. A. Zampese, *J. Mater. Chem.* **2011**, *21*, 16108.

24) R. H. Grubbs, *Angew. Chem. Int. Ed*. **2006**, *45*, 3760.

25) For selected examples, see: a) S. J. Miller, H. E. Blackwell, R. H. Grubbs, *J. Am. Chem. Soc*. **1996**, *118*, 9606; b) A. Fürstner, K. Langemann, *J. Org. Chem*. **1996**, *61*, 3942; c) T. J. Kidd, D. A. Leigh, A. J. Wilson, *J. Am. Chem. Soc*. **1999**, *121*, 1599; d) C. W. Lee, R. H. Grubbs, *Org. Lett*. **2000**, *2*, 2145; e) C. W. Lee, R. H. Grubbs, *J. Org. Chem*. **2001**, *66*, 7155; f) E. N. Guidry, S. J. Cantrill, J. F. Stoddart, R. H. Grubbs, *Org. Lett*. **2005**, *11*, 2129; g) S. Nawaz Khan, A. Kim, R. H. Grubbs, Y.-U. Kwon, *Org. Lett*. **2011**, *13*, 1582.

26) a) B. Mohr, M. Weck, J.-P. Sauvage, R. H. Grubbs, *Angew. Chem. Int. Ed*. **1997**, *36*, 1308; b) M. Weck, B. Mohr, J.-P. Sauvage, R. H. Grubbs, *J. Org. Chem*. **1999**, *64*, 5463; c) C. Dietrich-Buchecker, G. Rapenne, J.-P. Sauvage, *Chem. Commun*. **1997**, 2053; d) U. Lüning, F. Fahrenkrug, M. Hagen, *Eur. J. Org. Chem*., **2001**, 2161; e) S. Kang, B. M. Berkshire, Z. Xue, M. Gupta, C. Layode, P. A. May, M. F. Mayer, *J. Am. Chem. Soc*., **2008**, *130*, 15246; f) F. Arico, P. Mobian, J.-M. Kern, J.-P. Sauvage, *Org. Lett*., **2003**, *5*, 1887; g) P. Mobian, J. -M. Kern, J.-P. Sauvage, *Inorg. Chem.*, **2003**, *42*, 8633; h) M. Gupta, S. Kang, M. F. Mayer, *Tet. Lett*., **2008,** *49,* 2946; i) J. Frey, T. Kraus, V. Heitz, J.-P. Sauvage, *Chem. Comm*., **2005**, 5310; j) J. Frey, T.Kraus, V. Heitz, J.-P. Sauvage, *Chem. Eur. J*., **2007**, *13*, 7584.

27) M. Gonçalves, K. Estieu-Gionnet, T. Berthelot, G. Laïn, M. Bayle, X. Canron, N. Betz, A. Bikfalvi, G. Déléris, *Pharm Res.* **2005**, *8*, 1411.

28) R. Crabtree, *Acc. Chem. Res*. **1979**, *12*, 331.

29) a) C. A. Slinn, A. J. Redgrave, S. L. Hind, C. Edlin, S. P. Nolan, V. Gouverneur, *Org. Biomol. Chem*. **2003**, *1*, 3820; b) J. Huang, E. D. Stevens, S. P. Nolan, J. L. Petersen, *J. Am. Chem. Soc*. **1995**, *117*, 5503; c) M. S. M. Timmer, H. Ovaa, D. V. Filippov, G. A. van der Marel, J. H. van Boom, *Tetrahedron Letters*, **2000**, *41*, 8635; d) H. Clavier, S. P. Nolan, Eds. Springer *Metathesis Chemistry (NATO Science Series)*, **2007**, Vol: *243*, 29; e) M. D. McReynolds, J. M. Dougherty, and P. R. Hanson, *Chem. Rev*., **2004**, *104*, 2239; f) F. D.Toste, A. K. Chatterjee, and R. H. Grubbs, *Pure Appl. Chem.*, **2002**, *74* (1), 7; g) T. M. Trnka, R. H. Grubbs, *Acc. Chem. Res*., **2001**, *34*, 18. h) K. S. Dunne, S. E. Lee, V. Gouverneur, *J. Org. met. Chem*., **2006**, *691*, 5246.

30) A. Debe, M. J. Carlson, W. A. Goddard III, *Proc. Natl. Acad. Sci. USA* **1999**, *96*, 2596.

CHAPTER 4

Macrocyclic phenanthroline ligands for the preparation of heteroleptic Cu^{I} complexes

Conclusion

The development of phosphorescent materials based on Cu(I) coordination compounds has attracted a considerable interest in the last decade. When compared to compounds prepared from heavy metals, Cu(I) complexes represent an environmentally friendly alternative for applications in light emitting diodes and dye sensitized solar cells. Cu(I) complexes are in general thermodynamically stable compounds, however they are also kinetically labile and fast ligand exchange is often observed in solution at ambient temperature. As a result, the dynamic coordination of several species is sometimes difficult to control. As part of this research, we have systematically investigated the structural factors that affect the distribution of species in the case of heteroleptic Cu(I) complexes obtained from various phenanthroline and bis-phosphine ligands. Furthermore, we have also proposed two strategies allowing to drive the equilibrium towards stable Cu(I) complexes. The first strategy was based on the use of a P,N-ligand. We found that the treatment of 2-diphenylphosphino-6-methylpyridine (dpPyMe) with $Cu(CH_3CN)_4BF_4$ afforded a remarkably stable dinuclear Cu(I) complex, namely $[Cu_2(\mu\text{-dpPyMe})_3(CH_3CN)](BF_4)_2$ (**1**).

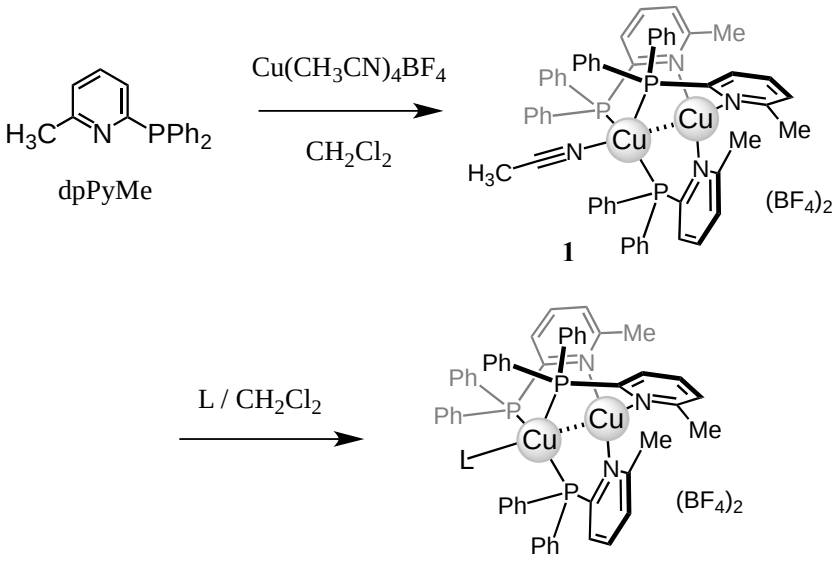

The methyl group in the dpPyMe ligand plays an important role in the stability of the complex as revealed by the comparison of the known analogous systems prepared from 2-diphenylphosphino-pyridine (dpPy). Whereas two isomers are observed for $[Cu_2(\mu\text{-dpPy})_3]^{2+}$,

we found that only the head-to-head isomer is obtained both in solution and in the solid state for the dinuclear complex prepared from dpPyMe. We have also shown that the labile CH_3CN ligand in **1** can be conveniently exchanged without disturbing the dinuclear core unit. The electronic properties of the resulting compounds have been systematically investigated. They are all weak emitters in solution, however particularly high emission quantum yields (up to 46%) have been found in a rigid matrix at room temperature. This is a remarkable achievement in the field of phosphorescent Cu(I) complexes and these results provide an interesting basis for future research on the development of Cu(I)-based materials for light emitting applications.

Heteroleptic Cu(I) complexes prepared from bis-phosphine (PP) and aromatic diimine (NN) ligands are characterized by remarkably high emission quantum yields from their long lived metal-to-ligand charge transfer (MLCT) excited state. However, a major limitation for the preparation of stable $[Cu(NN)(PP)]^+$ derivatives results from the exceptionally high thermodynamic stability of the corresponding homoleptic complexes and the preparation of stable $[Cu(NN)(PP)]^+$ derivatives in solution is a challenge.

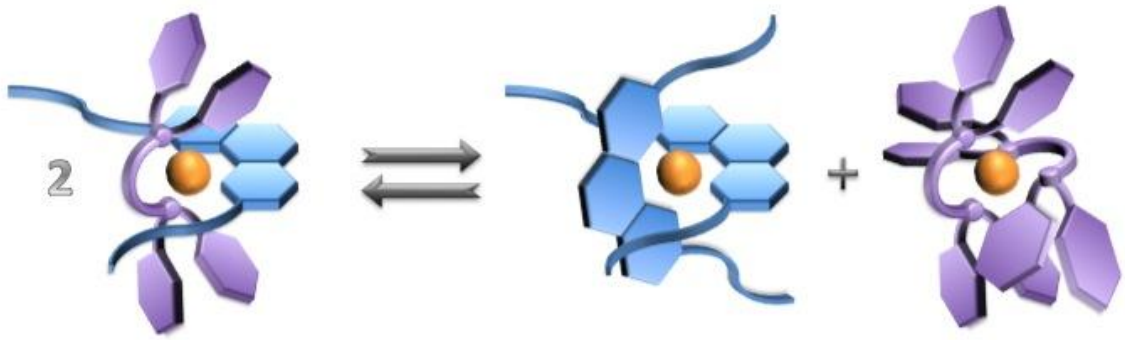

Based on the strategy developed by Sauvage and co-workers for the formation of stable coordination compounds consisting of two distinct phenanthroline ligands around a Cu(I) cation, we have shown that the formation of stable heteroleptic $[Cu(NN)(PP)]^+$ complexes is possible by applying the approach based on topological constraints. The 2,9-disubstituted-1,10-phenanthroline subunit has been incorporated in a macrocyclic structure. As a result, the formation of homoleptic complexes from the macrocyclic phenanthroline ligand being impossible, the maximum site occupancy principle favors the formation of stable heteroleptic Cu(I)-complexed pseudo-rotaxanes. This is the case when the macrocycle is large

and flexible enough (**m30** and **m37**) to allow the threading of the bulky diphenylphosphino moieties of the PP building block.

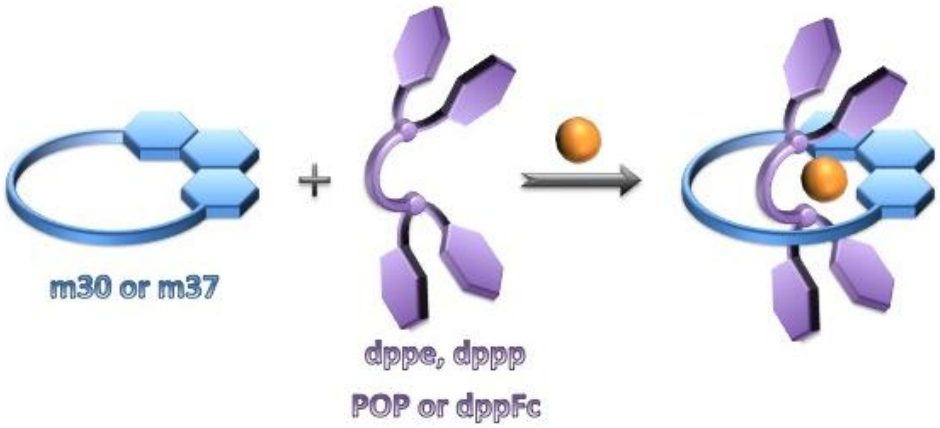

In contrast, when the phenanthroline-containing macrocycle (**M30**) is not large and flexible enough to allow the threading of the PP ligand, the combination of this steric constraint with the topological one resulting from the macrocyclic structure of the phenanthroline ligand plays a major role in the self-assembly process. The outcome depends actually on the adaptive capabilities of the PP ligand.

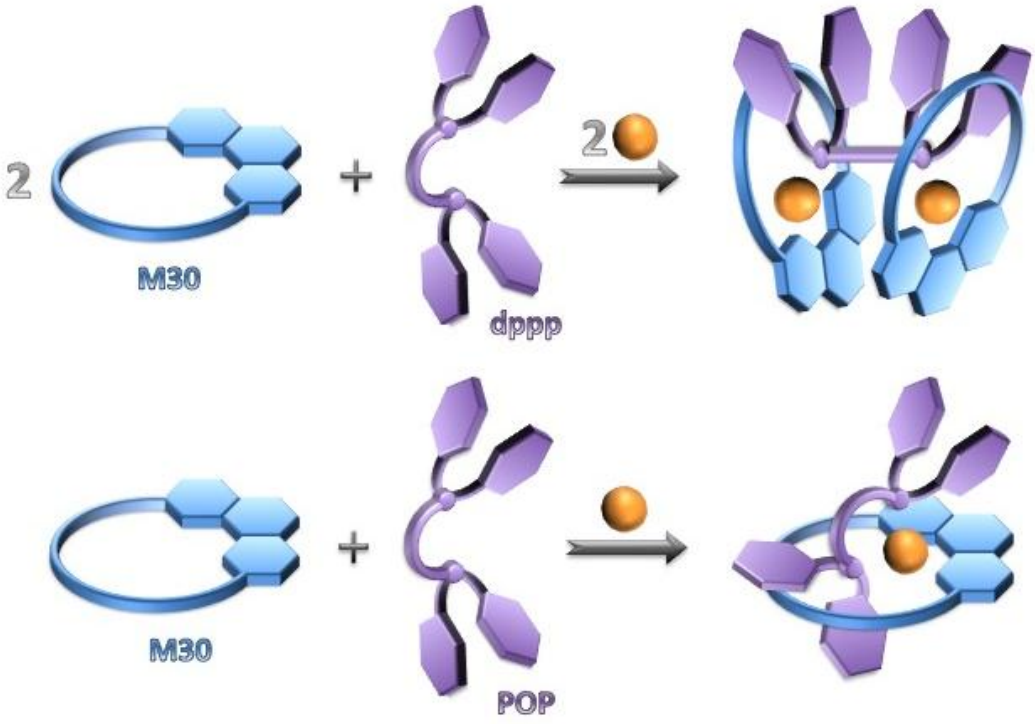

Meera MOHANKUMAR SREELATHA

Synthèse de complexes cuivreux luminescents

Résumé

La présente thèse décrit la préparation de complexes de Cu(I) stables grâce à l'ingénierie moléculaire de ligands permettant d'éviter la formation de plusieurs espèces en équilibre. Dans le cas de ligands P-N, la stratégie proposée repose sur l'utilisation d'un ligand ayant des substituants permettant de masquer un centre métallique et ainsi d'empêcher les réactions avec des nucléophiles permettant la dissociation du ligand. Dans le cas des dérivés $[Cu(NN)(PP)]^+$, l'approche synthétique développée repose sur l'utilisation de ligands phénanthrolines macrocycliques empêchant la formation des complexes homoleptiques $[Cu(NN)_2]^+$ correspondant. Des complexes stables et luminescents ont ainsi été préparés, les rendements quantiques d'émission allant jusqu'à 46% à l'état solide pour les meilleurs luminophores.

Cuivre(I) – Luminescence – Ligand P-N – Phosphine – Phénanthroline –Rotaxane

Résumé en anglais

The present PhD thesis descibes the preparation of stable Cu(I) complexes through appropriate ligand design to prevent the formation of several species in equilibrium. In the case of dinucleating P,N-ligands, the proposed strategy is based on the use of a ligand with additional substituents to shield the metal centers and thus to prevent nucleophilic attacks leading to ligand dissociation. In the case of the $[Cu(NN)(PP)]^+$ derivatives, the proposed synthetic strategy relies on the use of macrocyclic phenanthroline ligands preventing the formation of the corresponding homoleptic complexes $[Cu(NN)_2]^+$. Stable luminescent complexes have been thus prepared, the emission quantum yields being as high as 46% in the solid state for the best emitters.

Copper(I) – Luminescence – P,N-ligand – Phosphine – Phenanthroline – Rotaxane